http://researchcommons.waikato.ac.nz/

Research Commons at the University of Waikato

Copyright Statement:

The digital copy of this thesis is protected by the Copyright Act 1994 (New Zealand).

The thesis may be consulted by you, provided you comply with the provisions of the Act and the following conditions of use:

- Any use you make of these documents or images must be for research or private study purposes only, and you may not make them available to any other person.
- Authors control the copyright of their thesis. You will recognise the author's right to be identified as the author of the thesis, and due acknowledgement will be made to the author where appropriate.
- You will obtain the author's permission before publishing any material from the thesis.

Novel Compounds for Immunoassay of Small Biomolecules

This thesis is submitted in partial fulfilment of the requirements of the degree of Doctor of Philosophy in Chemistry at the University of Waikato

John Stanton Mitchell

University of Waikato

2005

Abstract

A series of progesterone-4-ovalbumin conjugates with different length intermediate linkers were applied as coating antigens in an enzyme-linked immunosorbent assay (ELISA) format to determine antibody-binding performance and assay parameters in cow whole milk. The use of an 18-atom linker gave higher binding than 4- or 11-atom linkers but no further increase was seen with increasing linker length. An ELISA constructed with the 18-atom linker conjugate gave a detection limit of 0.089 ng/mL progesterone and correlated well to an established radioimmunoassay procedure ($r = 0.94$). The assay has the advantages of a wide linear range (0.1 to 100 ng/mL) enabling full profiling of bovine estrous cycles, use of whole milk directly without extraction or pre-dilution, and employing more easily purified protein conjugates as coating antigens compared with commercial progesterone-enzyme conjugates.

Thioether-bridged derivatives of 17β-estradiol and estrone were produced with attachment at the 4-position of the aromatic A-ring using aromatic substitution of the corresponding bromoestrogens. These thioether derivatives were then modified further to attach oligoethylene glycol or polyethylene / polypropylene glycol chains of varying length ($n = 3$ and $n = 15$-19). The estradiol-oligoethylene glycol derivative was immobilised in situ in a surface plasmon resonance (SPR) biosensor and its antibody binding compared to conjugations through the steroid 2-position by Mannich reaction and the 3-position by hemisuccinate conjugation. 2-position conjugation gave 19% more binding than 4-position and 3-position hemisuccinate gave negligible binding to the antibody raised to a 6-position conjugate. The chip surfaces were then used to construct SPR assays of estradiol with and without secondary antibody signal enhancement and gave limit of detection (LOD) as low as 25 pg/mL.

Thioether-bridged derivatives of the catecholamines dopamine, nor-epinephrine and epinephrine were synthesised by electrolysis of the parent catecholamine to produce the corresponding *o*-quinone and then simply adding a thiol of three or 11-carbons in length with a terminal carboxylic acid function. A convenient cationic exchange method was developed for purification of the dopamine and nor-epinephrine products, whilst the epinephrine derivatives could

be purified on normal-phase silica. These reactions and separations were followed by reversed-phase HPLC. The dopamine propionate derivative was applied as coating antigen by in situ surface assembly with two different linkers and compared to conjugation through the amine. The antibody raised to a glutaraldehyde-linked conjugate showed highest binding to the amine-conjugated surface.

New surface plasmon resonance biosensor formats were developed using gold nanoparticles to amplify the binding signal of progesterone / antibody binding interactions. A very stable sensor surface with progesterone immobilised via an oligoethylene glycol chain was produced capable of withstanding more than 1100 binding and regeneration cycles without appreciable loss of binding capacity. Gold labelling of the monoclonal antibody was achieved via a biotin/streptavidin couple in both a preincubation of biotinylated antibody with streptavidin gold and a sequential addition of antibody and then gold label. Preincubation gave no signal enhancement but lowered the detection limit of the assay to 143 pg/mL compared with previous reports which had detection limited to 1 ng/mL. Sequential labelling resulted in a two-fold enhancement of signal and the detection limit was reduced to 23.1 pg/mL. Labelling with a secondary antibody alone produced signal enhancements of eight-fold and when secondary antibody was conjugated to colloidal gold it produced enhancements of 13-fold. The secondary antibody-gold labelling gave LOD of 8.6 pg/mL. There was no difference in enhancement between 10 and 20 nm colloid for the biotin/ streptavidin couple and colloid size did not affect enhancement for the secondary antibody-mediated format. This study is the first successful development of nanoparticle signal-enhanced immunoassay for small molecules using SPR and demonstrates how assay performance may be improved to levels comparable to or better than existing ELISA.

Acknowledgements

I would like to acknowledge the great mentoring that all my supervisors have given me. I would like to thank Yinqiu Wu of HortResearch for his boundless enthusiasm and helpful suggestions and whose insights have enriched this project. I wish to thank Lyndsay Main of the Chemistry Department at the University of Waikato for his patience in answering all my queries and for providing firm support for this project. I thank Christian Cook of HortResearch for being a great friend and advisor. I would also like to thank David Musgrave for giving a valuable biochemist's perspective into this work.

Many thanks must go to the Foundation for Research Science and Technology and later the Tertiary Education Commission for their generous provision of a Bright Future Top Achiever Doctoral Scholarship for this project. Your investment has been integral in the success of this work.

Thanks also to the people of the Bioengineering Sector of HortResearch who have been such a good group to work with; especial thanks to Mira Petcu and Richard Oliver for their input. Thanks to the Department of Chemistry of the University of Waikato for their support.

Finally, I would like to thank all my family for their constant love and encouragement. I am very lucky.

This thesis is dedicated to my parents Paul and Carol Mitchell

Whose love has no bounds

Contents

List of Figures

Appendix 3

Appendix 4

Note: Superscript numbers on captions for figures in Chapter 1 refer to the references from which the figure was reproduced in full or in part or was adapted.

List of Tables

Publications

This work has been published in the following forms as of 12/08/05:
Milk Progesterone Immunoassay Studies as:

Mitchell, J. S.; Wu, Yinqiu; Cook, C. J.; Main, L. Protein Conjugate-Based Immunoassay of Whole Milk Progesterone. J. Dairy Sci., **2004**, *87*, 2864-2867.

Estrogen conjugate synthesis and binding studies:
Submitted to Bioconjugate Chemistry

Catecholamine derivative synthesis:
To be submitted to Tetrahedron

Gold-enhanced surface plasmon resonance of small molecules as:

Mitchell, J. S.; Wu, Yinqiu; Cook, C. J.; Main, L. Sensitivity Enhancement of Surface Plasmon Resonance Biosensing of Small Molecules Anal. Biochem. **2005**, *343*, 125-135.

Provisional Patent in New Zealand
New Zealand Patent Application No. NZ 528323

PCT Patent Immunoassay. Patent No. PCT/NZ2004/000222

Conferences

Attended "The Eighth World Congress on Biosensors" in Granada, Spain 21 May 2004 – 23 May 2004

Attended "229th ACS National Meeting" in San Diego, USA 13 March 2005 -17 March 2005

Abbreviations

α: Significance level

AO: Acridinium oxime

BCA: 2-Bincinchonic acid

Boc: *Tert*-butoxy-carbonyl

Bp: Boiling point

CL: Corpus Luteum

CM5: Carboxymethyl 5

CMO: Carboxymethyloxime

COSY: Homonuclear Correlated Spectroscopy

CV: Coefficient of Variation

DA: Diazo

DBDC: Di-*tert*-butyl-dicarbonate

Dβ-H: Dopamine β-hydroxylase

DCC: 1,3-Dicyclohexylcarbodiimide

DCU: 1,3-Dicyclohexylurea

dH_2O: Deionised water

DMF: *N*, *N*-Dimethylformamide

D-MHPG: 3-Methoxy-4-hydroxyphenylglycol

DMAP: 4-(Dimethylamino)pyridine

DMSO: Dimethylsulfoxide

DNA: Deoxyribonucleic Acid

EDC: *N*-Ethyl-*N*-(3-dimethylaminopropyl)carbodiimide

EDTA: Ethylenediaminetetra-acetic acid tetrasodium salt

EIA: Enzyme Immunoassay

EI-MS: Electron Impact Mass Spectrometry

ELISA: Enzyme-Linked Immunosorbent Assay

EMIT: Enzyme Multiplied Immunoassay Technology

ES-MS: Electrospray mass spectrometry

Fab': A type of Fragment antibody

FAB-MS: Fast Atom Bombardment Mass Spectrometry

Fc: Flow cell

GA: Glutaraldehyde

HBS-EP: HEPES buffered saline with EDTA and P-20 surfactant

HEPES: *N*-[2-Hydroxyethyl]piperazine-*N*'-[2-ethanesulfonic acid]

hCG: Human chorionic gonadotrophin

HCV: Hepatitis C virus

Hinf: Restriction enzyme from *Haemophilis influenzae*

H_0: Null hypothesis

HPLC: High-performance liquid chromatography

HRP: Horseradish peroxidase

HS: Hemisuccinate

IC_{50}: Inhibitory Concentration at 50% Bound

Ig: Immunoglobulins

IgG: Immunoglobulin G (an antibody class)

IFC: Integrated Microfluidics Cartridge

K_d: Dissociation constant

K_m: Concentration of substrate that gives half maximum enzyme activity

LH: Luteinising Hormone

LOD: Limit of detection

mAb: Monoclonal antibody

MALDI-TOF: Matrix-Assisted Laser Desorption Ionisation Mass Spectrometry with Time-of-Flight Detection

Mp: Melting point

MIP: Molecularly imprinted polymer

MFP: Mean Free-Path

MPA: 3-Mercaptopropionic acid

MR: Mannich Reaction

μ: Mean of a data set

MUA: 11-Mercaptoundecanoic acid

NAD: Nicotinimide Adenine Dinucleotide

NBS: *N*-Bromosuccinimide

NHS: *N*-Hydroxysuccinimide

NMR: Nuclear Magnetic Resonance

NOESY: Nuclear Overhauser Enhancement Spectroscopy

NTA: *N*-(5-Amino-1-carboxypentyl)iminodiacetic acid

OEG: Oligoethylene glycol (sometimes called oligoethylene oxide)

OVA: Ovalbumin (eggshell albumin)

PBS: Phosphate buffered saline

PBS/T: 10 mM Phosphate buffered saline with 0.05% Tween 20, pH = 7.4

PCS: Photon Correlation Spectroscopy

PEG: Polyethylene glycol (sometimes called polyethylene oxide)

PNMT: Phenylethanolamine-*N*-methyltransferase

PVP: Polyvinylpyrrolidone

RBA: Relative Binding Affinity

R_f: Retention index – TLC

RIA: Radioimmunoassay

RP-HPLC: Reversed Phase High Performance Liquid Chromatography

R_t: Retention time (HPLC)

RU: Resonance Units

SD: Standard Deviation

SERS: Surface-Enhanced Ramen Spectroscopy

SPIA: Sol-particle Immunoassay

SPR: Surface Plasmon Resonance

TE: Thioether

TEM: Transmission Electron Microscopy

TFA: Trifluoroacetic acid

TMB: 3, 3', 5, 5'-Tetramethylbenzidine

θ_r: Resonance angle

THF: Tetrahydrofuran

TLC: Thin layer chromatography

UHQ: Ultra high quality

UV: Ultraviolet

V_H: Variable heavy chain

V_L: Variable light chain

Z_{avg}: Cumulant mean size representing the hydrodynamic diameter

Chapter 1 – Introduction

This chapter will cover firstly the basic theory and technology behind modern biosensors before moving on to showing how these technologies have been applied to the target molecules of relevance to this thesis, *i.e.* the steroid hormones and catecholamines. This is followed by a more detailed analysis of the chemistry of steroid hormone and catecholamine conjugation as applicable to biosensors and the chapter finishes by examining how this thesis covers several opportunities in optical biosensor research for small molecule analytes.

1.1 Biosensor Technology

1.1.1 Biosensing and Biomimetic Sensing

A biosensor may be defined as a system that converts biochemical states and changes in these states into an electrical response[1] with the purpose of gathering information concerning parameters in a sample. Biosensors should consist of a site (usually a modified surface) in which a biochemical interaction takes place, a system for delivering components to this site, *e.g.* a microfluidics system, a signal transduction device to convert the biochemical changes into an electrical signal, a data display and / or storage system and usually a system for regenerating the sensor ready for the next cycle. Biosensors may be represented schematically by the box diagram in Figure 1.1. The normal parameter being measured is the concentration of a particular analyte or analytes in a given sample. Biosensors may be classified according to the type of biochemical interaction employed, the type of signal transduction system used and according to the sensor target or analyte.

The most common biochemical interaction employed in diagnostics is the binding of an antibody to its target in the sample being analysed. This interaction is mostly used in immunoassays such as enzyme-linked immunosorbent assay (ELISA) but is also widely used in biosensors called immunosensors. Other

biosensor interactions can include enzyme catalysis and receptor / target interactions as well as microbe-mediated and deoxyribonucleic acid (DNA)-mediated interactions.[2] Transduction systems for immunoassays and biosensors include a wide range of technologies such as colorimetric changes catalysed by enzymes conjugated to antibodies as in ELISA, changes in electrical properties of the detection surface as in printed electrode systems, or changes in optical properties of the surface as in surface plasmon resonance (SPR) and spectroscopic properties as in surface-enhanced raman spectroscopy (SERS).

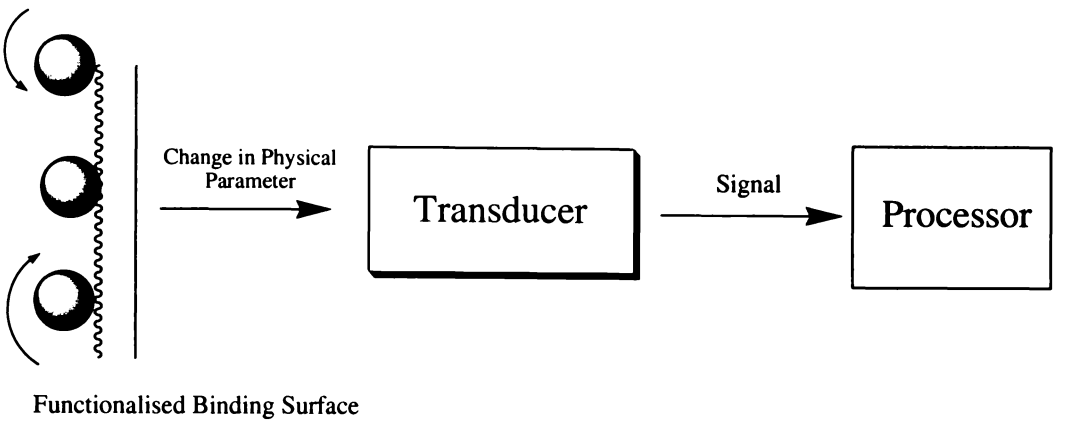

Figure 1.1 Biosensor Box Diagram

Immunosensors and immunoassays will form the main discussion in this thesis but it is worthwhile to consider the other biological interactions possible. Enzyme-based sensors were the first biosensors and are highly favoured due to their high specificity and the possibility to quite simply follow the throughput of chemicals in the active site. The usual methods of transduction are via amperometric or potentiometric determinations. Such systems have found wide application in detection of neurotransmitters and most famously in glucose sensors. It is also possible to use these systems to determine quantities of enzyme-inhibiting compounds. Microbe-based biosensors utilise the physiological changes in specific microorganisms to determine the quantities of the substances inducing these changes.

DNA biosensors utilise the specific binding interaction between complementary strands of DNA to detect the target. This technique is very useful for specifically identifying DNA strands that may be specific to a particular

organism[3] or even to bind to intercalating targets such as certain aromatic compounds.[4] Variations in just one base pair can greatly compromise binding giving rise to excellent specificity. This field is presently underdeveloped and is emerging as an important new biosensing platform. Nanotechnology is further boosting the options for biosensors with the unique electrical properties of carbon nanotubes being utilised to produce highly specific biosensors.[5]

As well as a vast number of proper biosensing systems there is also growing interest in biomimetic sensors, which employ chemical systems designed to mimic a biological recognition system. Perhaps the most well known of these systems are the molecularly imprinted polymer (MIP) sensors. These sensors employ a specially constructed polymer, which contains binding sites specific to a particular chemical compound.[6]

Immunosensors are a large and growing field and incorporate the advantages of high specificity, high binding affinity, broad applicability to any compound of sufficient size and functional characteristics and a wide range of applicable transduction technologies. Allied to the field of biosensors is that of immunoassays, techniques for the detection of concentrations of a target analyte by utilising the binding interaction between antibody and target. Biosensors are normally applied with the intention of using them in on-site or in-the-field situations whereas immunoassay includes the fields of ELISA and radioimmunoassay (RIA). In order to understand the functioning of immuno-detection systems it is necessary to have knowledge of antibody theory.

1.1.2 Antibody Theory

An antibody is a protein synthesised by the B-lymphocytes and subsequently excreted into plasma.[7] They are produced by the body of a vertebrate in response to a foreign agent and are generally referred to as immunoglobulins (Ig). In their monomeric state, Ig molecules are composed of two identical halves that are bound to each other via disulphide bridges. Each half consists of two chains, a heavy glycosylated chain (about 50 kDa) and a light non-glycosylated chain (about 25 kDa) connected by one disulfide bridge to be found close to the carboxyl end of the light chain. Altogether the molecule has a Y-shaped

configuration and is about 150 kDa. The heavy chain can also be further subdivided into the Fc and Fab regions. The Fc region is located at the carboxyl terminal and is bound to carbohydrate chains. The Fab region is located at the amino terminal. Each chain can also be divided into domains of ~110 amino acid residues. For immunoglobulin G (IgG) antibodies there are four in the long chain and two in the short. Basic IgG structure is shown in Figure 1.2

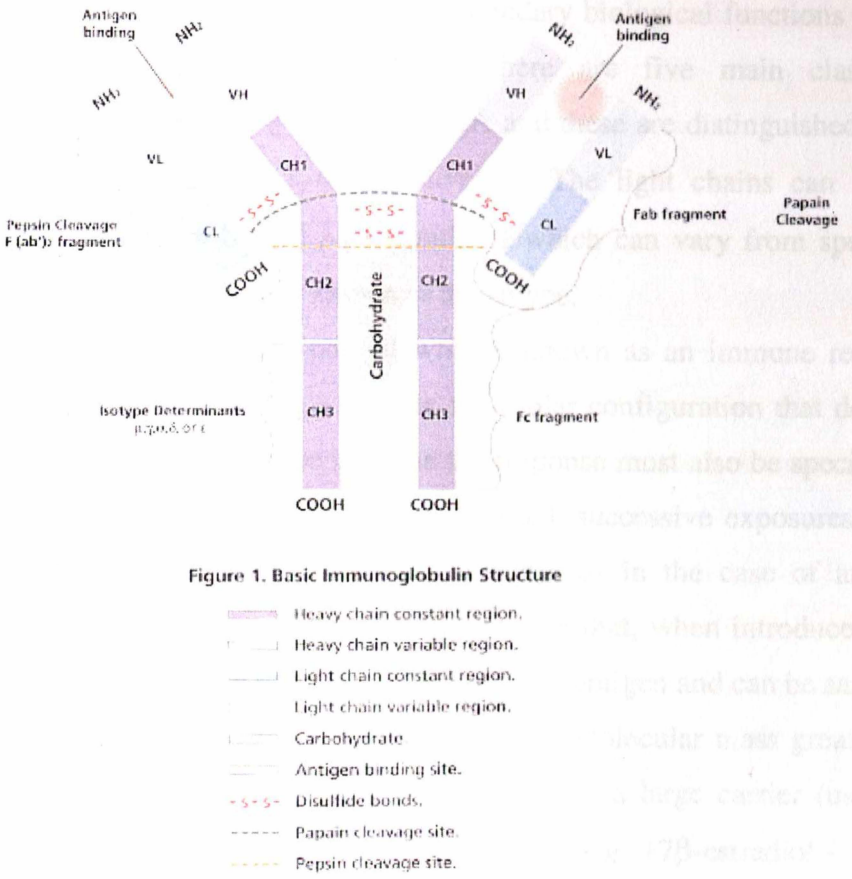

Figure 1.2 IgG structure[7]

There are also constant regions of low amino acid variability (constant or C region) and of high amino acid variability (variable or V region) from molecule to molecule. Protein folding of the variable regions of one light (V_L) and one heavy (V_H) chain forms a groove that can accommodate the antigen. In an IgG molecule, two antigen molecules can be bound. The antigen is held into place by the antibody through several interactions:

1. Hydrogen bonding: between carboxyl oxygens and amino groups

2. Ionic interactions: these include electrostatic interactions between protein antigens and antibody amino acid residues
3. Hydrophobic interactions: if an antigen orients its non-polar groups inwards and its polar functionalities outwards into the polar aqueous solvent then a hydrophobic pocket would be established enabling thermodynamically favourable binding to the hydrophobic antibody binding site.[8]

The constant region is used for certain secondary biological functions such as complement and macrophage binding. There are five main classes of immunoglobulin: IgG, IgD, IgM, IgE and IgA and these are distinguished by the type of heavy chain (γ, δ, μ, ε, α respectively). The light chains can also be divided into two classes (κ and λ) the ratio of which can vary from species to species. Each of these classes is known as an isotype.

Antibodies are employed as part of what is known as an immune response, defined as "altered reactivity to a specific molecular configuration that develops following contact with it".[8] To be immune the response must also be specific to a certain molecular structure and be repeated through successive exposures to this structure. An immune response can be humoral, as in the case of antibody immune responses, or cell-mediated. The substance that, when introduced to an organism, elicits an immune response is known as an antigen and can be said to be immunogenic. Immunogenic antigens must be of a molecular mass greater than about 2 kDa; smaller compounds must be coupled to a large carrier (usually a protein) in which case they are known as haptens, *e.g.* 17β-estradiol – bovine serum albumin (BSA) conjugates. Smaller molecules are not immunogenic, usually because they do not have suitable sites for simultaneous binding of a class II protein and a T-cell receptor, a vital part of antibody production.

1.1.3 Monoclonal Antibodies

Antibodies produced by simple immunisation of vertebrates will lead to production of polyclonal antibodies, that is a mixture of different antibody types directed to different parts of the antigen (antigenic determinants). Each antibody has somewhat different specificities and affinities and so this may cause problems

in certain assay formats where discrete specificities and affinities are required. Monoclonal antibodies, immunoglobulins with a discrete affinity and specificity directed to one epitope of the antigen, are produced by fusing B lymphocyte cells from the spleen with myeloma cells (cancerous immune system cells) after immunisation. The fused cells are then screened for correct antibody production, isolated and cloned and re-tested before culture as required, thus allowing large-scale production of the desired monoclonal antibody. Monoclonal antibodies are the preferred choice for immunoassay and are used for immunoassays described throughout this thesis.

1.1.4 Radioimmunoassay

Having discussed the basic theory of antibodies it is now best to consider the ways in which antibodies may be employed in immunoassay formats. Immunoassay relies upon a means of transduction and it is this that generally defines the types of immunoassay. The earliest form of immunoassay is radioimmunoassay, which detects binding between antibody and antigen by means of labelling either the antibody or the antigen with a radiochemical label, the radiation of which can be easily detected.

The first radioimmunoassay was developed for insulin in plasma by Berson and Yallow in 1960[9] and the technique has since then expanded greatly into a range of target antigens and radiolabels. The basic principle is to attach a label containing a radioactive isotope (commonly ^{3}H or ^{125}I) to the target analyte with some kind of molecular spacer in between to ensure antibody binding is not inhibited. Bound labelled antigen can then be determined by scintillation counting where counts will be inversely proportional to the amount of antigen present in the sample.

The usual format for such assays has the antibody bound to a solid surface, usually a customised micro-well plate and the labelled antigen passed over the surface either at the same time as the sample (competitive format) or after the antigen present in the sample has had time to bind (sequential non-competitive format). The antigen is incubated to allow time to bind and then un-bound

material is washed off the plate and the counts determined. These formats are illustrated in Figure 1.3.

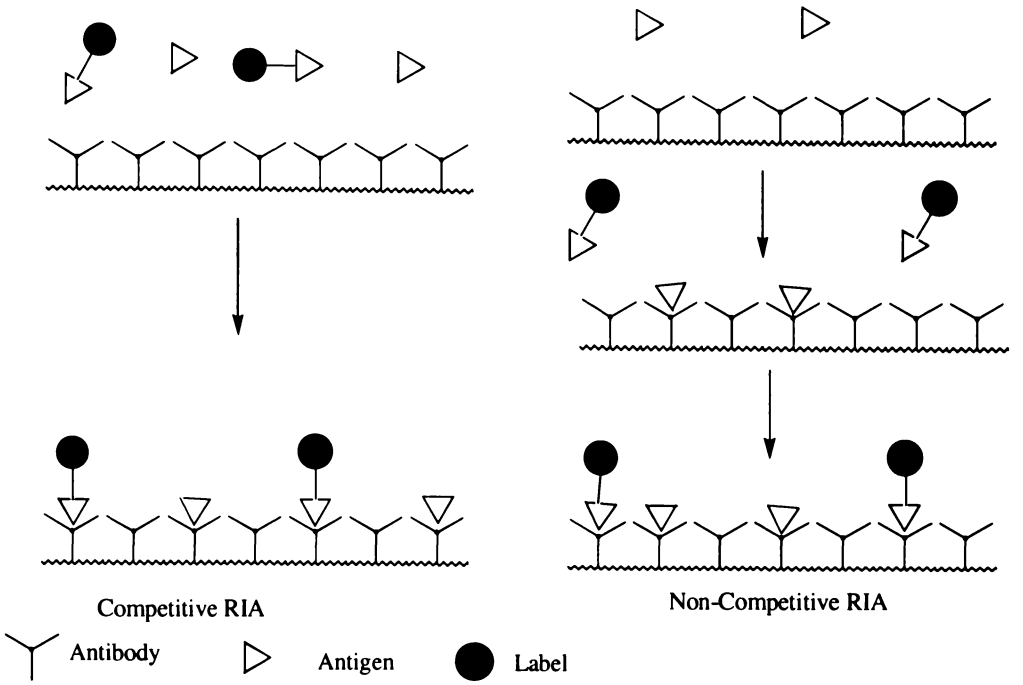

Figure 1.3 Competitive and Non-Competitive RIA[10]

RIA has several advantages, mainly very good sensitivity (down to a few picograms of analyte per well with high affinity antibodies) and with detection limits of the order of 10-100 pg/mL in the case of certain steroidal sex hormones.[11] RIA is now well established and has been successfully applied in a range of media including blood and milk. There are however several major disadvantages including the need to use and dispose of hazardous radioisotopes, their relatively high cost ($15-20 per sample) due to the radiolabels, and their limited shelf life. The radiolabelled compounds are often hard to completely purify and radiolabels can have a significant effect on antigen binding to antibodies. These restrictions have prevented radioimmunoassays being adapted successfully as biosensors for on-site use and has restricted them to laboratory-based assays only.

1.1.5 Enzyme Immunoassay

The breakthrough that helped enable future practical immunobiosensor technology was the development of the enzyme immunoassay (EIA) which was first produced for progesterone in 1975 by Dray et al.[12] The principle is much the same as that for radioimmunoassay except that the radiolabel is replaced by an enzyme label (commonly horseradish peroxidase (HRP)). The enzyme serves to catalyse signal generation in three main types of signal agent – colorimetric, fluorometric and chemiluminescent agents. By so doing, the enzyme produces a signal far larger than that of the background and enables detection whereby the response is inversely proportional to the concentration of target analyte in the sample. There has been a great deal of study in the area of enzyme immunoassay and these systems may be categorised according to their analyte (antigen or antibody), the labelled reactant (antigen or antibody), the method of incubation (competitive or non-competitive) and the way in which the bound and free label are separated from each other.[13]

Enzyme labelling can be of the antigen or of the antibody and usually, especially in the case of the antigen, a spacer is inserted between the two to prevent the label from sterically inhibiting the binding interaction. The most common method employed is to immobilise the antibody on the surface of a special microwell plate at appropriate pH by electrostatic interactions and incubate the sample over the surface either in the presence of the enzyme labelled antigen or separately (competitive and non-competitive respectively). In this case the response will be inversely proportional to the concentration of analyte. Competitive formats are usually used for small molecule antigens, as it is usually difficult to separate out the antibody/antigen conjugate.[14]

An alternative, lesser-used format is to immobilise the antigen on the surface and then expose the enzyme-labelled antibody simultaneously with the sample to the surface either after or during a period of incubation between antibody and sample. This method has been previously employed by the author in assay formats for progesterone.[10, 15, 16] This format requires that for small-sized antigens they be attached to the surface via a protein that has the required large number of ionic functionalities for surface attachment. This is done in the form of a protein

conjugate where the attached analyte is referred to as a hapten. These different formats can be seen in Figure 1.4. In all plate EIA the un-bound portions of the plastic wells must be blocked with protein (usually BSA, ovalbumin (OVA) or milk protein) to prevent non-specific binding that would compromise signal distinction. Between each stage of the assay the plate is washed thoroughly to remove un-bound material.

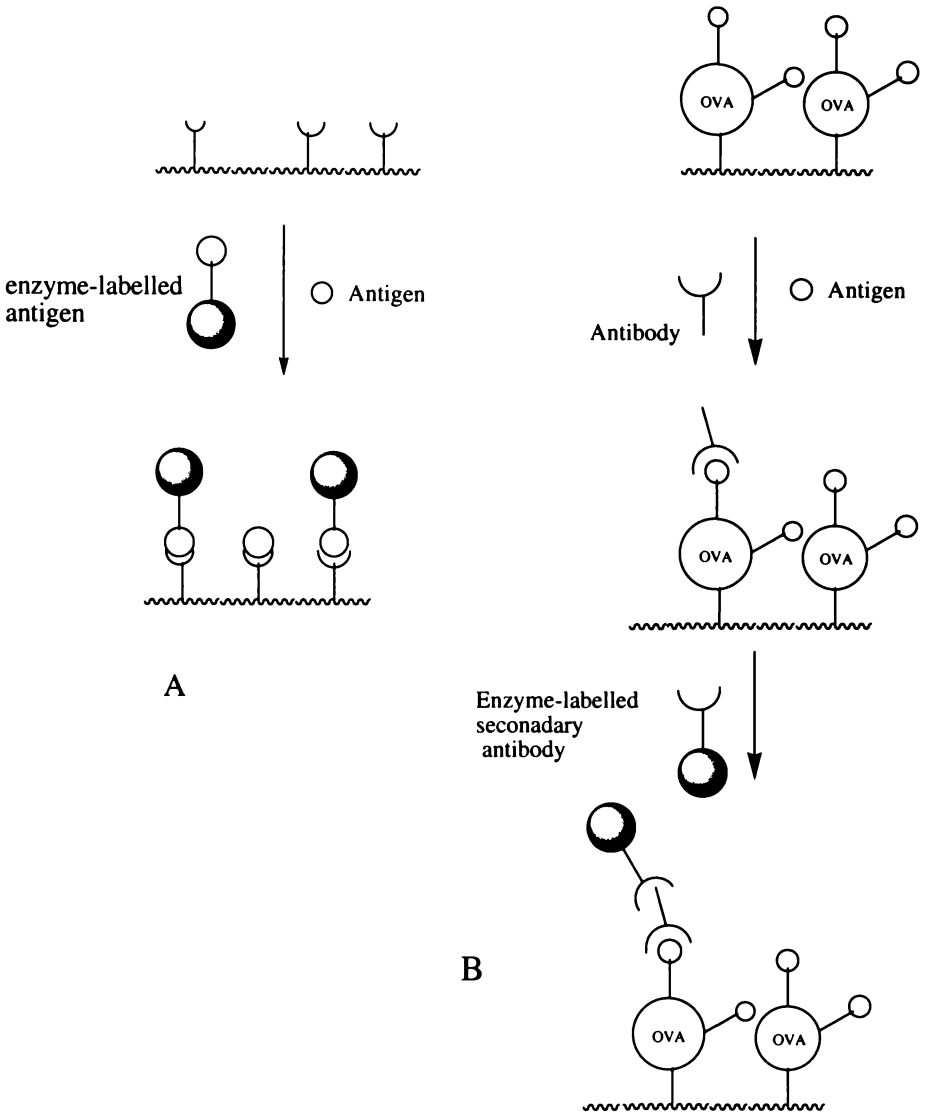

Figure 1.4 Antibody Bound (A) and Antigen Bound (B) EIA

To improve signal to noise ratios it is wise to carefully choose the enzyme label to ensure that it has a high turnover number, a low K_m for the substrate and a high K_m for the product and that it is highly stable under the conditions of the assay.[17]

Enzyme labelling of the antibody may be effected either directly through chemical modification of the antibody (usually also with an intermediate linker) or through use of a secondary antibody, *i.e.* an anti-immunoglobulin antibody conjugated to the enzyme. The latter method of enzyme labelling enables greater specificity as it improves the antibody binding cross-section, as there are two specific antibody binding steps[18] and so overall binding specificity is greatly improved. The secondary antibody-enzyme conjugate does not compromise the ability of the primary monoclonal antibody to bind either by chemically denaturing the antibody, blocking the binding site of the antibody by being attached over it or sterically disfavouring approach of the antigen. Enhancements in specificity are particularly important when considering complex biological media. The secondary antibody is always used somewhat in excess so its immunoreactivity can be slightly reduced.

In the case of larger molecules (> 2 kDa) it is possible to perform a different assay format known as a sandwich EIA (Figure 1.5). In this case the antibody is immobilised to the surface and the sample alone incubated with the antibody. The surface is then exposed to enzyme-labelled antibody that binds the already bound antigen, which is of sufficient size to bind to two antibody units at different non-overlapping epitopes simultaneously. In this format one has the advantage that the enzyme signal is directly proportional to the amount of analyte, hence one is directly measuring the analyte concentration rather than doing so indirectly through measuring the vacant antibody binding sites. A recent example of this format is the sandwich assay for hepatitis C virus (HCV) core protein from single hepatocytes.[19] One can also use antibodies that recognise primary antibody / antigen complexes such as for digoxin measured clinically.[20]

One can classify EIA also according to the separation steps employed. Heterogeneous EIA has the enzyme label retaining activity after binding to the antibody/antigen system. This is the more common variety and includes the much-used ELISA, a schematic example of which is found in Figure 1.6. ELISAs rely upon the enzyme catalysing the conversion of a substrate that has little or no colorimetric or fluorescent signal to one that has intense signal. Such substrates include the common 3, 3', 5, 5'-tetramethylbenzidine (TMB) using a peroxide initiator along with HRP to turn from colourless to intense blue, and then to yellow upon stopping with acid. Other substrates can produce fluorescent or

chemiluminescent responses and include aequorin, a calcium-activated photoprotein. The move from colorimetric to fluorescent to chemiluminescent systems can greatly increase assay sensitivities to the extent that chemiluminescent detection can give detection limits better than RIA.

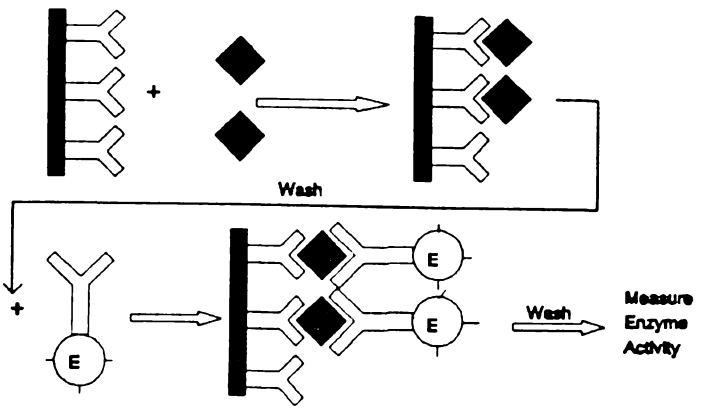

Figure 1.5 Sandwich EIA[13]

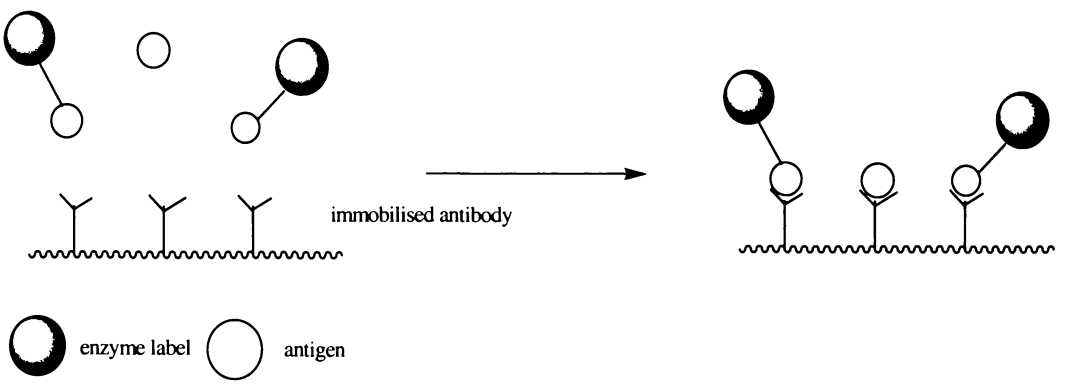

Figure 1.6 Heterogeneous EIA

Homogeneous EIA exposes the sample to an enzyme or modulator-labelled analyte or antibody that is activated in one solution including the reagent for signal development of the enzyme. This is known as direct signal modulation. This obviates the need for washing labelled analyte or antigen away making the assay much simpler. Modulation of the enzyme may occur by use of steric, allosteric or ionic effects, enzyme inhibitors, activation of apoenzymes or cofactors, use of enzyme antibodies and complexing of multiple enzyme systems by use of a channelling technique. An example is sol particle immunoassay

(SPIA) for measuring serum cystatin C, whereby the anti-cystatin C antibodies are coated on colloidal gold particles and the binding to the protein in the sandwich format is observed directly.[21] Figure 1.7 shows another example, enzyme multiplied immunoassay technology (EMIT), which functions by an enzyme label being inhibited by binding of antibody to antigen.

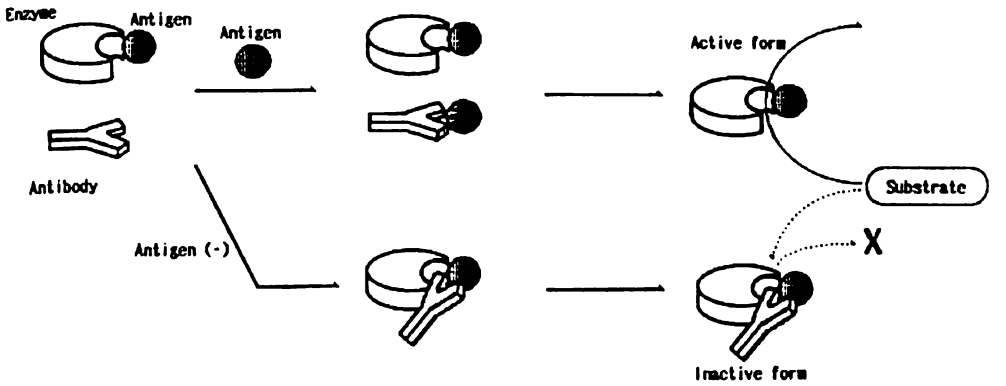

Figure 1.7 EMIT Homogeneous EIA[13]

There are many advantages in the use of EIA, principally, the sensitivity is high (in the case of chemiluminescent assays now generally better than RIA), reagents are less expensive and last longer, many simultaneous assays can be done, there is no radioactive hazard, many different formats are available and they are rapid and simple. Thus far we have considered the range of immunoassays available as RIA and EIA. However, these assays cannot be practically converted to use in on-site applications, they are restricted to laboratory use only. They are often labour intensive, usually take from several hours to two days making them unsuitable for applications that require timely results, and require a trained operator. Also, transport to a central laboratory can compromise samples. ELISA kits have been commercialised for use in certain applications on-site, *e.g.* milk progesterone determination for farmers, but have not seen widespread commercial success due mainly to their high labour requirements and lack of precision. Another factor to consider is the matrix effect whereby substances present in the background matrix of the sample can interfere with signal intensity. This can be minimised to a certain extent by increasing the sensitivity and thus reducing the volume of matrix per well.[22]

A further method for improving sensitivity is to use direct labelling of antigen or antibody with chemiluminescent or fluorescent labels such as the fluorescent *O*-(fluoresceinylmethyl)oxime-progesterone steroid conjugate[23] or chemiluminescent acridinium oxime-steroid conjugates[24] that can be applied in immunoassay like a radiolabel. EIA can also be adapted to amperometric assays as has been done for human chorionic gonadotrophin (hCG) on the Clarke oxygen electrode.[25]

Immunoassay is of vital importance to the diagnostic market and dominates such areas as biomedical laboratory testing. Immunoassays, principally through sandwich ELISA and new signal enhancement labels, are constantly being developed. Whilst they are not practical for on-site use their principles of operation are directly applicable to the design and science of biosensors and they provide an invaluable means of conducting fundamental studies into antibody / antigen binding interactions. Plate-based immunoassays are static immunosensing platforms in that the fluid-containing sample and labelled antigen or antibody does not flow over the immobilised surface in a concerted way. In most biosensor formats however, the sample and other components do flow over the immobilised surface as part of an in-line or on-line sensing system and as such ELISA models do not always match flow biosensor models. Surface plasmon resonance (SPR) biosensors are one such type of flow-biosensors with many advantages over ELISA.

1.1.6 Surface Plasmon Resonance

1.1.6.1 The Fundamental Principles

Surface Plasmon Resonance (SPR) is a quantum optical-electrical phenomenon that occurs at the surface of a SPR active substance when photons of light are incident upon its surface.[26] When a photon of light is incident upon a noble metal surface it can couple with the electrons in that metal and transfer its energy to them. This coupling occurs at a specific wavelength that is known as the resonance wavelength. The electrons then become excited and move as a single electrical entity known as a plasmon. Coupling will occur when the momentum

of the incoming photon equals that of the plasmon. The plasmons will move along the metal setting up an electrical field that extends for about 300 nm from the surface. If the surface features within 300 nm change, such as in the binding of proteins, then the plasmon will be perturbed and the wavelength needed for resonance will shift. Surface plasmon resonance is essentially a charge-density oscillation existing at the interface of media with dielectric constants of opposite sign. This charge density wave is associated with an electromagnetic wave and collectively can be termed a surface plasma wave.[27] It is possible to determine the resonance wavelength optically as other wavelengths will be simply reflected; hence a plot of reflected light intensity *vs* wavelength will show a distinct dip at the point of resonance. The surface is held in a fixed position and the plasmons are confined to the plane of the surface, so the resonance wavelength can be determined by scanning through angles of the incident photon beam to the surface until the resonance angle (θ_r) is found.[28] The resonance angle will then correspond to the angle at which the plane parallel component of the photon momentum equals the momentum of the plasmon. The angle must be greater than that required for total internal reflection and the illumination is from the back-side and is *p*-polarized onto the prism-coupled gold film.[29] Changes in resonance angle with changing surface coating can be expressed in terms of resonance units (RU) whereby 1 RU is said[30] to be roughly equivalent to a mass change on the surface of 1 pg/mm^2. SPR measurements are effectively measurements of changes in the refractive index of the surface with 1 RU unit being 1 x 10^{-6} of a refractive index unit allowing much finer measurement than would ever be possible with a refractomer. A computer plot can then be made of SPR response (RU) *vs* time and is known as a sensorgram. A schematic of the SPR system is given in Figure 1.8.

The most commonly used metal that exhibits SPR is gold. In most SPR set-ups a chip or plate is constructed with a thin layer of gold supporting a polymeric matrix that has functional groups needed to immobilise coating antigens or antibodies. A number of "home-made" SPR apparatus have been constructed due to their comparative simplicity[31, 32] but perhaps the dominant use of SPR is in biomolecular interaction analysis using the commercial BIAcore™ format. BIAcore is extensively used as a research tool for examining antibody / antigen[33],

receptor / target[34], oligonucleotide / complementary oligonucleotide[35] interactions. Host / guest binding interactions have also been examined by SPR.[36]

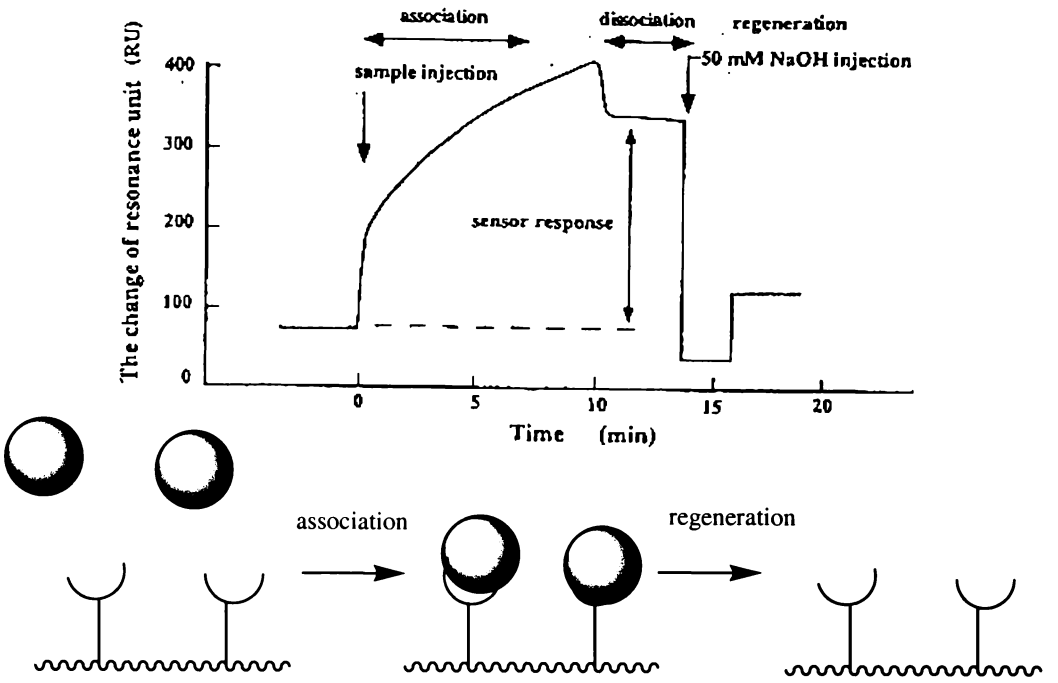

Figure 1.8 SPR Schematic Showing Binding Surface and Sensorgram[37]

Other companies have developed SPR systems of lower cost than the BIAcore system, such as Texas Instruments and their Spreeta™ Cell[38, 39] and Windsor Scientific's IBIS system.[38] BIAcore continues to dominate the research publications however due to its patented carboxy-methylated dextran coated chips and fluidic control systems.

1.1.6.2 BIAcore

The BIAcore system works on the basis of a removable self-contained sensor chip. These chips consist of a glass plate coated with a 50 nm thick gold film and encased in a plastic covering that can be slotted into the machine. On the gold surface is a layer of carboxy-methylated dextran with exposed carboxylic acid groups. The chip when inserted is in intimate contact with a milli-fluidics system,

UNIVERSITY OF WAIKATO
LIBRARY

which has four interconnected channels through which solutions may be passed. The chip is incubated at a set temperature (usually 25 °C) and is fed by an injection system, which can take fluids from racks of vials or from a 96-well microtitre plate. The systems available range from BIAcore X, which is manually fed, to BIAcore 3000, which is highly automated and can be used for screening of drug candidates. The binding is observed in real-time by a sensorgram, which is a plot of the response units *vs* time.

Either target or recognition compound may be immobilised on the sensor surface by first activating the carboxylic acid functions by applying *N*-ethyl-*N*-(3-dimethylaminopropyl)-carbodiimide (EDC) with *N*-hydroxysuccinimide (NHS) to produce the active ester. The compound to be immobilised is then passed over the surface at the pH that will produce maximum binding and amide linkages can be formed with the amino groups of the compound. The optimum pH for immobilisation can be determined by "pH scouting", that is passing solutions of the compound at various pHs over the non-activated surface and assessing the pre-concentration sensorgrams observed. The compound is concentrated by ionic interactions with the surface. Optimum pH should give a high sensorgram with an approximately 45° angle in the binding response. Once the compound has been immobilised then the remaining un-reacted carboxylic acid functions are deactivated by reaction with ethanolamine to ensure minimal non-specific binding and no further immobilisation. Immobilisation can be done automatically to a set response target or simply through multiple injections of the compound. Upon de-activation with ethanolamine, normally about 25% of the initial binding response is lost. Macromolecules are normally immobilised at low concentrations (20-100 μg/mL).[40] Immobilisation of macromolecules should be done at a pH below the pI of the protein in question to ensure adequate concentration of the protein in the dextran layer.[41] Immobilisation can also be done through disulphide bridges formed between thiolated ligand and disulphide modified binding compound or vice versa.[42] Some immobilisation techniques are shown in Figure 1.9.

A newly immobilised sensor surface may require a period of washing to remove unbound material and several binding cycles may need to be done to ensure repeatable response. The binding cycle consists of first setting the flow

rate over the surface; slower flow rates will enable higher binding but naturally take longer. The normal running buffer is a *N*-[2-hydroxyethyl]piperazine-*N*'-[2-ethanesulfonic acid] (HEPES)-buffered saline with ethylenediaminetetra-acetic acid (EDTA) and P-20 surfactant (pH 7.4) (HBS-EP). The sample to bind is then injected and the binding response followed by the rising sensorgram. Once the binding is finished one will normally observe dissociation of the bound material from the surface, the rate of which can also be instructive as to the binding kinetics.

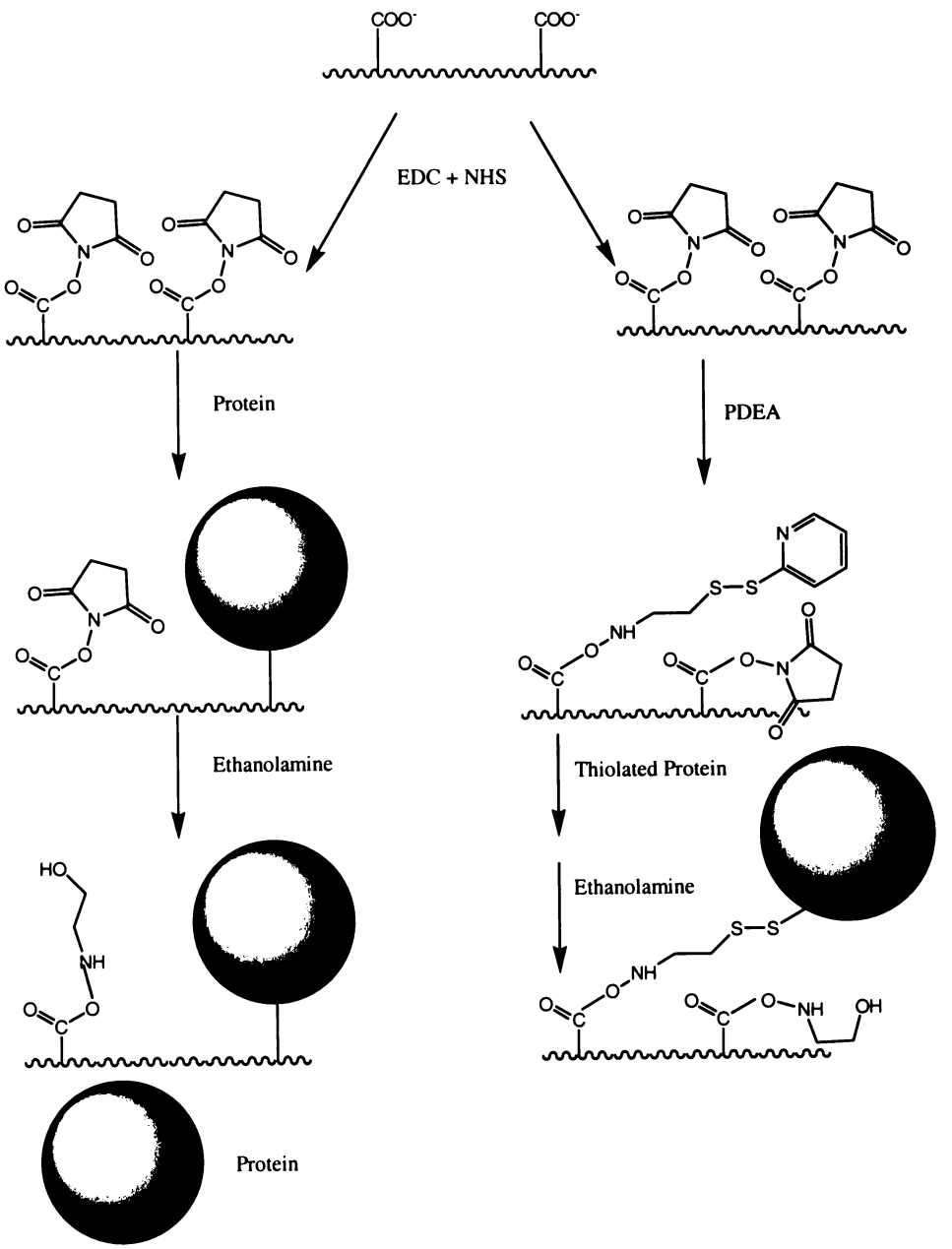

Figure 1.9 Immobilisation by Active Ester (Left) or Ligand Thiol Coupling (Right)

Once binding is over then the surface must be regenerated. This is done using a regeneration cocktail and there is an extensive range of these used.[43] Common cocktails include glycine, NaOH, HCl, sodium acetate and chaotrophic reagents[43] such as acetonitrile. Choice of regeneration cocktail is very important as it must properly regenerate the surface every time with no residual bound material but must not strip immobilised compound from the surface. Acidic pHs are favoured over basic. The regeneration process will ultimately destroy the chip with most chips only lasting for about 100 cycles. Binding responses are naturally highly dependent upon pH, temperature, and concentration of both immobilised compound and binding compound and flow rate. The total binding cycle is represented in Figure 1.10.

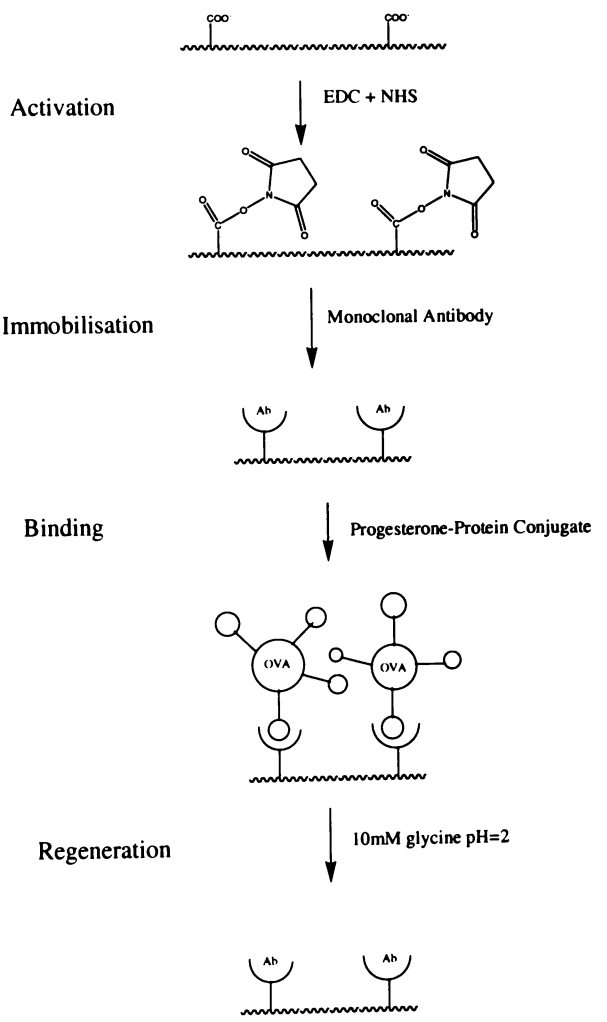

Figure 1.10 Activation, Immobilisation, and a Complete Binding and Regeneration Cycle Using BIAcore[10]

As mentioned above, the chips have four flow cells that can be monitored simultaneously. One flow cell is kept as a blank reference cell by activating and deactivating the chip without immobilisation of antibodies or analytes, so that it can be used to reference subtract bulk effects in the refractive index changes that could otherwise swamp the binding interactions. SPR in most applications is only essentially detecting mass changes on the surface and so small molecules binding will not be visible to the instrument and cannot be seen in the sensorgrams except at high concentrations. In order to get good signal one must usually use compounds of >2 kDa. If one wants to detect small molecule binding to immobilised antibody then one would have to conjugate the molecule to an appropriate high mass label, usually a protein. Alternatively of course, one could simply immobilise the protein conjugate and detect the antibody, which is better for higher signal as the antibody is larger than BSA or OVA, which are the common conjugate proteins.

As well as the carboxylic acid functions, BIAcore has chips modified with disulphide linkages that can be used to attach compounds with thiol functionalities, such as certain proteins. Other formats used by Texas Instruments include coating the surface with avidin and then applying biotinylated proteins to the surface.

BIAcore has proven itself to be an important research tool and as a first step to designing practical on-site biosensors. It enables direct monitoring of binding events and immunoassay in real-time including the ability to process sensorgram data to obtain binding kinetics information. It can be fully automated and runs can be set up with minimal human interference compared with labour intensive ELISA. The systems can be adapted to high-volume screening applications[44] particularly with the advent of BIAcore 3000.[45] Other advantages include:

1. The ability to detect in four channels simultaneously

2. The ability to use organic solvents in the buffers

3. The low levels of proteins required for immobilisation (~1 μg of protein is typically needed to coat one surface)

4. The system can avoid the use of labels and the synthetic complications and binding interferences these can involve.

5. The amount of complex at equilibrium can be measured without disturbing the equilibrium even in the presence of unbound compound

6. The stability of the immobilised ligand can be monitored continuously by assessing baseline stability and binding capacity with time

The main disadvantage is that the instrument is very expensive to purchase and uses consumables that are also quite expensive (chips now cost NZ$200-300) and the machine clearly is completely laboratory based and so is only a model for development of on-site biosensors. Other applications of BIAcore include optimisation of fluorescent immunoassay parameters.[46]

1.1.7 Immunoprobes, Electrochemical Biosensors and Developing Technologies

Immunoprobes offer the ability to combine immunoassay detection with a small probe suitable for insertion *in-vivo* and can yield valuable quantitation of small biomolecule analytes such as hormones.[47] Such probes are often connected to electrochemical detectors and the electrochemical detectors are quite widespread and make use of recent developments in electrode signal transduction.[48]

A field of immunosensing that is emerging as critically important in the field of drug screening is the miniaturized microarray-based multianalyte assays.[49] These involve application of antibody microspot arrays for the combinatorial screening of potential antibody targets. The arrays are scanned by laser based confocal microscopes and utilise fluorescent tags. These systems have particular use in identification of viral antigens or allergens in media such as transfusion blood and require only small samples and greatly reduce laboratory labour.[50] Another greatly promising field of immunosensing is in time-resolved fluorescence detection using labels such as the lanthanide chelates and these systems lend themselves to

multianalyte detection because of the number of lanthanide ions that can be detected simultaneously.[51]

1.2 Biosensors for Steroid Hormones and Catecholamines

Having now reviewed the concepts of biosensors and biomimetic sensors and reviewed immunoassay techniques and then the SPR transduction phenomenon and its application to biosensing in the form of BIAcore, it is now important to provide background in the fields of immunosensing study that this thesis will cover. The first of these is an examination of progesterone – protein conjugates applied in ELISA of whole cow milk. It is necessary therefore to discuss the biochemical role of progesterone in the cow and to review the application of milk progesterone determinations. The second area of interest is to examine biosensing of the estrogen class of steroid hormones, and then finally sensing technologies, conjugation and physiology of the catecholamines.

1.2.1 Steroid Hormones

1.2.1.1 Steroid Hormone Chemistry and Immunosensing

1.2.1.1.1 Progesterone Chemistry

Progesterone is a non-aromatic female sex steroid hormone of the pregnane class, (Figure 1.11). It was first isolated in sow ovaries in 1934.[52, 53, 54, 55] It has a C-4 – C-5 unsaturation (Δ^4) and a C-3 carbonyl (conjugated olefinic system) which give rise to its ultraviolet (UV) absorbance at 240 nm.[56] Progesterone in mammals sustains and controls pregnancy and has a major role in estrous and menstrual cycles.

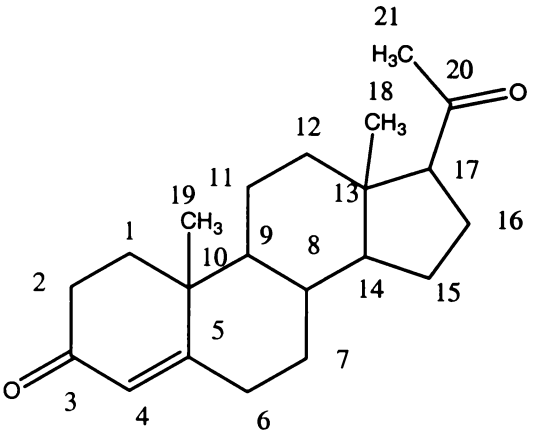

Figure 1.11 Progesterone

1.2.1.1.2 Bovine Estrous Cycle, Pregnancy and Progesterone

The bovine estrous cycle refers to cyclical changes in the reproductive system associated with the maturing and release of an oocyte from the ovaries. The bovine is polyestrus, that is it goes through several such cycles each breeding season. The cow ovary is composed of a cortex containing the oocytes and covered by epithelium tissue and a medulla that has the necessary blood vessels and connective tissue.[57] The primordial follicle (cortex and epithelium) grows and regresses during the estrous cycle. The estrous cycle is divided into estrus, luteal and pro-estrus phases with day 0 set at onset of estrus phase. Correspondingly, the follicle goes through three phases. The first is the follicular phase where the granulosa layer forms, the oocyte matures, a fluid filled cavity grows (antrum) and the follicle swells.[58] At this point the follicle either undergoes atresia (degeneration) or enters the next phase (ovulatory phase). Atresia accounts for all but ~0.1% of follicles and occurs by apoptosis[59, 60]. If the follicle survives it passes through phases of growth marked as the primordial, antral and Graafian before it is ready to ovulate. Approaching ovulation there is swelling to up to 2.5 cm and at ovulation the follicle ruptures and releases follicular fluid along with the oocyte. Ovulation occurs about 25-30 h after estrus on-set.[61] The follicle then enters the luteal phase in which the cavity left is filled with dividing cells and forms the corpus luteum (CL) or "yellow body" from which progesterone is

secreted from about day 4 to day 17 and then the CL regresses enabling the cycle to start over.

There are 2-4 growth waves of the follicle over the 7-10 days leading up to ovulation and atresia may occur at any stage and acts to reduce the number of follicles until dominant follicles are selected, only one of which will ovulate in each cycle.[62, 63] The average estrous cycle in a cow is 21 days with a range of 18-26 days.[62] Quiescent interludes are possible where the estrous cycle stops. The estrus phase lasts 12-16 h and is the period of increased sexual activity, which is the time for mating to occur. The luteal phase matches that of the follicle and is the phase of progesterone control. Pro-estrous is the phase of pre-ovulatory follicle maturity and increases in estradiol and pre-ovulatory luteinising hormone (LH).

Cyclicity in progesterone concentrations in both blood and milk reflect the stages of growth and regression in the CL, with near zero progesterone from days 0-4, rising progesterone from days 4-8, plateau at days 8-16 and then decline from days 16-21 back to near zero in a reasonably predictable cycle, Figure 1.12.

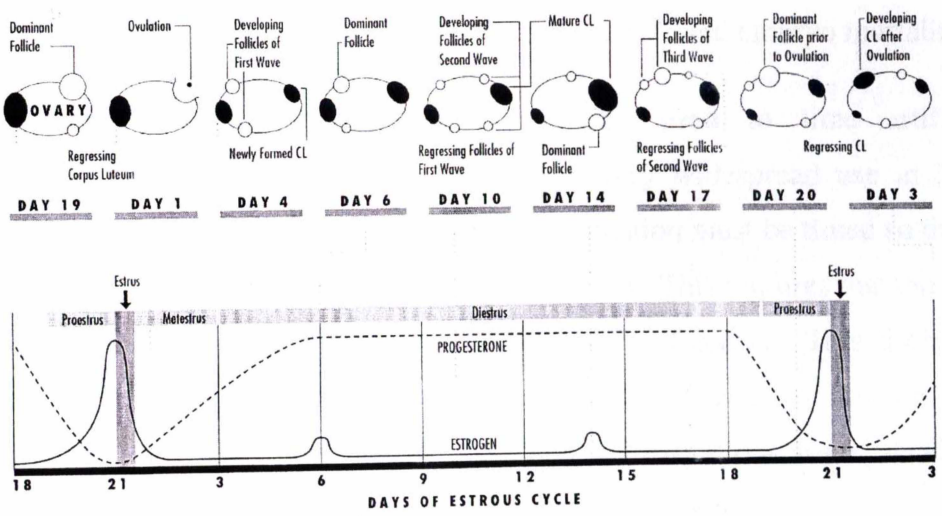

Figure 1.12 Cyclic Changes in Bovine Progesterone and Estrogen and Bovine Ovarian Stages[64]

1.2.1.1.3 Progesterone as a Physiological Marker

Progesterone can be used as a marker for the estrous cycle of a cow with progesterone fluctuating from less than 0.1 ng/mL at estrus to greater than 6 ng/mL at the luteal phase in blood plasma and from less than 4 ng/mL[65] to as high as around 50 ng/mL in whole milk. The exact amplitude of the fluctuation will vary from cow to cow. Clearly detection of progesterone in whole milk has the distinct advantages of higher concentrations and ability to detect it non-invasively.

Milk progesterone levels can also be used to help determine the pregnancy status of cows. The bovine placenta is unable to produce adequate progesterone to sustain a pregnancy and so the CL retains its progesterone secreting function into pregnancy. Progesterone rises steadily up to mid-luteal phase concentrations in pregnancy and so a sustained high reading of progesterone provides an indication of possible positive pregnancy. Early detection of pregnancy would be possible theoretically by taking a milk sample 21 days after insemination. Care is needed however when making assessments based on milk progesterone as one can get embryonic mortality and irregular life-span of the CL. Progesterone levels can also be used to mark failure of the cow to return to cyclicity after parturition which is a major veterinary concern to the farmer, and such conditions as abnormal pregnancies, follicular cysts,[66] anestrous cows[67] and embryo mortality.

Determination of milk progesterone may be used to time artificial insemination. Artificial insemination is now in very widespread use in New Zealand and abroad but in order to work, the insemination must be timed so that it overlaps the life of the sperm with the life of the ovum. This requires that the cow be inseminated between 6 and 28 h after first onset of estrus. This timing is presently very poorly done with only a less than 40% success rate on first insemination.[68] It is estimated that the US dairy industry alone loses >US$300 million per year through misdiagnosis or failure to detect estrus.[69]

1.2.1.1.4 Progesterone Detection Methods in Whole Milk

Many different techniques have been applied to determining estrus and pregnancy. Estrus monitoring by behavioural analysis involves inspection of

cows for biological indicators such as cows standing to be mounted by a bull, discharge of clear mucus from cervix and uterus, restlessness, and swelling of the vulva.[70] Techniques include pressure-activated heat mount detectors and contact indicating paint strips.[70] Progesterone determination in whole milk is extensively used in some areas.

Progesterone detection was first done by high performance liquid chromatography (HPLC) methods using solvent extractions from the sample and often multiple detector systems such as diode array with mass spectrometry.[71] Systems have been developed also for detection of progesterone metabolites in urine and faeces.[72] Detection however is dominated by enzyme immunoassay.

There have been a large number of publications in the field of milk progesterone EIA. Dominating these publications are those for ELISA techniques but there are a growing number that examine other methods. In all cases there are a number of factors that need to be considered when examining milk progesterone concentration. Progesterone is a lipophilic molecule and as such it concentrates in the fats of the whole milk with about 80% of progesterone being present in the fats.[73] The fat content of the milk however is a major matrix interference in the detection of progesterone, serving to impede binding of progesterone to its antibody. Many papers have sought to remove this interfering factor by using skimmed or de-fatted milk[74] but this has the obvious major disadvantage of removing most of the progesterone in the sample and this becomes a particular problem when considering low initial concentrations of progesterone. EIA's have been developed that can cope with up to 10% milk fat.[75] Major studies have been conducted that have built up estrous cycle and postpartum milk progesterone profiles for herds of dairy cows.[76] The use of preservatives has been found to be quite effective in keeping milk samples at room temperature for 10 days without significant changes in progesterone concentration.[77] ELISA immunoassay kits are now widely available to farmers in the USA and elsewhere as crude indicator tests taking 3-22 minutes[78] but are labour intensive.

As well as EIA methods using ELISA there has been a recent move to developing on-line sensors for milk progesterone. The objective is to have an automated sensing system that can sample directly from milking lines and give

real-time information to the farmer about the estrus or pregnancy status of the cows. Such systems usually consist of a detection membrane, transducer system and computer.[79] Claycomb et al. have developed such a system using a fluidic and fibre optic system for colorimetric EIA with 20 cycles per sensor.[80, 81] This work has been further extended and allows detection within 10 min and is sufficiently accurate to distinguish follicular phase from mid-luteal phase concentrations.[82, 83] Pemberton et al. have produced amperometric milk progesterone biosensors based on competitive immunoassay[84] whilst Kartoch et al. have synthesised nitroxide spin-labelled progesterone derivatives for use in biomembranes and immunoassay.[85]

Surface plasmon resonance is now becoming of interest in the application to biosensing of cow milk progesterone. This was demonstrated in aqueous medium by Wu et al.,[15] and a biosensor for detection in diluted cow milk was developed using BIAcore by Gillis et al. but suffered from a high detection limit (3.56 ng/mL) and all the limitations of BIAcore.[86] As well as progesterone, other milk components have also been analysed by SPR biosensing. These include detection of sulfamethazone residues[87] and staphylococcal enterotoxin B.[88]

1.2.1.1.5 Practical Aspects of the Design of Milk Immunoassays

Despite the large amounts of scientific study that have gone into the construction of milk progesterone immunoassays there is still a relative dearth of studies that consider:

1. The effects of different assay formats on experimental results, for instance immobilisation of antigen rather than antibody on the ELISA plate

2. The effects of the complex and often difficult to handle medium of cow milk on certain parameters of the immunoassay

3. The steric factors that influence the antibody binding and assay curves in milk progesterone ELISA

Existing commercial ELISAs rely on the use of progesterone-enzyme conjugates as competitive agents with the free milk progesterone for binding to

immobilised antibody.[89] Such enzyme conjugates have been used extensively and many different examples have been synthesised, the most common being to horse radish peroxidase (HRP).[90] The use of such conjugates has certain major disadvantages. There is no truly efficient and convenient method of purifying such conjugates. The only option to remove unbound enzyme from the reaction mixture is to employ affinity chromatography, which is very time-consuming and quite expensive, as it requires quite a lot of antibody. If the enzyme conjugates are not properly purified then unconjugated enzyme can bind to plate surfaces non-specifically producing high background signal and therefore lower signal to noise ratio and poorer detection capability. Furthermore, affinity chromatography is not usually 100% efficient in removing un-bound label. It has been found that some purification of progesterone-HRP conjugates with an affinity column allows a five-fold improvement in the detection limit.[91]

The enzymes are usually conjugated to analytes via the ε-amino groups of lysine residues. Most enzymes have multiple residues for analyte attachment. As the electrostatic and steric environment of the conjugated antigen greatly influences antigen / antibody interactions then changes to this environment can greatly impair the antibody binding affinity to the ligand.[92] In the production of the conjugate the number of analyte molecules attached per enzyme molecule cannot be easily controlled, so irregular binding, such as binding to multiple recognition sites is possible thus changing the conditions for competition with the analyte in the sample,[92] Figure 1.13.

The simplest way to avoid the need for enzyme-analyte conjugates is to immobilise an analyte-protein conjugate to the surface of the plate rather than the antibody. Competition can then be set up between sample progesterone and immobilised progesterone for limited free primary antibody. The bound antibody can then be detected using a secondary antibody conjugated to an enzyme.[90] Use of a secondary antibody has the following primary advantages:

1. The antibody-enzyme conjugate could be easily purified of unbound enzyme by simple dialysis

2. Multiple attachment to one enzyme is much less likely to occur, on steric grounds, and consistent conjugations can be expected as the enzyme and antibody are much closer in size than the enzyme and small-molecule antigen. Some slight conjugation variability is not as important anyway as the secondary antibody is applied in excess and is not involved in the critical analyte recognition part of the assay

3. Use of two antibodies increases the specificity of binding by increasing what is called the "reactive cross-section" of the binding interaction. This factor is of importance in complex biological media such as milk where many often related agents are present simultaneously.[18]

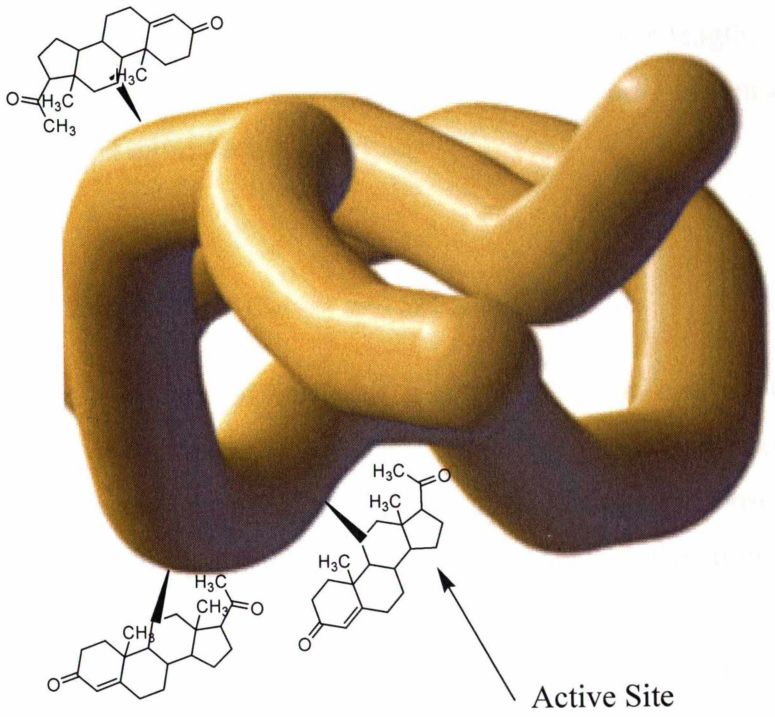

Figure 1.13 Binding Irregularities of Progesterone to Enzyme Label

Many studies have been conducted on the effect of changing media on immunoassay data[93] and some show large-scale changes in binding properties in the assay and require compensation for this. In the milk matrix there have been a number of early studies on the effects of changing the matrix in terms of parameters such as fat content and total nitrogen[94, 95] but there have been no systematic studies of the effects of the milk matrix relative to aqueous phase on

binding of progesterone-protein conjugates as immobilised antigen to monoclonal antibody. Protein conjugates are constructed with various types of intermediate linker between antigen and carrier protein and there have been no studies of the effects of incrementally increasing this linker length on the antibody binding to conjugates in the milk medium. Linker length has a major effect on steric hindrance to binding of antigen and antibody. In the aqueous medium it has been shown to have no effect on antibody binding in a static assay format[15] but this may well not be the same for whole milk assays.

There is clearly a need to develop and validate a protein-conjugate based ELISA system for the detection of whole milk progesterone and a need to study this format in the milk medium with respect to antibody binding properties and assay curve positions and shapes with incrementing linker length. The results of such a study could have further value in developing new biosensor formats for whole milk small biomolecule detection.

1.2.1.1.6 Assay Binding Curves and Statistical Analysis

There are a variety of different sets of data that can be obtained from immunoassay or immunosensor systems. The first group is data of how binding response (expressed as optical absorbance in ELISAs or response units (RU) in SPR) varies with changing concentration of either the immobilised agent (antibody or protein conjugate) or the free binding or competitive agent introduced with the sample (labelled antigen or antibody). Plots of this data may include plots of response *vs* coating protein conjugate concentration or response *vs* solution antibody concentration or dilution. Distinguishing binding response data points from each other using this system is comparatively easy by simply employing student's *t*-test to determine whether the response differences are significant.

Greater statistical difficulty is encountered when one considers the actual assay standard curves. Such curves are plots of binding response *vs* analyte concentration and their form will vary depending upon the format. In a sandwich immunoassay one gets a standard curve that at low analyte concentration is of low

response and flat. When the "active region" of the assay is reached then there is an increase in response with increasing analyte until finally a plateau region is reached where there is no further signal increase, corresponding to saturation of immobilised antibody binding sites. Such curves have an S-shape and can be expected to approximate to a straight line of positive slope in the mid-region of the curve.

Competitive and non-competitive non-sandwich immunoassays have a curve, which has high signal at low analyte and is a flat line. As the analyte is increased then label binding is inhibited leading to a drop in response down to near zero when inhibition of signal-generating binding is nearly total at which point the curve flattens out. This S-shaped curve is the inverse of the sandwich assay curve and once again approximates to a straight line in the mid-region.

The detection limit of an immunoassay is generally defined as the analyte concentration corresponding to the blank reading less two standard deviations (sometimes three) of the mean of the blank. The sensitivity of an assay can be defined in one of two ways:

1. As the slope of the active part of the curve, that is the signal change per unit concentration change. This is reflected in the height of the standard curve.

2. As the minimum detection level of the assay, that is the detection limit. This is usually reflected in the overall position of the curve along the concentration axis.

The linear range is the region in which data points from the standard curve may be fitted to a linear regression with good fit. The dynamic range refers to the range between 10 and 90% bound relative to the blank which is 100% bound. It is possible to simplify this non-linear relationship by simply considering the linear region and reducing all statistical consideration to a linear regression. This is not usually suitable though as the curve seldom fits at a wide range to a perfectly linear fit. It is far more common to fit a four-parameter logistic relationship to the data and use this to calculate concentration values from the equation of the curve.[96, 97] The logistic fitting can be described by the equation in Figure 1.14 and

the graphical representation is given in Figure 1.15. Some researchers use semi-log linear ranges but this is less common.[98] Some standard curves fit better to S-curve fittings and this may be more appropriate in certain cases.

$$y = \frac{(a-b)}{1+(x/c)^d} + b$$

y = response
x = concentration
a = maximum response
b = minimum response
c = concentration at 50% response
d = slope of the line at the mid-point

Figure 1.14. Four-Parameter Logistic Equation for Immunoassay Curves

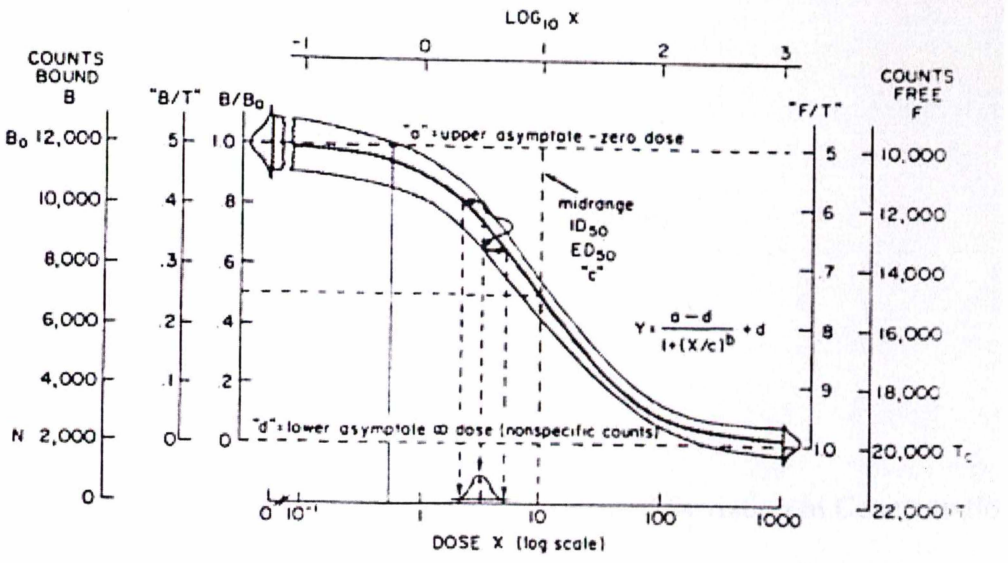

Figure 1.15 Four Parameter Logistic Fitting of Immunoassay Data[99]

For the determinations of errors in the concentration determinations from these non-linear curves one can use a number of options. Dudley et al. suggest that as at any given point upon the curve a tangent to the curve will give the slope of the curve at that point then this tangential slope can be used to calculate the standard error in the concentration from the standard error in the absorbance at that point.[99] The standard deviation in the response can either be used as the actual standard

deviation of the standard curve point nearest to the concentration or else by developing a response-error relationship. This is where an assay is done exactly the same way for a large number of times and so a plot is made of the average determined standard deviation at certain concentrations and is plotted versus those concentrations. This enables one to formulate an equation relating error to concentration that can be used in conjunction with the equation in Figure 1.14. This slope system will work well for regions where the curve is not too deviant from a straight line but it becomes more of an approximation as one moves to the ends of the curve.

There is no set procedure for dealing with errors in immunoassay concentrations, but given a four parameter logistic fit simple algebra suggests an adequate approximation would be the equation given in Figure 1.16. In such fittings this formula will apply quite well and has been adopted in this thesis.

$$Sdx \simeq x \times sd \log x \simeq \frac{x\, sd(y)\, (1 + (x / c)^d)^2}{d\, (a-b)\, (x / c)^d}$$

Where: sdx = standard deviation in x (in concentration)

x = concentration

sd(y) = standard deviation in y (in response)

a, b, c, d are parameters as for Figure 1.14.

Figure 1.16. Equation for the Calculation of Standard Deviation in Concentration From Immunoassay Curves.[100]

1.2.1.1.7 Estrogen Biochemistry

Another class of compounds that is very commonly the target of immunosensors and immunoassays are the estrogens. The estrogens are also of interest for their receptor binding properties as such binding is critically important to the human endocrine reproductive control system.

The estrogens are a class of C 18 female sex steroidal hormones that are part of the estrane series (Figure 1.17). The principal estrogens are 17β-estradiol and estrone and to a lesser extent estriol and are produced in the female ovary. Estrone was first isolated in 1929[101] and 17β-estradiol in 1936.[102]

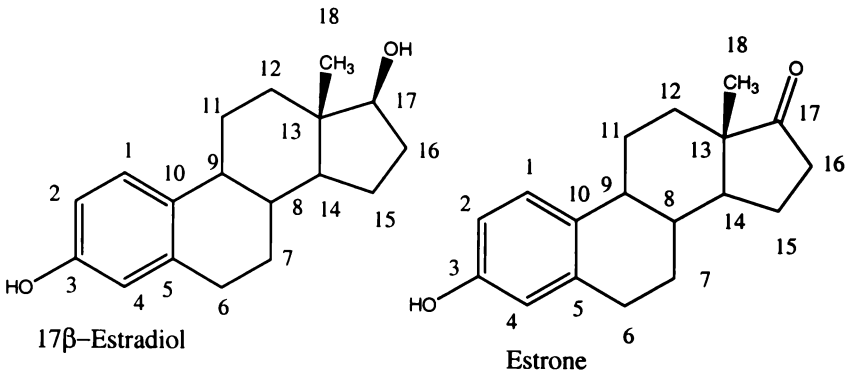

Figure 1.17 Estrogens: Estradiol (left), Estrone (right)

In human pregnancy, the hCG signalling from the blastocyst results in an increase in secretion rates of hormones including estradiol. Estradiol levels in pregnancy increase in maternal serum to levels of 20-30 ng/mL, about 100x higher than in a non-pregnant woman.

Estradiol levels in serum can be closely monitored to monitor follicle development and maturation, predict ovulation and prevent ovarian hyperstimulation in anovulatory women. Such levels can also be used for determination of postmenopausal status and for evaluation of men with gynecomastia. There are a number of EIA kits available for clinical determination of serum estradiol.[103]

1.2.1.2 Synthetic Chemistry of the Steroids for Antibody Interactions

1.2.1.2.1 Labelling, Carrier Proteins and Intermediate Bridges

As the sex steroids are of such importance in mammalian physiology, much research has been devoted to the production of derivatives of the steroid molecules for a number of different purposes. These purposes include the production of protein conjugates as immunogens to raise antibodies or to function

as coating antigens, the labelling of steroids with enzyme, fluorescent or chemiluminescent labels for biosensing of these steroids and the production of drug – steroid conjugates for specialised treatment of disease.

When antibodies are to be raised to small molecules (<2 kDa) then it is necessary to link or conjugate them to carrier proteins to provide enough size for the immune response to occur. Such protein conjugates consist of the antigen linked through some site on its structure to a straight chain chemical linker or bridge and then to the protein, usually BSA or OVA, Figure 1.18. Such protein conjugates may also be used as coating antigens on the surface in ELISA or biosensor applications. As well as proteins, one can also use such carriers as nucleic acid fragments[104] or *N*-vinylpyrrolidone copolymer.[105] Such protein conjugates have even been used in studies into their physiological effects in mammals.[106]

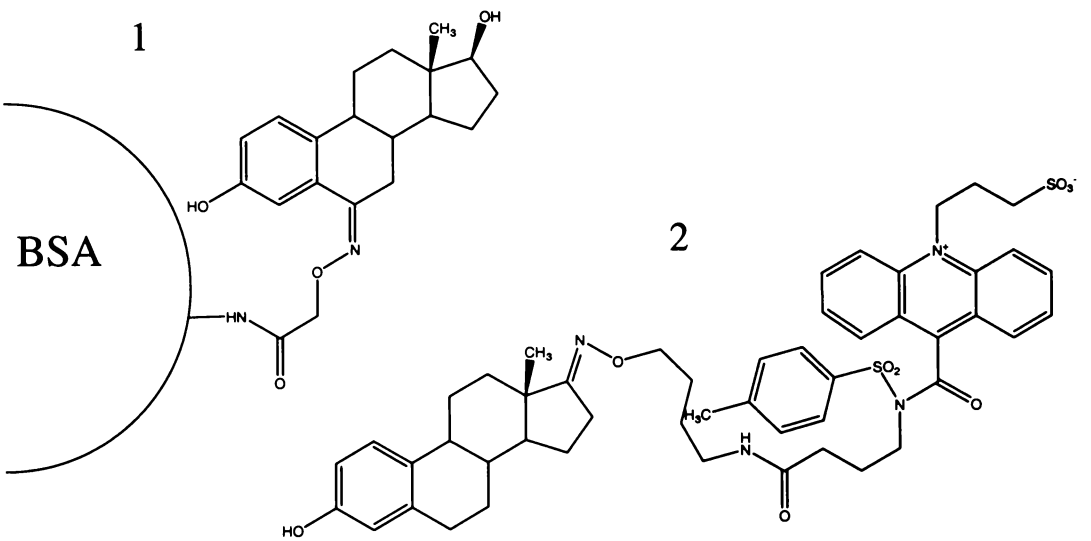

Figure 1.18 Estradiol – BSA Conjugate (1) and Estrone – Chemiluminescent Acridinium Oxime (AO) Conjugate (2)[108]

For antibody-immobilised formats for immunoassay and biosensors it is necessary to develop labelled antigen molecules for competition with free sample analyte. These conjugates consist of the antigen linked once again via a bridge to the label in question. Extensive studies have been done using enzyme conjugates, fluorescent labels[107] and chemiluminescent labels.[108] Conjugates of drugs to the estrogens are also of critical importance in the treatment of cancers in tissues

associated with estrogen receptors such as breast cancer[109, 110] and enable cytotoxic compounds such as daunorubicin to be directed with some selectivity.

1.2.1.2.2 Estrogen Site and Bridge Heterology

The production of linkages to estrone and 17β-estradiol were at first made via the existing functional groups in the steroids. This meant attachment via the 3-OH or 17-OH in estradiol or the 3-OH and 17-carbonyl in estrone. Attachment was via a hemisuccinate bridging through the alcohols or an (*O*-carboxymethyl)-oxime (CMO) through the carbonyl, Figure 1.19. The hemisuccinates of estradiol and estrone are widely available commercially and are a very common form of conjugation.[111, 112, 113] Whilst such conjugates are easy to produce, they suffer from being susceptible to base-catalysed decomposition[23] and compromise functional groups that are important in the antigenic recognition of the molecules.[23] Carboxymethyloximes derived from steroid carbonyl groups are viable alternatives as has been demonstrated for several steroids including progesterone (3- and 20-positions),[114] cortisol (3-position)[115] and testosterone (3-position)[116] as well as estrone (17-position)[23, 24] (Figure 1.19). This bridge attachment method will naturally only work if the antigen has a carbonyl group to attach through or if one can be introduced, and will compromise the antigenicity of the antigen unless a carbonyl group is introduced to the molecule at a position spaced from existing functional groups. This can be done by using the 6-oxo-estrogens that are commercially available to conjugate at the 6-position. This attachment has the advantage that only one stereochemical product can be produced and so there is no reduction in antibody recognition due to a mixture of stereoisomers.

Previous studies have examined the effect of changing attachment position on antibody binding and specificity. To this end steroid conjugates have been made at the 4-, 6- and 7-positions of progesterone and compared to those at the 11-position[117, 118, 119] for the raising of antibodies. The 4-, 6- and 7-positions are on the opposite side to the 11-position and it was thought that attachment on this side may give better antibody specificity and binding affinity. It was found that attachment at the 4-position resulted in no antibody cross-reactivity with phenolic

or C-19 steroids or with corticosterone. There was however large reactivity with 5α- and 5β-dihydroprogesterone that supports other observations of loss of specificity about the point of attachment. Hatzidakis et al. have reported for progesterone, that raising the antibody to a conjugate at the 7-position and using an enzyme conjugate at the 6-position gives greatest sensitivity and selectivity as opposed to conjugates attached at the 3- and 11-positions.[120] This tends to suggest that the 6/7 side of the steroid skeleton may be better for conjugate attachment.

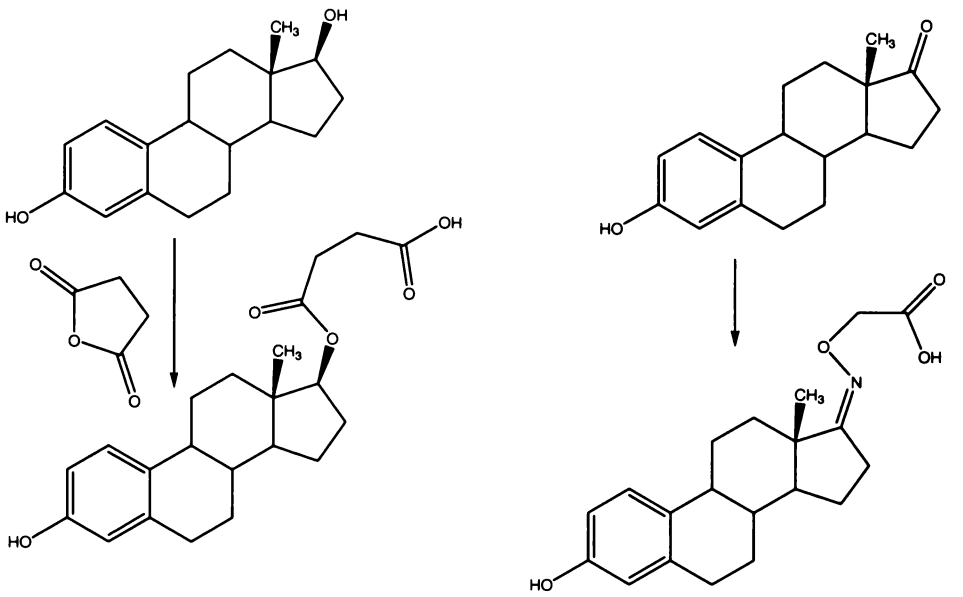

Figure 1.19 Production of Estradiol – Hemisuccinate (Left) and Estrone – Carboxymethyloxime (Right) Derivatives

The overall consensus for achieving best antibody binding and specificity is to use heterology of some kind.[121] There are two types of heterology. The first is site heterology whereby the antibody is raised to a conjugate with attachment at a different site from the labelling or carrier protein attachment site for the assay antigen. Bridge heterology is where different types of intermediate chemical bridges are used to connect the antigen to protein for immunisation and to label, or protein for immobilisation. Bridge heterology is very important, as if the same bridge is used for both immunisation and in the assay itself, then the antibody will bind not only to the antigen but also to the connecting bridge and so binding will be stronger to the labelled antigen than to the free sample antigen and so the assay will be less sensitive to changes in progesterone concentration and so will produce an inferior assay. There have been a number of studies on this phenomenon and

indeed in certain cases the bridge heterology has been shown to be more important than the site heterology.[122] In the case of the milk medium, Sauer et al. have shown that using an 11-α-hemisuccinate bridge and an 11-α-glucuronide label bridge[123] will greatly reduce bridge recognition.[124]

In the case of the estrogens, De Boever et al. found interestingly that raising monoclonal antibody to estradiol-6-carboxymethyloxime-bovine serum albumin (BSA) and using a homologous format with 6-carboxymethyloxime (6-CMO) labelling with isoluminol or HRP gave the lowest detection limit and highest sensitivity.[125] This is an interesting result and shows that it is possible to produce homologous assays with very good sensitivity and this has been confirmed by other reports so long as the 6-CMO attachment method is used.[126, 127] These results for 6-CMO have been carried through to chemiluminescent immunoassay also.[128] Linker and site heterologies have been employed for assaying follicular estradiol. Silvan et al. have used the 6-carboxymethyloxime to raise polyclonal antibodies and then used 3-hemisuccinate bridging for the HRP label.[129] Follicular fluid contains many other closely related steroids to estradiol and it was found that this format enabled detection of estradiol with low cross-reactivity with other steroids.

Another type of site heterology employed is the use of different stereoisomers. Webb et al. reported the raising of antibody to the 11β-hemisuccinate of estradiol and attachment of radiolabel at the 11α-position.[130] This was compared to the 3- and 6-positions that showed far less sensitivity. It was concluded that the bridge-binding phenomenon was dependent upon the site of conjugation employed as a homologous 3-CMO conjugated testosterone had very similar results to the estradiol assay across antisera from several different animals. This may help to explain the observations of de Boever et al.[128] Taking the heterology concept even further, Rao et al. have raised antiserum to testosterone-19-carboxymethylether-BSA conjugate and used 4-(17β-hydroxy-3-oxoestra-4,9-dien-11β-yl)butanoic acid conjugated to penicillanase as the enzyme conjugate.[131] This is an example of bridge, site and ring heterology and produced an assay of good sensitivity and selectivity.

Another method of conjugation that is applied to the aromatic A-ring of estrogens is the formation of an azo linkage, Figure 1.20. This involves selectively nitrating the aromatic ring at either the 2- or 4-positions, reducing the nitro group to an amine by reaction with sodium hydrosulfite and then formation of the diazide by reaction with sodium nitrite in hydrochloric acid and then conjugation of the diazo unit to the protein at a pH of 8.5-9.5.[132] This method has the clear disadvantages of needing a number of reaction steps and using diazo coupling which is not as consistent nor the product potentially as stable as in coupling via amide linkages from a carboxylic acid terminating derivative. Diazo coupling has also been employed for estradiol-17-glucuronides by approximately the same method.[133] The principal method of such diazonium conjugations is formation of diazo linkages with the tyrosine and histidine residues of the protein.[90] Diazonium conjugation works well for tyrosine-containing peptide haptens. As tyrosine groups are usually quite rare in a given peptide hapten there can be consistent orientation of hapten to carrier and near-identical cross-linking. The problems with diazo coupling however are immense. The rate of reaction is so fast that most of the total coupling potential can be lost by the diazo group undergoing intra-molecular coupling on the carrier protein. As they are formed they can react with active hydrogens on the aminophenyl precursor even before hapten is added. Even without the second active-hydrogen containing molecule, the diazonium-activated molecule will turn brown/black within one hour as it self-conjugates. Such problems lead to highly inconsistent conjugation reactions.[90]

As well as diazo coupling one can also couple to the A-ring using the glutaraldehyde and Mannich reaction methods. In the glutaraldehyde method the nitro derivative is formed at the position of attachment and then reduced as for the diazo method to the amine and then coupled to glutaraldehyde by addition at pH 6.8 along with the carrier protein, Figure 1.21. Once again this involves several steps and uses an amino group on the hapten, which is not as good for conjugation as a carboxylic acid as there is less control over the conjugation process. The conjugates formed are also usually of high molecular weight that may cause precipitation problems.[90]

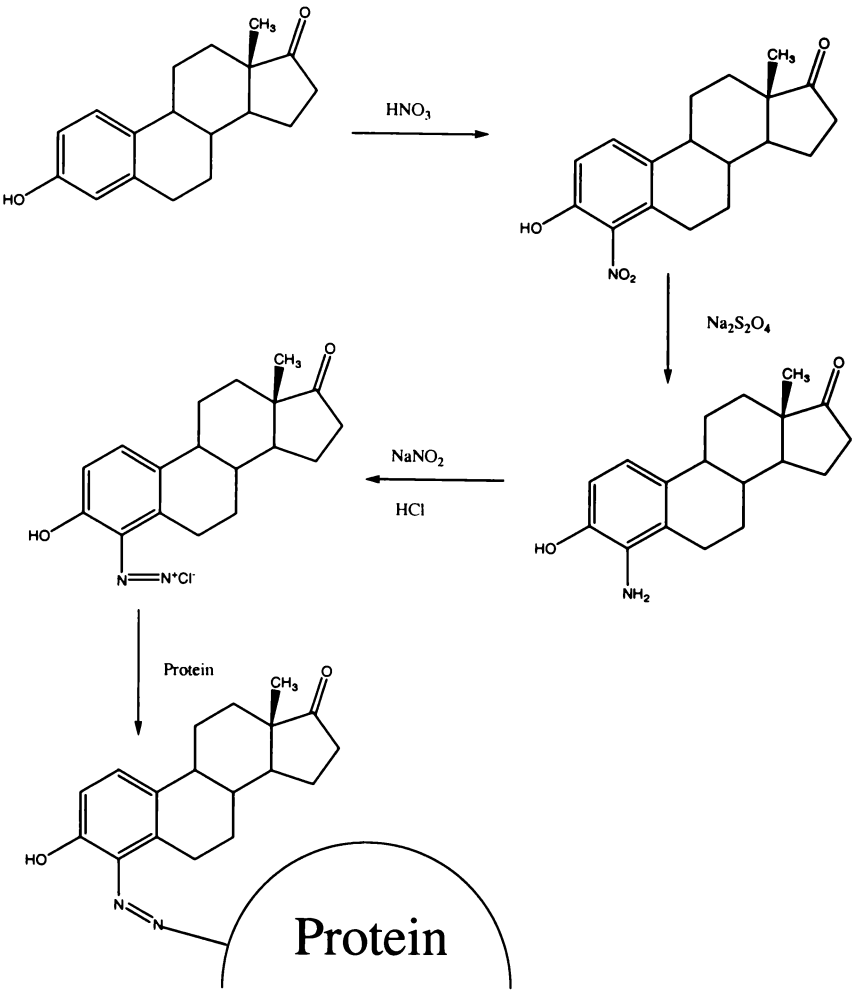

Figure 1.20 Diazo Coupling to Estrone[132]

The Mannich reaction proceeds by addition of estrogen with BSA and formalin solution, but in order for this method to work in any good yield it is necessary to first cationize the carrier protein usually by addition of diamines to the carboxylic acids of the protein thus introducing another labour-intensive step, Figure 1.22. Furthermore, the position of attachment on the steroid A-ring is not controlled which may well compromise antibody affinity and selectivity. It is thought that attachment is *ortho* to the hydroxyl group but this could be either 2- or 4- conjugation. The yields of conjugation are quite variable with this method and depend upon the reactivity of active hydrogens on the hapten.[90] Such reactions should obviously never be used for haptens containing free amine groups as hapten polymerisation may occur preferentially to conjugation to the carrier.

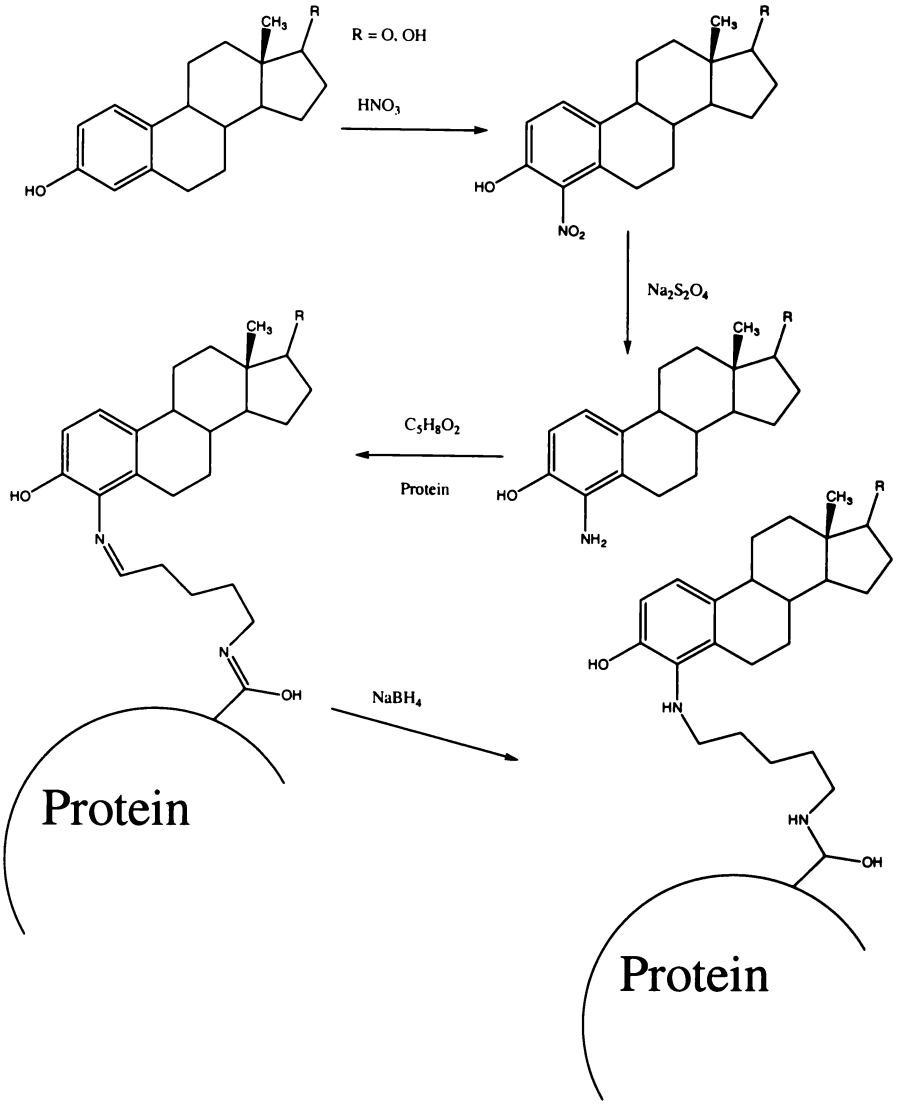

Figure 1.21 Glutaraldehyde Conjugation of Estrogens to Protein

1.2.1.2.3 Linker Length Effects

Another area of key interest is on the effects of changing bridge or linker length on the amount of antibody binding and the performance of the assay. It is intuitive to expect that as the bridge length is incrementally increased that this will increase the amount of antibody binding up to a certain point as the steric hindrance to binding is gradually relieved. Studies of linker length effects are therefore of great interest not just for studying immunoassay interactions but also when considering the binding of conjugated targets to antibodies and receptors in histology and drug-delivery, Figure 1.23. In the case of steroids, it has been found that for cortisol and 11-deoxycortisol conjugated at the 4-position, use of a bridge shorter than that used to raise the antibody leads to an increase in assay sensitivity

whilst one longer than the immunogen has no positive effect.[134, 135] This is intuitively reasonable as the shorter the bridge of the labelled antigen, the less the antibody will bind and so the more it will tend to favour free progesterone and thus the more sensitive it will be to changes in free progesterone concentration. The other factor to consider is that the shorter the linker between antigen and label, the lower will be the antibody binding and hence the lower the signal. This will have a major effect on the signal : noise-type sensitivity of the assay by reducing the slope of the assay curve. The same can apply when the label is on the antibody. Indeed, this has been found in systematic studies of the linker length when enzyme or microparticle label of monoclonal and polyclonal antibody respectively is employed.[136] When linker was increased from 9- to 23-atoms long there was a 64% signal increase and from 9- to 30-atoms there was an 82% signal increase for enzyme-labelled α-fetoprotein antibody.[136]

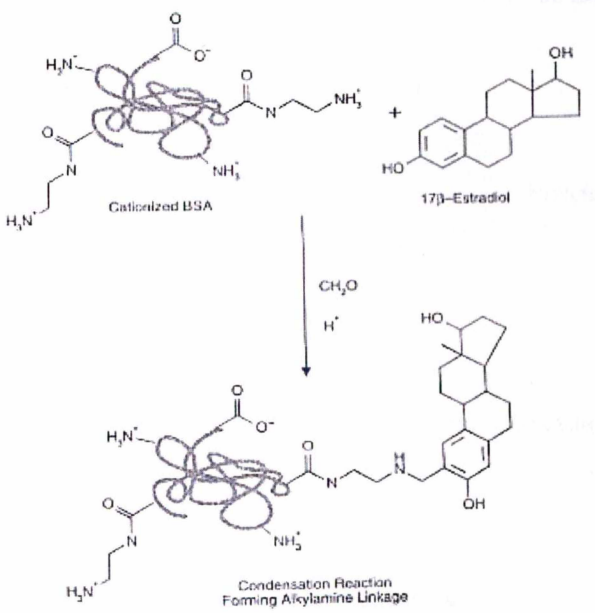

Figure 1.22 Mannich Reaction at the 2-position of Estradiol[90]

There has been an extensive study on the effects of incrementing linker length on antibody binding to protein conjugates attached to progesterone via the 4-position.[10] This study has found that antibody binding to conjugates ranging from 4-atoms to 18-atoms is identical in static ELISA formats as is binding to 4- and 7-position conjugates. However, in SPR, a flow-through format, that is one where one binding partner is flowed over a surface immobilised with the second partner,

there is a substantial increase in binding with increasing linker length and there is much higher binding at the four position than at the seven position.[10] Studies have been made on estrone-protein conjugates used to raise antibodies via an azo bridge to the aromatic ring.[137] In this case the addition of a short aliphatic chain (4-amino-*n*-butyric acid) gave antisera that cross-reacted with estrogens with D-ring structures different to that of estrone. The explanation was given that it is possible for the linker chain to twist and allow the D-ring region to be surrounded by the carrier protein thus inhibiting binding to that determinant and diminishing specificity.

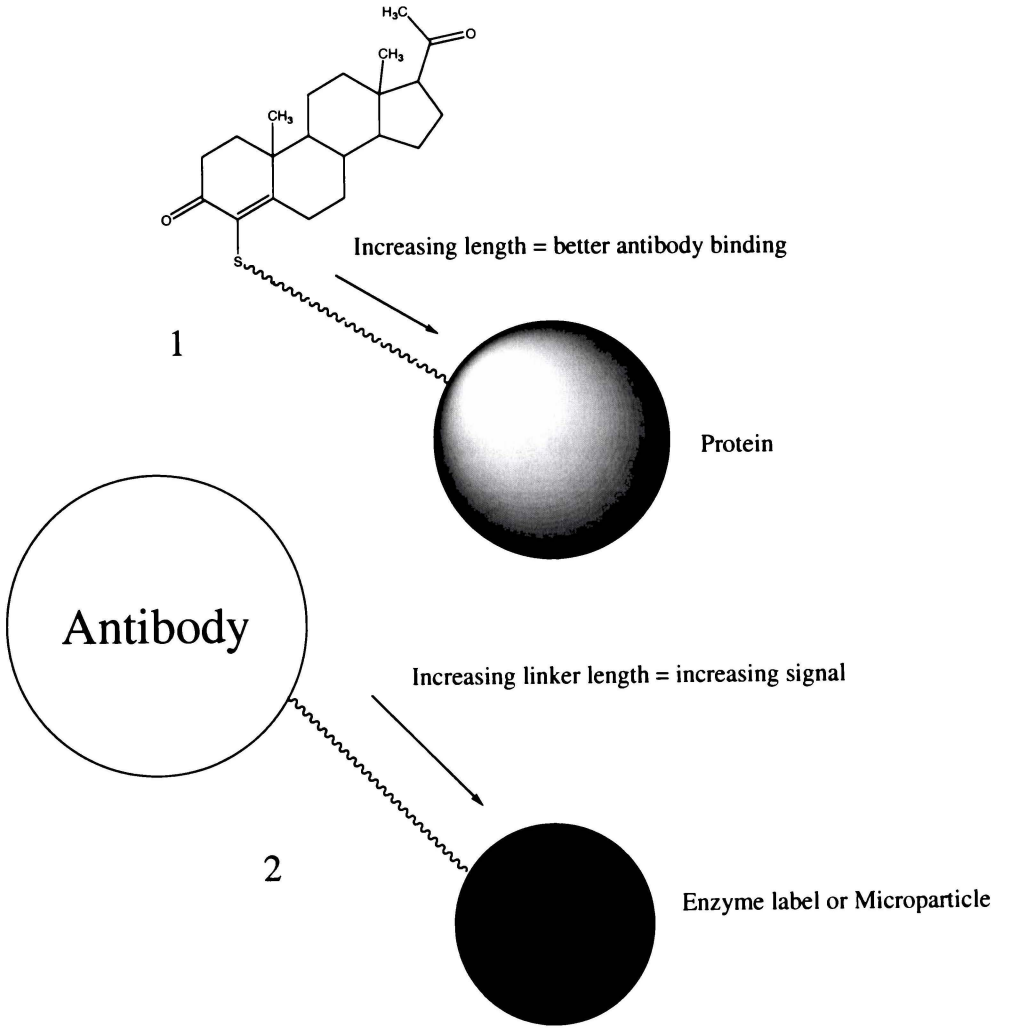

Figure 1.23 Linker Length Effect for Progesterone-Protein Conjugate[10] and Antibody-Enzyme Label / Microparticle Conjugate[136]

Polyethylene glycol (PEG) or oligoethylene glycol (OEG) polymer chains offer several advantages as intermediate linkers in hapten-carrier or antigen-label conjugates. They can lend water solubility through their multiple ether linkages to an analyte that might otherwise be insoluble or sparingly soluble in water. This can be of great advantage in protein conjugations as use of organic solvents can affect the repeatability of conjugations.[10] The chains have been used extensively in antibody binding interaction studies as they have been found to not interfere with antibody binding to the target analyte but rather serve to reduce non-specific binding. PEG chains have been attached to certain estrogens. PEG chains of $n \simeq 66$ and $n \simeq 133$ have been attached to estradiol via the 3-OH in an ether connection[138] as has estrone[139], and polyestrones have been synthesised by multiple conjugation to a PEG chain.[140] PEG has been used extensively in the immobilisation of target analytes in such applications as affinity chromatography[141] and for the modification of proteins including enzymes and hormone antagonists.[142]

1.2.1.2.4 Thioether Bridging

Thioacids have been extensively used as bridging agents in steroid conjugates. The coupling is via a thioether to the ring structure of the steroid with a protruding carboxylic acid functionality. The thiol group acts as an efficient nucleophile for attachment to the steroid whilst the carboxylic acid can via appropriate activation form an amide linkage to lysine residues in the carrier protein. Thioether derivatives of progesterone have been examined with carboxymethyl alkylthio derivatives being synthesised at the 7α-position[143] and 3-mercaptopropionic acid (MPA) derivatives being synthesised at the 4- and 7α-positions[144] as linkers for enzyme attachment, Figure 1.24. Methods for MPA attachment have also been developed for the 4- and 6-positions of 11α-hydroxyprogesterone.[119] Production of the 4- and 7-thioethers on a non-aromatic ring in a steroid proceeds by first brominating the steroid at the 6-position by simple reflux treatment of the steroid with *N*-bromosuccinimide (NBS). This is then followed by reflux with the 3-mercaptopropionic acid in methanolic KOH to give the 4-thioether or treatment with sym-collidine to produce the diene and then addition across the 6-7 double

bond by treatment with the 3-mercaptopropionic acid and sodium methoxide in tetrahydrofuran (THF).

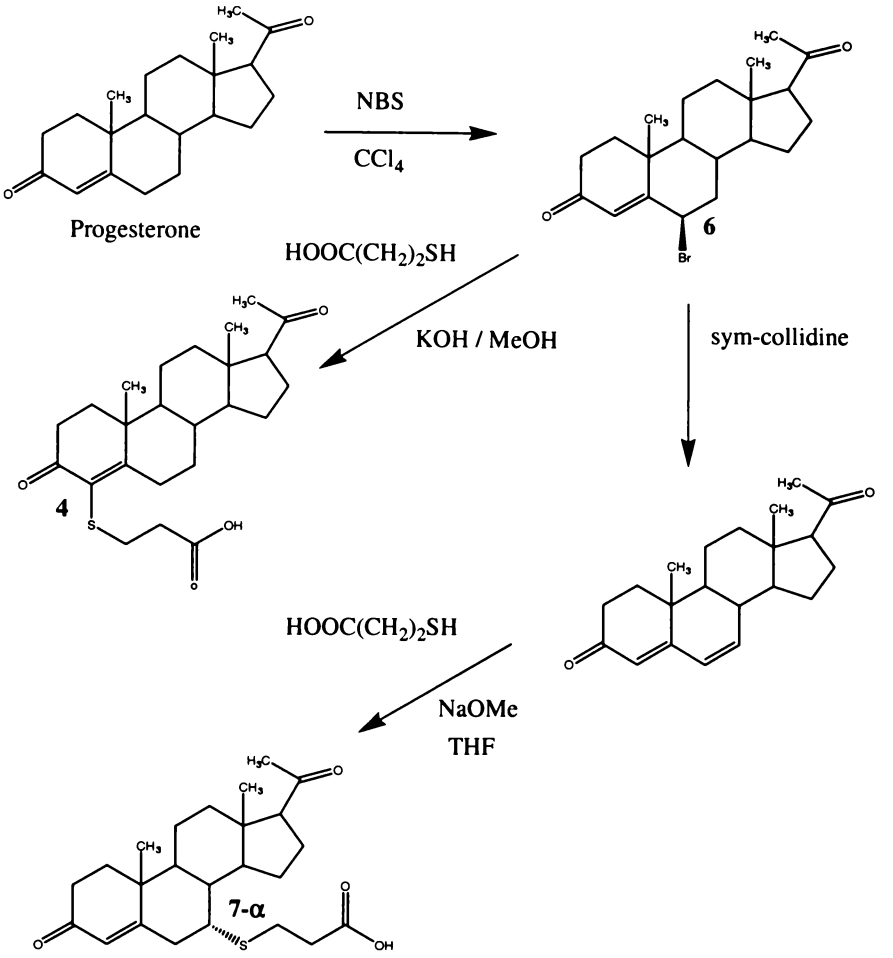

Figure 1.24 Progesterone Thioether Derivatives

The estrogens readily form thioether conjugates in vivo by reacting with the thiol-containing amino acid cysteine and the tripeptide glutathione as a means of metabolising the steroids and eliminating them from the body. These were first identified by incubating ^{14}C-estradiol with rat liver fractions.[145] 2-Hydroxy-17β-estradiol has been used to produce glutathione and cysteine conjugates by production of the *ortho*-quinone by treatment with acetic acid and sodium metaperiodate and then extraction into dichloromethane, followed by addition of glutathione or cysteine in acetic acid.[146] Such a reaction system could not be used to easily produce a thioether conjugate of 17β-estradiol as the product still has an additional hydroxyl group on the aromatic ring that cannot be removed easily

without damaging the thioether linkage. Furthermore, the chemistry involved does not have high pure yields (about 10%), as the product does not crystallise well.

Another method for the production of thioether estrogen derivatives from the aromatic ring is to start with the epoxide 4β,5β–epoxy-17β-hydroxyestr-1-ene-3-one and produce 4-ethylthioestradiol by stirring the epoxide with ethanethiol and sodium metal under nitrogen.[147] The 4-position 3-mercaptopropionic acid derivative of 17β-estradiol was synthesised using the epoxide method from 19-nortestosterone (nandrolone) by Meltola et al. in three steps,[107] Figure 1.25. This is less than ideal as there are three quite complex steps and this route starts from a restricted drug.

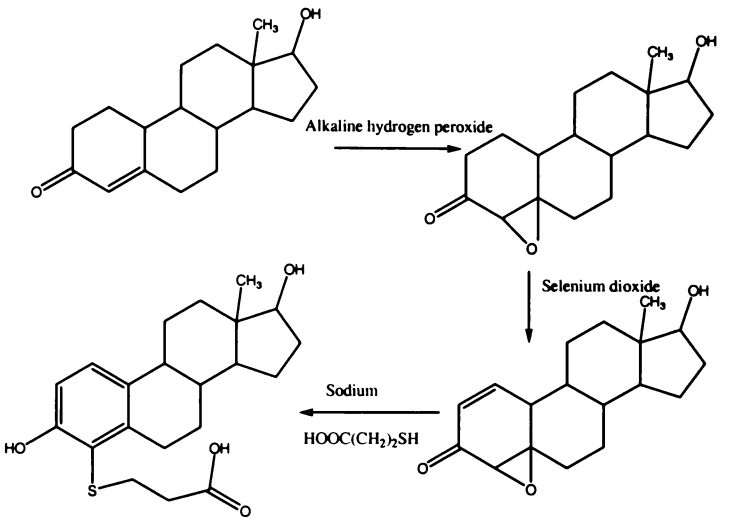

Figure 1.25 The Epoxide Method for Formation of Estradiol Thioether

Rather than adopting an *ortho*-quinone or epoxide method it should be possible to utilise aromatic substitution of a halogen derivative on the aromatic A-ring as a means of producing thioether conjugates to the 4-position of the estrogens. Bromo derivatives should offer the best possibilities for this as they have sufficiently weak C-Br bonds but are more stable than the chloro or fluoro analogues. The first report of "regioselective" bromination of estradiol and estrone was by Slaunwhite et al. who used a method of stirring in acetic acid with bromine to produce bromoestrone derivatives, and refluxing with *N*-bromosuccinimide for estradiol.[148] Finely divided iron powder was used to block production of the 4-bromo compound to get pure 2-bromo. This estrone bromination method has since been shown to be somewhat unreliable with

dibromination occurring and yields being variable. The production of pure bromoestrones has posed a significant synthetic challenge. Most brominations reported have led to either an isomeric mixture of the 2- and 4-bromoestrones in about equal quantities or have yields that cannot be readily reproduced.[149, 148, 150] Page et al. have reported the production of 4-bromoestrone **5** from estrone **3** via 2,4-dibromoestrone **4** by *N*-bromosuccinimide reaction in ethanolic solution followed by reduction of the dibromo with 10% palladium on carbon under reflux in formic acid and *N,N*-dimethylformamide (DMF)[151] (Figure 1.26). It has been thought that production of pure 4-bromoestrone may have to proceed by a formic acid debromination of the 2,4-dibromoestrone over palladium on carbon (Figure 1.26). This has also been reported by Numazawa et al. who have also produced the 4-bromoestradiol this way.[152] Numazawa et al. also used potassium iodide and ascorbic acid as dehalogenating agents. These results as well as the work of Utne et al. conflict with the paper of Slaunwhite et al. Utne et al. however produce only pure 2- and 4-bromoestradiol using *N*-bromoacetamide, and do so only with the aid of column separation.[149]

In the case of estradiol, the 2,4-dibromoestradiol can be prepared simply by direct bromination with bromine in near quantitative yields.[153] Formation of 4-bromoestradiol from this dibromo- has been achieved by regioselective hydrogenation[154] with remarkable selectivity. 2-Bromoestradiol can also be synthesised by alkylation of estradiol with chloromethyl methyl ether to give either the 3,17β-bis(methoxymethyl) ether or the 3-methoxymethyl ether.[153] Either of these protected estradiols can then be used to react with butyllithium and then trimethylsilyl chloride to give the 2-trimethylsilyl derivatives, which can be converted into 2-bromo or 2-iodoestradiol. Yet another method for 2-bromoestradiol and 2-bromoestrone synthesis is the reaction of the corresponding 2-phenylselenyl derivatives with iodine monobromide producing compounds in ~70% yield.[155] Lovely et al. have very briefly mentioned a method for production of the 4-bromoestradiol **2** from estradiol **1** by simple bromination with *N*-bromosuccinimide in ethanol[156] (Figure 1.26). Under this method the desired 4-bromoestradiol simply precipitates out of solution upon reaction. No details of this synthesis were given other than the yield of 55% and so the careful control

needed of the ratios of reactants and solvent will need to be determined again for this method.

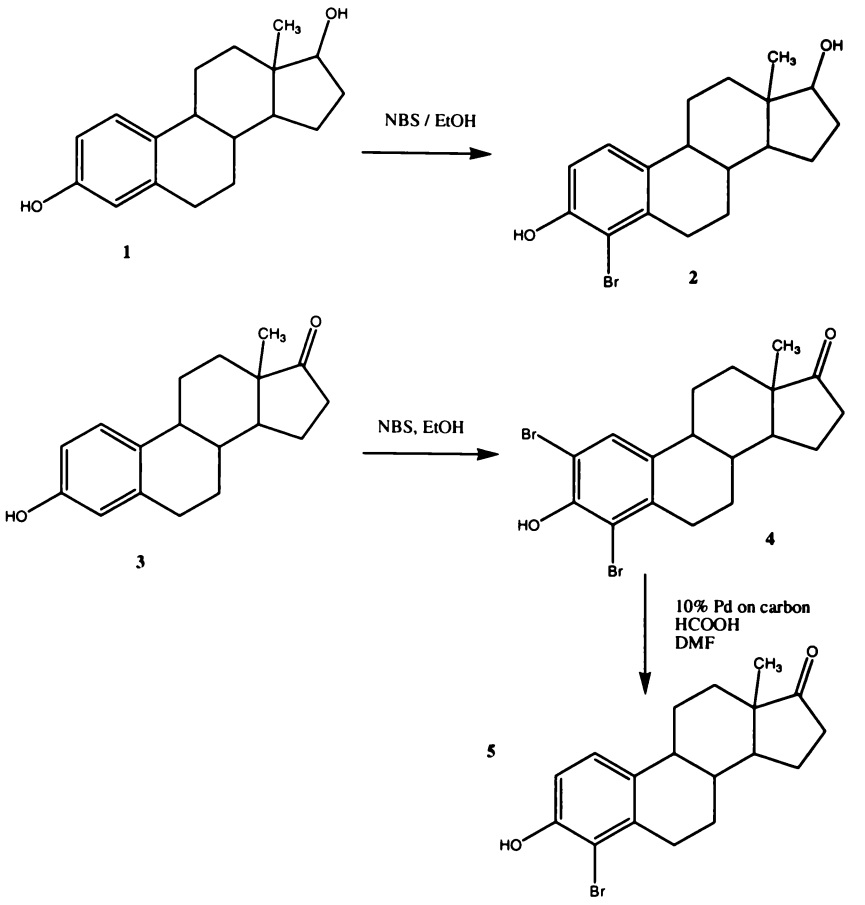

Figure 1.26 Bromination Methods for the Estrogens

Whilst there have been no reports of thioether conjugation to the A-ring of estrone and only one epoxide-mediated method for estradiol, there has been work done on uses of such a conjugation at the 7-position of 1, 3, 5 (10), 6-estratetraenes to give estra-1, 3, 5 (10)-trienes substituted at the 7-position with 3-thiopropionic acid side chain in a light-catalysed radical reaction yielding α and β-epimers.[157] These were then conjugated to BSA with 25-30 steroid residues per albumin molecule that was then used to raise specific antibodies. This reaction is the photolytic equivalent of the 7-mercaptoprogesterone reflux method mentioned above. Previous experiments with the progesterone conjugates have demonstrated that the 4-position gives much higher antibody binding than the 7-position in flow-through formats.[10] This method demonstrates the efficacy of the thioether linkage for conjugation and reinforces the possible usefulness of attachment at the

4-position by thioether conjugation. Numazawa et al. have also reported the thioether linkage at the 16-position of the androsten-17-ones[158] from the corresponding 16-bromo derivative by a direct S_N2 displacement. Miller et al. have also produced 7-thiosubstituted estratriene derivatives by reacting the 6-carbonyl 7-bromo equivalent with *p*-thiophenol, sodium hydride and DMF followed by sodium borohydride and ethanol and then TFA and Et_3SiH to produce the *p*-thiophenol thioether derivative.[159]

Clearly, production of conjugates linked at the 4-position on the aromatic A-ring of the estrogens is of great interest as this position has demonstrated superior antibody binding over 7- and 11-position protein conjugates of a steroid with a non-aromatic A-ring, progesterone.[10] Furthermore, this position is stereochemically fixed so there can be no contamination of different epimers at a saturated carbon that could reduce antibody binding affinity and / or specificity. Theoretically, the best attachment method would be via thioether conjugation of a mercapto carboxylic acid as this would produce a highly stable connection and the terminal carboxylic acid unit would allow easy conjugation to a protein carrier via *N*-hydroxysuccinimide activation that has been shown to be a very consistent and easily controlled means of conjugation. The active esters are highly reactive towards the amino groups of the carrier and form stable amide linkages. Previous studies have found this conjugation method to produce highly consistent conjugations with respect to hapten number.[10,15] This method allows easy attachment of heterobifunctional linker agents to the antigen to provide spacing between hapten and carrier. The formation of thioether linkages should be able to be effected by simple aromatic substitution of the bromo-derivative.

It has previously been found that for fluoroimmunoassays, that fluorescent tracers conjugated to estradiol via a C-4 thioether linkage give binding to an antibody raised to the 6-position whereas conjugates via the C-2 position do not.[107] Furthermore, C-4 conjugates were found to give more sensitive immunoassay curves than C-6 conjugates.[107]

The attachment positions that have been used to date are summarised in Figure 1.27.

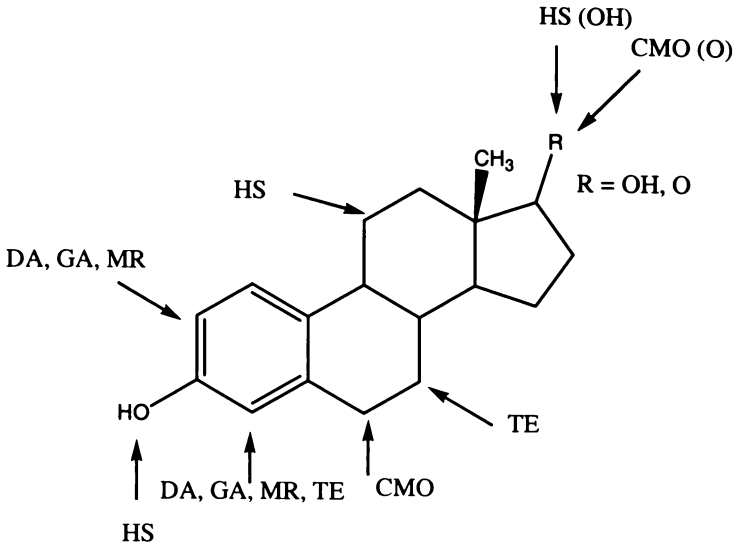

Figure 1.27 Attachment Positions to the Estrogens: DA: diazo, GA: glutaraldehyde, MR: Mannich reaction, HS: hemisuccinate, CMO: carboxymethoxime, TE: thioether

1.2.1.3 Detection of Estrogen Binding Interactions

Estrogen binding interactions have been determined using a number of different techniques. One of the most commonly employed is the estrogen receptor binding assay. This involves taking a sample of estrogen receptor prepared from an appropriate tissue source, *e.g.* lamb uterine cytosol[160] and competing estrogen analyte with tritiated estrogen to determine the relative binding affinities (RBA).[159] These tests have been used by Miller et al. to determine the selectivity of 7-thiosubstituted estratriene derivatives[159] and have shown that the selectivities are sensitive to the type of thioether chain used.

A developing field of research is the use of SPR to determine estrogenic binding properties. SPR has been used to study the binding between 17β-estradiol and estrone to polyclonal antibodies[161] for homogenous energy transfer immunoassay and chemiluminescent estradiol conjugate antibody binding has been studied also.[162] Estrogen receptor binding assays have been conducted using estradiol immobilised to the biosensor surface via a short aliphatic spacer chain attached via the 17-OH of the estradiol and leaving a free amine group for

attachment to the biosensor surface.[163] The estrogen receptor is then used as the high molecular mass binding agent and dissociation constants calculated. Fractal analysis has also been used as a means of modelling binding and dissociation kinetics using SPR.[164] SPR thus offers an interesting means of studying the binding patterns of new estrogen derivatives or conjugates.

1.2.2 Catecholamines

1.2.2.1 Catecholamine Biochemistry

Apart from the steroid hormones, another class of compound is of integral importance in physiological signalling within the mammalian body. A neurotransmitter is defined as a chemical substance that is synthesized in a neuron and is released at the synapse of a neuron where it influences another neuron or an effector cell in some particular way.[165] Further conditions include that it must be found in the synapses at reasonably high concentration, be blocked by agents that block synaptic transmission and be removed from the extra-cellular space.[165] Broadly speaking, one can divide the neurotransmitters into two categories: the small molecule neurotransmitters and the neuropeptides. The former group will be considered here and include the class known as the catecholamines, compounds that contain a 3,4-dihydroxybenzene ring and an amino group. Examples of catecholamines include dopamine, nor-epinephrine, epinephrine and L-DOPA, Figure 1.28.

1.2.2.2 Catecholamine Biosynthesis

The catecholamines are synthesised in the nerve terminals and then packed into the synaptic vesicles. This synthesis allows continuous replenishment of the synaptic vesicles. They are produced from tyrosine by the action of tyrosine hydroxylase, which produces L-dopa and requires oxygen and reduced pteridine as cofactors.[166] The L-dopa is then decarboxylated by pyridoxal phosphate-

dependent aromatic L-amino acid decarboxylase to dopamine.[166] In noradrenergic nerve terminals the dopamine is further acted upon by dopamine-β-hydroxylase (DβH) to give norepinephrine, which is then methylated in the presence of phenylethanolamine-*N*-methyltransferase (PNMT) with methyl donation from S-adenosylmethionine.[166]

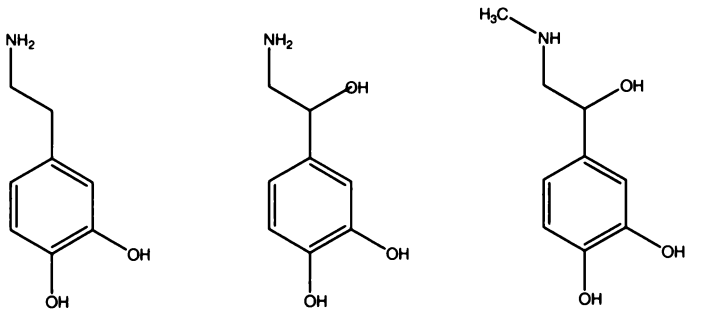

Figure 1.28 Structures of (left to right) Dopamine, Nor-epinephrine and Epinephrine

1.2.2.3 Synthetic and Conjugation Chemistry of the Catecholamines

1.2.2.3.1 Thioether-Catecholamine Synthesis

The chemical means by which thioether conjugates of catecholamine compounds can be synthesised has been studied to provide standards for analysis of quantities of these conjugates in biological fluids and tissues ranging from urine through to human brain samples. The conjugates that have been synthesised have been the glutathione and cysteine conjugates of dopamine, nor-epinephrine and epinephrine.[167, 168] The first step is the formation of catecholamine *o*-quinones, which is well studied. Whilst biochemical production works via enzymatic and electrochemical routes, the chemical processes involve electrolysis of the catecholamine in concentrated acid solution.[169] Shen et al. suggest 0.1 M HCl with 5.7 mg of dopamine in 30 mL of acid at 1.0 V for 30 min.[169] This should turn the solution from colourless to bright yellow. The thiol unit is then added and by simple stirring there is conjugation to the *o*-quinone and formation of the hydroxyl groups once again to give the thioether conjugate.[169]

This simple reaction procedure should apply to all *o*-dihydroxy catecholamines and to all thiol molecules provided steric hindrance is not great and the nucleophilic interaction is strong enough. The reaction must be done under acid conditions not only to provide the electrolyte but also to ensure that the catecholamine does not undergo radical oxidation. Under basic conditions dopamine is rapidly oxidised by dissolved oxygen to produce hydrogen peroxide and dopamine *o*-quinone. The oxidation is mediated by superoxide that acts as the chain propagating radical.[170] Dopamine has been shown to be stable at 0.1 N HCl, pH < 1.[171]

As well as the thiol-containing amino acids, it should be possible to use this electrolysis technique to produce straight chain linker derivatives that terminate in carboxylic acid functions. Such derivatives would be of great use as drug carriers or probes to study receptor and antibody binding properties. This reaction method allows the attachment of a linker unit directly to the aromatic core of the catecholamine rather than through existing functional groups.

1.2.2.3.2 Catecholamine Conjugate Chemistry for Binding Studies

There have been very few studies of catecholamine conjugates for antibody binding or raising of antibodies. Protein conjugates to epinephrine, nor-epinephrine, dopamine and L-dopa were developed to raise antibodies using conjugation by the Mannich technique,[172, 173] Figure 1.29. This technique suffers from the need to protect the amino group before conjugation. Miwa et al. have done this by maleylation of the primary amine but this will produce a secondary amine that theoretically could condense with an additional molecule of aldehyde and amine.[174] It is also possible for a Mannich base to condense with excess formaldehyde. A further problem is that the position of attachment cannot be determined with certainty in protein conjugation. A study was made on position of attachment when 4-methylcatechol is reacted with ethylamine by the Mannich reaction and found attachment at the 5-position,[175] but this is a very rough estimation and it is quite conceivable that multiple Mannich reaction products are formed that would greatly compromise the specificity and affinity of the antibody. Also, Mannich reaction without cationisation of the protein will take up to five

days. Dopamine antibodies were also raised using a Mannich conjugation to protein carrier.[176] The Mannich reaction has also been applied to production of protein conjugates of 3-methoxy-4-hydroxyphenylglycol (D-MHPG) in an analogous way.[177] Hirose et al. introduced the use of a caproic acid unit as the Mannich base with D-MHPG in a protein conjugate with isolation of the linker derivative and determination of position of attachment.[177] Position of attachment could not be determined if the reaction was done in one step as it usually is and if used with catecholamines bearing primary amine groups the amine groups would still need to be protected. The production of carboxyl terminals and subsequent NHS esterification and conjugation will give the most consistent and well-controlled conjugation and these terminals can be produced by either using the thioether derivative with carboxylic acid terminal or using the Mannich reaction with a heterobifunctional caproate unit as the Mannich base. With both of these techniques one can increase the length of the spacer by simply using different length thioacid or caproate chains. These conjugations direct to the aromatic ring are clearly beneficial for production of conjugated catecholamines without danger of compromising existing functional groups. It is therefore of interest to study their binding properties to antibodies to assess their efficacy as coating antigens in biosensors or as immunogens in protein conjugates or their receptor interactions to assess their efficacy as carriers of drugs or labels to receptor sites.

1.2.2.3.3 Purification of Catecholamine Derivatives

The catecholamine derivatives discussed are quite polar molecules. Dopamine is only freely soluble in water and slightly soluble in methanol, nor-epinephrine only freely in water and epinephrine is only freely soluble in acid or NaOH and KOH solutions.[178] Any direct ring-conjugation to a carboxylic acid terminating thioacid would not be expected to greatly reduce the polarity. This has posed a problem for researchers wanting to purify catecholamines from biological samples or to purify synthesised derivatives.

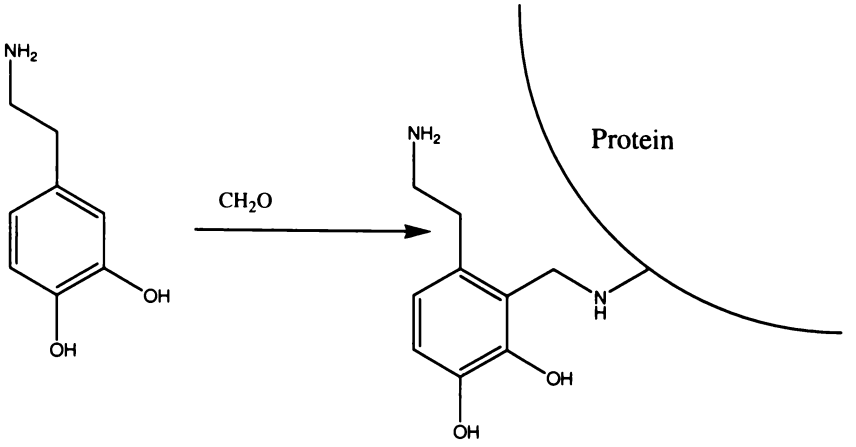

Figure 1.29 Mannich Condensation to Form Protein Conjugates of Dopamine

For catecholamines in biological samples the method of choice has been ion-exchange chromatography.[179] This has been applied in the HPLC format[180] and as a separate gravity or low-pressure column.[181] The low-pressure system used with success uses a strong cation exchange column and elution of the compound with acid/organic solvent mixtures,[181] Figure 1.30. The organic solvent serves to compress the volumes of elution. The acid used is 4-6 N aqueous HCl and the solvent is ethanol.[181] It is also possible to elute such columns with NaOH[182] but this may cause problems with base degradation of compounds. The ion-exchange columns have only been employed for low concentrations of catecholamines. The method preferred for purification of synthesised catecholamine derivatives appears to be preparative reversed-phase HPLC[169] but this is often a very time-consuming process that will yield only small amounts of product and often requires many repeated runs to get that small amount of product.

From this background one can see that there is an opportunity to produce thioether-linker straight-chain catecholamine derivatives connected via the aromatic ring directly and with an acid functionality that could be equally used in protein conjugations and as a connection point for labels or drugs. It would also be of interest to study the antibody or receptor binding properties of these analogues using the SPR capabilities of BIAcore and compare them to those conjugated via existing functional groups on the catecholamines.

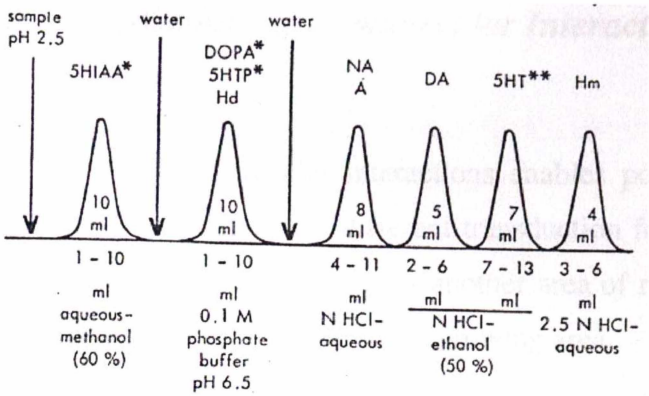

Figure 1.30 The Separation of Catecholamines by Gravity-Fed Ion-Exchange Column[181]

1.2.2.3.4 SPR Studies of Receptor Binding

The advent of SPR technology has enabled real-time biointeraction analysis for the binding of receptors to catecholamine targets. However, there are no papers that report the use of this technique for catecholamines. A possible reason is that most such studies are done in vivo and as such cannot be done in an SPR format. A number of different methods have been used for receptor binding studies and perhaps the most common is the use of radiochemical techniques. In such methods a cell clone sample expressing the desired receptor is incubated with a ^{3}H-labelled antagonist for the receptor. The receptor / antagonist complex is then incubated with the sample and the sample displaces the radiolabelled antagonist in proportion to its affinity for the receptor. The dissociation constant (K_d) can be determined by comparison of the radioactivity after a set time to that of the original radiolabelled antagonist before sample incubation.[183] Such tests are now nearly routine and this technique has become the dominant research method.[184, 185] Biomimetic chemical receptors for the catecholamines have been tried in biosensors[186] and evanescent wave biosensors have been developed for detection of adrenaline by absorption of the evanescent wave by adrenaline oxidation products at a Laccase interface.[187]

1.3 Nanoparticle Labelling of Biomolecular Interactions

Nanoparticle labelling of biomolecular interactions enables potentially large increases in binding signal in a number of different transduction formats such as surface plasmon resonance (SPR), and this forms another area of research in this thesis. This section summarises the research in this growing area.

1.3.1 Nanoparticle Labelling

The growing field of nanochemistry has embraced the labelling of biomolecular interactions such as the binding of complementary strands of DNA, of antibodies and antigens, of receptors and targets and of host / guest interactions. Perhaps the most wide spread applications of this nanobiochemistry are in two areas:

1. Self-assembly of nanoparticles

2. Signal enhancement of biomolecular interaction analysis systems

The first area involves using biochemical binding, principally complementary DNA interactions[188] and antibody / antigen[189] analysis to assemble nanoparticles that are connected to them to produce nanoscale structures or more generally changes in the order or spatial arrangement of the nanoparticles. This is a very new and fast developing area that has already been employed in the detection of small quantities of specific oligonucleotide strands[190] through self-assembly of gold colloids by binding of complementary strands (Figure 1.31).

The second area is of relevance to this thesis and makes use of a wide range of different nanoparticle properties to detect binding interactions with much improved sensitivity. Perhaps the most widespread application of this is the use of gold colloids[192] and fluorescent nanocrystals[193] to amplify binding in microarrays for the purpose of high-throughput screening or in biological imaging. The use of gold colloid labels in histology for staining of tissues has

been well developed and employs immunolocalisation to target nanoparticles to specific regions of tissues.[194] The developing field of surface-enhanced raman spectroscopy (SERS) is also utilising nanoparticle localisation.[195] An area of emerging interest is the use of nanoparticles as labels to enhance the signal from biomolecular interactions detected by surface plasmon resonance (SPR).

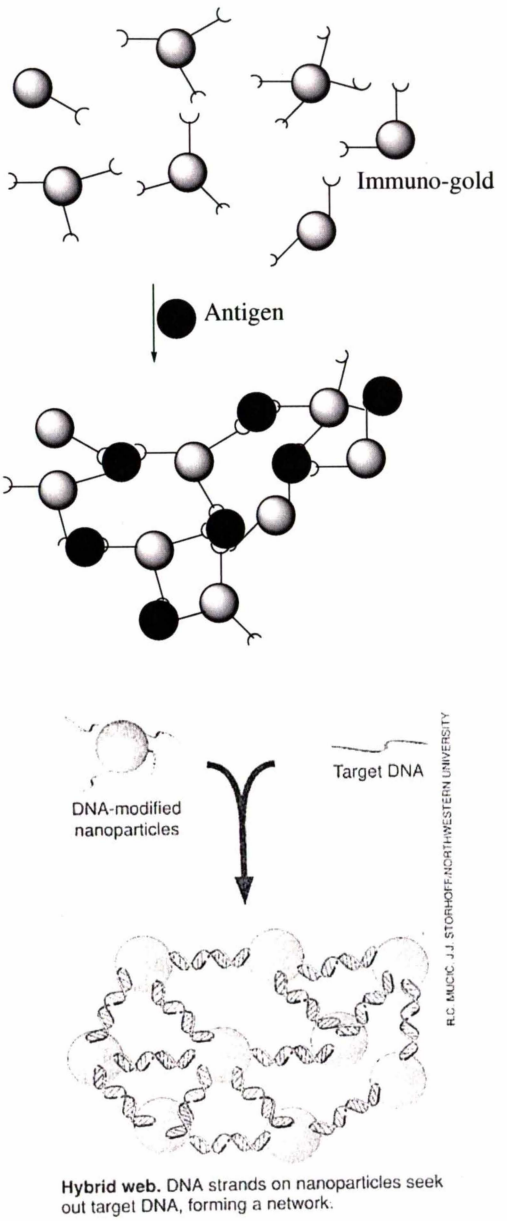

Figure 1.31 Top: Antibody/Antigen Interactions to Order Gold Nanoparticles, Bottom: DNA Interactions to Order Gold Nanoparticles[191] (from R. C. Mucic, J. J. Storhoff / Northwestern University).

1.3.2 Nanoparticle Enhancement of SPR Signal

The detection of small molecule binding interactions by SPR is very challenging in that the small molecules by virtue of their small mass produce only very slight changes in refractive index of the surface upon binding. Binding of a small molecule (<2 kDa) will typically produce RU changes of 10-50 RU at most[196] and often needs a dimethylsulfoxide (DMSO) component to ensure solubility.[196] There have been some reports using gradient immobilisation (multiple flow cells with different amounts immobilised) for low molecular-weight antigens binding to immobilised antibody but this method still produces very low sensitivity.[197] There are two potential ways of overcoming the problem of low signal. The first is to immobilise antigen and detect the compound by using antibody binding to the surface[10] and the second is to tag the binding agent (antigen or antibody) with a high mass label that will enhance the observed binding signal intensity.

Enhancement of binding signal intensity in SPR has two functions in improving biosensor sensitivity. The enhancement will increase the slope of the calibration curve allowing for finer distinction of different concentrations and secondly it will allow lower concentrations of bound material to be distinguished from the background. In short, the enhancement increases the changes in resonance angle ($\Delta\theta_r$) enabling one to measure this change more accurately. In the case of a sandwich immunoassay, this means that smaller concentrations of analyte bound can be distinguished from zero analyte bound as the bound analyte signal is amplified. For inhibition assays such as those for small molecules, the signal enhancement will mean that smaller amounts of inhibition will be able to be distinguished from 100% bound. In both these cases, signal amplification should result in a drop in detection limit.

The signal that is obtained upon the binding of a large molecule or binding complex in solution to an immobilised SPR chip surface agent is dependent upon several factors:

1. The total mass of the chemical entity binding to the surface, the larger the mass the greater the response

2. The extent to which the binding agent is able to undergo surface plasmon resonance itself

3. The distance of the binding agent's centre of mass and / or surface plasmon resonance active component from the gold surface.

A number of different types of nanoparticle have been suggested for use as signal enhancement tags. These include liposomes, latex particles, proteins and gold colloids. The first three classes of tag rely solely upon their large mass to induce larger changes in refractive index on the gold surface and hence enhance biomolecular binding interaction signals. The gold colloids however are capable of employing not only large mass but also a reinforcing SPR effect in the nanoparticles themselves that will yield an enhancement much greater than that expected by mass increases alone.

Liposomes (large membrane-like spherical units that assemble from phospholipid molecules) have been used to enhance signal (Figure 1.32). Liposomes range in size from 100-1000 nm and Wink et al. have used them as labels of protein immunoassays by immobilising antibody, passing protein antigen and then antibody again (*i.e.* sandwich format) which is biotin-labelled. Avidin is then used as a bridge from biotinylated antibody to biotinylated liposome.[198] Under this format the slope of the calibration curve has been raised to ~40,000 times that of the un-enhanced calibration curve and the detection limit dropped by over three orders of magnitude.[198]

Latex particles have also been employed and can be used in one of two ways. The first is in the same way as liposomes, as a high mass label of the binding interaction and secondly, as a means of increasing chip surface area available for immobilisation and thus increasing the binding sites on the chip and thus allowing greater binding. In the first case, latex nanoparticles ranging from 40-210 nm have been used with a refractometric transducer to give enhancements of five-fold over unenhanced sandwich immunoassay for thyroid stimulating hormone and a greater than three orders of magnitude reduction in the detection limit.[199] In the

later case, the molecular capacity of the evanescent field can be increased by increasing the effective sensor area.[200] This can also be done by use of a hydrogel matrix.[201]

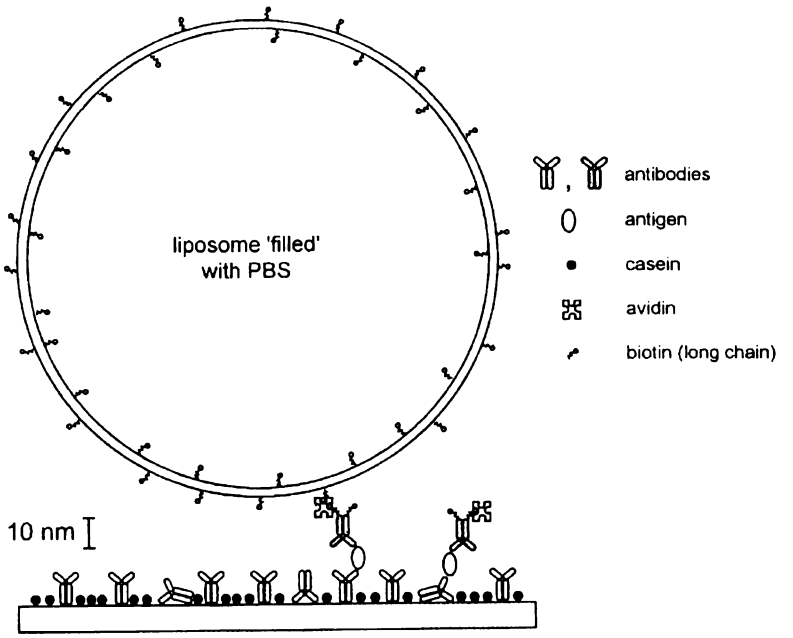

Figure 1.32 Liposome-Enhanced SPR Binding[198]

Proteins can also be used as high mass labels for binding interactions. Such a system was employed to label the binding interactions of progesterone with its immobilised antibody by forming a protein conjugate[10,15] and indeed this is an effective method for detecting small molecules whose binding to immobilised antibody would otherwise be undetectable, but is limited by the size that the protein can get to before steric crowding prevents approach of the conjugated small molecule to the surface and is also limited by the limited ability of proteins to increase antigen mass. The enhancement will at best bring the small molecule antigen up to the signals obtained for un-labelled protein assays. A better system of labelling is to use a protein label as a secondary label that recognises the bound complex. This can be done for antibody immobilised on a chip, binding of protein antigen, binding of antibody again in a sandwich format and then addition of a protein label such as a secondary antibody, or streptavidin to a biotinylated antibody. Such a system has been employed for DNA interactions whereby a

DNA strand is immobilised on the surface and binds a biotinylated complementary strand, which is then labelled with streptavidin to enhance mass and signal.[202] Here, a four-fold improvement in detection limit is observed. Amplification has also been achieved by immobilisation of an enzyme on the sensor surface with competitive binding between an inhibitor and a biotinylated target and signal amplification by anti-biotin antibody.[203]

As well as the attachment of labels, the use of improved transducer technologies has also led to an enhancement of signal. These include the use of a resonant mirror[204] or a grating coupling.[205] Perhaps the one method of signal enhancement that has received the most attention though is the use of colloidal gold nanoparticles as signal enhancement agents. Colloidal gold nanoparticles employ surface plasmon resonance effects within the colloid as well as mass effects to gain signal enhancement. Some understanding of the physics of this process is required.

1.3.3 Physics of Gold Colloid SPR Signal Enhancement

The basis for much of the gold enhancement effect lies in surface plasmon resonance coupling between the gold nanoparticle and the gold film of the SPR chip. Each gold colloid nanoparticle has an enhanced electric field that can be many orders of magnitude higher than the incident fields.[206] These fields are caused by the surface plasmon resonance induced by incident radiation. These fields are confined to a small distance out from the nanoparticle surface, typically weak beyond 300 nm, and thus produce a very strong field gradient.[206] When a gold nanoparticle approaches another gold domain such as the gold sensor surface or another gold nanoparticle these electric fields can overlap and the surface plasmon modes couple to each other (Figure 1.33). This strong optical coupling then produces a large shift in refractive index and thus in plasmon angle that is much greater than would be expected from a simple mass increase. These changes in the corresponding SPR curve are ~25 times larger than those observed in binding without the gold colloid.[207] Theoretically, if the gold colloid coating is such that colloid nanoparticles are close enough to each other to couple then a

continuous evanescent wave can move down both gold film and through the gold colloid layer. Studies have shown that such coupling produces a large shift in plasmon angle, a broadening plasmon resonance and an increase in minimum reflectance, all of which results in increased SPR sensitivity.[208]

Naturally, this coupling interaction is very much dependent upon the distance of the gold colloids from the gold film surface. If the colloids are far away from the surface then no coupling of electric fields is possible and so no plasmon resonance signal enhancement will be observed. This factor must be considered when constructing biosensor formats based around this phenomenon. Research has been done on using poly-ion multilayer spacers to calibrate the distance dependence of the SPR effect when applied to organic separation layers.[209] The coupling distance between the gold film and the labelling nanoparticles can be optimised and researchers have utilised this to space the nanoparticles at the optimum distance from the chip film by use of a 30 nm SiO_2 layer immobilised upon a gold film surface of 50 nm.[29] Another factor that will have a great effect on the plasmon angle shift is the size and shape of the gold nanoparticles. It has been found that as the colloidal gold diameter increases from 30-59 nm on a 47 nm thick film, the plasmon angle, minimum reflectance and curve breadth all increase with increasing nanoparticle size and coverage until a plateau is reached when SPR attenuation is maximised.[210] The relationship between colloid size and the mean free path (MFP) of the plasmon electrons is also important. Plasmon bandwidth will increase as the colloid size decreases below the MFP and increases with increasing size above the MFP.[211] It has also been found that the extent of the sensing distance range out from a gold nanoparticle surface can be tuned by adjustment of the composition, shape, in-plane width and out of plane height of the nanoparticles.[212] As well as gold colloids, silver colloids can also undergo SPR but are not as extensively used principally because of the difficulties of producing stable silver colloids. Studies have also been done on the effects of changing either substrate film or nanoparticle from gold to silver using 2-aminoethanethiol immobilisation.[213]

1.3.4 Gold Nanoparticle Enhanced Binding in SPR

The use of gold nanoparticles for SPR enhancement of binding interactions falls into two main areas:

1. The analysis of oligonucleotide binding interactions and their applications to oligonucleotide assays

2. The analysis of the binding between antibodies and large size antigens, *i.e.* proteins and oligopeptides

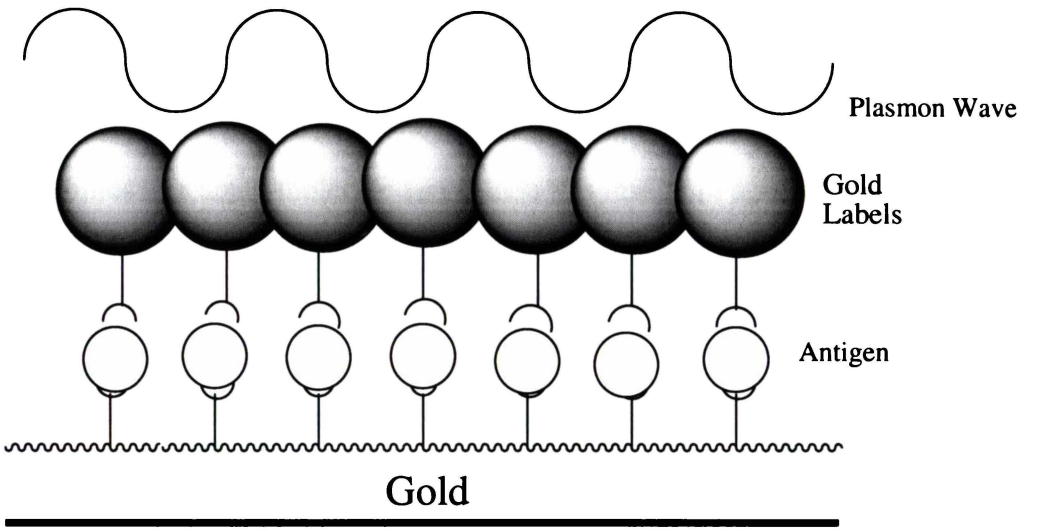

Figure 1.33 Schematic of the gold nanoparticle enhancement effect in SPR showing overlapping gold electric fields (which also overlap with the gold surface) and the plasmon wave (offset)

The sensitive detection of oligonucleotides is of great interest for the rapid diagnosis of many genetic diseases. SPR has been used to detect DNA for some years but it is only comparatively recently that work has been done using gold nanoparticles to label the binding interactions between complementary strands for the purposes of signal enhancement. He et al. used oligonucleotides linked by either a thiol terminus or a biotin / streptavidin linkage to gold colloids of 12 nm diameter and obtained signal enhancements of more than 1000-fold over the un-

labelled and a detection limit of ~10 pM[214] (Figure 1.34). Further work has utilised gold "nanoislands" immobilised on glass for hybridisation detection through thioether-mediated coupling[215] (Figure 1.34). The use of gold labelling of DNA interactions has been patented.[216, 29]

Antibody / large antigen interactions with gold enhancement have been studied for somewhat longer. Gold amplification is applied to sandwich immunoassay formats (Figure 1.35). Studies include detection of immunoglobulin G where a 25-fold signal enhancement and picomolar detection was observed for binding of an ~11 nm colloidal gold label.[207] IgG Fab' fragments have been immobilised upon the gold sensor surface and anti-IgG antibody added labelled with 40 nm gold.[217] This gave reported sensitivity enhancements of about 300-fold.[217] Gold labelling of binding proteins has also been applied to high-throughput screening applications that exploit the SPR effect of the nanoparticle.[218] When the binding protein binds to a small molecule target then this results in a shift in the SPR band of the gold and has been utilised in simple photometric type experiments in association-dissociation assays.[218] It has been concluded that clustering of gold colloid particles leads to greater signal enhancement in SPR.[219] Gold-labelled secondary antibodies have been applied extensively in formats such as the Nycocard colorimetric system and binding properties have been assessed using BIAcore with binding to a capture antibody.[220] Technologies have been patented for the use of small gold colloids to amplify the signal when attached to large-size antigens binding immobilised antibody in competitive assay.[216] Another format developed has gold labelling of antibody and binding in a sandwich assay format with immobilised antibody.[216] These systems use small gold nanoparticles to diffuse into the system and then amplify the size by attachment of Ag nanoparticles.[216]

To date there have been no reports of gold nanoparticle-enhanced binding responses in SPR for small molecule immunoassay. There has only been one paper that employs gold labelling of small molecules for SPR studies.[221] This example uses tiopronin-capped gold nanoparticles to label *N*-(3-aminopropyl)-*N*'-methyl-4,4'-bipyridinium to follow electrochemical deposition of the modified gold upon the SPR gold surface and in amplified SPR detection of nicotinamide

adenine dinucleotide NAD(+) and NADH cofactors.[221] This detection is by indirect means through the NAD^+ / NADH redox couple with the bipyridinium causing changes in bipyridinium oxidation state and thus level of electrochemical deposition on the surface. This paper makes no mention of the enhancement degrees obtained, and has detection ranges that are quite poor ($1x10^{-4} - 2x10^{-3}$ M) and uses an indirect technique for assay by using partial biocatalyzed dissolution of the bipyridinium radical cation film in the presence of diaphorase.[221] Some papers have made allusions to the ability of reported systems to be adapted to function for small molecule immunoassay but this has not been followed up by reported research.[217, 207] There are several possible reasons for this:

1. Small biomolecules are easily sterically swamped by the larger gold colloids and so methods have to be constructed such that the small molecule labelled with gold can still bind the antibody to an appreciable extent.

2. The small molecules cannot be immobilised directly upon the sensor surface as can proteins and so some linkage needs to be constructed to bind them to the surface either via a protein or through some other intermediate linker.

3. The proteins can be bound intimately onto the surface of the gold colloid and cover it but the small molecules are constrained to being attached by intermediates which could push the gold colloid too far away from the gold of the chip and thus spatially prevent enhancement effects.

4. The small molecules cannot be assayed in a sandwich format and as such the gold enhancement will only help in indirectly detecting free antigen / antibody binding, forcing the detection to be by inhibition.

5. Small molecule antigens cannot block the surface of the gold colloids in the way that large molecules can and so special blocking and regeneration procedures may need to be used if antigen-colloid conjugates are used.

6. The regeneration of the colloidal gold-small molecule systems may introduce problems with the strength and nature of regeneration cocktail needed and surface stability under regeneration.

Another point to note is that the existing gold colloid enhanced immunoassay research has not used the BIAcore format except for that of Johne et al. who have used it in analysis of their Nyocard conjugate.[220] The other studies have rather relied upon in-house SPR systems where it is possible that there has not been the same degree of system control as is possible with BIAcore. The principle reasons for use of in-house systems is that they circumvent patent considerations around immobilisation by dextran layer and also the dextran layer can in some cases cause problems in enhancement due to its thickness (about 100 nm from the gold film) pushing the gold colloid further out from the gold film of the sensor surface. Another possible limitation is that specific binding sites on the surface may not be accessible to larger molecules such as proteins or larger labels such as gold colloids as the dextran forms a three-dimensional array out from the gold film surface and thus one can get non-specific binding of proteins to the dextran layer.[29] A major drawback in not using the dextran layer or some other equivalent coupling matrix is that SPR reflectivity changes within uniform substrates, such as monolayers of bifunctional organic cross-linkers, are quite often so small as to be undetectable.[29]

1.3.5 Immobilisation, Regeneration and Linkage Technologies

In any consideration of gold labelling of binding interactions for small molecules the methods of immobilisation, regeneration and the linkage technologies for labelling will be critical. Immobilisation for the protein-based nanogold-enhanced systems has employed immobilisation of an alkanethiol layer on the naked gold film that is carboxylate-modified, *e.g.* 3-mercaptopropionic acid (MPA), and thus uses carbodiimide coupling to the immobilised protein.[207] Alternatively, modification with a straight chain thiol amine followed by treatment with *N*-succinimidyl-3-(2-pyridyldithio)propionate enables antibody

fragments to be attached via a disulfide linkage.[217] Immobilisation of small-molecule antigens would naturally require a specific chemical spacer and immobilisation technique to project the antigen from the surface and thus eliminate the steric constrictions of the gold film surface, or dextran matrix if used. Other linkers used in non-gold-labelled applications include 11-mercaptoundecanoic acid (MUA) linkers for proteins[222] and stable chelating *N*-(5-amino-1-carboxypentyl)iminodiacetic acid (NTA) linkers allowing reversible immobilisation of oligohistidine tagged proteins.[223] Some general immobilisation linkers are shown in Figure 1.36.

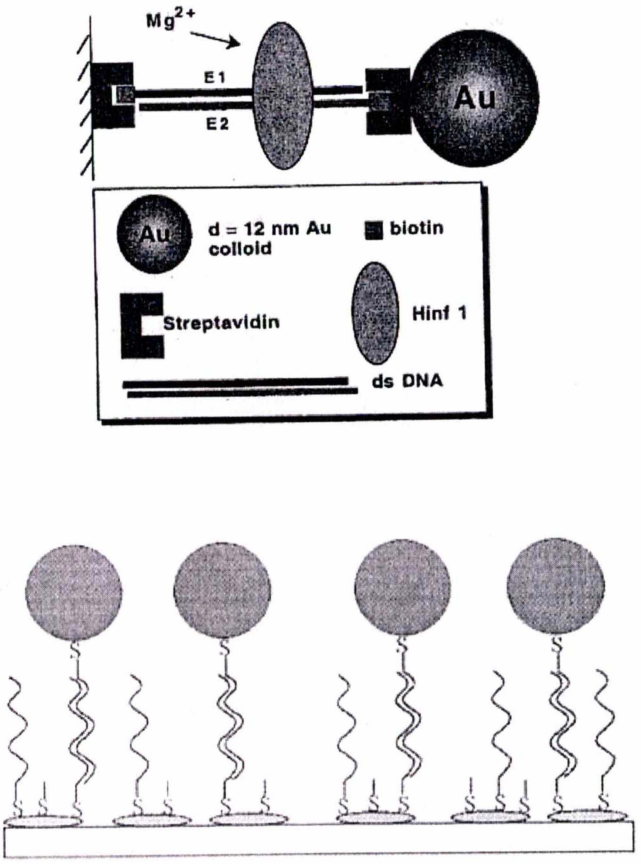

Figure 1.34 Gold Nanoparticle Enhanced SPR of DNA Binding. Top: Streptavidin / Biotin Binding for Labelling of Complementary Strands.[214] Bottom: Gold Nanoisland Method[215]

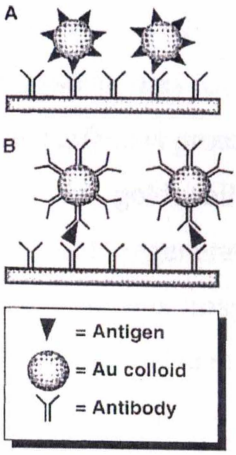

Figure 1.35 Gold-labelled Competitive SPR Immunoassay (A) and Sandwich SPR Immunoassay (B)[207]

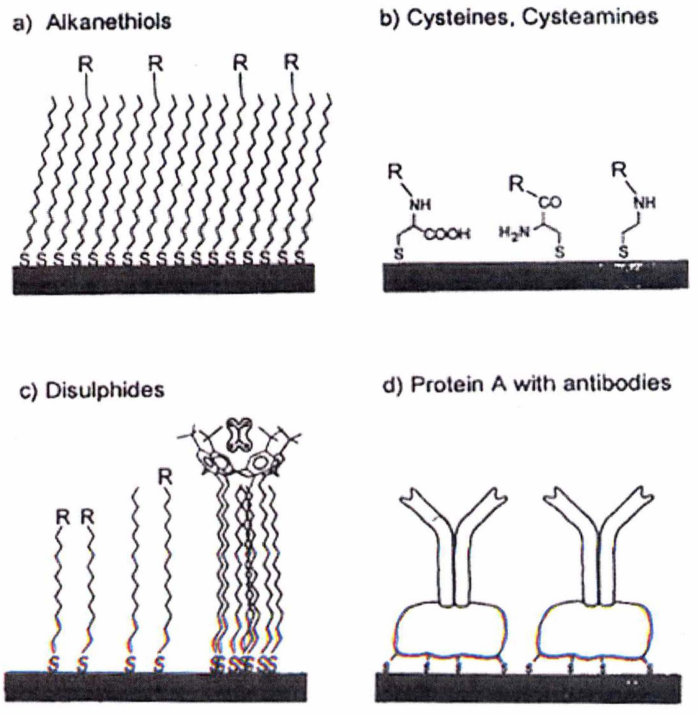

Figure 1.36 Various Thiol-Terminating Linkers used for Spatial Distancing of Binding Agents from the Gold Surface[224]

None of these papers include mention of regeneration of the surface after gold label binding except that of Johne et al. who used a 100 mM HCl regeneration pulse between sandwich assays.[220] The reason for lack of reference to regeneration methods is unclear, but clearly to develop a biosensor that will be of

practical use the system must have reliable regeneration steps. The introduction of large nanoparticles into the system may conceivably lead to problems of surface stability, particularly if the surface is protein-functionalised. This is due to non-specific interactions between the gold colloid and the surface removing immobilised material or if stronger regeneration conditions (compared to unlabelled proteins) are needed then this may lead to chemically induced degradation of the immobilised surface. There are a number of regeneration cocktails that have been considered with perhaps the most common being 10-100 mM HCl or 10 mM glycine pH 1.7-2.2.[225] It is critically important to ensure complete regeneration of the surface or the surface properties will not be constant and there will be drift changes from assay to assay.

There are a number of linkages that can mediate the gold binding interaction. These linkages can be constructed before the assay or some biomolecular interaction used to mediate the gold colloid attachment in situ. Perhaps the simplest technique is to immobilise antibody or protein antigen electrostatically on the surface of the colloid by simple pH adjustment of the colloid to mildly basic pH and then to add protein and briefly incubate and then block with some other protein such as BSA.[90] Another possible method is use of the biotin / streptavidin linkage to label the antibody or protein. In this case biotinylated antibody can be incubated with streptavidin or avidin-coated gold colloid and the resulting complex used as the labelled binding unit in the assay. Biotinylation of antibodies is a well established technique[90] though has the disadvantage that it has been known to interfere with antibody recognition in protein / antibody interactions using BIAcore.[226] The biotin / streptavidin interaction is the strongest non-covalent binding interaction known in nature and has been widely used with nanoparticles in a range of formats such as organisation of iron oxide nanoparticles in ferritin.[227] Streptavidin-gold labelling of biotinylated antibodies has been employed in staining of tissue sections[90] (Figure 1.37). Furthermore, the streptavidin / biotin interaction can be utilised to immobilise steroidal antigens in SPR with the streptavidin functioning as a molecular spacer unit.[228] The use of streptavidin-gold conjugates is extensive and some are commercially available.[229]

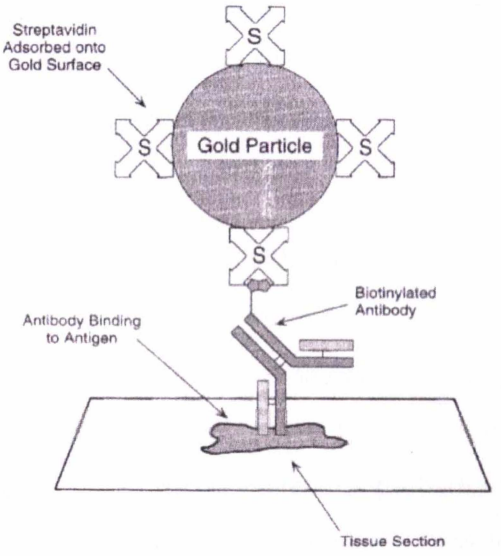

Figure 1.37 Streptavidin-Gold Labelling of Biotinylated Antibody[90]

1.3.6 Gold Nanoparticle Production and Modification

The production of gold nanoparticles with reproducible mean diameters was first made possible with the work of Frens in developing citrate reduction of gold colloids.[230] By adjustment of the volume of citrate solution added to a solution of $HAuCl_4$ one can adjust the mean colloid diameter from 1.6 nm to 147 nm.[230] Colloids of high size are more difficult to reproduce due to the low citrate quantities having less control in blocking the aggregation of colloid particles. The mean particle diameters can be determined by transmission electron microscopy (TEM) through taking microscope pictures and measuring diameters on the images compared to reference standards run at the same time. Usually this will require at least 100 readings to determine the average. Another possible alternative is the use of photon correlation spectroscopy (PCS) that has been extensively developed for the measurement of mean particle diameters.[231] PCS obtains particle size data by examining the different velocities of different sized particles undergoing Brownian motion. A correlator analyses the variable intensity of scattered light with time to determine particle size. This technique has been applied in the commercial instrument known as the Malvern Zetasizer™ that involves placing the sample in a four-directional cuvette under temperature

control and taking a series of readings after having first established a correlellogram for the sample.[232] These readings give the average particle size, and multiple readings on different sub-samples can give an estimation of particle size spread.

Once produced, these nanoparticles then need to be immobilised with the binding partner required for the labelled interaction. Immobilisation of functional groups has been done via a wide range of methods including modification with 2-mercaptosuccinic acid to present carboxylic acid functions at the surface.[233] Immobilisation of proteins direct to the surface is probably the most widely used system and is adequate in most cases for antibody binding to a gold label. Other possibilities as well as the use of ionic interactions include the use of hydrophobic interactions and the formation of dative bonds through thiol groups either originally present or introduced to the antigen or antibody (Figure 1.38).

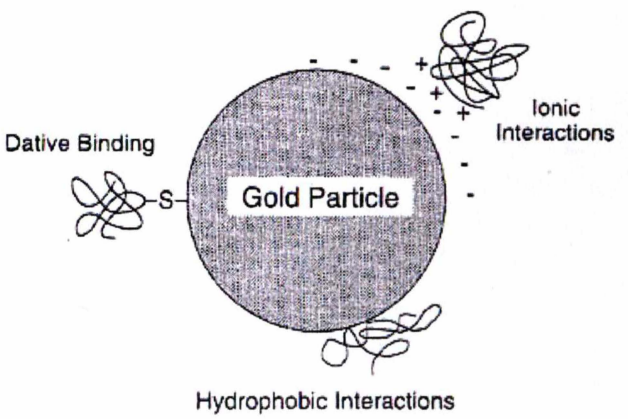

Figure 1.38 The Methods of Conjugation to Gold Nanoparticles[90]

Non-specific binding to gold nanoparticles can be a problem when developing gold-labelled complexes for immunosensing and there has been some investigation of ways of minimising it.[234] Another factor to consider is the need to prevent aggregation of the gold colloid particles, which is a particular problem when using larger gold nanoparticles. A number of methods have been investigated for preventing this. The use of protein coating such as coating with

BSA is quite common. Polymers have been shown to prevent aggregation and polyethylene glycol is a major example because of its water solubility and the ability to terminally functionalise it with such groups as mercapto and acetal terminals.[235] PEG and protein immobilisation stabilise the gold colloid through steric repulsion effects. Varying amounts of PEG added at formation of the colloid can vary the size of the colloid produced and PEG terminals have even been functionalised with biotin to enable streptavidin-induced aggregation of the gold colloids.[236] PEG has been used extensively in the surfaces of biomedical devices because it increases biocompatibility and reduces thrombogenicity[237] and has been extensively used for protein modification and is highly suitable for the formation of drug carriers or in antibody or receptor binding targets because of its suppression of protein binding, low toxicity and because it is non-immunogenic and is very biocompatible.[238] PEG has also been used as a linker in the modification of antigens for labelling with biotin in streptavidin/biotin systems and could potentially be used to label antigens with colloidal gold-streptavidin (Figure 1.39).

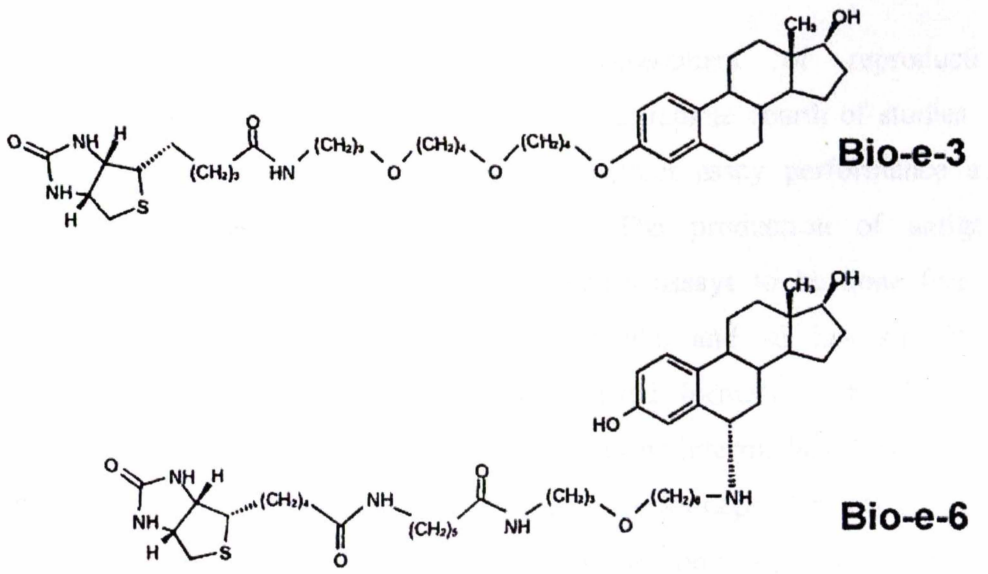

Figure 1.39 Biotinylated Estradiol with PEG linkers[228]

It is clear that the development of gold nanoparticle-enhanced immunoassay of small molecules by SPR is of great benefit in the development of more sensitive

immunoassays for these compounds by SPR. The development of such a system clearly poses significant challenges for the chemist in terms of gold colloid linkage, assay formats, regeneration and surface immobilisation.

1.4 Research Aims

1.4.1 Opportunities

The field of biosensing technology is a vast and rapidly growing one where there is much scope for the development of new and improved assay systems, chemical modification of targets and technologies that will enable the production of more robust and practical biosensors. In order to improve biosensors and develop new ones it is very important to have a fundamental understanding of the binding interactions that are taking place and the ways that changing chemistry, format and kinetics change the performance of antibody / antigen and receptor / target interactions and thus influence biosensing assays.

Milk progesterone determinations for assessment of reproductive endocrinology are widespread, however there is a complete dearth of studies on how changing assay format and medium will affect assay performance and antibody / progesterone binding behaviour. The production of antigen-immobilised ELISA for milk progesterone enables assays to be done free of enzyme-antigen labels and their inherent problems and so has significant advantages over conventional antibody-immobilised formats. The study of antibody binding patterns in whole milk with increasing intermediate linker length enables comparison to aqueous results to observe media-dependent effects. The assay performance can then be assessed with these conjugates to give greater understanding of the medium-dependent effect influencing antibody binding patterns in whole milk ELISA.

Estrogens have been traditionally labelled via existing functional groups or via epimeric positions on the molecule. There have been no immunoassay or antibody binding studies done with regioselective attachment at the 4-position of

estradiol and estrone in flow-through formats despite its demonstrated superior antibody binding in flow-through formats for progesterone. This gives the possibility of novel aromatic substitution chemistry to produce thioether conjugates with water-soluble intermediate linkers and then subsequent analysis of antibody binding in flow-through SPR formats.

The catecholamines have been extensively studied for their receptor binding properties yet conjugates attached directly to the aromatic ring have not been studied for antibody or receptor binding. By thioether bridging to the aromatic ring it is possible to form such conjugates without the inherent problems of the Mannich reaction. Through ion-exchange chromatography and HPLC analysis it should be possible to purify these compounds and then apply them as immobilised targets to assess their antibody binding properties by SPR.

Small-molecule assay by SPR is a burgeoning field and yet whilst there have been a number of studies employing nanoparticles in labelling of large-molecule binding interactions, there have been no studies for small-molecule / antibody binding interactions. There is clearly an opportunity to develop the chemistry necessary to produce such gold nanoparticle-enhanced assays with respect to assay format, labelling technologies, surface immobilisation and regeneration to produce a practical biosensing system.

1.4.2 The Objectives of the Project

The objectives of this project can be divided into four separate but interrelated areas. All of these areas of research are devoted to the same set of basic research aims, which can be summarised as:

1. To develop fundamental understanding of how changes to parameters in a small biomolecule immunosensing system produce changes in the performance of this system. The parameters may include sample medium, intermediate linker length and/or chemical identity, position of modificational attachment to antigens or targets, and the nature of any

labels. Performance of the system may be assessed by factors such as detection limit, sensitivity and active assay range.

2. To develop new immunosensing formats for small biomolecule targets that utilise innovative chemistries to produce substantial improvements in the immunosensing system.

3. To develop fundamental understanding on how chemical modification of targets affects the binding properties of the target to antibodies or receptors.

1.4.2.1 Protein Conjugate-Based ELISA of Whole Milk Progesterone

Progesterone-ovalbumin conjugates with different length intermediate linkers will be applied as coating antigens in ELISA plate immunoassay of cow whole milk progesterone. The linker lengths will be four, 11, 18 and 25 atoms long. The patterns of binding to antibody and comparison of the assay performances of these conjugates will be determined. An ELISA for whole milk progesterone will be validated based on this data and compared to existing RIA methods. It is envisaged that as well as eliminating antigen-enzyme conjugates this assay will require no pre-dilution of milk and will deliver more than adequate accuracy and precision for estrus monitoring and pregnancy prediction.

1.4.2.2 Introduction of Carboxylate Linker Groups by Thioether Derivatisation of Bromoestrogens with Mercaptopropionic Acid at the Aromatic A-ring – Synthesis and Antibody Binding Studies

The estrogens, 17β-estradiol and estrone will be conjugated by formation of thioether linkages at the 4-position on the aromatic A-ring by substitution of the corresponding bromo-compounds to produce 3-mercaptopropionate derivatives, which can then be further derivatised by attachment of water-soluble OEG or PEG linkers of varying length. These derivatives will then be used as immobilising

antigens in SPR studies of their binding interactions relative to hemisuccinate and Mannich conjugated controls.

1.4.2.3 Introduction of Carboxylate Linker Groups by Thioether Derivatisation of Catecholamines with Mercaptoalkylcarboxylic Acids – Synthesis, Purification, HPLC Studies and their Antibody Binding Properties

Thioether derivatives of the catecholamines dopamine, nor-epinephrine and epinephrine will be synthesised from the corresponding *o*-quinones, purified by ion-exchange chromatography or conventional silica chromatography as required and analysed by HPLC to monitor their purification. The compounds will be analysed by nuclear magnetic resonance (NMR) spectroscopy to determine their attachment positions and assessed as antibody binding targets in SPR *vs* the equivalent amine-bound control. This work will provide new thioether linked carboxylic acid derivatives of catecholamines and yield information on the effect of attachment position on antibody binding. This work will be of potential future use in raising specific antibodies and designing catecholamine-transported drug candidates or biomarker compounds.

1.4.2.4 Gold-Enhanced SPR Immunosensing of Small Molecules

Methods for gold nanoparticle enhancement of small-molecule binding to antibody will be developed using progesterone as a model compound. Technologies for surface immobilisation, colloid stabilisation and regeneration will be developed. Different methods of gold linkage for labelling will be developed and the effects of different colloid size, assay format and immobilization level will be examined. The levels of signal enhancement will be systematically compared and assay performance and antibody binding properties will be determined in each case and related to enhancement of signal. The fundamental binding effects in this system will be examined for each format.

Chapter 2 – Protein Conjugate-Based Immunoassay of Whole Milk Progesterone

2.1 Introduction

Whole milk progesterone concentration is a well-established indicator of the bovine estrous cycle[239] and has been used extensively to help diagnose pregnancy.[66] By establishing a progesterone profile with time across the estrous cycle for each cow, the farmer can make decisions about timing of artificial insemination to coincide with the estrus phase. At the estrus part of the cycle, the progesterone concentrations are at their lowest, often around 0.5 ng/mL,[240] so being able to accurately identify these low concentrations is very important for successful insemination. Furthermore, by comparing milk progesterone concentration at the time of insemination at estrus to the concentration 21 days afterwards, the analyst can have a possible early indicator of pregnancy status. If the cow is still cycling then progesterone levels can be expected to be low again, and if pregnant, the progesterone levels will be high (5 ng/mL is one previously used cut-off[241]).

There have been a large number of immunoassay systems developed for milk progesterone, particularly in the enzyme-linked immunosorbent assay (ELISA) format. These ELISA systems have relied upon immobilisation of antibody to the plate and the use of progesterone-enzyme conjugates to compete with free progesterone in milk for binding to limited antibodies on the ELISA plate. Such conjugates have been demonstrated to be unreliable in their responses due to their multiple antigen bindings to one enzyme molecule, antigens obstructing the active site of the enzyme and chemical modification affecting the chemical environment and thus the performance of the enzyme.[92] This all results in quite variable enzyme performance, which is a major problem when using the enzyme to label un-bound sites, as for this one requires fixed and repeatable enzyme response per unit antibody bound. A further major disadvantage is the difficulty of purifying these conjugates, as this requires expensive and time-consuming affinity

chromatography that never completely purifies the conjugate. Un-conjugated residual enzyme will produce significant non-specific signal in the assay thus lowering the signal : noise ratio and reducing the sensitivity of the assay.

It is thus desirable to eliminate the antigen-enzyme conjugate, and this can be done by immobilisation of protein conjugate instead and competition between the protein conjugate and sample progesterone for limited monoclonal antibody followed by a secondary antibody-enzyme conjugate. This not only eliminates the antigen-enzyme conjugate but also improves the specificity of the assay by giving a higher "antibody cross-section" by having two specific binding interactions involved in labelling.[18] This is particularly important in complex biological media such as whole milk where other components may bind non-specifically. Furthermore, there is much less inconsistency in conjugation as the enzyme and antibody are closer in mass and so could be expected to conjugate in a much better defined ratio and the secondary antibody-enzyme conjugate is used in excess so all antibody-bound material will be maximally labelled. Removal of unconjugated enzyme label is potentially simpler as it could be done by dialysis with the smaller enzyme label being passed out through the dialysis membrane.

Further disadvantages with existing methods are that they usually rely on some form of pre-dilution of the whole milk or else some extraction of the milk, *e.g.* use of skim milk, de-fatted milk. These steps are highly labour intensive and inevitably result in a reduction in the tested concentration of the progesterone. Any attempt to remove fat from the milk may also result in inaccurate results as the lipophilic progesterone concentrates in the fat. Dilution is mostly done to gain consistent binding results with minimised fat interference. It would be advantageous if the development of a new format could largely minimise these interferences without the need for prior dilution.

Currently available ELISA systems also suffer from narrow dynamic ranges, *i.e.* the range of progesterone concentrations that the assay can detect. ELISA for milk progesterone have ranges no wider than about 1 to 30 ng/mL.[89] These ranges often are inadequate for fully profiling the estrous cycles of individual cows. Many cows have estrous cycle progesterone peaks of around 50 ng/mL and so existing assays tend to truncate the tops of the progesterone cycles. At the low end of the cycle, progesterone often drops as low as 0.1 ng/mL and so once again the lower parts of the curve are often truncated, making determination of the exact

point of estrus difficult. Exact determination of estrus is critical in timing of artificial inseminations.

There has been a great dearth of studies on the effects of fundamental changes to ELISA formats particularly in the area of protein conjugate-based immunoassay. There has been recent evidence that formation of protein conjugates to progesterone through the 4-position and the use of linkers up to 18-atoms significantly improves antibody binding ability in flow-through formats[10,15] but this has not been applied to the milk medium of ELISA so any medium-dependent linker length effects are not known. Caproic acid-based linkers may perform better in the high lipid medium of whole milk compared to water as they are relatively non-polar and so may orientate into the lipid phase. Protein conjugates produced in this way using an NHS-mediated coupling have been shown to be very consistent in hapten number and so lend themselves well to comparative studies of binding abilities. The protein conjugate structures used in this study are given in Figure 2.1

There have also been no reports of progesterone-protein conjugate-mediated ELISA of whole milk progesterone, despite protein conjugates being potentially more stable as coating agents for long-term storage relative to sensitive antibody and despite the ability of such a system to do away with progesterone-enzyme conjugates.

Reported below are the antibody binding relationships with increasing linker length up to 25-atoms in the whole milk medium, of a new protein-conjugate based ELISA format. The format uses ovalbumin (OVA) protein conjugated to progesterone at the 4-position via ε-aminocaproic acid linkers attached end-on-end via amide linkages to increment the linker length. Also reported are the assay standard curves and performance parameters for increasing intermediate linker length of protein conjugate in the whole milk medium. From this, the first reported protein conjugate-mediated ELISA for whole milk progesterone, one that requires no pre-dilution of sample, is developed and validated against an established RIA method and used to profile estrous cycles in the dairy cow. The test is also used as a rough predictive tool for pregnancy diagnosis in a small herd.

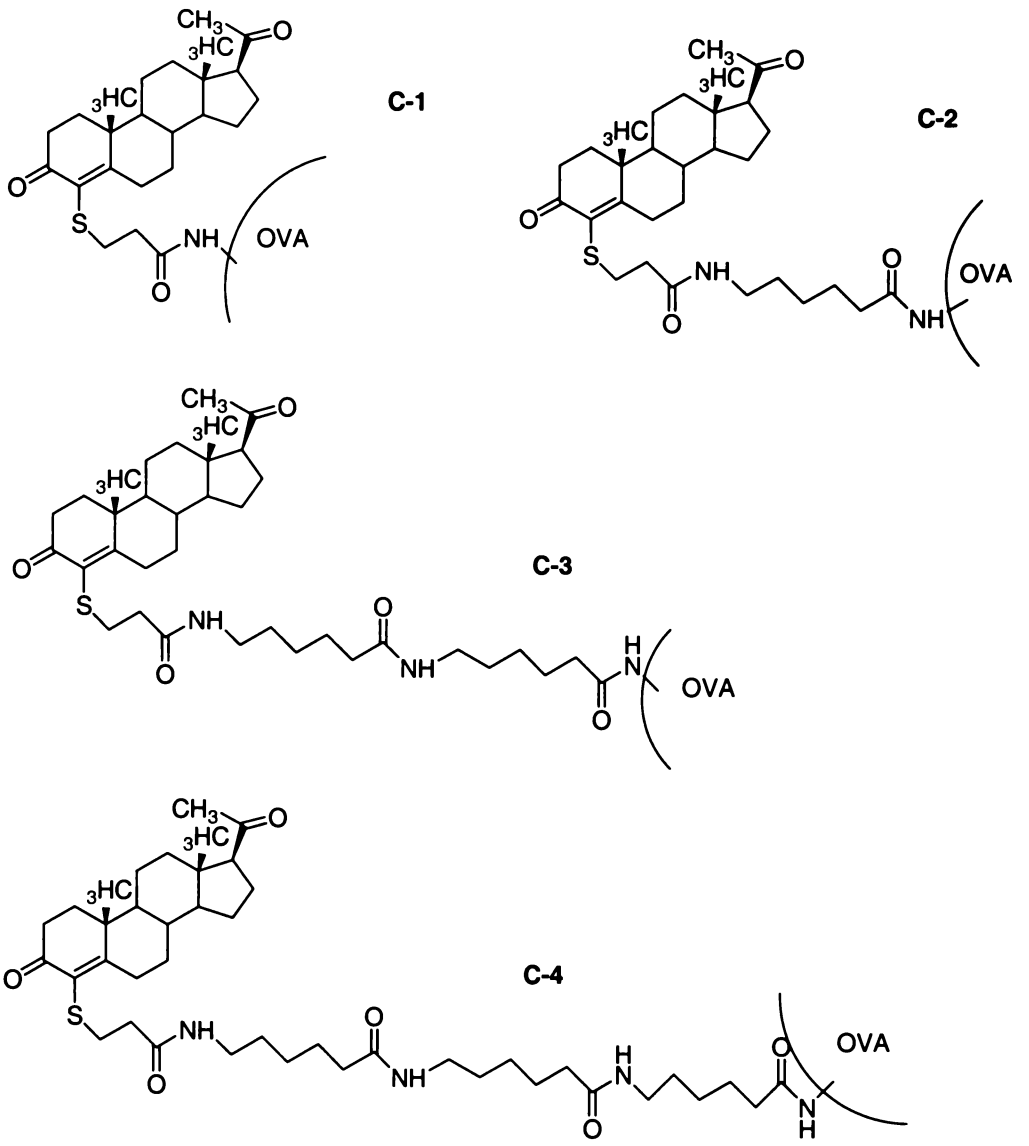

Figure 2.1 Progesterone – Linker – Protein Conjugate Structures

2.2 Experimental

2.2.1 Materials and Instruments

2.2.1.1 General

ELISA plates were Maxisorp (Nunc, Denmark). The buffers and substrate solutions were prepared as described in Appendix 1. All water used was ultra high quality (UHQ) deionised water. 3, 3', 5, 5'-Tetramethylbenzidine (TMB)

was from Roche (Mannheim, Germany) and hydrogen peroxide was from BDH (Poole, UK). The plates were read on an Organon Teknika Reader 230 S and washed on an Organon Teknika Microwell System Washer 430.

The monoclonal antibody from Sigma (St Louis, MO, USA) was raised to progesterone-7-BSA and was IgG1 Clone no. 2H4 derived from the hybridoma produced by the fusion of mouse myeloma cells and splenocytes from immunised rats (Sigma P1922). The secondary antibody-HRP conjugate was Anti-Rat IgG (whole molecule) Peroxidase (Sigma A5795) developed in rabbit using purified rat IgG as immunogen and conjugated to peroxidase by protein cross-linking.

Statistical analysis was done with the aid of Minitab 14.1 Statistical Software. Graphing was done with the aid of Origin 5.0 and Sigma Plot 8.0S. RIA was done by Dexcel Ltd. using a Coat a Count Progesterone RIA (Diagnostic Products Corp. Los Angeles, USA) validated for milk.[242]

2.2.1.2 Milk Samples

Whole milk samples were taken from New Zealand dairy cows of a variety of breeds but principally Friesian Holstein. All whole milk samples were collected directly from the cow at milking time in plastic sample vessels and were immediately preserved with potassium dichromate preserving tablets and then frozen. Once thawed (at 4 ^{0}C) the samples were used for measurement within three days and were not re-frozen. Blank whole milk was obtained directly from a cow 14 days after giving birth and was found by RIA to have negligible progesterone concentration. This milk was then spiked with a small volume of aqueous progesterone to give a 1 μg/mL stock solution, which was then serially diluted with the zero progesterone milk to give all the required standards for the assays. Milk standards were frozen until use and never re-frozen.

2.2.1.3 Progesterone – OVA Conjugates

Progesterone was conjugated via its A-ring 4-position through heterobifunctional caproate linker units linked end-on-end to produce linkers of 4-, 11-, 18- and 25-atoms. The progesterone-ovalbumin conjugates used in this section were synthesised exactly according to the procedures laid out in the

author's Masters thesis[10] and the concomitant paper.[15] The hapten numbers for these conjugates were exactly the same as those previously reported[10, 15] and are reproduced here in Table 2.1 as determined by matrix assisted laser desorption ionisation mass spectrometry with time of flight detection (MALDI-TOF). The protein conjugates will now be referred to by their numbers: **C-1** – 4-atoms, **C-2** – 11-atoms, **C-3**- 18-atoms and **C-4** – 25-atoms in the intermediate linker.

Table 2.1 Hapten Numbers of Progesterone Protein Conjugates

Progesterone-OVA Conjugates	Average MW	Hapten Number
OVA	44270	0
C-1	45850	3.9
C-2	46450	4.1
C-3	46830	4.1
C-4	45980	2.3

The lower number for the 25-atom conjugate occurs because the progesterone-linker derivative is not very soluble in the polar solvents needed for conjugation.

2.2.2 Antibody Binding Studies of Progesterone-Protein Conjugates in the Whole Milk Medium

Standard 96-well flat microtitre plates were coated with the progesterone – OVA conjugates **C-1**, **C-2**, **C-3** and **C-4** at protein concentrations of 0, 0.1, 0.5, 0.75, 1 and 5 μg/mL in 0.05 M bicarbonate buffer, pH = 9.6 with eight replicates, 100 μL per well except for the blank wells that had no antibody coated. The plates were shaken at 400 rpm for 2 h and then refrigerated overnight. The plates were then drained, washed with 3 x 300 μL of phosphate buffered saline with Tween-20 pH = 7.4 (PBS/T) and blotted dry. The plates were then blocked with OVA (1%w/v in PBS/T, 200 μL per well) and the plates shaken at 400 rpm for 2 h. The plates were then drained and washed as before and PBS/T (75 μL/well) was added followed by the blank milk (25 μL per well, no prior dilution) added to the plates. Monoclonal antibody was added (5 μg/mL in PBS/T, corresponding to approximately 1/1600 dilution; 100 μL per well). The plates were then shaken at

400 rpm for 1 h at room temperature. The plates were then drained and washed as before and IgG – horseradish peroxidase (HRP) secondary antibody conjugate (1/12500 dilution in PBS/T, 200 μL / well) was added and the plates shaken (400 rpm, 1 h). The plates were then washed and drained as before and TMB colour substrate added (125 μL of 1.5% H_2O_2 solution in water and 125 μL of 1 mg/mL TMB in dimethyl sulfoxide (DMSO) were added to 12.5 mL of 0.1 M sodium acetate buffer pH = 4.0) (100 μL/ well) and the plates shaken immediately (400 rpm, 5 min). The plates were developed in the dark before stopping solution was added (2 M sulfuric acid, 50 μL/ well). The plates were then read at 450 nm. Four replicates were done of each point.

2.2.3 Assay Curve Determination for Progesterone-Protein Conjugates in Whole Milk

Protein conjugates **C-1**, **C-2**, **C-3**, and **C-4** were immobilised on an ELISA plate (1 μg/mL in 0.05 M bicarbonate buffer, pH = 9.6) by shaking for 2 h and then refrigerated overnight. The plates were then drained, washed with 3 x 300 μL of PBS/T and blotted dry. The plate was blocked with OVA (1%w/v in PBS/T) by shaking for 2 h. The plates were then drained and washed as before and PBS/T (75 μL / well) was added to the plate followed by milk standards (0, 0.01, 0.1, 1, 5, 10, 100, 1000 ng/mL progesterone, 25 μL/well). The plate then had monoclonal anti-progesterone (5 μg/mL in PBS/T, 100 μL / well) added immediately. The plate was shaken for 1 h at room temperature before washing (as before but six times) and then adding IgG – HRP (1/12,500, 200 μL / well) and shaking for 1 h at room temperature. The plate was then washed (as before but six times) and colour development and reading done as above. The standards were run in triplicate or quadruplicate.

2.2.4 Assay Validation

The ELISA tests for estrous cycling and assay validation were done as for the standard curves but with actual milk samples as well as standards. The standards

used on each plate were 0, 0.1, 1, 2.5, 5, 7.5, 10, 50 ng/mL, and 25 ng/mL where needed. Three or four replicates were done of each point for the samples and three for the standards. The intra-assay coefficient of variation was calculated as the mean of the co-efficient of variation of binding response of triplicates of the same sample on the same assay plate (used 22 separate samples across the progesterone range of 1.6 to 21 ng/mL). The inter-assay coefficient of variation was calculated as the mean of the coefficient of variation for replicates of the same sample across different runs (three different assays on separate plates of six different samples). The % recovery was defined as the concentration of the ELISA determination as a percentage of the actual theoretical progesterone concentration from the serial dilution of spiked progesterone standard at five concentrations (0, 1, 2.5, 5, 25 ng/mL) with three replicates per concentration. The comparison with RIA results was made over 45 samples with the RIA being conducted by Dexcel within 24 h of the ELISA being done and assayed in three batches, with most assayed as one batch.

2.2.5 Estrous Profiling and Pregnancy

Two cows were selected and had their estrous profiles followed by the ELISA and RIA for two complete cycles with twice weekly sampling, *i.e.* sampling intervals of three or four days. A set of 12 cows were analysed for pregnancy by the ELISA by assessing milk taken within three days of servicing with a bull and then again at 17-24 days after servicing using the standard assay validated method. Veterinary ultrasound pregnancy tests were conducted 49-88 days after service and used as a standard for comparison to the ELISA predictions.

2.2.6 Statistical Methods

All determinations were made to the number of replicates stated above. The mean, standard deviation and coefficient of variation were taken for all samples. Absorbances were taken as outliers where they lay outside two standard deviations of the mean of the other replicates. Standards were run with every plate and used to formulate a standard curve for every sample plate. To determine

the standard errors (SE) and standard deviations (SD) of the blank-corrected absorbances the standard errors and standard deviations were combined for standard and sample absorbances with the standard deviation or standard error in the blank by the method of least-squares. Standard curve data were fitted to a 4-parameter logistic relationship and errors in the concentration were determined by the use of the formulaic approximation given in Figure 1.16.

The detection limits were calculated as the concentration reading corresponding to the absorbance reading that is 2 SD of the absorbance reading of the blank below the mean absorbance of blank milk. This value is a value widely used in statistical considerations of detection limit.[22, 128, 129] As the detection limit point is a theoretical point on the curve of best fit there is no actual standard error value ready to be used directly in determining detection limit error. It is therefore necessary to approximate the error in this point. This may be done by production of a standard error *vs* concentration plot, which is generalised for use in all the plots. This method is certainly appropriate if the standard errors are showing a set pattern with changing concentration and indeed this is normally the case, with the error increasing with increasing binding response. This pattern has however not been observed with this ELISA format nor has any other pattern been observed. This suggests that the error is more dependent upon the actual sample used and so it would be more accurate to use the error in the point on the given standard curve closest to the detection limit. It would not be appropriate though to use any point that was not in the active region of the curve, *i.e.* was reading 100% or close to 0% as these points are out of the dynamic concentration range. This method was applied to the calculation of standard errors.

Binding absorbances were compared using the student *t*-test (two-tailed unless otherwise stated) as were the detection limits of the assay curves to determine if a significant difference existed. All error bars represent +/- one SD of the mean. Correlation of the ELISA with the RIA was determined by fitting a linear correlation and determining the equation and R^2 using Origin 5.0 graphing software. The coefficient of variation of the slope of the correlation line was determined as a measure of spread of the data about the correlation line. Errors quoted in the text are standard errors unless otherwise stated.

2.3 Results and Discussion

2.3.1 Progesterone-Protein Conjugate Antibody Binding Studies in the Whole Milk Medium

Binding studies were conducted on all four conjugates using the same ELISA format that was eventually developed for the whole milk samples. This format is illustrated schematically in Figure 1.4, part B. By using blank milk in place of real milk samples it was possible to accurately simulate the medium that the protein conjugates will operate in under the ELISA conditions. By relating binding strength as measured by the enzyme catalysed colour absorbance to the concentration of protein conjugate used, a clear picture can be obtained of the binding of the antibody to the protein conjugates and the changes in binding that occur as the protein conjugate coating concentration is altered. From such studies one can determine the optimum coating concentration, that is the concentration that gives maximum binding but where the antibody is not in excess, so changing the concentration of free antibody available to bind a fixed level of conjugate will lead to significant change in signal and hence good sensitivity. In other words, high binding signal is preferable but the antibody must not be in excess relative to the coating protein conjugate. Figure 2.2 shows the plot of antibody binding absorbance *vs* monoclonal antibody concentration for all four conjugates.

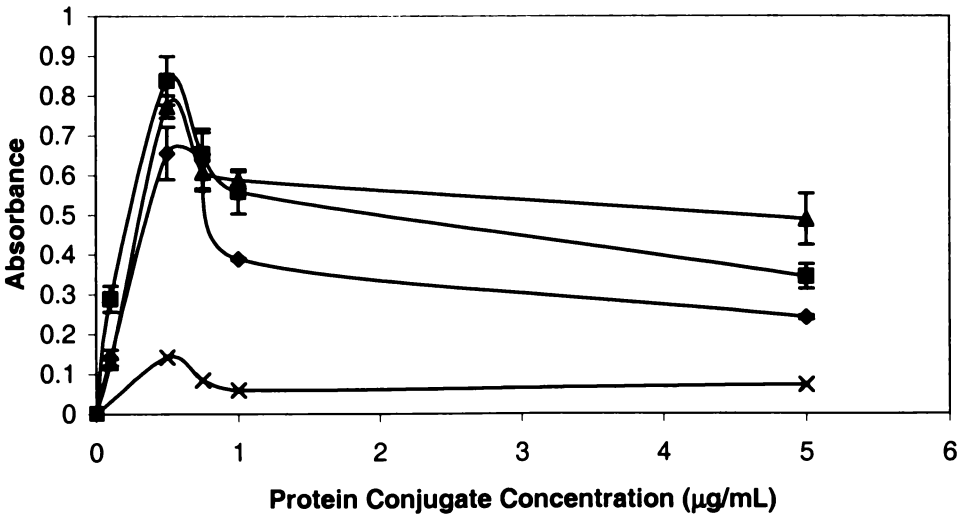

Figure 2.2 Plot of Antibody Binding Signal (Absorbance) *vs* Protein Conjugate Concentration (µg/mL) **C-1 ◆, C-2 ■, C-3 ▲, C-4 ✕**.

All conjugates showed a sharp rise in binding response from 0 μg/mL conjugate up to maxima at 0.5 μg/mL for all conjugates. This increase in binding response is due to increasing conjugate concentration enabling more antibody to bind. From this one can conclude that the antibody is in excess up to these maxima points, *i.e.* conjugate binding sites are maximally bound. All conjugates then show a sharp decrease in signal by ~35% for conjugates **C-1, C-2** and **C-3** and by ~90% for conjugate **C-4**. This is most likely due to the conjugates crowding together on the plate and preventing antibody binding through steric constriction. Clearly the antibody is no longer in excess. The drop is particularly pronounced in conjugate **C-4** which is possibly due to the longer linker producing more substantial steric crowding of the binding sites with more linker-antigen folding occurring. From 1 μg/mL to 5 μg/mL there is only a very slight drop in binding for conjugates **C-1**, **C-2** and **C-3** and no drop for **C-4** suggesting that an equilibrium has been established at the surface whereby no more conjugate can bind as all available spaces are taken and steric constriction of binding is no worse. Conjugate **C-4** has substantially less binding than all the other conjugates and a principal reason for this is that it has a lower hapten number than the others. This lower hapten number arose due to the poor solubility of the three-caproic acid unit linker derivative in water, making conjugation more difficult. To prevent this decrease in progesterone attachment, more polar linkers would need to be used, but these will not be so lipophilic and so therefore may not extend into the milk medium so well.

The binding curves have shown that overall antibody binding increased with increasing linker length in the whole milk medium up to 18 atoms. 1 μg/mL coating concentration appears to be the best concentration to use, as at this antibody concentration one has sufficient conjugate coating to bind the available antibody, *i.e.* the antibody is not in excess and small variations in conjugate coating concentration are unlikely to cause substantial variations in response allowing more consistent plate production.

At 1 μg/mL coating concentration, increasing the linker from 4 to 11 atoms enhanced binding by 32% and incrementing from 11 to 18 atoms produced a further increase of 18% at 1 μg/mL. However, extending the linker to 25 atoms decreased binding by 96% compared with the 18-atom linker at 1 μg/mL. This

drop is partly due to the lower hapten number caused by poor linker solubility, but cannot be completely explained by this. A further reason may be that the linker is folding over the progesterone and preventing approach to the antigen by the antibody.

The un-paired *t*-test was used to decide upon statistical differences in sets of ELISA data. The null hypothesis (H_0) in all cases was H_0 μ_1 (mean of data set 1) = μ_2 (mean of data set 2) and cut-off was α (significance level) = 0.05. Determination of whether the data should be pooled in a pooled *t*-test, *i.e.* whether variances are equal, $\sigma^2_1 = \sigma^2_2$, was determined by the use of the F-distribution table. All results are quoted by using their *P*-value, taking into account whether the *t*-test is one or two-tailed. The two-tailed *t*-test is used more commonly here, though one-tailed *t*-test can also be validly used to determine if one value is significantly below or above another. The standard error in the antibody binding figures was determined by the least-squares combination of the standard errors of the blank and individual binding values at 1 μg/mL concentration. The blank was set as the same for all curves. A two-tailed, un-paired *t*-test was used on each of the nearest values. More comparisons are not necessary as all these *t*-test comparisons show greatly significant difference and thus all other comparisons will also result in significant differences. In all cases the *P*-values are <0.0001 so there can be no doubt that there is a significant difference between all binding points compared. The data for 5 μg/mL coating concentration likewise shows all significant differences and the same order of conjugate binding as for 1 μg/mL.

It can be hypothesised that with increasing linker length higher binding is seen because of the longer linker enabling better access to the conjugated progesterone in whole milk. The linker is lipophilic so speculatively it could be projecting the progesterone out into the lipid milk medium quite effectively. These patterns were not observed in previous studies for the aqueous medium where all conjugates except **C-4** showed identical binding patterns.[10,15] There is clearly a medium effect in operation here and speculatively one could suggest that the lipophillic linkers are projected much better by the lipid-laden milk than by the polar water medium and so linker length effects in progesterone / antibody binding are evident in milk but not in aqueous medium.

2.3.2 Assay Parameters With Changing Linker Length

As well as considering the antibody binding patterns it is also important to see how these changes are reflected in the performance of the assay constructed around these conjugates. The assays were set up exactly as it was intended to run the final fully validated assay. The curves were determined over a broad range to fully define the active regions and completely cover all physiological ranges. The range chosen was 0.01-1000 ng/mL. The assay curves for the conjugates are given in Figure 2.3.

The assay curve plot shows clearly how the assay curves differ as the linker length is increased. All the conjugates give full inhibition at 1000 ng/mL. The changes come in the limits of detection of the curve. Clearly, conjugate **C-3** reaches saturation surface binding at lower progesterone concentration than conjugate **C-2** as does conjugate **C-2** relative to conjugate **C-1.** This therefore causes the assay curves to slope back more, producing a shallower assay slope and thus a broader active range for the assay. This has the effect of changing the detection limits of the assays and this is reflected in the assay parameters given in Table 2.2.

One can see a clear pattern of decreasing limit of detection (LOD) with increasing linker length up to 18-atoms. Curiously this does not cause the upper concentration limit to decrease with the detection limit, and so, as the detection limit decreases the assay curve slope also decreases. The inhibitory concentration at 50% bound (IC_{50}) figures of the curves showed there has been some shift in the curves despite the near identical upper concentration limits, with conjugate **C-1** being much higher than **C-2** and **C-3**, with **C-4** even higher again. The IC_{50} values were calculated as a parameter of the curve fitting by four-parameter logistic. Conjugate **C-4** was not plotted in Figure 2.3 as it does not demonstrate significant inhibition until 30 ng/mL and so does not plot well. The antibody binding to this conjugate is so low that no practical assay could be constructed around it. The detection limit pattern was confirmed by analysis using student's *t*-test. These results showed that the detection limits for **C-2** and **C-3** were highly significantly different ($P < 0.001$). The high detection limit errors in **C-1** and **C-4** were caused by low curve slope and low antibody binding respectively and made some

detection limit comparisons with them statistically difficult, though by one-tailed *t*-test, the 18-atom linker detection limit is lower than both the 4- and 25-atom linkers (one-tailed *t*-test *P* values of 0.05).

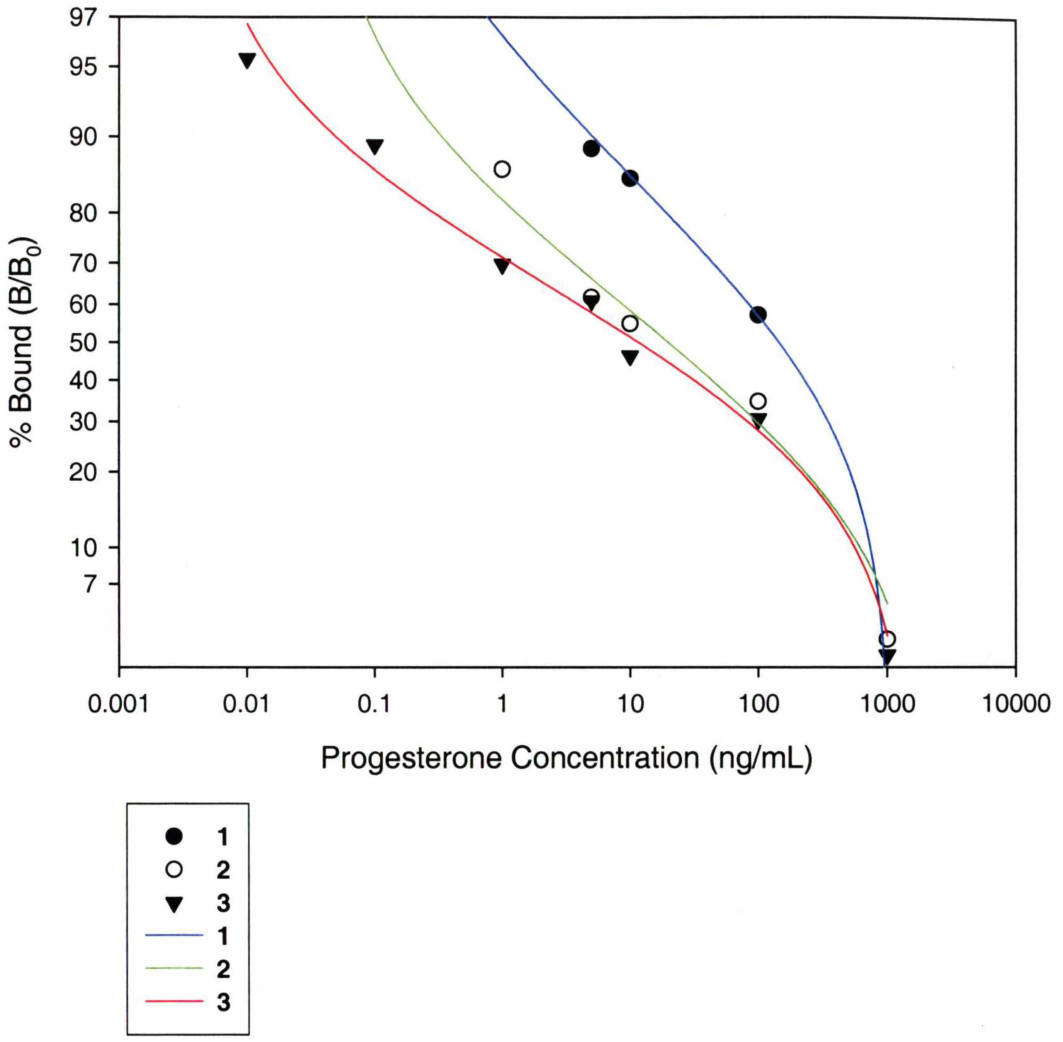

Figure 2.3 Assay Curves of **C-1, C-2** and **C-3** as a logistic / log plot of % Bound *vs* Progesterone Concentration (**C-1** $R^2 = 0.999$, **C-2** $R^2 = 0.986$, **C-3** $R^2 = 0.991$).

Table 2.2 Assay Parameters

Conjugate	LOD (ng/mL)	IC50 (ng/mL)
C-1	2.7 ± 0.9	25 ± 1.2
C-2	0.87 ± 0.08	3.5 ± 0.25
C-3	0.089 ± 0.016	3.4 ± 0.68
C-4	30 ± 10	89 ± 0.62

This pattern combined with the antibody binding data suggests that the detection limit enhancement is probably due to the higher antibody binding enabling higher signal: noise ratio and thus increasing the sensitivity of the assay. It does not appear that any higher steric preference of the antibody to bind the free progesterone over the conjugate has occurred, which might have resulted in a greater inhibition of antibody binding and a lower detection limit through moving the entire curve to lower concentrations. This is supported by the curves all being the same at 1000 ng/mL progesterone. Clearly there are milk medium-dependent effects here also as the previous studies done in aqueous medium have shown no difference between conjugate assay performance in the ELISA format with increasing linker length.[10,15] Once again, the better performance can be attributed to the lipophilic nature of the linker allowing better projection of progesterone in milk rather than in aqueous medium. These patterns are of great interest in the fundamental study of enzyme immunoassay (EIA) formats and dynamics as they suggest that tailoring of the linker to the medium in which the assay is conducted can allow for higher antibody binding responses and better assay performance. It was decided to validate and use the assay based on conjugate **C-3** as it had the best detection limit, good coefficients of variation and covered the physiological range of progesterone in milk.

2.3.3 ELISA Method Development

In developing the ELISA format there were several factors that needed to be included in the assay. The first of these was that the milk must be delivered direct to the plate without pre-dilution. This is a major problem to solve as milk fat is as high as 15% w/w in whole milk and the assay must be robust enough to produce good results despite high fat levels that have the capacity to interfere with the antibody binding. By adding PBS/T first to hydrate the wells, and then the whole milk sample followed by antibody, it was possible to effect a final 1/8 dilution in the microwells without pre-diluting the milk. This dilution was enough to achieve consistent binding results from the milk samples whilst not significantly increasing the labour involved in the assay and not diluting the milk so much that

detection was not possible. The assay is quite rapid with the binding and detection processes being over within three hours from a pre-coated and blocked plate. The washing steps in the assay were particularly important as they ensured that the high fat milk was completely cleaned from the wells before adding secondary antibody to ensure minimal non-specific binding of enzyme label. A standard range of 0.1 – 50 ng/mL was decided upon as this covers the whole normal physiological range and the use of regular points of 1, 2.5, 5, 7.5 and 10 ng/mL ensures good coverage of the central range of concentrations for estrous cycle profiling.

One of the principal benefits with this assay is that the active region of the assay is quite broad with a linear range of 0.1-100 ng/mL ($r = 0.99$). This allows the whole estrous cycle to be plotted from trough to peak in one assay, rather than having truncated physiological progesterone plots or needing two assays to cover the range. This represents a substantial increase in convenience for the analyst, saving time, sample and money. Furthermore, by immobilizing a carrier protein conjugated to the antigen, one produces a plate with a much longer lifetime than if antibody was immobilised. Antibody-immobilized plates can be quite easily destroyed if not stored correctly, and usually have at most a six-month lifetime.

2.3.4 Assay Validation

The ELISA then had to be validated to ensure that the results obtained were consistent and accurate compared to existing validated methods. The first test was the co-efficient of variation for replicates of a single sample within a plate and between plates. The within-plate or intra-assay coefficient of variation was determined as the average of 22 different samples each with three replicates. This gave 5.5%, which compares favourably with other ELISA plate systems for milk progesterone[22,74] and indicates consistency of determination between wells. The lack of pre-dilution has not adversely affected the repeatability between replicates. The between-plate or inter-assay coefficient of variation was determined from six different samples each repeated for a total of three times. The average coefficient of variation (CV) was 12.5%, which also compares well to other existing ELISAs. The inter-assay CV is higher than the intra-assay as differences can occur between

plates that affect the results and increase the errors. These figures indicate that the ELISA is indeed adequately precise in its determinations and that the wide active region of the assay has not compromised the precision.

Validation to determine accuracy was also needed. The first of these was the determination of the % recovery, which measures how close the determinations of the standards are to the spiked concentrations. This was done for multiple concentrations, four replicates each and the results are summarised in Table 2.3.

Table 2.3 % Recovery Figures for the ELISA

Actual Progesterone Concentration (ng/mL)	Determined Progesterone Concentration (ng/mL)	Recovery (%)
1	1.11	111
2.5	2.78	111
5	4.91	98
25	24.9	100
50	44.7	90

This range is quite comparable to other milk progesterone ELISA,[22,74] with an average recovery of 102%. Greater deviations from 100% recovery seem to come at points distant from the IC_{50} of the curve as expected when the curve slope decreases. The best way of determining accuracy is by comparing the method to an already established and validated assay. For milk progesterone this is RIA, which is as close to a "gold standard" for milk progesterone determination as is possible, having been extensively developed and tested for decades. The RIA used in this case has been previously validated for use in milk progesterone determinations[242] and was conducted by an independent professional commercial laboratory (Dexcel). The ELISA was compared to RIA for 45 samples and a scatter plot of commercial RIA *vs* EIA measurements was constructed and a linear regression line fitted, which enabled calculation of the coefficient of variation in the slope of the line. This plot is given in Figure 2.4.

The line can be described by the equation: RIA = 0.81EIA + 1.1, so the RIA results whilst giving linear fit with the EIA results, are somewhat lower overall than those determined by the EIA, differences having been seen in other studies also.[22,240] The correlation is very good with an r-value of 0.94 and a *P*-value of <0.0001. This indicates that the EIA and RIA results have a linear

relationship, which is an indication of a good level of accuracy. The percentage error in the slope of the regression line was 5.6% indicating that the data is quite tightly spread about the line of regression, so the relationship between RIA and EIA results is fairly predictable.

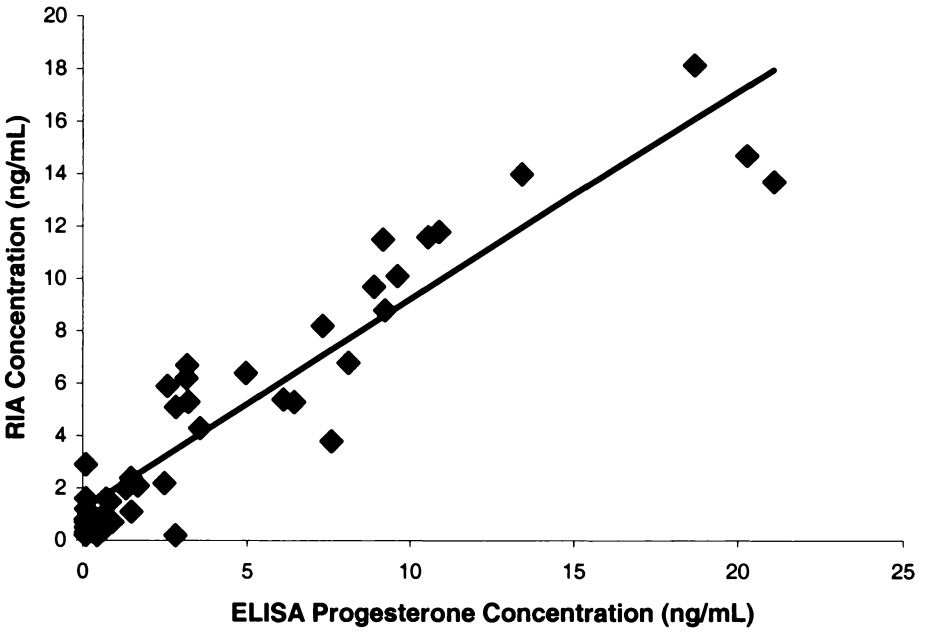

Figure 2.4 Correlation Scatter Plot of RIA Progesterone Determinations (ng/mL) *vs* ELISA Progesterone Determinations (ng/mL)

From these four different parameters one can conclude that this ELISA has good precision and accuracy and thus is validated for the determination of progesterone in whole milk. The assay method may therefore be applied reliably to real determinations of endogenous progesterone in bovine whole milk.

2.3.5 Determination of Estrous Cycles in the Dairy Cow

Two cows had their milk analysed for progesterone using the ELISA to form a hormonal profile through two whole estrous cycles with determinations twice weekly, *i.e.* three or four days between samples. These plots are given in Figure 2.5.

The progesterone cycles are clearly visible in the plots, with cow **1** cycling between 0 and 25 ng/mL and cow **2** between 0 and 12 ng/mL for ELISA determinations. The ELISA shows that the cows are cycling with a 20-21 day cycle as expected. For comparison the RIA results are superimposed on the EIA results and one can see that there is overall a close agreement between them further validating the assay. One can see how variable the amplitudes of the progesterone waves are between cows further emphasising the need for individual profiles for each cow. Larger error bars on some points reflect that these points are averages of determinations on different plates with their errors combined by least squares addition.

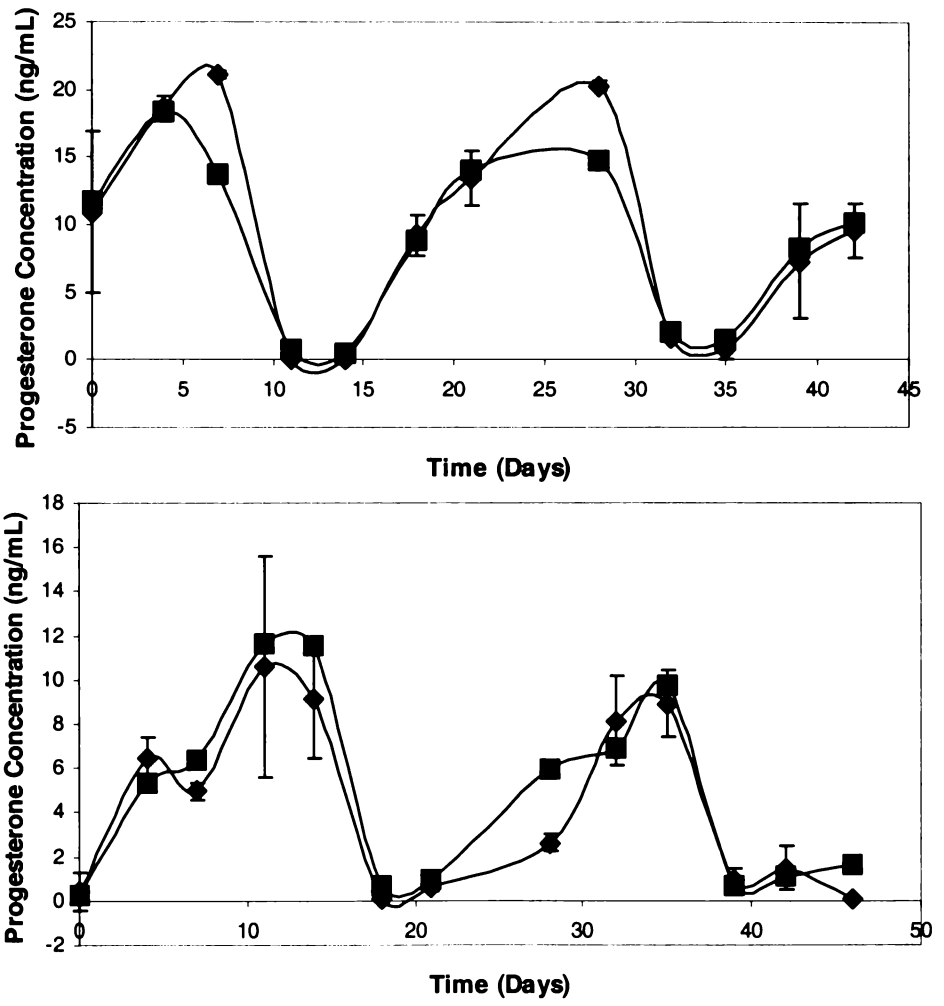

Figure 2.5 Plots of Progesterone Concentration in Whole Milk (ng/mL) *vs* Time (Days) for Two Cows, **1** top, **2** bottom. ♦ ELISA, ■ RIA (Diagnostic Products Corp.)

2.3.6 Pregnancy Prediction by ELISA

It follows that if the estrous cycle progesterone levels can be determined for estrus prediction then the assay should also function as an aid in pregnancy prediction. To this end a small herd of 12 cows was monitored at time of servicing with a bull and then around 21 days later when the progesterone should be back down to insemination sample levels if the individual cow has failed to conceive or progesterone levels will be high if it has conceived successfully. The measured progesterone levels are given in Table 2.4.

Table 2.4 Pregnancy Assessment Results for 12 cows Using Multiple Progesterone Determinations (ng/mL Whole Milk Progesterone)

Time (days)	1	2	3	4	5	6	7	8	9	10	11	12
0	1.9	<0.1	<0.1	4.8	<0.1	<0.1	6.1	<0.1	<0.1	<0.1	<0.1	<0.1
17		5.5			<0.1							
21			<0.1	16.9			29.4		4.3	4.5	<0.1	3.6
22								3.8				
24	5.2	5.2				6						
42							>50			5.7	<0.1	

Of the 12 cows, nine were inseminated when near estrus as determined by very low assayed levels of progesterone (<0.1 ng/mL). The other three were assayed at concentrations between 1.9-6.1 ng/mL, *i.e.* the lower half of the cycle. As none of these cows were fully estrous-profiled these concentrations may be reasonably close to the estrus trough. A concentration of 5 ng/mL at around 21 days was used as the arbitrary cut-off for pregnancy. Tests done at 17-24 days revealed that five of the cows were definitely pregnant using this criterion, three cows were definitely not pregnant and the status of four was uncertain though were tentatively assigned as pregnant. Further testing at 42 days was done of one positive test, one negative test and one uncertain test as determined at 17-24 days. These later tests confirmed the positive and negative determinations and suggested that the uncertain one was pregnant. Assuming all uncertain results as pregnant then the test would have predicted correctly for all the cows studied as otherwise determined by veterinary ultrasound. This is a very rough test and by

no means a perfect test for pregnancy as progesterone alone cannot be used as a complete pregnancy determination, but is a further indication of the efficacy of this ELISA technique.

2.4 Conclusions

The use of a protein conjugate-based ELISA format for determination of milk progesterone has major advantages over progesterone-enzyme conjugate-based assays. This format eliminates the need for enzyme-analyte conjugates, which have problems of inconsistent enzyme activity and conjugation and difficulties of purification. The format also enables two antibody recognition events to be employed to further increase specificity. The binding of monoclonal antibody to protein-progesterone conjugate increases with increasing linker length up to 18-atoms in the whole milk medium. The assay detection limits decrease with increasing linker length up to 18-atoms. These linker effects are seen in whole milk but not in aqueous medium and may be due to the lipophilic nature of the linkers.

A valuable new protein conjugate-based ELISA has been developed around conjugate **C-3**. The ELISA obviates the need for any pre-treatment or predilution of the milk and allows a wide dynamic range for clear estrous cycle profiling. The ELISA was validated against RIA, and tested for variability and found to be acceptable. The ELISA was applied to profiling of estrous cycles in dairy cattle and in a rough test to aid early pregnancy diagnosis and showed good correlation in both cases against established techniques.

These results show that there are medium effects in the binding and performance of protein conjugate-based immunoassay and indicate the importance of a fundamental understanding of the immunoassay format being applied. This ELISA system is the first reported protein-conjugate based ELISA in bovine whole milk and offers a generic format that may be of great use for other small molecules in high-lipid media.

Chapter 3 – Thioether Derivatives of the Estrogens – Synthesis and Antibody Binding Studies

3.1 Introduction

The estrogens are an extremely important class of steroid hormones and much research has been devoted to developing immunoassay systems for these compounds. As well as studying estrogen derivatives as immunosensing agents through conjugation to enzyme, chemiluminescent or fluorescent labels, and conjugation to proteins for raising antibodies, there has been much study of estrogens as carriers for drugs directed to specific tissues expressing estrogen antibodies or receptors. It is therefore of great importance to develop estrogen conjugation technology to ensure that the optimum antibody or receptor binding for the estrogen is achieved. In order to do this it is necessary to consider the effects that changes to the conjugate structure may have on the ability of the antibody or receptor to bind to the target estrogen.

One of the key conjugate parameters is the position at which a linker is attached to the steroidal backbone. If the point of attachment obstructs a major functional group or is bonded through an existing functional group, then this may greatly interfere with the specificity of the binding and the level of recognition and binding to the antibody or receptor. The position of attachment must also be considered in relation to the position of attachment used in the conjugate to which the antibody is raised. Site heterology, *i.e.* use of a different position of attachment to the one used in raising the antibody, is important for maximising recognition. In studies of the non-aromatic steroid progesterone, it has been found that in flow-through binding assay formats the A-ring 4-position of the steroid offers higher binding than does the 7-position and offers the further advantage of providing stereochemical purity due to the 4-5 unsaturation in the A-ring.[10,15]

The estrogens have generally similar structures to the progesterone family with the major difference being the presence of an aromatic A-ring phenol instead of the non-aromatic 4-5 unsaturated 3-carbonyl ring. Attachment to progesterone at the 4-position has been previously done by bromination at the 6-position followed by methanolic KOH reflux with 3-mercaptopropionic acid.[117] This method cannot be applied exactly to the estrogens but suggests a method by which thioether bridging could be achieved. Formation of the bromoestrogens is well established including bromination at the 4-position. By formation of the 4-bromo derivatives it should be possible to effect an $S_{RN}1$-type substitution of the bromo derivative to produce the corresponding thioether-bridged acid-terminating derivative. Thioether bridging by this method has never been attempted before for the estrogens.

Previous studies have attached the linker unit via the Mannich reaction for protein conjugation. This is done in a one-step process where there is no control over the position of attachment with both 2- and 4-positions being possible. Production of the 4-position thioether derivative of estradiol via the 4,5-epoxide has been previously reported[107] but proceeds through a complex three-step process as detailed in Chapter One. Once the thioether linker acid compound is attached then one can modify the linker to make it more water-soluble by attachment of versatile oligoethylene glycol (OEG) chains of varying lengths, which also provide a means of extending the linker length. OEG chains also can be connected quite stably via amide linkages and are non-immunogenic, their length providing an inert means of distancing the target estrogen from the conjugated compound, whether it be a drug, signal label or immunogen carrier protein.

The conjugated derivatives thus produced, can be studied conveniently by SPR through the BIAcore technology, as the flow-through conditions of the BIAcore enable controlled studies of the binding interactions in an environment not dissimilar to that in the human body, particularly the flow-through nature of the environment. Binding in real-time enables the analysis of binding kinetics and shows clearly the differences between different conjugation techniques and linker types.

SPR has been used to study binding interactions of estrogen steroids conjugated to chemiluminescent labels and in the study of binding interactions between steroid derivatives and estrogen receptors.[162,163] There has been a

deficiency of studies that systematically use SPR to probe the effects of changing conjugation position on the ability of an antibody to bind the hapten. To produce effective biosensors and to further understand the ways in which antibodies interact with target molecules, one must understand the effect of conjugation position and thus modification of the antigen on the levels of antibody binding that can be obtained. Higher antibody binding will allow greater signal strength in optical assays, which reduces signal: noise ratio and therefore increases the signal sensitivity of the assay. In inhibition assays where the antibody is pre-incubated with free sample antigen this higher signal should decrease the limit of detection (LOD) by enabling better discrimination of low antigen concentrations from the blank or otherwise by enabling a lower monoclonal primary antibody concentration to be used.

The development of new sensitive estrogen assays is very important as most estrogen assays are restricted to ELISA, which whilst being quite sensitive is labour-intensive, laboratory-based and time-consuming. SPR-based assays offer a means of determining estrogen concentrations in an automated system, which can be potentially adapted for use outside of the laboratory. BIAcore systems provide a convenient means of developing such assays. SPR however suffers from inferior sensitivity compared to ELISA.

Studies of antibody binding to conjugated estrogens are not only critical for biosensor design, but also for understanding how such conjugates are recognised by antibodies in vivo. With the growing development of drug conjugate technology for specific delivery to tissues in the human body, an understanding of how such conjugates bind to proteins is essential to optimise the conjugate production. Conjugation of anti-cancer drugs to estrogens to target estrogen receptor bearing cells for the treatment of breast cancer is but one example of the emerging applications of estrogenic conjugates to the treatment of disease. Clearly, designing conjugates to maximise such binding interactions is of great interest.

Reported below is the synthesis and characterisation of 17β-estradiol and estrone thioethers synthesised through aromatic substitution of the corresponding bromoestrogens at the 4-position. Also reported is a method for production of 4-bromoestrone without need of debromination of the 2,4-dibromoestrone derivatives. These thioether-linked derivatives are then used to produce OEG

chain derivatives of varying chain length, one of which is then applied in SPR binding studies by coupling to the sensor chip surface, and compared to conjugations via the 3-hemisuccinate and 2-position Mannich reaction as control comparisons.

3.2 Experimental

3.2.1 Materials and Instruments

3.2.1.1 General

17β-Estradiol was purchased from ICN (Aurora, USA, 101656); estrone was purchased from Acros Organics (New Jersey, USA, 117840050). Di-*t*-butyl dicarbonate and 4,7,10-trioxa-1,13-tridecanediamine were purchased from Fluka Chemie (Buchs, Germany) and triethylamine from BDH (Poole, UK). All other reagents were purchased from Aldrich Chemical Company (Milwaukee, WI, USA) and were used without further purification. *N*-Bromosuccinimide was purchased fresh at 99% and used without recrystallisation. Silica gel was Merck 60Å, grade 9385, 230-400 Mesh. Thin layer chromatography (TLC) was run on silica gel 60 F_{254} plates, aluminium-backed. All solvents used were of analytical grade for synthesis and purification and of Hipersolv chromatography grade for HPLC analysis. Molecular sieves were of type 4A 4-8 Mesh. Petroleum spirit used was 60-80 ^{o}C bp range.

Melting point determinations were done using a Reichert Thermopan instrument and were uncorrected. Proton and carbon-13 NMR spectra were acquired using both a 300 MHz Bruker AC300 FT-NMR and a 400 MHz Bruker Avance DRX400 FT-NMR and Dept 135 spectra were run also. Chemical shifts (δ) are reported in parts per million (ppm). Electrospray mass spectra were acquired using a VG Platform II Electrospray Mass Spectrometer (ES-MS) instrument in either positive or negative ion mode as appropriate. Analytical reverse phase high performance liquid chromatography (RP-HPLC) was done using a Sphereclone C_8 3 μm column (100 x 4.60 mm) on a Shimadzu instrument. High resolution fast atom bombardment mass spectrometry (FAB-MS) and high resolution electron impact mass spectrometry (EI-MS) was done by Michael

Walker of Auckland University using a VG 70-SE mass spectrometer with MASPEC 2 data analysis software. BIAcore SPR analysis was done using a BIAcore 3000 instrument at the School of Science and Technology, Waikato University with CM5 sensor chips (research grade). Monoclonal anti-17β-estradiol antibody was from US Biologicals (E3550-29) and was raised to estradiol-6-CMO-BSA conjugate as mouse anti-human. It had a calculated affinity constant of ~1 x 10^{10} L/M. The whole antiserum polyclonal anti-estradiol antibody was from Sigma (E2885) and raised using 17β-estradiol-6-BSA conjugate from rabbit and stored in lyophilised form. The whole antiserum polyclonal estrone antibody was from Sigma (E3135) and raised using estrone-6-thyroglobulin from rabbit and stored in lyophilised form. Secondary antibody was anti-mouse IgG (whole molecule) raised in rabbit as the IgG fraction of the antiserum in aqueous solution (Sigma, M7023). Immobilisation amine coupling kit was from BIAcore (BR-1000-50) consisting of 1-ethyl-3-(3-dimethylaminopropyl)-carbodiimide hydrochloride (EDC) and NHS solutions. BIAcore experiments were run using HEPES buffered saline with EDTA and P-20 (HBS-EP) as running buffer, see Appendix 1. For full details of the statistical methods and graphical fittings used, see Chapter 5. All error bars on graphs are +/- 1 SD and all errors given in the text are standard errors.

3.2.1.2 HPLC Methods for Determination of Compound Purity

All HPLC analysis was performed by injection of the sample of the compound in question run according to the conditions detailed in each experimental section. The injection volume was the maximum that the column could withstand without overloading. The product peak was collected entirely to give the pure standard, which was then dried in vacuo. The pure standard and dried raw sample were then both made to 1 mg/mL concentration and three or four replicate injections of 10 μL each of both standard and raw sample were made. The peak integrals were calculated using the computer program and averaged. The percentage purity was determined by:

$$\% \text{ Purity} = \frac{\text{mean raw sample area}}{\text{mean standard area}} \times 100$$

3.2.2 Synthesis of Estrogen Thioethers[1]

3.2.2.1 ***4-Bromo-17β-estradiol (1)***

This was adapted from a previous method[156] that did not itself stipulate molar ratios of reactants or volume of solvent. 17β-Estradiol (800 mg, 2.94 mmol) was dissolved in dry EtOH (40 mL, dried over molecular sieves) and *N*-bromosuccinimide (522 mg, 2.94 mmol in 15 mL of dry EtOH) was added drop-wise to the vigorously stirring solution. A white solid formed within 1 h of reaction and the mixture was stirred for a further 24 h. The solid was removed and recrystalised from $CHCl_3$ to yield **1** as a white crystalline solid. Yield: 55% (572 mg, 1.63 mmol). Mp 203-205 °C (lit.[148] 207-208 °C). TLC retention factor (R_f) = 0.89 (15:1 $CHCl_3$: MeOH). IR (KBr disc): 1053 (aromatic vibration), 1437 (CH_2/CH_3 deformation), 2926 (CH_2 asymmetric υ), 3242 (OH υ), 3504 cm^{-1} (OH υ). ^1H NMR ($CDCl_3$ + CD_3OD) δ: 0.80 (3H, s, 18-CH_3), 1.98 (2H, d of d, *J* = 2.7 Hz, *J* = 12 Hz, 12-H), 2.16 (2H, m, 11-H), 2.72 (1H, m, 9-H), 2.93 (1H, d of d, *J* = 5.6 Hz, *J* = 11.9 Hz, 17-H), 3.75 (2H, q, *J* = 7.0 Hz, 6-H), 5.59 (1H, s, OH), 6.88 (1H, d, *J* = 8.5 Hz, 2-H), 7.21 (1H, d, *J* = 8.3 Hz, 1-H). ^{13}C NMR ($CDCl_3$) δ: 11.1 (18-CH_3) 23.2 (C-6), 26.7 (C-15), 27.4 (C-7), 27.6 (C-11), 30.0 (C-16), 31.3 (C-12), 36.8 (C-8), 38.2 (C-9), 43.3 (C-13), 44.3 (C-14), 81.6 (C-17), 113.1 (C-4), 113.5 (C-2), 125.2 (C-1), 134.1 (C-5), 137.2 (C-10), 151.2 (C-3). ES-MS *m/z* (MeOH –45 V) 349.1, 351.1 $[M-H]^-$.

3.2.2.2 ***2,4-Dibromoestrone (2)***

Estrone (400 mg, 1.48 mmol) was dissolved in dry ethanol (25 mL) with warming. *N*-Bromosuccinimide (790 mg) was added and the mixture stirred vigorously for 24 h in the dark. The solvent was removed from the deep purple solution and the solid separated on a silica gel column using in succession, petroleum spirit, 4:1 petroleum spirit: ethyl acetate eluant to yield **2** as an off-white solid. Yield: 53% (336 mg, 0.784 mmol). Mp 230 °C (lit.[151] 235-236 °C).

[1] See p. 120 for reaction scheme of 4-position derivatives and p. 121 for 3- and 2-position derivatives. Full bromination reaction scheme is given on p.123.

TLC R_f = 0.41 (4:1 petroleum spirit: ethyl acetate). IR (KBr disc): 1462 (CH_2 deformation), 1720 (C=O υ), 2925 (CH_2 asymmetric υ), 3337 cm^{-1} (OH υ). ^1H NMR ($CDCl_3$) δ: 0.93 (3H, s, 18-CH_3), 1.27-2.98 (m), 5.90 (1H, s, OH), 7.43 (1H, s, 1-H). ^{13}C NMR ($CDCl_3$) δ: 14.1 (18-CH_3), 21.9 (C-15), 26.5 (C-6), 26.8 (C-7), 30.1 (C-11), 31.3 (C-12), 31.8 (C-16), 36.2 (C-8), 37.7 (C-9), 44.3 (C-13), 48.1 (C-14), 106.9 (C-2), 113.6 (C-4), 128.9 (C-1), 135.4 (C-5), 137 (C-10), 147.7 (C-3), 220.6 (C-17). ES-MS *m/z* (MeOH –20 V) 425 – 429 isotope pattern $[M-H]^-$.

3.2.2.3 ***4-Bromoestrone (3A) from 2,4-dibromoestrone (2)***

2,4-Dibromoestrone (300 mg, 0.70 mmol) was dissolved in dimethylformamide (DMF) (10 mL) and 3%w/w palladium on carbon (333 mg) was added followed by formic acid (270 μL). The mixture was then refluxed for 105 min, cooled to room temperature and the catalyst filtered off and washed with ethyl acetate (2 x 4 mL). The combined filtrate and ethyl acetate washings were further diluted in ethyl acetate and washed with aqueous saturated sodium bicarbonate solution (twice) and distilled water (twice). The organic phase was then dried over magnesium sulfate and the rose pink solution was separated on a silica column (using in succession, petroleum spirit, 4 : 1 petroleum spirit : ethyl acetate, 3:1 petroleum spirit: ethyl acetate, 2:1 petroleum spirit: ethyl acetate) to yield 4-bromoestrone as a white solid. Yield 30% (74 mg, 0.21 mmol). Mp 258-259 °C (lit.[150] 264-265 °C). TLC R_f = 0.23 (4:1 petroleum spirit: ethyl acetate). ^1H NMR ($CDCl_3$) δ: 0.90 (3H, s, 18-CH_3), 0.90 (1H, s), 1.26 – 2.96 (m), 5.37 (1H, s), 6.86 (1H, d, J = 8.6 Hz, 2-H), 7.18 (1H, d, J = 8.6 Hz, 1-H). ^{13}C NMR ($CDCl_3$) δ: 14.1 (18-CH_3), 21.9 (C-15), 26.3 (C-6), 27.0 (C-7), 30.1 (C-11), 31.4 (C-12), 31.9 (C-16), 36.2 (C-8), 37.9 (C-9), 44.5 (C-13), 50.7 (C-14), 113.3 (C-4), 115.6 (2-C), 125.9 (C-1), 134.0 (5-C), 136.5 (10-C), 150.6 (3-C), 221.1 (17-C=O). ES-MS *m/z* (-40V MeOH) 346.7 and 348.7 $[M-H]^-$.

3.2.2.4 ***4-Bromoestrone (3B) from estrone***

Estrone (400 mg, 1.48 mmol) was dissolved in dry EtOH (10 mL) and acetone (10 mL). *N*-Bromosuccinimide (263 mg, 1.48 mmol) was added to the vigorously

stirring solution and the stirring continued at room temperature for 24 h. The white solid formed was filtered off and washed with ethanol. The filtrate solvent was removed and the resultant solid from the filtrate was recrystallised from chloroform to increase yield and then added to the filtered solid yielding **3B**. Yield 43% (221 mg, 0.63 mmol). Mp 264-265 °C (lit.[150] 264-265 °C). TLC R_f = 0.23 (4:1 petroleum spirit 60-80°C : ethyl acetate). IR (KBr disc): 1472 (CH_2 deformation), 1731 (17 C=O υ), 3420 cm^{-1} (OH υ). ^1H NMR ($CDCl_3$) δ: 0.90 (3H, s, 18-CH_3), 0.90 (1H, s), 1.26 – 2.96 (m), 5.37 (1H, s, OH), 6.86 (1H, d, *J* = 8.6 Hz, 2-H), 7.18 (1H, d, *J* = 8.6 Hz, 1-H). ^{13}C NMR ($CDCl_3$) δ: 14.0 (18-CH_3), 21.8 (C-15), 26.3 (C-6), 26.9 (C-7), 31.2 (C-11), 31.7 (C-12), 36.2 (C-16), 37.8 (C-8), 44.4 (C-9), 49.1 (C-13), 50.5 (C-14), 113.2 (4-C), 118.9 (2-C), 125.3 (1-C), 133.3 (5-C), 137.0 (10-C), 151.4 (3-C), 222.6 (17-C). ES-MS *m/z* (-40V MeOH) 346.7 and 348.7 $[M-H]^-$; High resolution (HiRes) Electron impact-MS: Calculated: 348.0725 and 350.0705, Found: 348.0727 and 350.0708 (M^+).

3.2.2.5 3-(3,17β-Dihydroxyestra-1,3,5(10)-trien-4-yl)thiopropanoic acid (4)

1 (200 mg, 0.57 mmol) was dissolved in dry MeOH (20 mL). Methanolic potassium hydroxide (20 mL, 7.8 mg/mL) was added followed by 3-mercaptopropionic acid (550 μL). The solution was refluxed under dry conditions (oven-dried glassware, drying tube and solvent dried over molecular sieves) for 24 h in the dark. The solvent was removed and the sample reconstituted in distilled water (50 mL). The aqueous phase was washed with EtOAc (2 x 25 mL, 1 x 50 mL). The EtOAc phase was then back washed with distilled water (50 mL in total). TLC analysis revealed that the R_f of the product was too close to that of 3-mercaptopropionic acid to allow column separation and so the solvent was removed in vacuo and the product was reacted directly through to the next stage. TLC R_f = 0.52 (5:1 $CHCl_3$: MeOH). ^1H NMR ($CDCl_3$) δ: 0.81 (3H, s, 18-CH_3), 1.38-2.3 (m, steroidal backbone), 2.75 (3H, t, *J* = 4.6 Hz, 17-CH), 2.81 (2H, m, S-CH_2), 6.89 (1H, d, *J* = 6.3 Hz, 2-H), 7.22 (1H, d, *J* = 6.7 Hz, 1-H); incomplete assignment as the spectrum was obtained overlaid with 3-mercaptopropionic acid (MPA) peaks. ^{13}C NMR ($CDCl_3$) δ: 14.2 (18-CH_3), 21.2 (C-15), 21.4 (C-6), 22.8 (C-7), 23.1 (C-11), 24.0, 25.4, 26.8, 29.1 (S-CH_2), 29.8, 30.2, 31.0 (C-12), 33.8

(CH_2-COOH), 34.2 (C-16), 37.1 (C-8), 50.9 (C-14), 74.6 (C-17), 90.5, 171.5 (COOH), 194.0; ES-MS *m/z* (+ve ion mode, MeOH) 399.1 $[M+Na]^+$, (-ve ion mode, MeOH) 406.8 $[M+OMe]^-$.

3.2.2.6 3-(3-Hydroxyestra-1,3,5(10)-trien-17-on-4-yl)thiopropanoic acid (5)

3 (150 mg, 0.43 mmol) was dissolved in dry MeOH (20 mL, dried over molecular sieves) and potassium hydroxide (15 mL, 23 mg/mL in dry MeOH) was added whilst stirring, followed by 3-mercaptopropionic acid (425 μL) and the solution heated under reflux with oven dried glassware and a drying tube for 24 h. The sample was then cooled and the solvent removed. The sample was reconstituted in distilled water (25 mL) and washed with EtOAc (2 x 12.5 mL, 1 x 25 mL). The water was removed in vacuo and the sample column separated using 1:1 $CHCl_3$: MeOH eluant to yield **5** as a white solid. Yield 27% (43 mg, 0.11 mmol). Mp 108-112 °C. TLC R_f = 0.65 (10:1 $CHCl_3$: MeOH). IR (KBr disc): 1241 (CH_2-S υ), 1400 (CH_3 deformation), 1698 (acid C=O υ), 1735 (17 C=O υ), 3429 cm^{-1} (OH υ). ^1H NMR ($CDCl_3$ + CD_3OD) δ: 0.93 (3H, s, CH_3-18), 2.54 (2H, t, J = 9.4 Hz, CH_2-COOH), 2.88 (2H, t, J = 8.8 Hz, CH_2-S), 6.81 (1H, d, J = 11 Hz, H-2), 7.22 (1H, d, J = 11 Hz, H-1). ^{13}C NMR ($CDCl_3$ + CD_3OD) δ: 13.8 (18-CH_3), 21.6 (C-15), 26.2 (C-6), 26.7 (C-7), 29.5 (S-CH_2), 31.0 (C-11), 31.5 (C-12), 35.9 (CH_2-COOH), 37.4 (C-16), 38.5 (C-13), 44.0 (C-9), 48.0 (C-13), 50.3 (C-14), 113.0 (C-2), 125.4 (C-1), 133.6 (C-5), 136.5 (C-10), 150.6 (C-4), 156.2 (C-3), 175.4 (COOH), 223.0 (CO). ES-MS *m/z* (MeOH) 397.4 $[M+Na]^+$, 373.4 $[M-H]^-$.

3.2.3 Synthesis of Polyethylene Glycol Derivatives of the Estrogens

3.2.3.1 2,5-Dioxo-1-pyrrolidinyl 3-(3,17β-dihydroxyestra-1,3,5(10)-trien-4-yl)thiopropionate (6)

The entire semi-solid from the ethyl acetate phase of the **4** reaction was dissolved in dry DMF (1 mL) and dicyclohexylcarbodiimide (DCC) (176 mg in 1 mL of dry DMF) was added drop-wise followed by NHS (98 mg in 1 mL of dry

DMF). A white solid precipitated out within 1 h and the mixture was left sealed stirring in the dark overnight. The solvent was removed in vacuo and the sample separated by silica column using in succession, $CHCl_3$, 15:1 $CHCl_3$: MeOH, 10:1 $CHCl_3$: MeOH and then 2:1 $CHCl_3$: MeOH as eluant to yield **6** as a white solid. Yield 52% (141 mg, 0.297 mmol) from **1**. Mp 194-196 °C. TLC R_f = 0.48 (10:1 $CHCl_3$: MeOH). IR (KBr disc): 1242 (CH_2-S υ), 1576 (aromatic υ), 1626 (aromatic υ), 1736 (NHS C=O out of phase υ, C=O υ active ester), 1783 (NHS C=O in-phase υ), 2851 (CH_2 symmetric υ), 2929 (CH_2 asymmetric υ), 3327 cm^{-1} (OH υ). ^1H NMR ($CDCl_3$ +CD_3OD) δ: 0.79 (3H, s, 18-CH_3), 2.97 (4H, s, NHS), 3.05 (t, *J* = 6.7 Hz, CH_2-S, overlaid with H-9 ^1H to make 3H group), 3.75 (1H, t, *J* = 10.9 Hz, H-17), 6.87 (1H, d, *J* = 11.3 Hz, H-2), 7.20 (1H, d, *J* = 11.4 Hz, H-1). ^{13}C NMR ($CDCl_3$ + CD_3OD) δ: 11.1 (18-CH_3), 23.1 (C-6), 24.7 (C-15), 25.0 (NHS ring CH_2), 25.5 (NHS ring CH_2), 26.6 (C-7), 27.4 (C-11), 30.7 (CH_2-COO), 31.2 (S-CH_2), 32.4 (C-16), 32.9 (C-12), 38.1 (C-8), 43.2 (C-9), 44.2 (C-13), 52.9 (14-C), 81.9 (C-17), 112.8 (C-2), 113.8 (C-5), 125.6 (C-1), 134.4 (C-10), 136.5 (C-4), 150.2 (C-3), 162.6 (ester C=O), 169.0 (NHS C=O), 179.3 (NHS C=O). ES-MS *m/z* (40 V, MeCN) 515.5 $[M+MeCN+H]^+$.

3.2.3.2 ***2,5-Dioxo-1-pyrrolidinyl-3-(3-hydroxyestra-1,3,5(10)-trien-3-ol-17-on-4-yl)thiopropionate (7)***

5 (100 mg, 0.268 mmol) was dissolved in dry DMF (1 mL) and DCC (72 mg, 0.348 mmol, in 0.5 mL dry DMF) was added to the rapidly stirring solution drop-wise. This was followed by NHS (40 mg, 0.348 mmol, in 0.5 mL of dry DMF). The solution was left stirring at room temperature overnight in the dark. The solvent was removed in vacuo and the resulting semi-solid separated on a silica column using 15:1 $CHCl_3$: MeOH eluant to yield **7** as a white solid. Yield 32% (40 mg, 0.085 mmol). Mp 193-197 °C. TLC R_f = 0.96 (15:1 $CHCl_3$: MeOH). IR (KBr disc): 1576 (aromatic υ), 1627 (aromatic υ), 1736 (NHS C=O out of phase υ, 17 C=O υ), 1780 (NHS C=O in-phase υ), 2851 (CH_2 symmetric υ), 2929 (CH_2 asymmetric υ), 3328 (OH υ) cm^{-1}. ^1H NMR ($CDCl_3$ + CD_3OD) δ: 0.90 (3H, s, 18-CH_3), 2.89 (4H, s, NHS), 4.31 (1H, d, *J* = 9.4 Hz), 6.85 (1H, *J* = 11.4 Hz, H-2), 7.16 (1H, *J* = 11.4 Hz, H-1). ^{13}C NMR ($CDCl_3$ + CD_3OD) δ: 13.9 (18-CH_3), 21.6

(C-15), 24.8 (NHS CH_2), 25.0 (NHS CH_2), 25.5 (C-6), 25.7 (C-7), 26.2 (C-11), 26.7 (CH_2COO), 31.1 (CH_2-S), 32.9 (12-C), 34.0, 36.6 (C-16), 37.6 (C-8), 44.2 (C-9), 48.0 (C-13), 52.8 (C-14), 113.0 (C-2), 125.5 (C-1), 133.6 (C-5), 136.4 (C-10), 150.6 (C-4), 157.1 (C-3), 162.7 (ester C=O), 179.3 (NHS C=O), 220.9 (17 C=O). ES-MS *m/z* (MeOH 40 V) 471.6 $[M+H]^+$.

3.2.3.3 N-(t-Butoxycarbonyl)-4,7,10-trioxa-1,13-tridecanediamine (8)

Adapted from the method of Wilbur et al.[243] 4,7,10-Trioxa-1,13-tridecanediamine (OEG) (1.9 g, 8.60 mmol) was dissolved in 20 mL of molecular sieves-dried methanol in a round bottom flask (50 mL). Di-*tert*-butyl dicarbonate (DBDC) (1 g) was dissolved in dry methanol (10 mL). Triethylamine (1 mL) was added to the vigorously stirred OEG solution under a septum. The DBDC solution was then added drop-wise under a septum to the vigorously stirred solution via syringe. The solution was stirred overnight. The solvent was removed and the sample dried in vacuo. The resultant oil was then column separated by flash chromatography using successively 4:1 CH_2Cl_2: MeOH, 32:8: 1 CH_2Cl_2: MeOH: AcOH, 16:4:1 CH_2Cl_2: MeOH: AcOH to yield **8** as a clear, colourless oil. To return to free amine form **8** can be washed with aqueous sodium bicarbonate solution. Yield: 69% (1.925 g, 5.93 mmol). TLC R_f = 0.85 (16: 4: 1 CH_2Cl_2: MeOH: AcOH). IR (film): 1113 (CH_2-O υ), 1555 (Boc amide), 1694 (Boc amide C=O υ), 2874 (-NH_3^+ υ, CH_2 symmetric υ), 2931 cm^{-1} (CH_2 asymmetric υ). ^1H NMR ($CDCl_3$, **8** as acetate salt) δ: 1.43 (s, 9H, *t*-butoxy carbonyl (Boc) methyl), 1.77 (quin, 2H, J = 6.3 Hz, C**H**$_2$-CH_2-NH_3^+), 1.94 (quin, 2H, J = 5.8 Hz, C**H**$_2$-CH_2-NH-CO), 3.09 (2H, t, 6.1 Hz, C**H**$_2$-NH_3^+), 3.19 (2H, d of t, J_d = 5.9 Hz, C**H**$_2$-NH-CO), 3.53 (2H, t, J = 6.0 Hz, CH_2-O), 3.58 (2H, t, J = 3.3 Hz, CH_2-O), 3.62 (6H, m, CH_2-O), 3.66 (2H, t, J = 5.6 Hz CH_2-O). ^{13}C NMR ($CDCl_3$) δ: 28.4 (Boc Me), 29.7 (CH_2-**C**H_2-CH_2), 33.4 (CH_2-**C**H_2-CH_2), 38.4 (CH_2-NH), 39.6 (CH_2-NH_2), 69.4 (CH_2-O), 70.19 (CH_2-O), 70.22 (CH_2-O), 70.57 (CH_2-O), 70.60 (CH_2-O), 156.1 (C=O). ES-MS *m/z* (MeOH): 321.1 $[M+H]^+$. Purity: 97% (HPLC, retention time (R_t) = 1.34 min, 60:40 MeOH: H_2O, λ_{max} = 201 nm).

3.2.3.4 N-(13-(t-Butoxycarbonylamino)-4,7,10-trioxatridecanyl)-3-(3,17β-dihydroxyestra-1,3,5(10)-trien-4-yl)thiopropanamide (9)

6 (50 mg, 0.075 mmol) was dissolved in dry DMF (1 mL). **8** (Na_2CO_3 washed, 21 mg, 0.064 mmol in 0.5 mL of $CHCl_3$) was added drop-wise with vigorous stirring followed by triethylamine (100 μL, dried over molecular sieves). The solution was stirred in the dark at room temperature over 60 h. Solvent was then removed and the product separated on a silica column using successively 15:1 $CHCl_3$: MeOH, 10:1 $CHCl_3$: MeOH, 5:1 $CHCl_3$: MeOH, 1:1 $CHCl_3$: MeOH and then MeOH as eluant to yield **9** as a clear, colourless oil. Yield: 86% (44 mg, 0.064 mmol). TLC R_f 0.50 (15:1 $CHCl_3$:MeOH). IR (film): 1542 (Boc amide), 1655 (amide C=O υ), 1695 (Boc amide C=O υ), 2919 (CH_2 asymmetric υ), 3410 cm^{-1} (OH υ). ^1H NMR ($CDCl_3$) δ: 0.77 (3H, s, CH_3-18), 1.44 (9H, s, Boc CH_3), 2.56 (2H, t, *J* = 7.1 Hz CH_2COO-), 2.99 (2H, t, *J* = 7.1 Hz Ar-S-CH_2), 3.6 (12H, m, PEG CH_2-O), 3.73 (1H, t, *J* = 8.5 Hz, H-17), 6.85 (1H, d, *J* = 8.5 Hz, H-2), 7.17 (1H, d, *J* = 8.5 Hz, H-1). ^{13}C NMR ($CDCl_3$) δ: 11.0 (CH_3-18), 23.2 (15-C, C-6), 27.2 (C-7), 28.1 (C-11), 28.4 (Boc CH_3), 28.5 (Boc Me), 28.9 (Boc Me), 29.2 (OEG chain), 29.5 (OEG chain), 29.7 (CH_2S), 31.1 (C-16), 34.2 (C-12), 35.9 (CH_2CO), 36.5 (CH_2NH steroid end), 37.9 (CH_2NH Boc end), 38.1 (C-8), 43.2 (C-9), 44.2 (C-13), 49.9 (C-14), 69.5 (OEG CH_2O), 69.9 (OEG CH_2O), 70.1 (OEG CH_2O), 70.2 (OEG CH_2O), 70.5 (OEG CH_2O), 81.8 (Boc C-O), 82.3 (C-17), 112.8 (C-2), 113.7 (C-4), 125.4 (C-1), 134.2 (C-10), 136.5 (C-5), 150.3 (C-3), 156.1 (ester), 170.9 (ester). ES-MS *m/z* (H_2O, 60 V) 718.9 $[M+H_2O+Na]^+$.

3.2.3.5 O-(N-(t-Butoxycarbonyl)-2-aminopropyl),O'-(2-aminopropyl) polypropylene glycol-block-polyethylene glycol-block polypropylene glycol (10)

Polyethylene glycol 800 (O, O'-Bis-(2-aminopropyl)polypropylene glycol-block-polyethylene glycol-block polypropylene glycol, Fluka 14527) (2 g, approx. 2.22 mmol as exact chain length varies) was dissolved in dry MeOH (20 mL) and dry triethylamine (1 mL) was then added. Di-*tert*-butyl dicarbonate (Boc) (0.486 g, 2.22 mmol) was dissolved in dry MeOH (10 mL) and added drop-wise to the rapidly stirring PEG solution over 20 min using a syringe and septum. The

solution was then left to rapidly stir overnight at room temperature. The solvent was then removed and the sample separated on a silica column using successively 32:1:1, 32:2:1, 32:4:1, 16:4:1 CH_2Cl_2 : MeOH : AcOH as eluant to yield **10** as a clear colourless semi-solid. Yield: 41% (911 mg, approx. 0.91 mmol). TLC R_f = 0.53 (32:2:1 CH_2Cl_2 : MeOH : AcOH). IR (film): 1105 (CH_2-O υ), 1699 (Boc amide C=O υ), 2875 (CH_2 symmetric υ), 3411 cm^{-1} (-NH_2 υ). ^1H NMR ($CDCl_3$) δ: 1.13 (s, 8H), 1.27 (s, 3H), 1.44 (s, 9H, Boc CH_3), 2.00 (s, 6H), 3.45 (s, 7H), 3.65 (s, 65H, ethylene protons); ^{13}C NMR ($CDCl_3$) δ: 15.0, 15.3, 15.4, 16.1, 16.8, 16.9, 17.0, 17.9, 18.8, 22.5, 28.4 (Boc CH_3), 46.6, 47.1, 47.2, 48.4, 70.3 (cluster, OCH_2), 72.5, 72.6, 74.4, 74.9, 75.2, 75.5, 76.2, 155.5, 176.1 (Boc carbonyl). ES-MS (MeOH 40V) multiple peaks corresponding to different n-values of the PEG chain. Note: the PEG chain varies slightly in length so this is not one discrete compound but rather a mixture with a narrow distribution of chain lengths.

3.2.3.6 ***O-2-[3-[(3,17β-Dihydroxyestra-1,3,5(10)-trien-4-yl)thiopropanoyl]aminopropyl), O'-2-(N-(t-butoxycarbonyl)-2-aminopropyl) polypropylene glycol-block-polyethylene glycol-block polypropylene glycol (11)***

6 (50 mg, 0.106 mmol) was dissolved in dry DMF (1 mL) and stirred rapidly whilst **8** (372 mg, approx. 0.372 mmol (as exact Mr is variable), dissolved in 5:1 $CHCl_3$: MeOH, 3 mL) was added drop-wise followed by triethylamine (0.5 mL). The solution was stirred at room temperature for 60 h in the dark. The solvent was then removed and the resulting orange oil separated on a silica column using successively 15: 1 $CHCl_3$: MeOH, 10: 1 $CHCl_3$: MeOH, 5: 1 $CHCl_3$: MeOH as eluant to yield **11** as a clear, colourless oil. Yield 27% (40 mg, 0.029 mmol). TLC R_f = 0.52 (5:1 $CHCl_3$: MeOH). IR (film): 1106 (CH_2-O υ), 1659 (amide C=O υ), 1711 (Boc amide C=O υ), 2873 (CH_2 symmetric υ), 3340 (OH υ) cm^{-1}. ^1H NMR ($CDCl_3$) δ: 1.14 (14H, m), 1.44 (9H, s, Boc CH_3), 2.58 (2H, t, *J* = 7.1 Hz, CH_2-COO-), 2.73 (2H, t, *J* = 7.0 Hz, S-CH_2-, H-9 overlapping to give 3H total), 2.97 (6H, m), 3.47 (m), 4.91 (1H, s), 6.75 (1H, t of d, *J* = 34.9 Hz, *J* = 7.9 Hz); ^{13}C NMR ($CDCl_3$) δ: 16.7, 17.1, 17.6, 18.0, 28.5 (Boc CH_3), 29.7 (CH_2S), 34.1 (CH_2CO), 34.3, 36.2 (17-CH), 45.1 (C-9), 45.5 (C-13), 70.6 (PEG C-O), 71.9 (PEG C-O), 72.1 (PEG C-O), 72.4, 72.6, 73.4, 74.0, 74.5, 75.1, 75.3, 75.6, 75.9,

118.8 (2-C), 126 (1-C), 128 (4-C), 130 (5-C), 155.7 (3-C), 170.8 (C=O), 174.4 (C=O). ES-MS (MeOH, 40 V) multiple peaks from range of PEG chain n-values. Note: as for **10** this is a mixture of estradiol derivatives with slightly different PEG chain lengths. The large PEG component of the derivatives has made discrimination of some estradiol NMR peaks difficult.

3.2.3.7 N-(13-(t-Butoxycarbonylamino)-4,7,10-trioxatridecanyl)-3-(3-hydroxyestra-1,3,5(10)-trien-17-on-4-yl)thiopropanamide (12)

7 (37 mg, 0.079 mmol) was dissolved in dry DMF (1 mL). A solution of **8** (51 mg, 0.159 mmol, in 750 μL of dry $CHCl_3$) was added drop-wise to the stirring steroid solution. Triethylamine (dry, 250 μL) was then added and the reaction stirred in the dark at room temperature for 2.5 days. After the second day another 250 μL of dry $CHCl_3$ was added to aid solubility. The solvent was removed under vacuum and the sample separated on a silica column using successively $CHCl_3$ and 15:1 $CHCl_3$: MeOH as eluant to yield **12** as a waxy white solid. Yield: 50% (27 mg, 0.040 mmol). IR (film): 1626 (aromatic υ), 1655 (amide C=O υ) 1702 (Boc amide C=O υ), 1736 (estrone C=O υ), 2850 (CH_2 symmetric υ), 2928 (CH_2 asymmetric υ), 3327 (OH υ) cm^{-1}. ^1H NMR ($CDCl_3$) δ: 0.91 (3H, s, 18-CH_3), 1.44 (9H, s, Boc CH_3), 3.63 (13H, m, OEG), 4.62 (1H, d, J = 10.0 Hz), 6.83 (1H, d, J = 11.3 Hz, 2-H), 7.15 (1H, d, J = 11.7 Hz, 1-H). ^{13}C NMR ($CDCl_3$) δ: 13.8 (18-CH_3), 21.6 (C-15), 25.0 (C-6), 25.6 (C-7), 26.2 (C-11), 28.4 (Boc Methyl), 29.6 (CH_2 chain), 31.1 (CH_2 chain), 31.5 (CH_2-S), 33.8 (C-12), 36.0 (**C**H_2CO), 37.6 (C-16), 38.2 (CH_2-NH), 39.3 (C-8), 44.1 (CH_2-NH), 48.9 (C-9), 49.0 (C-13), 50.3 (C-14), 69.4 (CH_2-O), 69.9 (CH_2-O), 70.2 (CH_2-O), 70.5 (CH_2-O), 79.2 (O-**C**-$(Me)_3$), 113.0 (C-2), 117.5 (C-5), 125.3 (C-1), 133.3 (C-10), 136.6 (C-4), 157.5 (C-3), 161.9 (C=O), 178.7 (C=O), 221.8 (17 C=O). ES-MS *m/z* (MeOH 40V): 695.6 $[M+H_2O+H]^+$. Purity: 96% (HPLC, 203 nm, R_t = 12.76 min, 65% MeOH).

3.2.3.8 N-(13-Amino-4,7,10-trioxatridecanyl)-(3,17β-dihydroxyestra-1,3,5(10)-trien-4-yl)thiopropanamide (13)

9 (28 mg, 0.041 mmol) was dissolved in formic acid (4 mL) and stirred at room temperature for 4 h before removal of acid under vacuum. The compound **13** could not be column separated on normal phase silica due to its high polarity and so was used as is (though shown to be quite pure by TLC apart from the Boc unit). TLC R_f = 0.12 (5:1 MeOH: acetic acid). ES-MS *m/z* (MeOH) 615.2 $[M+2H_2O+H]^+$, 637.3 $[M+2H_2O+Na]^+$.

3.2.3.9 N-(13-Amino-4,7,10-trioxatridecanyl)-(3-hydroxyestra-1,3,5(10)-trien-17-on-4-yl)thiopropanamide (14)

12 (15 mg, 0.022 mmol) was dissolved in formic acid (2 mL) and stirred at room temperature for 5 h before removal of solvent under vacuum. The compound **14** could not be column separated on normal phase silica due to its high polarity and so was used as is (though shown to be quite pure by TLC apart from the cleaved Boc). TLC R_f = 0.28 (1:1 methanol: acetic acid). ES-MS *m/z* (20 V, MeOH): 577.5 $[M+H]^+$.

3.2.3.10 17β-Hydroxyestra-1,3,5(10)-trien-3-yl hemisuccinate (15)

17β-Estradiol (100 mg, 0.367 mmol) was dissolved in pyridine (9 mL). Succinic anhydride (37 mg, 0.367 mmol in 1 mL of pyridine) was added drop-wise to the rapidly stirring solution. The reaction was then stirred at 45 °C for 24 h. The pyridine was then dried off in vacuo and the resultant sample purified by flash chromatography using successively $CHCl_3$, 15:1 $CHCl_3$: MeOH, 10: 1 $CHCl_3$: MeOH as eluant to yield **15** as a semi-solid. Yield: 24% (33 mg, 0.088 mmol). IR (film): 1588 (COO^- υ), 1739 (C=O υ ester), 3584 (OH υ) cm^{-1}. ^1H NMR ($CDCl_3$ + CD_3OD) δ: 0.77 (3H, s, 18-CH_3), 2.74 (2H, t, *J* = 8.9 Hz, C**H**$_2$-ester), 2.84 (2H, t, *J* = 7.3 Hz, C**H**$_2$-acid), 6.55 (1H, m, 4-H), 6.84 (1H, m, 1-H), 7.28 (1H, m, 2-H); ^{13}C NMR ($CDCl_3$ + CD_3OD) δ: 11.1 (18-CH_3), 23.1 (C-15), 26.2 (C-7), 27.1 (C-11), 27.3 (**C**H_2CO), 29.1 (C-6), 29.5 (**C**H_2COOH), 36.7 (C-

12), 38.6 (C-16), 43.2 (C-8), 44.2 (C-9), 49.8 (C-13), 50.1 (C-14), 81.6 (17-C), 118.5 (2-C), 121.4 (4-C), 126.4 (1-C), 131.7 (5-C), 138.0 (10-C), 148.4 (3-C), 171.6 (C=O), 174.9 (COOH). ES-MS *m/z* (MeOH, 40 V) 395.3 $[M+Na]^+$.

3.2.3.11 ***N-(13-(t-Butoxycarbonylamino)-4,7,10-trioxatridecanyl)-3-(17β-hydroxyestra-1,3,5(10)-trien-3-yl)oxycarbonylpropanamide (16)***

15 (72 mg, 0.194 mmol) was dissolved in 1:1 DMF: $CHCl_3$ (2.5 mL, dried over molecular sieves). This solution was stirred whilst DCC (60 mg, 0.292 mmol, in 500 μL of DMF dried over molecular sieves) was added drop-wise followed by NHS (34 mg, 0.292 mmol, in 500 μL of DMF dried over molecular sieves) also drop-wise. The solution was stirred in the dark overnight. White solid was filtered from the solution and washed with $CHCl_3$ and DMF before removing all solvent in the filtrate under vacuum. The resultant white semi-solid was reconstituted in 1:1 DMF: $CHCl_3$ (2 mL, dried over molecular sieves) and **8** was added (94 mg in 3.25 mL of 2:1 DMF: $CHCl_3$ dried over molecular sieves) drop-wise to the stirring solution. Triethylamine (1 mL, dried over molecular sieves) was added and the reaction stirred in the dark overnight. The solvent was removed and the sample dried under vacuum. The sample was then column separated using $CHCl_3$, 15:1 $CHCl_3$: MeOH and 10:1 $CHCl_3$: MeOH as eluant to yield **16** as a white semi-solid. Yield: 49% (64 mg, 0.095 mmol). IR (film): 1627 (aromatic υ), 1654 (amide C=O υ), 1702 (Boc C=O υ), 1736 (ester C=O υ), 2850 (CH_2 symmetric υ), 2926 (CH_2 asymmetric υ), 3326 (OH υ) cm^{-1}. ^1H NMR ($CDCl_3$ + CD_3OD) δ: 0.77 (3H, s, 18-CH_3), 1.44 (9H, s, Boc methyls), 2.47 (2H, t, J = 9.3 Hz, hemisuccinate CH_2-amide), 2.65 (2H, t, J = 9.4 Hz, hemisuccinate CH_2-ester), 6.62 (1H, m, 2-H), 6.79 (1H, m, 4-H), 7.12 (1H, m, 1-H); ^{13}C NMR ($CDCl_3$ + CD_3OD) δ: 11.1 (18-CH_3), 23.2 (C-15), 25.7 (C-7), 26.5 (11-C), 27.4 (**C**H_2CO), 28.5 (Boc Me), 28.9 (Boc Me), 29.5 (Boc Me), 29.6 (CH_2 OEG chain), 29.8 (CH_2 OEG chain), 30.1 (C-6), 30.8 (C-16), 33.9 (**C**-CO), 36.8 (C-12), 37.5 (CH_2-NH steroid end), 39.1 (CH_2-NH Boc end), 44.1 (C-8), 48.8 (C-9), 48.9 (C-13), 50.2 (C-14), 69.6 (CH_2O), 70.2 (CH_2O), 70.2 (CH_2O), 70.6 (CH_2O), 70.6 (CH_2O), 81.7 (C-17) 83.3 (O**C**Me_3), 118.6 (2-C), 121.5 (4-C), 126.4 (1-C), 131.8 (5-C), 138.0 (10-C), 148.5 (3-C), 158.0 (C=O), 172.1 (C=O), 173.8 (C=O). ES-

MS *m/z* (MeOH, 40 V) 697.5 $[M+Na]^+$. HiRes FAB-MS: Calculated 675.4202, Found 675.4202 (MH^+).

3.2.3.12 ***Estra-1,3,5(10)-trien-17-on-3-yl hemisuccinate (17)***

Estrone (200 mg, 0.740 mmol) was dissolved in THF (5 mL). Succinic anhydride (140 mg, 1.39 mmol, in 1mL of THF) was added to the stirring estrone solution. Triethylamine was added (240 μL) and then 4-(dimethylamino)pyridine (DMAP) (90 mg) and the reaction solution was stirred at 60 ^{0}C for 24 h. The solvent was then removed and the sample purified by flash chromatography using $CHCl_3$ and 10:1 $CHCl_3$: MeOH eluant to yield **17** as a white powder. Yield: 25% (69 mg, 0.185 mmol). TLC R_f = 0.39 (15:1 $CHCl_3$: MeOH). Mp 211-212 °C (lit.[245] 215-217 °C). IR (film): 1711 (acid C=O υ), 1735 (estrone 17- C=O υ), 1755 (ester C=O υ) cm^{-1}. ^{1}H NMR ($CDCl_3$) δ: 0.91 (3H, s, 18-CH_3), 2.74 (2H, t, *J* = 6.9 Hz, C**H$_2$**-amide), 2.85 (2H, t, *J* = 6.9 Hz, C**H$_2$**-acid), 6.81 (1H, s, 4-H), 6.85 (1H, d, *J* = 9.3 Hz, 1-H), 7.26 (1H, d, *J* = 8.5 Hz, 2-H). ^{13}C NMR ($CDCl_3$) δ: 13.9 (13-CH_3), 21.6 (15-CH_2), 25.8 (7-CH_2), 26.4 (11-CH_2), 29.0 (CH_2-ester), 29.4 (6-CH_2), 31.6 (**C**H$_2$-COOH), 35.9 (C-12), 38.1 (C-16 and C-8), 44.2 (C-9), 48.1 (C-13), 50.5 (C-14), 118.7 (2-C), 121.5 (4-C), 126.4 (1-C), 137.5 (5-C), 138.1 (10-C), 148.6 (3-C), 171.5 (ester), 174.8 (COOH), 221.8 (17 C=O). ES-MS *m/z* (MeOH, 60 V) 392.6 $[M+Na]^+$.

3.2.3.13 ***N-(13-(t-Butoxycarbonylamino)-4,7,10-trioxatridecanyl)-3-(estra-1,3,5(10)-trien-17-on-3-yl)oxycarbonylpropanamide. (18)***

17 (64 mg, 0.173 mmol) was dissolved in dry DMF (1 mL). DCC (47 mg in 500 μL of dry DMF) was added dropwise to the rapidly stirring solution. This was followed by NHS (26 mg in 500 μL of dry DMF) and the reaction was stirred overnight in the dark. The reaction sample was filtered to remove 1,3-dicyclohexylurea (DCU) and the filtrate was dried under vacuum. The sample was reconstituted in dry DMF (1 mL) and **8** (79 mg, 0.260 mmol in 2:1 DMF: $CHCl_3$ (dry, 3 mL)) was added drop-wise to the rapidly stirring solution. This was followed by triethylamine (1 mL) and the solution was stirred overnight in the

dark. The solvent was removed and the dried sample purified by flash chromatography using in succession $CHCl_3$, 15: 1 $CHCl_3$: MeOH, 10: 1 $CHCl_3$: MeOH, 2: 1 $CHCl_3$: MeOH to yield **18** as a waxy white solid. Yield: 91% (106 mg, 0.157 mmol). TLC R_f = 0.55 (15:1 $CHCl_3$: MeOH). IR (film): 1141 (CH_2O υ), 1649 (C=O υ amide), 1710 (Boc amide C=O υ), 1738 (estrone 17- C=O υ, ester C=O υ), 2858 (CH_2 symmetric υ), 2929 (CH_2 asymmetric υ) cm^{-1}. ^1H NMR ($CDCl_3$ + CD_3OD) δ: 0.92 (3H, s, 18-CH_3), 1.44 (9H, s, Boc CH_3), 2.85 (2H, m, CH_2-hemisuccinate amide, OEG end), 2.88 (2H, m, CH_2- hemisuccinate ester, aromatic end), 3.53-3.73 (10H, m, OEG CH_2-O), 6.62 (1H, m, 4-H), 6.83 (1H, m, 2-H), 7.19 (1H, m, 1-H). ^{13}C NMR ($CDCl_3$ + CD_3OD) δ: 13.9 (18-CH_3), 21.7 (C-15), 25.1 (C-7), 25.8 (C-11), 25.9 (C-6), 26.5 (Boc CH_3), 28.5 (Boc CH_3), 29.0 (Boc CH_3), 29.5 (CH_2CO), 29.6 (CH_2 OEG chain), 31.6 (CH_2CO), 31.7 (C-12), 33.9 (C-16), 36.1 (CH_2NH), 38.2 (CH_2NH), 44.1 (C-8), 44.3 (C-9), 48.7 (C-13), 50.6 (C-14), 69.4 (CH_2O), 69.5 (CH_2O), 70.2 (CH_2O), 70.2 (CH_2O), 70.6 (CH_2O), 79.3 (CMe_3), 118.8 (2-C), 121.6 (4-C), 126.4 (1-C), 131.0 (5-C), 137.8 (10-C), 148.7 (3-C), 156.8 (C=O), 163.3 (C=O), 172.1 (C=O), 222.3 (17 C=O). ES-MS *m/z* (MeOH, 40 V): 695.5 $[M+Na]^+$.

3.2.3.14 ***2-(N-(13-(t-Butoxycarbonylamino)-4,7,10-trioxa-1,13-tridecanyl)-(aminomethyl)-3,17β-dihydroxyestra-1,3,5(10)-triene) (19).***

Estradiol (100 mg, 0.367 mmol) was dissolved in absolute EtOH (10 mL). **8** (236 mg, 0.734 mmol in 4:1 EtOH:water (5 mL)) was added gradually to the solution whilst stirring. This was followed by 37% v/v formaldehyde solution (222 μL, 8.06 mmol) and the solution was heated under reflux with stirring for 6 h. The solvent was removed under vacuum and the sample reconstituted in chloroform before column separation with $CHCl_3$, 15:1 $CHCl_3$: MeOH, 10:1 $CHCl_3$: MeOH as successive eluants to yield **19** as a clear colourless oil. Yield: 13% (30 mg, 0.048 mmol). IR (film): 1692 (C=O υ Boc amide), 3584 (OH υ) cm^{-1}. ^1H NMR ($CDCl_3$ +CD_3OD) δ: 0.77 (3H, s, 18-CH_3), 1.43 (9H, s, Boc methyl), 2.80 (2H, m, CH_2-Ar), 3.60 (14H, m, OEG CH_2-O), 6.51 (1H, s, 4-H), 6.88 (1H, s, 1-H). ^{13}C NMR ($CDCl_3$ + CD_3OD) δ: 11.1 (18-CH_3), 23.2 (C-15), 26.5 (7-C), 27.3 (C-11), 28.2 (Boc Me), 28.4 (Boc Me), 28.5 (Boc Me), 29.4 (CH_2 OEG

chain), 29.6 (C-6), 30.1 (16-C and 5-C), 36.8 (12-C), 38.2 (CH_2NH Boc end), 39.0 (8-C), 43.3 (9-C), 44.1 (CH_2NH), 48.3 (CH_2NH), 48.9 (13-C), 49.5 (14-C), 69.1 (CH_2O), 69.3 (CH_2O), 69.5 (CH_2O), 70.2 (CH_2O), 70.6 (CH_2O), 72.1 (CH_2O), 81.6 (Boc $\mathbf{C}Me_3$), 82.4 (17-C), 116.0 (4-C), 117.3 (2-C), 124.4 (1-C), 133.0 (5-C), 136.5 (10-C), 151.8 (3-C), 155.1 (amide C=O). COSY NMR ($CDCl_3$) showed no coupling of aromatic protons. ES-MS *m/z* (MeOH, 40 V) 605.5 $[M+H]^+$.

3.2.3.15 ***2-(N-(13-(t-Butoxycarbonylamino)-4,7,10-trioxatridecanyl)-(aminomethyl)-3-hydroxyestra-1,3,5(10)-trien-17-one) (20).***

Estrone (100 mg, 0.37 mmol) was dissolved in absolute ethanol (10 mL). **8** (238 mg, 0.74 mmol in 4:1 ethanol: water, 5 mL) was added gradually to the solution whilst stirring, followed by formaldehyde, (37%, 224 µL, 8.13 mmol). The solution was heated under reflux with stirring for 6 h. The solvent was removed in vacuo and the compound purified on a silica column using $CHCl_3$, 15:1 $CHCl_3$: MeOH, 10:1 $CHCl_3$: MeOH, 5:1 $CHCl_3$: MeOH, 2:1 $CHCl_3$: MeOH as successive eluants to yield a clear, colourless oil. Yield: 15% (33 mg, 0.054 mmol). IR (film): 1114 (CH_2O υ), 1691 (Boc C=O υ), 1736 (17 C=O υ estrone) 2868 (CH_2 symmetric υ), 2929 (CH_2 asymmetric υ), 3403 (OH υ) cm^{-1}. ^1H NMR ($CDCl_3$ + CD_3OD) δ: 0.90 (3H, s, 18-CH_3), 1.43 (9H, s, Boc CH_3), 2.83 (2H, m, C-6), 3.60 (14H, m, OEG CH_2-O), 6.70 (1H, d, J = 9.7 Hz, C-4), 7.03 (1H, s, C-1). ^{13}C NMR ($CDCl_3$ + CD_3OD) δ: 13.9 (18-CH_3), 21.6 (15-C), 26.0 (7-C), 26.6 (11-C), 28.4 (Boc Me), 28.5 (Boc Me), 29.2 (C-$\mathbf{C}H_2$-C Boc end of OEG), 29.3 (6-C, C-$\mathbf{C}H_2$-C steroid end of OEG), 29.7 (16-C), 31.6 (12-C), 35.9 (CH_2-N), 38.3 (8-C), 43.9 (9-C), 44.0 (CH_2-Ar), 46.2 (CH_2-NH estrone end), 48.0 (13-C), 50.1 (14-C), 69.0 (CH_2-O), 69.1 (CH_2-O), 69.4 (CH_2-O), 70.2 (CH_2-O), 70.4 (CH_2-O), 70.6 (CH_2-O), 78.9 (Boc $\mathbf{C}Me_3$), 116.1 (C-4), 124.3 (C-2), 131.2 (C-1), 132.1 (C-5), 136.1 (C-10), 152.1 (C-3), 156.1 (Boc C=O), 220.8 (17 C=O). ES-MS *m/z* (MeOH, 40 V) 603.5 $[M+H]^+$. COSY NMR: No coupling between aromatic signals.

3.2.3.16 ***(13-Amino-4,7,10-trioxatridecanyl)-3-(17β-hydroxyestra-1,3,5(10)-trien-3-yl)oxycarbonylpropanamide (21).***

16 (48 mg, 0.071 mmol) was dissolved in formic acid (4 mL) and stirred at room temperature for 2.5 h before adding chloroform (1 mL) to improve solubility. Stirring was continued for an additional 1.5 h. Solvent was removed in vacuo and the compound column separated using 10:1 MeOH: AcOH eluant to yield **21** as a semi-solid after drying in vacuo. IR (film): 1414 (CH_2 or CH_3 deformation), 1561 ($-NH_3^+$), 1638 (amide C=O υ), 3434 (OH υ) cm^{-1}. ^1H NMR ($CDCl_3$) δ: 2.52 (2H, t, *J* = 6.0 Hz, CH_2-amide), 2.65 (2H, t, *J* = 7.2 Hz, CH_2-ester), 2.81 (2H, d, *J* = 12.0 Hz), 3.09 (2H, t, *J* = 7.4 Hz), 3.23 (2H, m), 3.55 (3H, m, OEG CH_2-O), 3.66 (11H, m, OEG CH_2-O). ^{13}C NMR ($CDCl_3$) δ: 21.1 (6-C), 23.3 (15-C), 29.8 (CH_2-ester), 38.8 (CH_2-NH_2), 70.1 (CH_2-O), 70.4 (CH_2-O), 83.4 (17-C), 174.8 (C=O amide). Note: NMR weak due to low solubility. ES-MS *m/z* (MeOH) 575.2 $[M+H]^+$.

3.2.3.17 ***2-(13-Amino-4,7,10-trioxa-1,13-tridecanyl)-(aminomethyl)-3,17β-dihydroxyestra-1,3,5(10)-triene) (22).***

19 (21 mg, 0.034 mmol) was dissolved in formic acid (3 mL) and stirred for 4 h at room temperature before removal of acid in vacuo. The product was column purified using 2:1 methanol: acetic acid to elute the product. TLC R_f = 0.33 (10:1 methanol: acetic acid). IR (film): 1134 (CH_2O υ), 1421 (CH_2-S/CH_2 or CH_3 deformation), 2981 ($-NH_3^+$ υ or CH_2 υ), 3438 (OH υ) cm^{-1}. ^1H NMR (CD_3OD) δ: 0.89 (3H, s, 18-CH_3), 2.83 (2H, m, C-7), 3.64 (m, OEG CH_2-O). ES-MS *m/z* (MeOH) 505.3 $[M+H]^+$.

3.2.3.18 ***(13-Amino-4,7,10-trioxa-tridecanyl)-3-(estra-1,3,5(10)-trien-17-on-3-yl)oxycarbonylpropanamide (23).***

18 (55 mg, 0.081 mmol) was dissolved in formic acid (3 mL) and stirred for 4 h at room temperature before removal of solvent in vacuo. The compound was too polar to be column separated on normal phase silica and so was used as is. TLC R_f

= 0.68 (1:1 methanol: acetic acid, very streaky). ES-MS *m/z* (MeOH 40 V) 573.5 $[M+H]^+$.

3.2.3.19 ***2-((13-Amino-4,7,10-trioxatridecanyl)-(aminomethyl)-3-hydroxyestra-1,3,5(10)-trien-17-one) (24).***

20 (18 mg, 0.030 mmol) was dissolved in formic acid (2 mL) and stirred for 4 h at room temperature before removal of solvent in vacuo. The compound was too polar to be column separated on normal phase silica and so was used as is. TLC R_f = 0.19 (1:1 methanol: acetic acid, very streaky). ES-MS *m/z* (MeOH 40 V) 503.5 $[M+H]^+$.

3.2.4 BIAcore Binding Analysis Studies

3.2.4.1 Immobilisation of Estradiol Derivatives

A carboxymethyl 5 (CM5) sensor chip was docked in the BIAcore instrument and primed x 2 with running buffer. The surface was activated with 1:1 EDC: NHS (50 µL, 5 µL/min). An ~1 mg/mL solution of the estrogen derivative to be immobilized (in 1%v/v DMF in PBS/T buffer, pH = 9.7) was injected after centrifugation to remove any insoluble material (1 x 20 µL, 1 x 80 µL, 1 x 100 µL, 1 x 200 µL, 5 µL/min). This was immediately followed by injections of estrogen derivative (~1 mg/mL, 1%v/v DMF in PBS/T buffer, pH = 11.7, 1 x 200 µL, 2 x 100 µL) and then deactivation with 1.0 M ethanolamine (50 µL, 5 µL/min). **21** was immobilized in flow cell 2, **22** in flow cell 3 and **13** in flow cell 4. Flow cell 1 was activated with EDC/NHS as for the others and then immediately deactivated with ethanolamine (50 µL, 5µL/min) without immobilisation of estrogens to serve as a reference flow cell.

3.2.4.2 17β-Estradiol Antibody Binding Studies

Plots of response *vs* primary antibody concentration with no secondary antibody enhancement were prepared using a wizard program by injecting

primary monoclonal antibody (60 μL, at 0, 0.25, 0.5, 1, 2, 5, 10 and 25 μg/mL, 5 replicates of each, 20 μL/min) and waiting 120 s before regeneration with two pulses of 50 mM NaOH, 10% v/v MeCN (20 μL each, 20 μL/min).

Plots of response *vs* secondary antibody concentration for secondary antibody signal enhancement were prepared by injecting monoclonal primary antibody (60 μL, 20 μL/min, 0.5 μg/mL) followed immediately by secondary antibody (60 μL, 0, 10, 20, 50, 100, 200, 300 μg/mL, 10 μL/min) and then a 120 s wait before regeneration as above.

Plots of response *vs* monoclonal antibody concentration with secondary antibody enhancement were prepared by injecting monoclonal primary antibody (60 μL, 0, 10, 25, 50, 100, 200, 350, 500 ng/mL, 20 μL/min) immediately followed by secondary antibody (60 μL, 200 μg/mL, 10 μL/min), a 120 s wait and then regeneration as above.

3.2.4.3 SPR 17β-Estradiol Assays.

Assay curves for 17β-estradiol assay without secondary antibody enhancement were prepared by mixing monoclonal primary antibody (70 μL, 1 μg/mL) with 17β-estradiol solutions (70 μL, 0, 1, 5, 10, 50, 100, 500 pg/mL, 1, 5, 10 ng/mL, five replicates each, in HBS-EP pH=7.4 serially diluted from a 10 mg/mL stock in DMF) in a microwell plate, mixing using the automatic mixing function, incubating for 5 min at 25 °C and then injecting (60 μL, 20 μL/min) and then after a 120 s wait regenerating as above.

Assay curves for 17β-estradiol assay with secondary antibody enhancement were prepared by mixing monoclonal primary antibody (50 ng/mL, 70 μL) with 17β-estradiol solutions (70 μL, 0, 0.5, 1, 5, 10, 50, 100, 500 pg/mL, 1, 5 ng/mL, five replicates each, in HBS-EP pH=7.4) in a microwell plate, mixing and incubating and injecting as above. This injection was then immediately followed by injection of secondary antibody (60 μL, 200 μg/mL, 10 μL/min), a wait of 120 s and then regeneration as above. Assay curve data was fitted to four parameter logistic curves as described in Chapters 1 and 5. All CVs mentioned in the text are of the binding responses and the errors mentioned in the text are standard errors. Error bars on the curves are one standard deviation of the mean.

3.3 *Results and Discussion*

The complete reaction schemes for all the thio-bridged compounds are given in Figure 3.1 and the reference compounds in Figure 3.2. Each part of the synthesis is described in detail below.

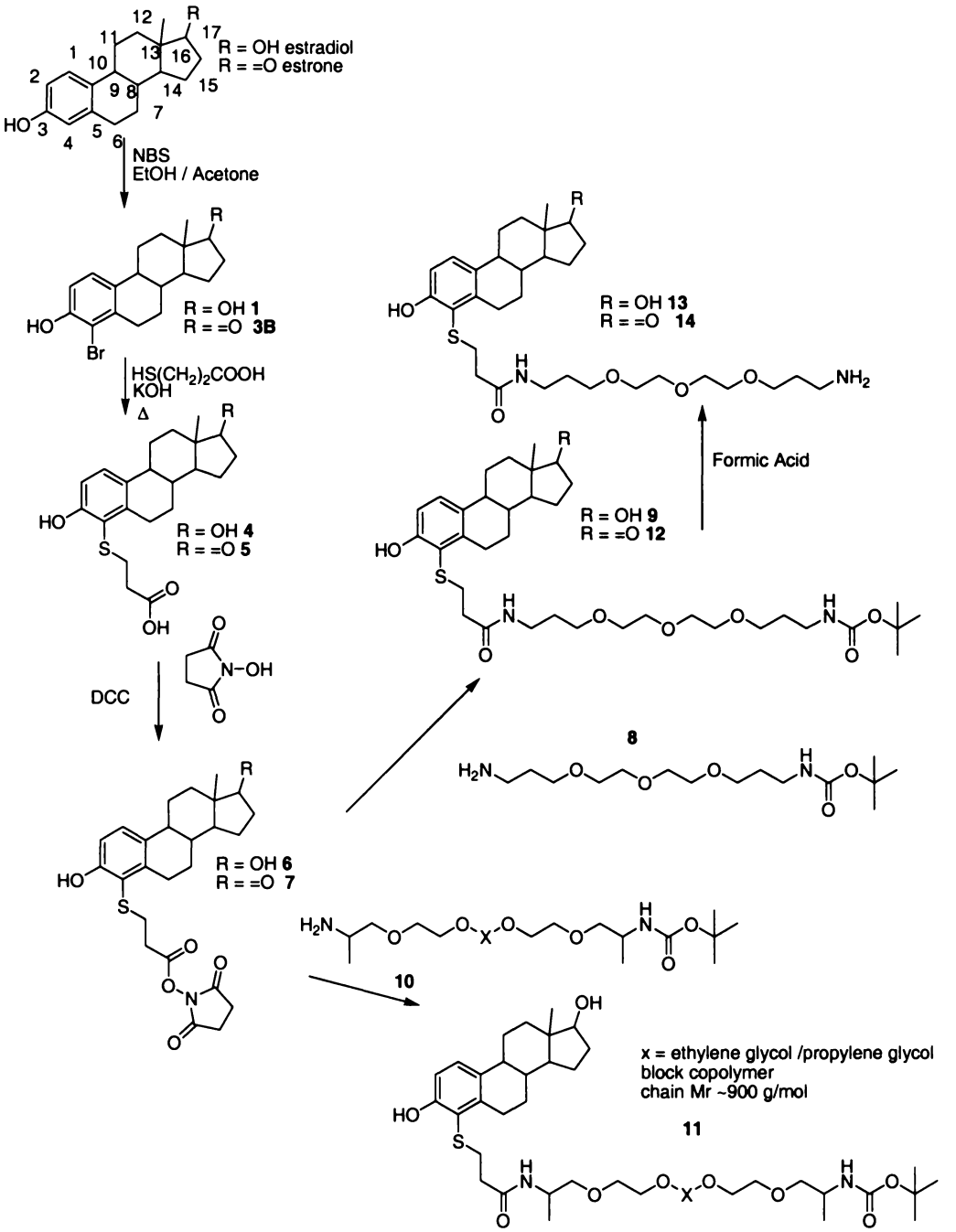

Figure 3.1. Synthesis of 4-position thiopropionate derivatives of 17β-estradiol and estrone and the attachment of oligoethylene glycol (OEG) chains.

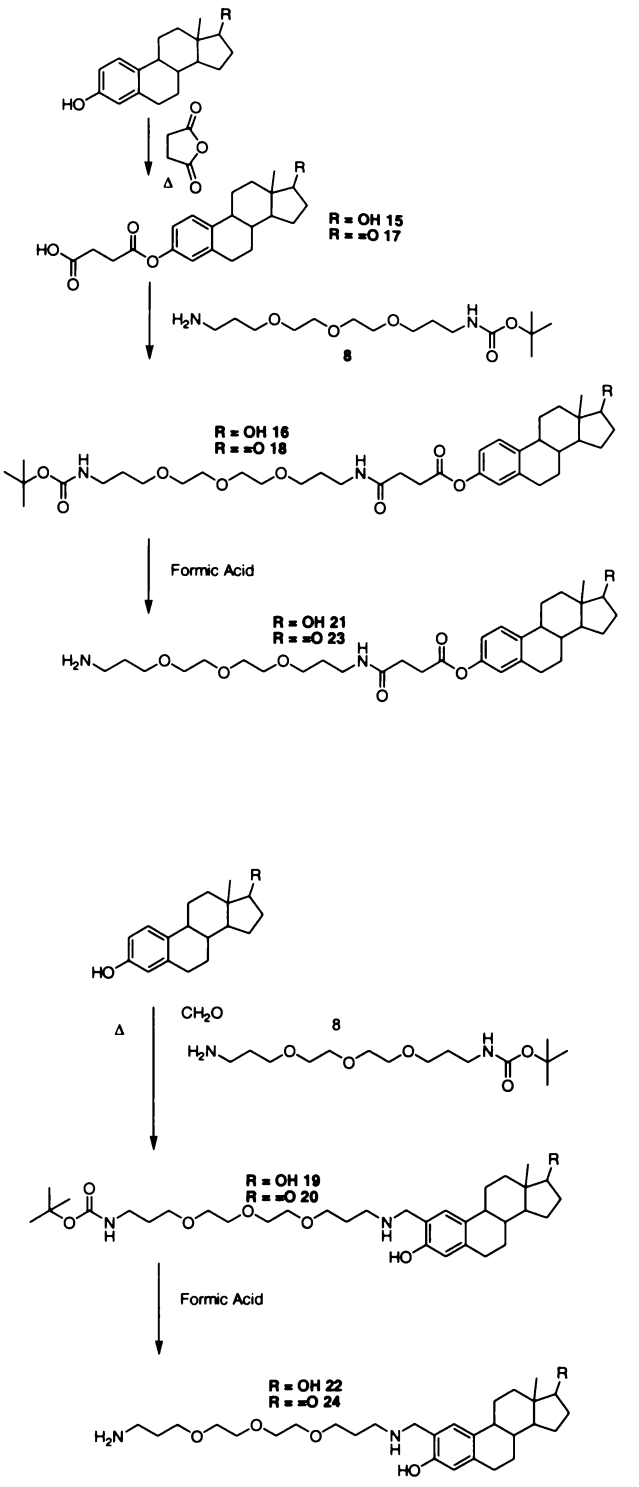

Figure 3.2. Synthesis of reference compounds. Synthesis of 3-hemisuccinate derivative of estradiol and estrone and attachment of an oligoethylene glycol (OEG) chain (top) and synthesis of 2-position Mannich reaction derivatives and attachment of OEG chain (bottom).

3.3.1 Synthesis of Estrogen Thioethers

The synthesis of 4-bromo-17β-estradiol **(1)** was achieved using an adaptation of the method of Lovely et al.[156] In their paper, they give no explicit directions on the experimental procedure and so the exact conditions used were determined by experimentation. The volume of ethanol used is critical for the successful precipitation of the brominated product from solution. TLC indicates that there is clearly some 4-bromo-17β-estradiol left in the solution, which can be recovered by column separation to further improve the 55% yield. The quality of the crystallised product was good with only one recrystalisation necessary to purify the compound, see Appendix 4. The NBS was used in a 1:1 molar ratio[244] to minimize any production of the 2,4-dibromoestradiol, and the 4-bromoestradiol is less soluble than any 2-bromo and so was precipitated out of the ethanol pure. NMR analysis showed no sign of 2-bromo or dibromo and so any such contaminant could be envisaged to be less than 1 %. The same applies to the bromination of estrone.

The synthesis of the 4-bromoestrone (**3**) gave somewhat more synthetic challenge. It has been previously asserted that this product should be made via the 2,4-dibromoestrone in order to get pure product uncontaminated by 2-bromoestrone.[151,152] In this thesis this method was applied successfully to produce the 4-bromoestrone (**3A**) by regioselective debromination of the 2,4-dibromoestrone (**2**) using palladium on carbon and formic acid in DMF. The overall yields involved in this two-step process were 16%, which is far too low for the production of a precursor compound at the beginning of a multi-step synthetic sequence. The original one-step method was successfully adapted to produce 4-bromoestrone (**3B**) in acceptably pure form and reasonable yield from simple reaction with *N*-bromosuccinimide (NBS). The key to this reaction was the use of a solvent combination of ethanol / acetone 1:1. This enabled the product to precipitate out of solution in the same way as for the 17β-estradiol bromination. The melting point was quite sharp and the NMR spectrum showed only the 4-bromoestrone. FAB-MS revealed a weak dibromo peak but this was not detectable under electrospray. The bromoestrogen products gave very distinctive

ES-MS spectra with the 1:1 bromo isotope pattern being very clearly visible, Figure 3.3. The brominations are shown in Figure 3.4.

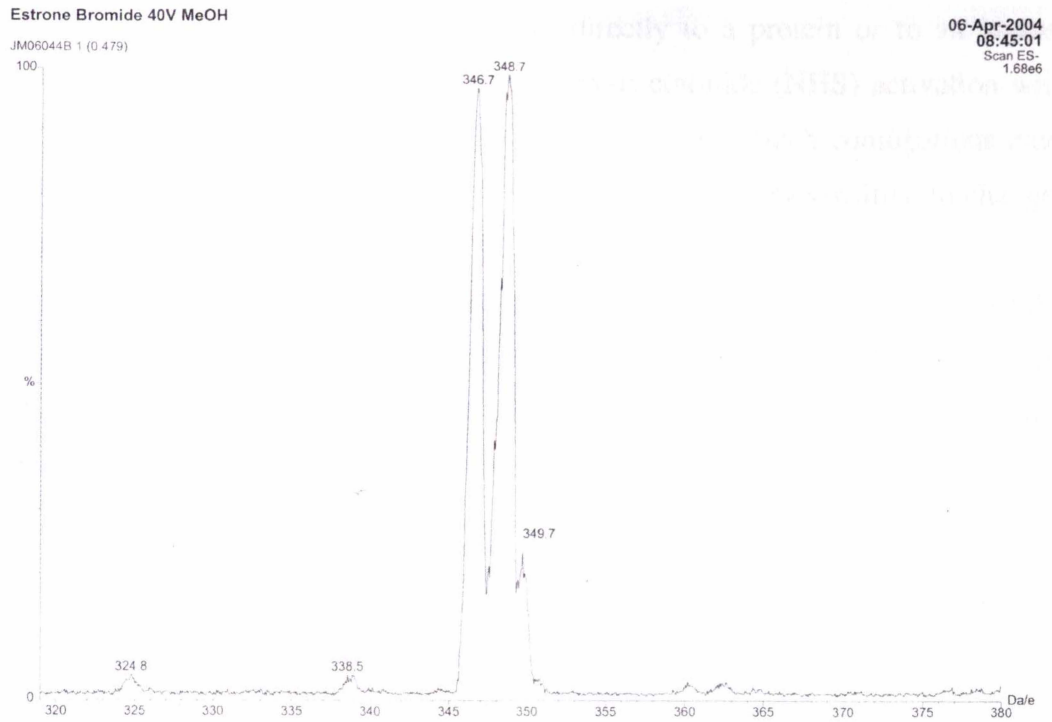

Figure 3.3 Electrospray mass spectrum of 4-bromoestrone **3B**.

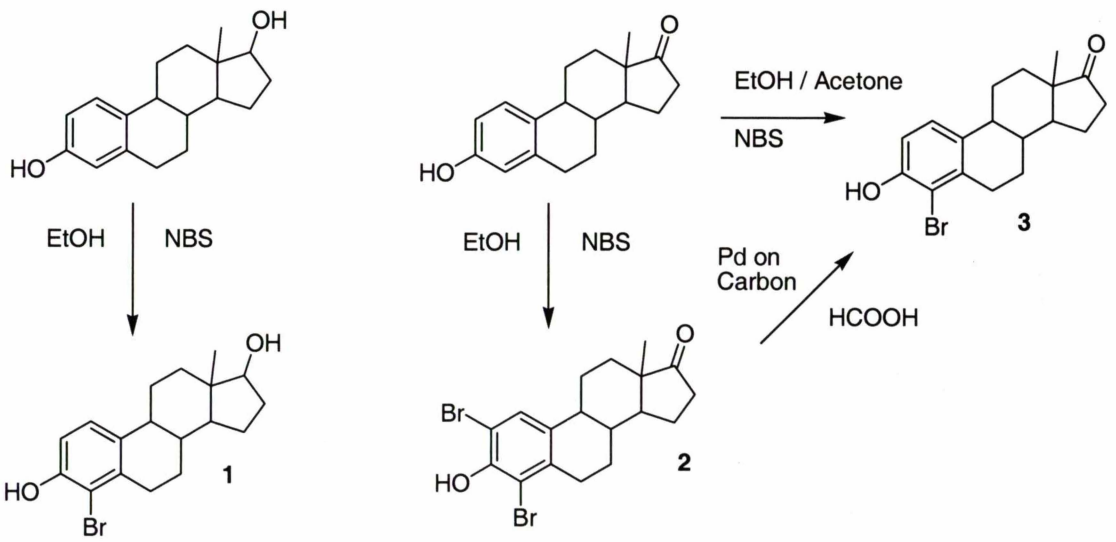

Figure 3.4 Bromination of estradiol and estrone to obtain 4-bromoestrogens.

The next step in the reaction sequence was to perform the aromatic substitution of the bromoestrogens with 3-mercaptopropionic acid (MPA). This unit is very

useful for conjugations as it can form the thioether linkage without interference from the carboxylic acid function. The thioether linkage is very stable, and the carboxylic acid enables attachment either directly to a protein or to an amine-terminating intermediate linker by *N*-hydroxysuccinimide (NHS) activation with dicyclohexylcarbodiimide (DCC) as dehydrating agent. Such conjugations have been demonstrated to be very repeatable as they are not very sensitive to changes in reaction conditions.[10, 15]

The aromatic A-ring of the estrogens does not lend itself to nucleophilic substitution because of the presence of the electron donating hydroxyl moiety, which will deactivate nucleophilic substitution at the *ortho* position. However, radical-mediated substitutions of halogens on aromatic rings by thiol compounds is widely known and usually proceeds via an $S_{RN}1$ mechanism.[174]

By regioselectively synthesising the 4-monobromo product it is possible to directly substitute to the 4-position exclusively. This exclusive attachment at the 4-position is not possible when using the Mannich reaction, which produces a mixture of products at the 4- and 2-positions that is seldom purified but rather reacted straight through to protein conjugation in one step. The use of a 4-bromo derivative provides a labile leaving group for the substitution whilst the 4-bromo derivative is quite stable when stored at room temperature in the dark. To effect the substitution, base is used to abstract the proton from the –SH group of the 3-mercaptopropionic acid (MPA) to produce $R\text{-}S^-$.

The reflux is done under dry conditions to minimise risk of hydrolysis of the bromo derivative. The substitution was performed in both cases by reflux with the MPA in methanolic KOH. The reaction scheme for the thioether formation is given in Figure 3.1.

For estradiol, the reflux was for 24 h, in the dark to ensure no photolytic degradation of the 4-bromoestradiol reactant. The product (**4**) was extracted into the ethyl acetate phase from water and the organic phase washed to remove as much MPA as possible (product and MPA were found in both phases). Upon TLC analysis, it was seen that the product spot was overlapping with that of the MPA and this was confirmed by NMR which showed strong MPA peaks overlaying the estradiol-thioether structure whose CH_2-S and CH_2-COOH peaks could be seen offset slightly from those of the unreacted MPA. The NMR overall corresponds to the literature data but the coupling constants for the propionic acid

chain are somewhat distorted by the MPA though they are much clearer for the later pure compounds **6** and **9** at around 7.1 Hz, which is the coupling constant observed for the acid propionate chain in the literature.[107] Presence of the product was further confirmed by mass spectrometry with a clear $[M+Na]^+$ peak. There was no presence of 4-bromoestradiol signals and their characteristic double peak. In order to completely remove the MPA and obtain a pure sample it was necessary to proceed directly to the next step without further purification. Attempts were also made to purify the product by precipitation from the aqueous phase by pH adjustment to acid. This method proved to be unreliable.

The only previous synthesis of **4** was done through the 4,5-epoxide in three steps from nandrolone.[107] This reaction is rather complex and starts from a restricted drug making it a less desirable method to use.

For production of the estrone MPA derivative (**5**) the same reaction method was employed. The sample was worked up by reconstituting the raw reaction mixture in water and then washing it with ethyl acetate to remove unreacted 4-bromoestrone. The aqueous phase was then separated by flash chromatography. The lower polarity of the estrone MPA compared with the estradiol MPA product allowed complete column purification at this stage so NMR could be obtained of the pure sample, Figure 3.5. Once again further conclusive mass spectra were obtained and there was once again no sign of unreacted bromo-derivative in the final pure sample. In both samples the risk of hydrolysis of the bromo-estrogen was minimised by using thoroughly dried solvents. In both steroid derivatives attachment at the 4-position was verified by the aromatic proton substitution pattern, which showed two doublets at 6.89 and 7.22 ppm for estradiol and 6.81 and 7.22 ppm for estrone. This is consistent with two single aromatic protons coupling to each other *ortho*, which can only occur for the protons 1 and 2. There are no other aromatic proton signals, so this emphatically shows 4-substitution. The same sorts of pattern can of course be seen in the corresponding bromoestrogens, with 6.88 and 7.21 ppm and J = 8.5 and 8.3 Hz respectively for 4-bromoestradiol and 6.86 and 7.18 ppm and J = 8.6 Hz for both for 4-bromoestrone.

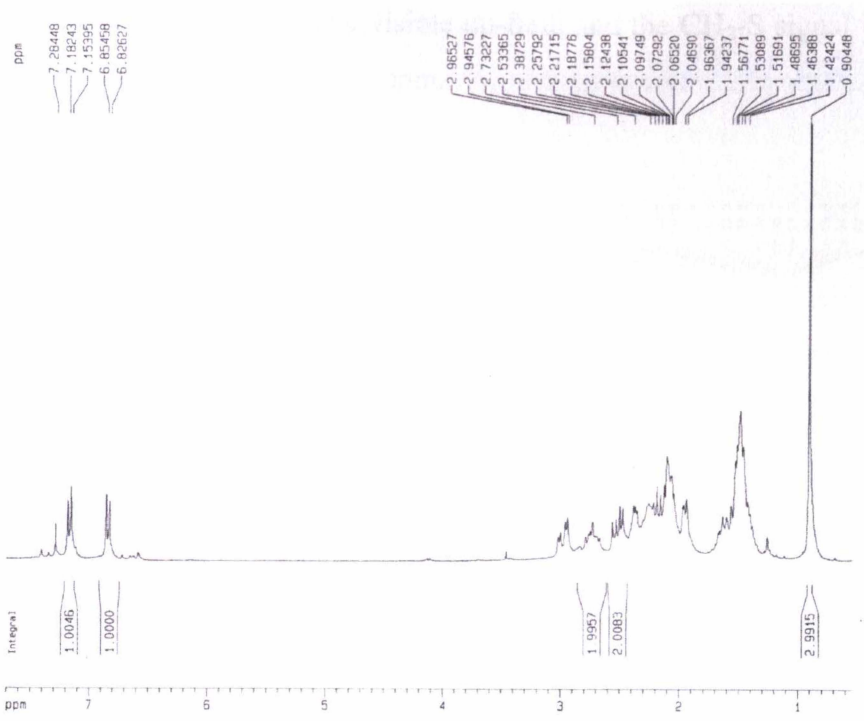

Figure 3.5 ^{1}H NMR Spectrum of **5**

3.3.2 Synthesis of Polyethylene Glycol Derivatives

The NHS active ester of **4** was synthesised by simply dissolving the steroid derivative in dry DMF and adding DCC and NHS. As the compound was somewhat impure with MPA, a large excess of NHS was used to produce the active ester. The DCC acts as a dehydrating agent in the reaction, removing water released upon active ester formation to produce dicyclohexylurea (DCU) and so push the reaction further forward. The active ester product (**6**) could be purified well by flash chromatography, as the polarity was now much lower and was quite different from that of any contaminating MPA or MPA ester. There was no sign of the MPA or MPA ester in the NMR or TLC analyses indicating that purification at the ester stage has been successful.

The Dept 135 spectrum (Figure 3.6) shows that there are only two CH aromatic carbons in the structure, showing that 4-position attachment of the propionate unit has been retained under the reaction conditions. The chemical shifts are consistent with those expected for the 1-H and 2-H protons. The estradiol steroid peaks for

the non-aromatic rings are clearly visible up-field and the CH_2-S signal is seen at 29.7 ppm and the NHS CH_2 at 24.7 ppm.

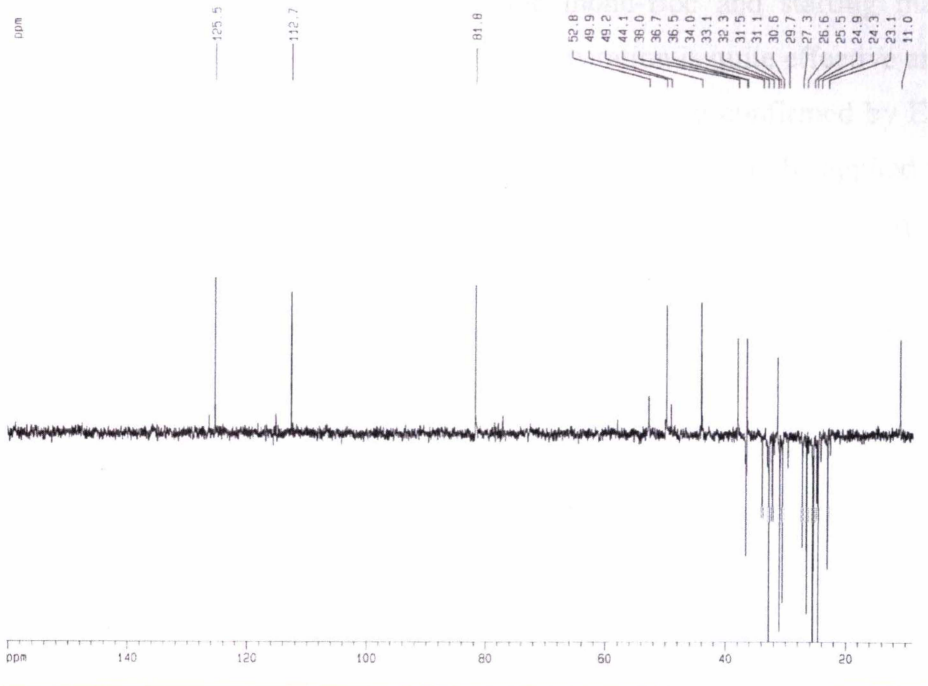

Figure 3.6 Dept 135 Spectrum of **6**

The formation of the estrone-NHS ester **(7)** occurred as expected. The expected electrospray peak was clearly observed and the NHS proton peak at 2.89 ppm was seen at the expected 4H intensity. Throughout these reactions the aromatic proton peaks at 1- and 2-positions have been retained as expected. The ^{13}C NMR spectrum is given in Figure 3.7.

The next step in the reaction sequence was to produce oligoethylene glycol derivatives of the steroids. To do this one uses amine-terminating OEG chains. To prevent dimerisation of the steroid it was necessary to protect one of the amine terminals and react the other with the NHS active ester of the steroid. The most effective way of doing this is to attach a *tert*-butoxy carbonyl moiety (Boc) to one of the terminal amine groups through reaction with di-*tert*-butyl dicarbonate (DBDC). Boc is a very common protecting group and can be easily attached to amine groups. When it needs to be removed this can be done by treatment with formic acid, Figure 3.1. The production of the mono-Boc protected OEG **(8)**[243] proceeds simply by adding the DBDC to a stirring solution of the OEG under

septum, drop-wise with vigorous stirring to ensure that the minimum of di-Boc product is formed, after adding triethylamine as a weak base. The reaction can be clearly visualised by ninhydrin treatment of the TLC plate, with the di-Boc producing only a very weak signal and the mono-Boc and starting material producing much stronger colour. The column separation is quite effective and the yields are quite good at 69%. The reaction can clearly be confirmed by ESMS, which gives a very strong product peak. The same reaction can be applied to the longer PEG-900 chain (**10**) with a yield of 41%. The electrospray mass spectrometry of this sample produces a large number of peaks arising from multiple charging of the polymer chain whereas the shorter OEG chain produces one discrete $[M+H]^+$ peak only. The short OEG chain has three ethylene glycol monomeric units whereas the longer PEG chain has on average n = 15-19 ethylene glycol and/or propylene glycol units.

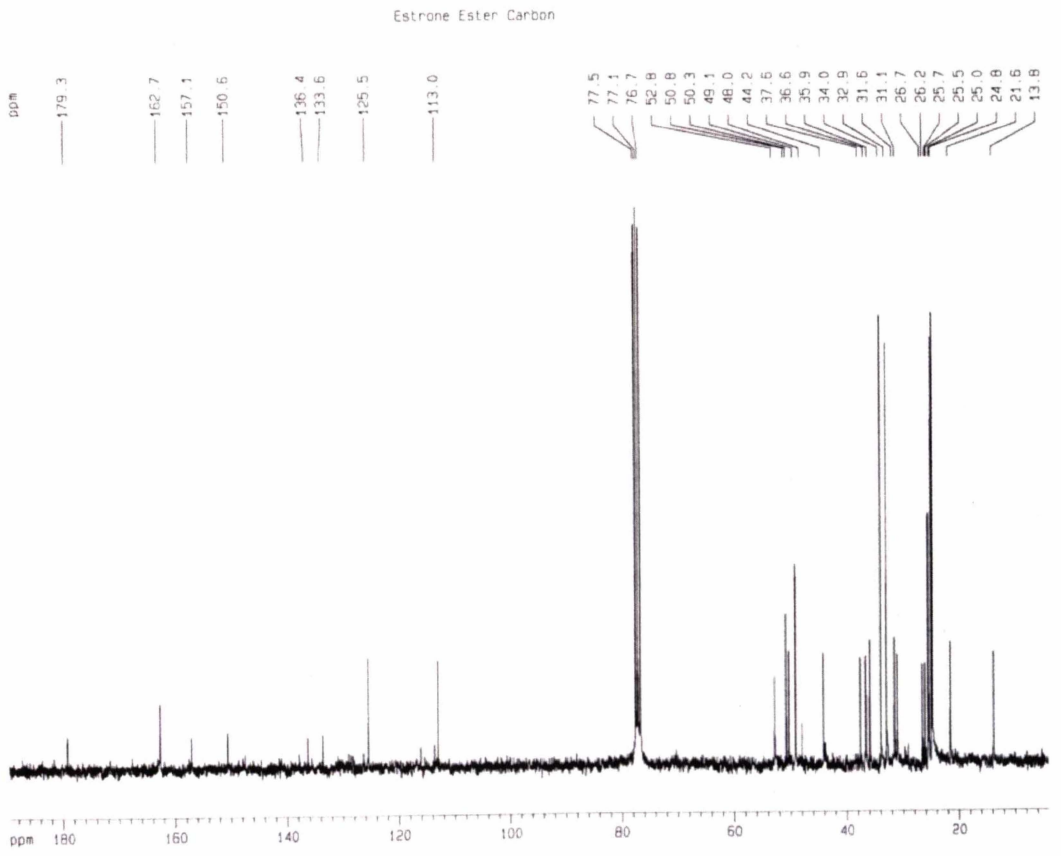

Figure 3.7 ^{13}C NMR of **7**

The mono-Boc protected OEG (**8**) was then reacted with the activated acid unit of the steroid to attach the OEG chain through the 4-position of the steroid. This could be achieved simply by addition of the mono-Boc OEG to the steroid active ester under dry conditions and addition of some triethylamine as mild base. The active ester is very reactive with the amine under these conditions and the amide linkage is formed to the OEG chain. For estradiol this was done by reaction of the active ester derivative and purification by simple flash chromatography to produce the amide (**9**) in 86% yield. The oil-nature of the OEG chain means that the product is also an oil. The compound in this Boc-protected form is quite stable for extended periods with no highly reactive functional groups. When it is ready to use it is a simple matter of removing the Boc protecting group of the compound to expose the terminal amine and proceed as required either with further reaction or immobilisation. The various characteristic groups of the estradiol derivative can be seen quite clearly in the NMR spectrum with the CH_2-S at 2.99 ppm J = 7.1 Hz, and CH_2-CO-N at 2.56 ppm J = 7.1 Hz. The Boc trimethyl protons are very characteristic at 1.44 ppm as a 9H singlet. The repeating ethylene glycol units can also be seen at 3.6 ppm for the CH_2-O and 12H intensity (six CH_2-O in the chain). The ^{1}H NMR spectrum for the estradiol short OEG derivative (**9**) is given in Figure 3.8.

The same general procedure was applied for the long PEG-900 derivative synthesis, though the yield was somewhat lower at 27%, compared with 86% for the shorter chain. This could possibly be due to approach to the amine terminal being sterically hindered by the much longer PEG chain folding over its amine terminals in solution. TLC analysis shows that the longer chain derivative (**11**) is noticeably more polar than the shorter chain derivative indicating that the longer the PEG chain the more polar the end steroid derivative becomes. This is as expected as the estrogens are not very polar whilst the PEG chain is. Once again the characteristic peaks are present in the NMR of the Boc 9H at 1.44 ppm and the CH_2-COO- at 2.58 ppm, J = 7.1 Hz and the CH_2-S- at 2.73 ppm, J = 7.0 Hz. In the ESMS there is a multiple charging pattern as expected.

For estrone, the analogous short OEG compound (**12**) was synthesised successfully in good yield (50%) and gave consistent NMR (very similar to the estradiol compound) and appropriate mass spectral data.

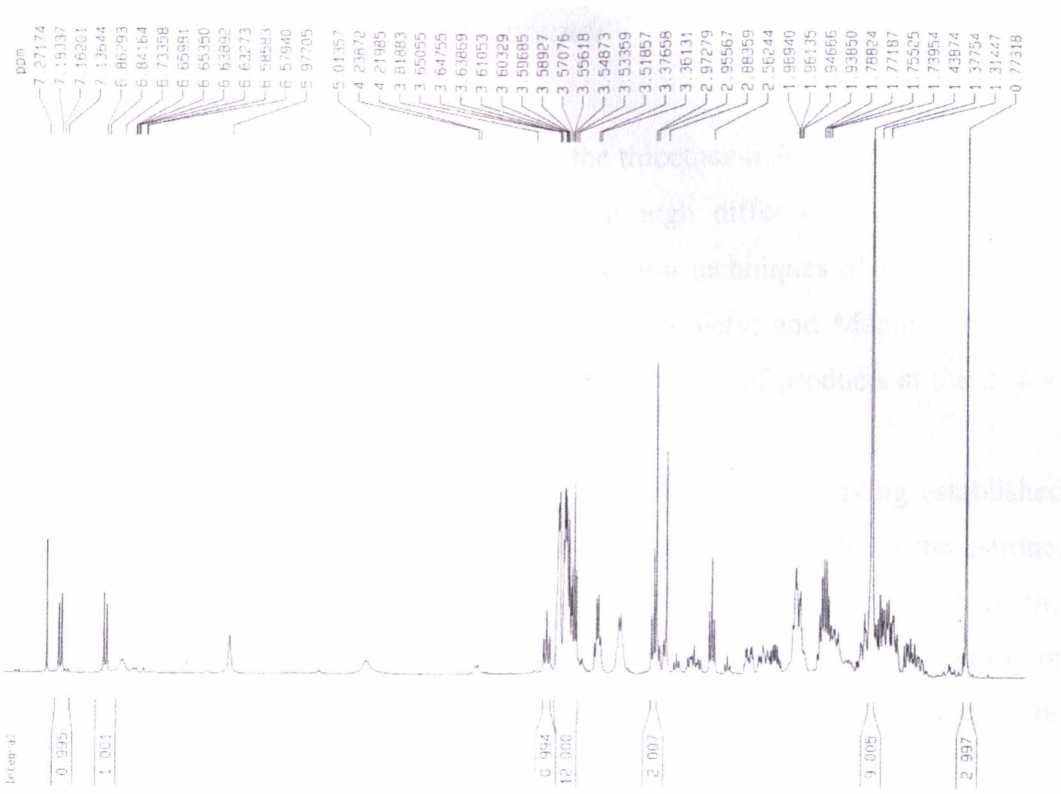

Figure 3.8 ^{1}H NMR Spectrum of **9**

The active esters of the propionic acid derivatives are quite versatile in as much as any of a number of different amine bearing linkers may be attached. In previous studies we have attached caproate linkers through these esters to form progesterone-protein conjugates.[10,15] The ethylene glycol-based linkers have been selected as they are highly water-soluble and so make the estrogen derivatives much more water-soluble. These derivatives when conjugated to a sensor surface should thus project themselves well in the aqueous medium, particularly in flow-through biosensing formats such as SPR. The oligo- and polyethylene glycol chains have the further advantage that they are non-immunogenic and so they are not recognised by the antibody, thus avoiding problems of bridge recognition by the antibody. Such linkers have potential use as biocompatible linkers for drug conjugates of the estrogens and so these derivatives have other potential uses outside of biosensing.

3.3.3 Synthesis of Reference Compounds

To provide conjugates for comparison to the thioether-linked conjugates, it was necessary to attach the OEG linker chain through different positions on the steroid, in this case using the common conjugation techniques of hemisuccinate linkage through the existing 3-position hydroxyl moiety; and Mannich reaction direct to the aromatic A-ring, which produces a mixture of products at the 2- and 4-positions.

The hemisuccinate of estradiol (**15**) was synthesised by adapting established methods through reflux in pyridine with succinic anhydride.[245] With the estrone, the same procedure could not be adopted as it was not soluble enough in the pyridine and so THF was used as the polar aprotic solvent and a combination of triethylamine and DMAP were used as the bases instead to produce the hemisuccinate product (**17**) by adapting the method of Won et al.[246] DMAP is commonly used as a base in hemisuccinate-linked protein conjugations. The hemisuccinates with their exposed carboxylic acid groups could now be activated with NHS in the presence of DCC and reacted with the free amine terminal of the mono-Boc protected OEG chain (**8**). This reaction was done without purification of the active ester. The ^{1}H NMR spectrum for the estradiol-hemisuccinate-OEG-Boc derivative (**16**) is given in Figure 3.9. ^{13}C NMR showed that some of the hemisuccinates would hydrolyse slightly with time (as shown by the development of peaks at 113 and 115 ppm and sometimes 154 ppm corresponding to the parent steroid). Any hydrolysis products were purified away at each step and final products checked by mass spectrometry and / or NMR immediately before use in BIAcore experiments to ensure the hemisuccinate linkages were intact.

Conjugation via the Mannich reaction is widely used for protein conjugations in immunology, where the reaction is done in one step with hapten and protein both present. This means that the exact position of attachment, 2- or 4-, cannot be precisely determined. Attempts have been made with reference compounds to simulate this process and it is widely acknowledged that the reaction gives rise to a mixture of conjugates. In this thesis, the reaction was used to conjugate the steroid to the amine-bearing linker, not a protein, and so this allowed the possibility of isolating a Mannich product to one position only on the aromatic

ring. The conjugation was done much as it would be for a protein, with formaldehyde solution providing the methylene spacer between aromatic ring and amine. TLC analysis showed that the reaction mixture was quite complex and careful column chromatography was needed to purify out the main product. For estradiol (**19**), the position of attachment in the purified Mannich product was found to be the 2-position. This was seen in the lack of coupling between the two aromatic protons and in their matching the expected chemical shifts. In 4-conjugated systems the coupling of the 1- and 2-protons is quite clear and this was not seen for the Mannich product. The position was further confirmed for the estradiol product by 2-D homonuclear correlated spectroscopy (COSY), which definitely showed no significant coupling between the two aromatic protons. The COSY spectrum is given in Figure 3.10.

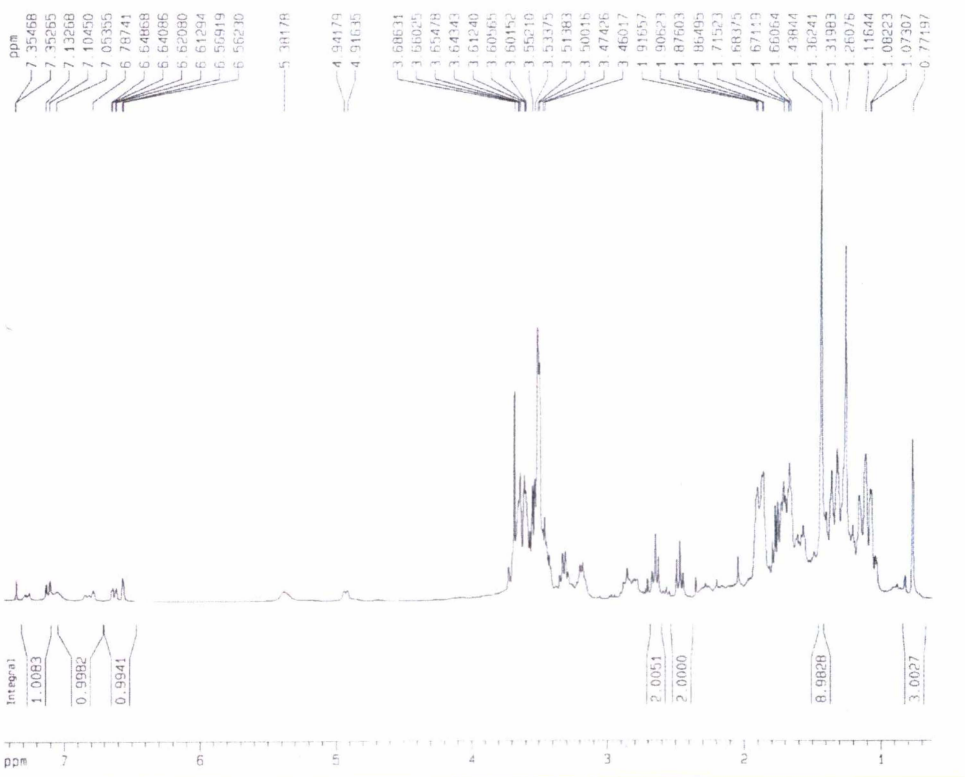

Figure 3.9 ^{1}H NMR of **16**

The yield for the Mannich reaction is quite low (13%) and this is consistent with previous observations.[90] In the case of estrone (**20**), the position of attachment was the 2-position as there was no aromatic coupling in the COSY. The yield for this reaction was also low (15%).

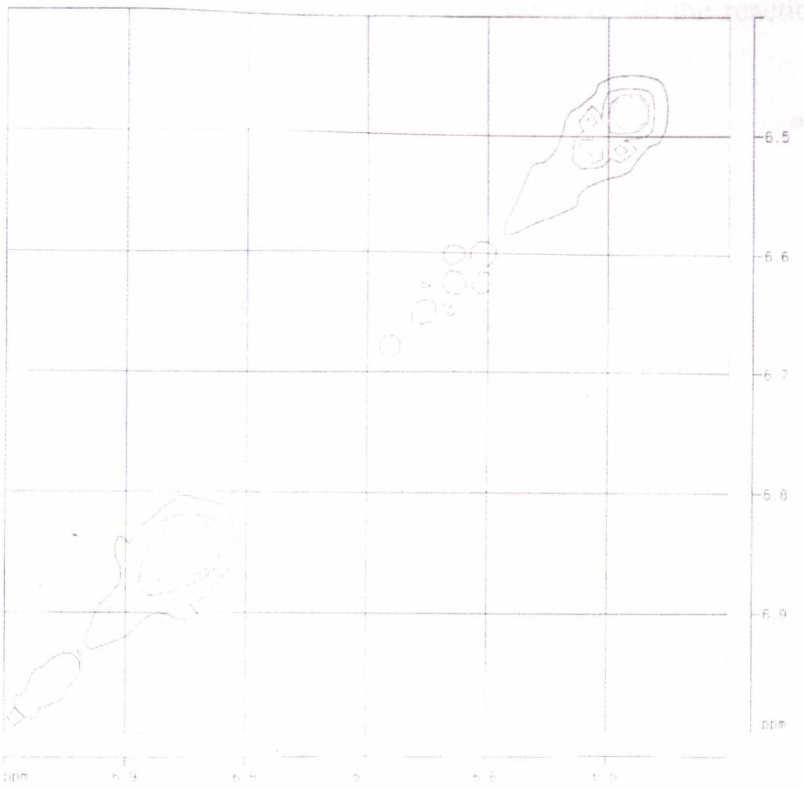

Figure 3.10 COSY of **19** showing the aromatic proton signals with no cross-peaks, indicating 2-position conjugation

3.3.4 Removal of Protecting Groups

Removal of the Boc protecting groups was easily achieved in all cases through simply stirring in formic acid. TLC analysis of the products showed that most were far too polar to give separation on a normal phase silica flash chromatography column and so would need a reversed phase column. As such columns are very expensive and the only remaining impurity of note would be the Boc protecting group, most of the compounds were used without further purification. The Boc-protected compounds were fully purified. It was possible to purify the estradiol-hemisuccinate derivative (**21**) and the estradiol Mannich derivative (**22**) but the thioether (**13**) was too polar to purify. The hemisuccinate, being conjugated through the 3-hydroxyl moiety, was of sufficiently low polarity to be columned. All these free amine compounds were analysed by mass

spectrometry and appropriate peaks found in each case. The electrospray mass spectrum for (**13**) is given in Figure 3.11. The yields of all the reactions in this reaction series are summarised in Table 3.1.

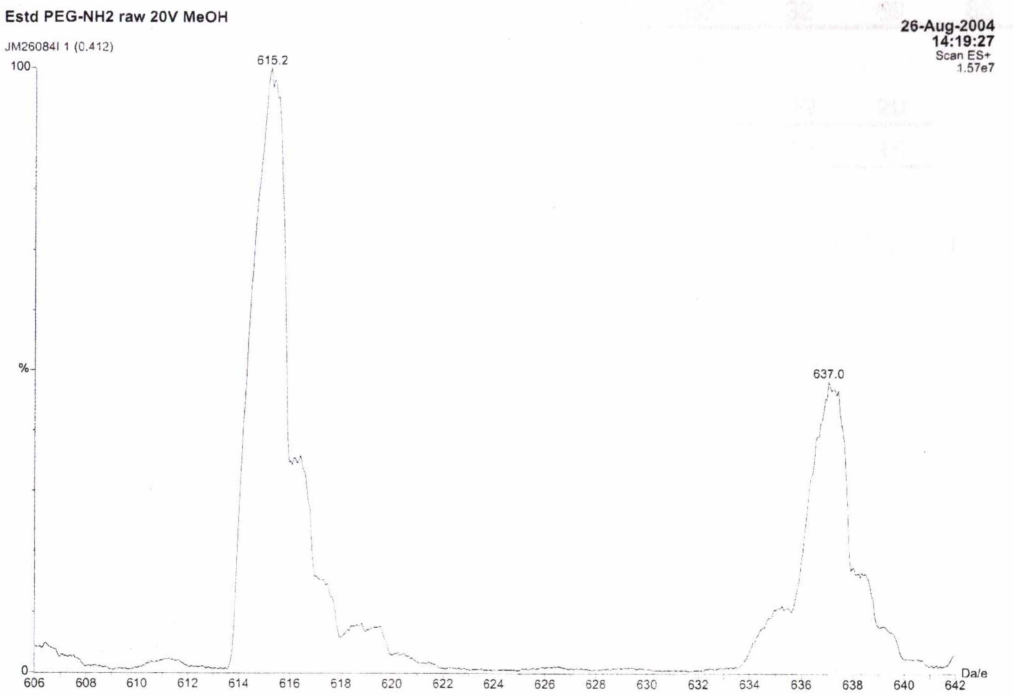

Figure 3.11 Electrospray Mass Spectrum of **13** 615.2 = $[M+2H_2O+H]^+$, 637.3 = $[M+2H_2O+Na]^+$.

In summary, it has been shown how linkage to the 4-position of estrogens can be achieved with complete regioselectivity and by a simple series of reactions starting from the parent steroid. No complex reaction procedures are needed and one does not need to begin with a controlled drug such as nandrolone. The 4-position carboxylic acid derivative enables attachment of any of a range of different linkers tailored to the individual requirements of the chemist. Such derivatives can be used as drug carriers, in the attachment of fluorescent or chemiluminescent labels or in the formation of enzyme conjugates.

One of the most important potential applications of these derivatives is their use as coating antigens in the production of stable and highly sensitive biosensors by conjugation via their free amine terminal. It is this application that is explored below in the BIAcore SPR flow-through biosensor.

Table 3.1 % Yields for Estrogen Derivatives

Compound	1	2	3A	3B	4	5	6	7	8	9
%Yield	55	53	30	43	*	27	52*	32	69	86

Compound	10	11	12	15	16	17	18	19	20
%Yield	41	27	50	24	49	25	91	13	15

* **4** is reacted through to **6** without complete purification, the 52% is for both steps.

3.3.5 Immobilisation of Free Amine Derivatives of Estrogens on the BIAcore Dextran Chip

The BIAcore biosensor has a range of sensor chips that can be used in its system. One of the most widely used is the CM5 carboxymethylated dextran chip, which presents carboxylic acid units to the surface and enables conjugation of primary amine-bearing compounds. Such compounds are usually antibodies or receptors immobilised through their amino acids. In a converse format, it is possible to immobilise a coating antigen on the surface to form a surface-bound conjugate and to use the high mass of the antibody in detection of the binding events. This is particularly important for small molecules that lack the mass to label the binding interaction themselves. Immobilisation by this method will result in the formation of stable covalent amide linkages.

It is possible to immobilise primary amine containing compounds directly onto the carboxymethylated dextran surface of the BIAcore CM5 chip. This can be done by first activating the chip with EDC and NHS coupling reagents. This was done at a slow flow rate (5 μL/min) and with a high loading of EDC and NHS to ensure that the maximum number of carboxylic acid sites had been activated. The primary amine containing estradiol derivatives were then immobilised under alkaline pH in situ also at the slow flow rate (5 μL/min). In order to ensure saturation of all binding sites on the chip, the amines were immobilised at very high concentration (1 mg/mL) and at very slow flow rate (5 μL/min). The compounds were injected at two different pH. The first, pH 9.7, is below the

estimated pKa for the free amine but is still quite basic and so should result in a significant proportion of the primary amines being in the $-NH_2$ form whilst not risking any damage to the active ester before reaction. The second pH was 11.7 and is significantly above the projected pKa of the free amine and so can ensure any unreacted surface sites are bound to the free amine and saturation of the surface has been attained. Under both pH conditions the volumes used for immobilisation were very high (400 μL per flow cell for each pH). Flow cell one was activated with the EDC / NHS and then deactivated with the ethanolamine to serve as a blank reference flow cell. Flow cell two was immobilised with the 3-hemisuccinate linked derivative (**21**) and flow cell three with the 2-Mannich linked derivative (**22**) and flow cell four with the 4-thioether linked derivative (**13**). All derivatives were immobilised under identical conditions. These thorough immobilization conditions will ensure that the surfaces are in each case immobilised to saturation and so comparisons between flow cells will be valid and not subject simply to differences in the amounts immobilised.

After initial immobilisation, the surfaces were extensively flushed with running buffer (HBS-EP) until stable baseline was obtained. This flushing enabled loosely bound material to be removed from the sensor surface. Binding to the surface was then examined for both polyclonal anti-estradiol and monoclonal anti-estradiol antibodies. The polyclonal antibody showed no binding whatsoever to the immobilised surface. The possible reasons for this include firstly, that the polyclonal antibody is not directed specifically to the epitope of the estradiol molecule and so only a sub-set of the polyclonal anti-serum will bind to the surface thus resulting in lower binding compared to a monoclonal antibody. Also, the affinity constant of the polyclonal antibody is 7.3×10^9 L/M compared to 1×10^{10} L/M for the monoclonal antibody and it was supplied as a somewhat dilute solution, though it was used here undiluted and still gave no binding. Monoclonal antibody binding on the other hand was found to be very strong indeed and so once the baseline had stabilised the surface was used in antibody binding studies.

A BIAcore sensor chip was similarly immobilised with the corresponding estrone conjugates on another chip, and polyclonal anti-estrone antibody binding was tested. As for the estradiol, no antibody binding was seen. Monoclonal antibody binding could not be done as we lack a reliable commercial source of monoclonal anti-estrone, with most antibodies being directed to estrone-3-sulfate

or estrone-3-glucuronide. If we find such a source then comparable studies could be done on estrone.

3.3.6 Antibody Binding Studies of the Estradiol Conjugated Surface

Monoclonal antibody (mAb) bindings were studied for a range of mAb concentrations on all three flow cells to assess the level of antibody binding that could be achieved with each different method of conjugation. Plots of response (RU) *vs* mAb concentration could then be prepared, Figure 3.12.

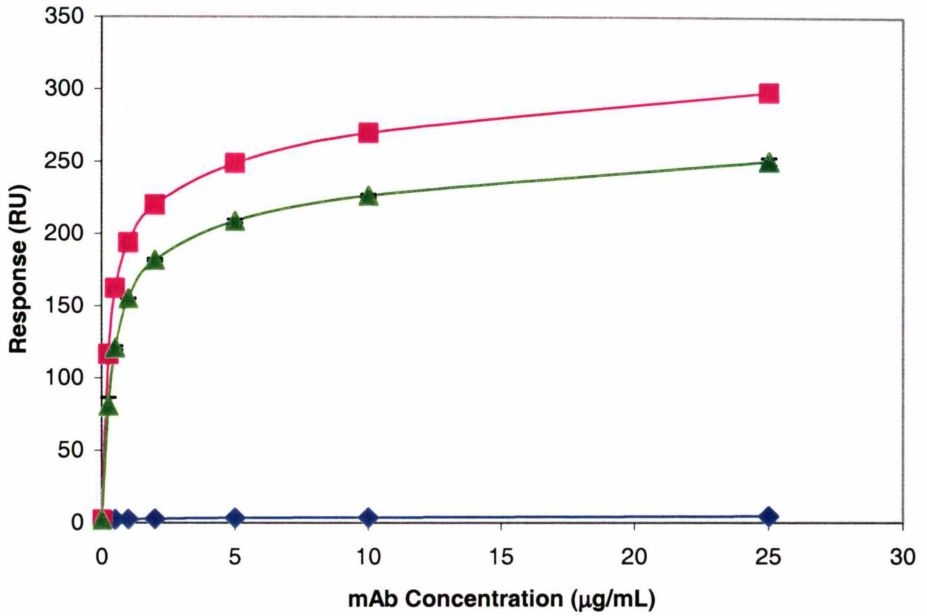

Figure 3.12 Plot of Response (RU) *vs* Monoclonal Antibody (mAb) Concentration (µg/mL) for Hemisuccinate (♦), Thioether (▲), Mannich (■) (Error bars are too small to see)

From this plot, one can clearly see that the hemisuccinate conjugate has given very little binding at all, whereas the conjugations that have not compromised an existing functional group on the A-ring give much higher binding despite being attached at very similar points on the A-ring (2-, 3- and 4-). Saturation binding is shown by the curve flattening off to horizontal and occurs at around 25 µg/mL mAb concentration. At saturation, the binding to the 3-position hemisuccinate is only 2% that of the 2-position conjugate, which in turn gives binding that is 19% higher than that of the 4-position conjugate. The low binding of the hemisuccinate

in a flow-through format can be explained by the conjugate modifying the 3-hydroxyl moiety of the estradiol and so removing one of the key functional groups that the antibody recognises. This low binding has important ramifications for the use of 3-position conjugates, as it suggests that such conjugates will give much lower antibody binding than those that are not conjugated through the hydroxyl, and so give much lower signal in flow-through SPR biosensing. 3-position hemisuccinate conjugates are widely used as enzyme conjugates in ELISA, and for the attachment of chemiluminescent labels, but they are clearly of no use in a flow-through format such as SPR for estradiol. The low hemisuccinate binding is unlikely to be due to alkaline hydrolysis of the ester linkage as the hemisuccinate was immobilised on another SPR chip at pH $\simeq$ 4.2 for comparison and still showed the same low antibody binding compared to strong binding for a Mannich linked surface (hemisuccinate gave ~ 4% of the Mannich binding).

Another important result from this data is that the Mannich 2-position conjugate is giving significantly more antibody binding than the 4-position thioether. The mAb has been raised to a conjugate at the six position and so one would expect that modification of the opposite side of the estradiol molecule to that of the immunogen conjugate attachment would result in significantly lower antibody binding response. It appears that the 2-position is not so far round the other side of the estradiol as to result in diminished binding. Mannich reaction conjugation at the 2-position has the same advantages as the 4-position, *i.e.* no epimerisation, and no functional group conjugation, but gives a slightly better mAb binding response.

These results differ from those previously reported for fluorescent conjugates in non-flow-through fluoroimmunoassay where conjugates through the 2-position (carboxypentyloxime linkage) were found to give no binding to an antibody raised to a 6- position CMO conjugate, whereas thioether conjugation of the fluorescent label through the 4-position showed binding to the antibody.[107] The differences observed for the 2-position are due to the different binding formats used (flow-through and non-flow-through) and / or the conjugation method employed. This shows how important the format and / or conjugation linkage of the assay or binding test are in determining the amount of antibody binding. Speculatively, the linker may be covering over the side of the steroid opposite the 6-position in the plate-based fluoroimmunoassay whereas in a flow-through format the linker is

held out from the steroid by the fluid flow with the linker end anchored to a solid surface so potentially allowing much better access by the antibody.

3.3.7 17β-Estradiol Assay

With this antibody binding data in mind, it is wise to consider the ways this might affect the performance of an inhibition assay of estradiol. An assay was constructed using the antibody concentration of 1 μg/mL (diluted to 0.5 μg/mL when estradiol solution is added). The assay standard curves are given below in Figure 3.13.

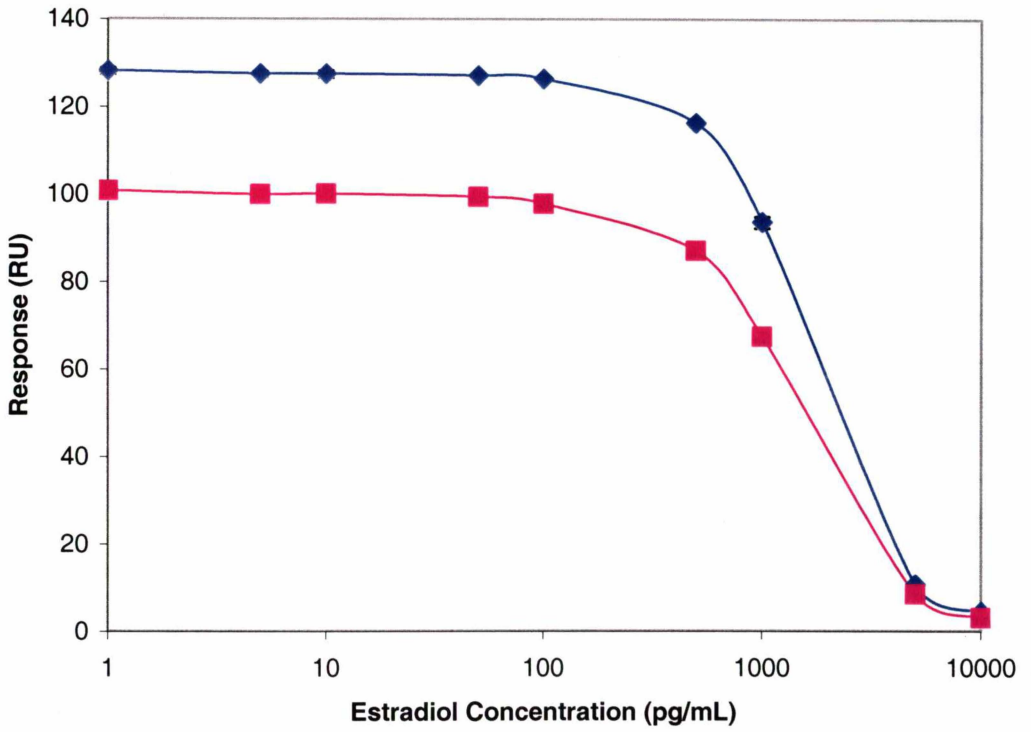

Figure 3.13 Assay Standard Curves for 4-Position Thioether (■) and 2-Position Mannich (♦) (Error bars are too small to see)

One can see once again that the Mannich conjugated surface is giving higher binding response than the thioether surface. An assay could not be run for the hemisuccinate surface, as the binding responses were too low. The limits of detection (LOD) are 96 ± 32 pg/mL and 111 ± 33 pg/mL for 2- and 4-position conjugation respectively. The higher signal has not significantly improved the

LOD of the 2-position conjugate assay over the 4-position. The high standard errors are due to the low curve slope around the LOD. The coefficients of variation (CV) of the responses for these assays are quite low (1.4% and 2.6% for 2-position and 4-position respectively). The inhibitory concentration at 50% bound (IC_{50}) values are also very similar, suggesting no significant curve position difference. It is of interest to try and lower the detection limit by use of signal enhancement techniques. Such techniques are detailed fully in Chapter 5. One such technique developed in Chapter 5 is the use of a secondary antibody that binds the bound primary antibody to enhance the signal of the binding interaction and so hopefully produce a more sensitive assay.

3.3.8 Secondary Antibody Signal Enhancement

Binding of anti-mouse IgG secondary antibody to the bound primary mAb raised in mouse should result in a significant signal enhancement due to the additional large mass of the secondary antibody. This was studied at a primary mAb concentration of 0.5 μg/mL and a plot prepared of the response *vs* secondary antibody concentration, Figure 3.14. The binding is achieved by first injecting primary mAb over the surface and then immediately injecting the secondary antibody. In this way binding attributed to the primary mAb and the total binding with secondary antibody labelling can be determined. The time between primary mAb injection and secondary antibody injection is very short and so there is minimal dissociation of primary mAb before injection of the labelling secondary antibody.

One can see that the final binding response has increased greatly from that of the primary mAb alone. Saturation binding of the bound primary mAb is occurring by 200 μg/mL, with only a 4% increase in signal from 200 to 300 μg/mL. As the higher secondary antibody concentration will possibly produce more non-specific binding, it was deemed best to use the 200 μg/mL secondary antibody concentration for the primary mAb binding tests and for the assay.

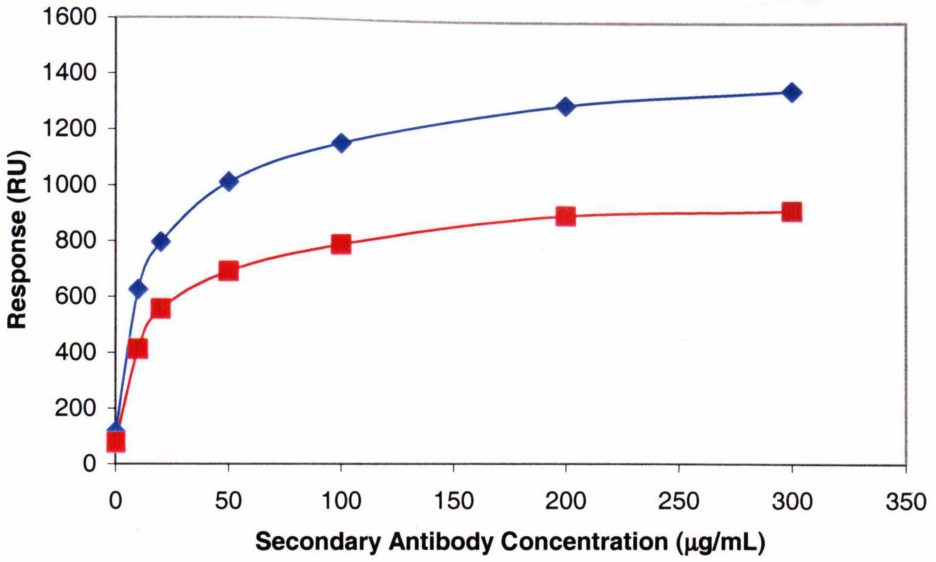

Figure 3.14 Plot of Total Response (RU) *vs* Secondary Antibody Concentration (µg/mL) for 4-Position Thioether (■) and 2-Position Mannich (♦) (Error bars too small to see)

To determine the effect of changing primary mAb concentration on the total signal, a plot of response *vs* primary mAb concentration was prepared at fixed secondary antibody concentration (200 µg/mL), Figure 3.15.

This plot shows the high level of signal enhancement obtained with secondary antibody labelling. With higher primary mAb levels, the enhanced signal is levelling off, suggesting that maximum secondary antibody binding has been achieved at the high mAb concentrations. A higher secondary antibody concentration would keep the binding line linear by having enough to fully label the primary mAb at higher concentrations, but would also potentially increase non-specific binding. The 4-position thioether surface gives very similar curves to this but at slightly lower signal. The linear range of these curves for the 2-position conjugated surface is plotted below in Figure 3.16.

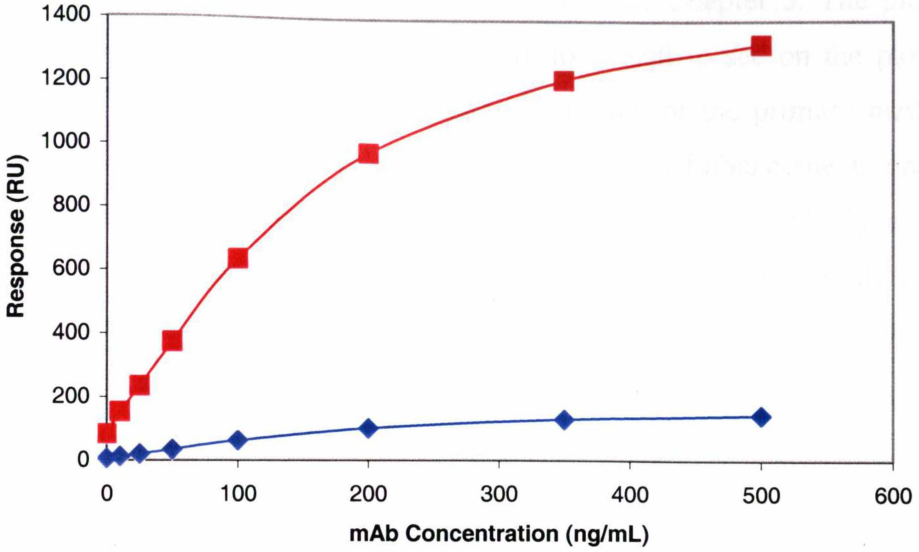

Figure 3.15 Plot of Response (RU) *vs* Primary mAb Concentration (ng/mL) for Primary mAb only (♦) and Secondary Antibody Enhanced Response (■) for 2-Position Mannich Conjugation (Error bars too small to see)

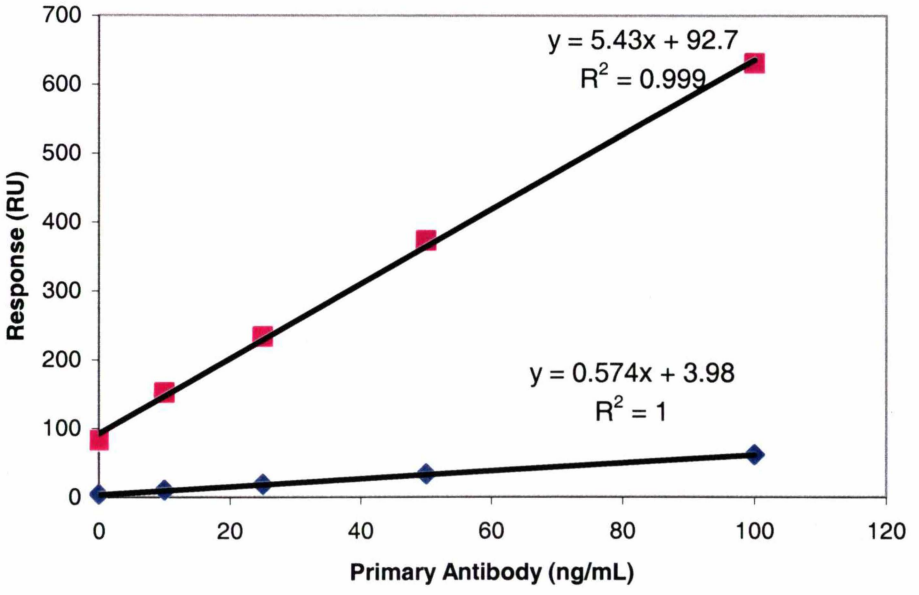

Figure 3.16 Linear Plot of Response (RU) *vs* Primary mAb Concentration (ng/mL) for Primary mAb only (♦) and Secondary Antibody Enhanced Response (■) for the 2-Conjugate Surface (Error bars too small to see)

From the slopes of the linear plots one can determine the degree of signal enhancement obtained. These plots show signal enhancements of 9.5-fold for the 2-position and 8.9-fold for the 4-position. This is much larger than would be

expected for simple 1:1 mAb to secondary antibody binding on the basis of mass alone. For a fuller discussion of this phenomenon see Chapter 5. The plots are very linear (R^2 near 1) and the error bars are too small to see on the plot. The intercepts of these lines give the non-specific binding of the primary mAb (4.0 RU) and the secondary antibody enhancement (93 RU). Enhancements obtained here are slightly better than those obtained with secondary antibody alone in Chapter 5. The difference is likely simply due to differences in binding affinity between the two antibodies. About 100 RU of specific binding response is all that is needed for a reliable inhibition assay and this was obtained at a primary mAb concentration of about 25 ng/mL. The CVs for the entire antibody binding studies have been very low, resulting in small error bars on the plots and demonstrating the excellent stability of the coated surface.

An assay was then constructed for estradiol using the 25 ng/mL final primary mAb concentration and secondary antibody signal enhancement at a loading of 200 μg/mL. The assay standard curve is plotted in Figure 3.17 with the 4-parameter logistic regression line shown.

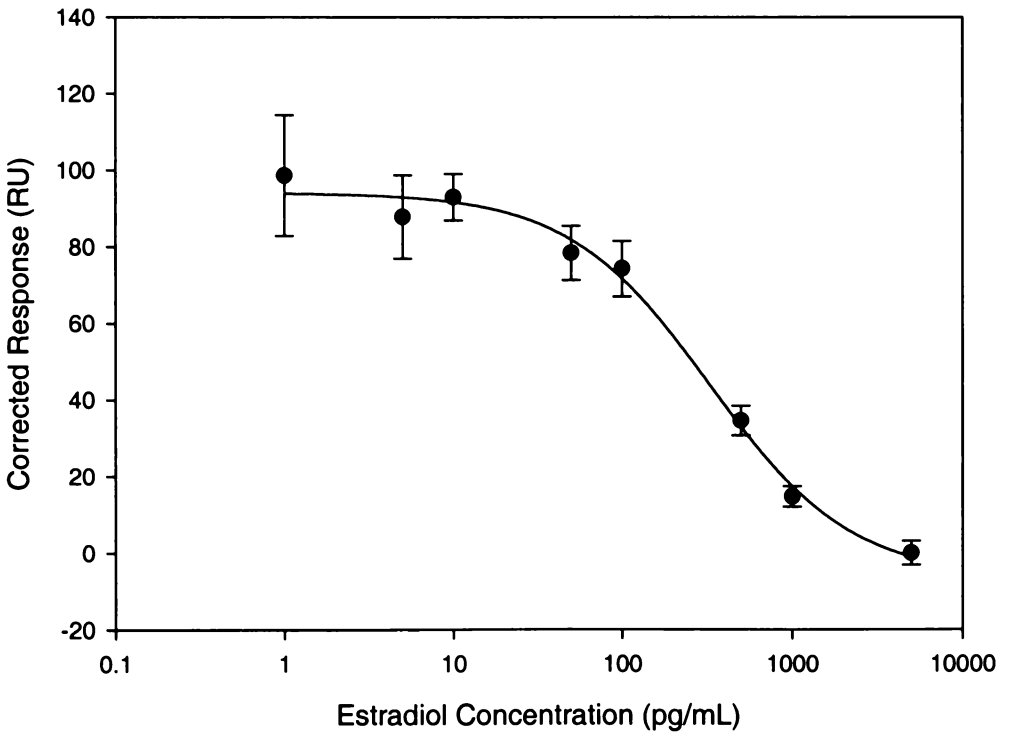

Figure 3.17 Assay Standard Curve for Secondary Antibody Enhanced Inhibition Assay of Estradiol Using 2-position Conjugated Surface Using a 4-Parameter Logistic Curve Fitting

The parameters for all the assays mentioned in this chapter are summarised in Table 3.2. All the assay curve data has been fitted to 4-parameter logistic relationships as mentioned in Chapter 1. This fitting gave good R^2 values with the data and is in line with standard methods for immunoassay curve data fitting.

The LOD for the primary mAb only part of the assay, appear to have decreased somewhat for 2-position Mannich conjugate but not for the 4-position, however it is very difficult to draw firm conclusions as the standard errors in the LOD are too large, caused by shallow curve slope and slightly higher CV. The LOD for the enhanced assay is significantly lower for the 2-conjugate but not the 4-conjugate and in any event has not lowered anywhere near as much as one would expect with this level of primary mAb concentration reduction. The primary mAb concentration has been reduced to $1/20^{th}$ of what it was originally and so one would expect an LOD of around 5 pg/mL; instead the best LOD is 5-times that. The reason for this is unclear.

Table 3.2 Assay Parameters For Estradiol SPR Assays

Assay Format	Conjugation Position	Primary mAb Concentration (ng/mL)	LOD (pg/mL)	IC50 (pg/mL)	Sensitivity (RU.mL/ng)	Enhancement Ratio
mAb Only	2	500	96 ± 32	1457 ± 9.6	22	n/a
mAb Only	4	500	111 ± 33	1432 ± 14	16	n/a
mAb Only	2	25	66 ± 27	414.9 ± 5.9	6.9	9.5
mAb Only	4	25	95.2 ± 32	351 ± 14	4.1	8.9
Secondary Antibody	2	25	25 ± 22	324 ± 21	65	9.5
Secondary Antibody	4	25	61 ± 39	396 ± 28	41	8.9

[a]All errors quoted are standard errors

The IC_{50} values show a drop to about $1/3^{rd}$ of their original value when the primary mAb concentration is dropped, and this is seen in both enhanced and non-enhanced assays and so is due to the lowering of the primary mAb only, as expected. This drop in IC_{50} has not been in direct proportion to the lowering of primary mAb concentration and in fact has dropped less than the LOD. The slope sensitivity of the assay is significantly improved with enhancement, changing from 16-22 RU.mL/ng to 41-65 RU.mL/ng. This occurs more because the assay curve has shifted to lower concentrations, as the total signal is about the same

because the primary mAb concentration has been dropped. The standard curve in Figure 3.17 has been corrected for non-specific binding from the secondary antibody, though this non-specific binding does not appear to in any way affect the performance of the assay. The absorbance CVs for the assay, at an average of 4.6% and 6.1% for the 2- and 4-position assays respectively, showed good precision for the assays.

These estradiol assays represent the most sensitive reported SPR immunoassays of estradiol. The only previous report of estradiol SPR immunoassay relies upon unstable estradiol-BSA surface coatings and demonstrates an LOD of 200 pg/mL, *i.e.* 8-fold higher than is reported here.[247] Furthermore, they require manual mixing and manual injections of solutions and 1 h incubations at 4 °C making the assay unsuitable for rapid, automated testing and do not use site or bridge heterology.[247] Previous SPR studies have also used receptor binding assay for estradiol.[163,248] One system[163] uses amine-mediated immobilisation of estradiol through the 17-hemisuccinate and estradiol assayed through competition assay with human estradiol receptor-α. This assay gave a very poor LOD for estradiol (5 nM corresponding to 1.4 μg/mL, *i.e.* about 5 orders of magnitude higher than the assay reported here). Another study demonstrated inhibition of receptor binding to an estradiol-BSA functionalised surface by estradiol but did not fully develop an estradiol assay.[248] Estradiol is a very important marker of ovarian function in women. Monitoring of estradiol levels is needed for in vitro fertilisation monitoring as well as in environmental sampling of estrogen levels. Many biological fluids, such as saliva, have only very low levels of estradiol present, *i.e.* high fg/mL or low pg/mL concentrations. The assay results presented here represent a significant improvement in the ability of optical biosensors to detect low (pg/mL) quantities of estradiol. The results show how optical biosensors could be used as replacements of ELISA technology for routine analysis of estradiol samples thus greatly improving sensory technology in this area.

There has been a dearth of studies in the area of estrogen binding interactions with antibodies studied using SPR technology, particularly with a view to producing optical biosensors. Estrone-3-glucuronide has been detected with Texas-instruments-based SPR technology, but this has only produced LOD of 10 ng/mL.[249]

The use of the estrogen – OEG compounds, as coating antigens has been vital to ensuring the long-term stability of the surface. The surfaces produced here have shown stable binding responses over more than 200 cycles and are likely to be stable for over 1000 cycles in light of the success achieved with comparable progesterone surfaces, see Chapter 5. If an antibody had been coated or a protein conjugate produced and then coated on the surface, the stability would certainly be much poorer than the covalently immobilized surface used. Lack of surface stability in biosensors is a major problem limiting their widespread use. Production of such surfaces using the covalent attachment method and non-immunogenic OEG chains has been shown to go a long way to overcoming these problems. The use of the OEG bridge minimises bridge recognition. It does this by being non-immunogenic and also because it is a different linker to that employed in the conjugate used to raise the antibody and so introduces bridge heterology. If binding to the bridge were to occur, this would reduce the specificity of the binding interaction and potentially its binding to the bridge could be stronger than that to free estradiol and so reduce the levels of inhibition attained and increase the LOD of the assay.

Throughout all of the binding studies and assays, the regeneration cocktail used has been a combination of sodium hydroxide and the chaotrophic reagent acetonitrile. This combination regenerated the OEG-linked surfaces quite well with no deterioration in the surface detectable. The surfaces seem quite stable and there is no decline in binding capacity from cycle to cycle. In the early cycles over the surface, the regeneration pulses removed loosely bound material from the surface. All surfaces were fully stabilised before antibody binding studies and assays were commenced. Less alkaline regeneration solutions such as sodium carbonate or bicarbonate and lower concentrations of sodium hydroxide proved ineffective in regenerating the surface, as did solutions without acetonitrile. This combination has been used to good effect in the studies in Chapter 5 for progesterone and seems equally as effective with estradiol. For a more thorough discussion of these factors, see Chapter 5.

These results show how important it is to have a thorough knowledge of the factors affecting assay antibody binding before developing immunoassays of small molecules. The widely used hemisuccinate method of linkage is clearly not appropriate for use in flow-through immunoassay of estradiol, giving very poor

antibody binding. Binding at either 2- or 4-positions is much better. Surprisingly it has been seen in these results that if the antibody is raised to the 6-position, then conjugation to the 2-position is still close enough to the same side of the antigen as to result in high antibody binding, even better than the 4-position. Conjugation on the opposite side of the molecule to that used for antibody generation could be expected to result in loss of shape recognition and so greatly diminished binding. The Mannich reaction still has major limitations when used as a one-step method for protein conjugation but if it is used to attach linkers to the steroid structure, then it can give excellent binding results when such a linker derivative is used as a coating antigen. The 4-position thioether method still gives strong antibody binding, and in these studies has similar assay performance to the 2-position Mannich conjugation.

3.4 Conclusions

Thioether bridging can be applied to estrogens where there is an aromatic A-ring. This has been done through substitution of the corresponding estrogen brominated at the 4-position. By using 3-mercaptopropionic acid as the thiol, one can introduce a carboxylic acid group to the compound and thus allow attachment of a wide range of linkers through amide coupling. OEG linkers of varying length have been attached to estradiol and estrone through the 4-propionate using NHS activation of the carboxylic acid and protection of one of the linker terminal amine functions. Once attached, the Boc protecting group may be removed by formic acid exposure when the compound is ready for use.

Estrogen-OEG-amine derivatives can be conjugated to the surface of an activated carboxymethylated dextran surface in situ using high loadings of estrogen derivatives and slow flow rates and varied pH to ensure saturation of the surface. The thioether-conjugated surface was then compared to reference compounds also with the same OEG linkage attached to the steroid through the 3-hemisuccinate or the 2-position Mannich reaction. Antibody binding studies showed that the 2-position Mannich conjugation was best for flow-through binding formats, followed by the 4-position, and the 3-position giving very little antibody binding at all.

Assays for estradiol were constructed with and without secondary antibody signal enhancement and showed LOD of 96-111 pg/mL without enhancement and 25-61 pg/mL with enhancement. Secondary antibody enhancement ratios varied from 8.9-9.5. The surface was completely stable throughout all binding studies and assays (over 200 cycles). This represents the most convenient, sensitive and robust reported SPR immunoassay of estradiol.

These results have clearly indicated that conjugation of the estrogens through an existing functional group (3-OH) is highly inferior to conjugation through other aromatic A-ring positions not bearing functional groups (2- or 4-position) for flow-through immunoassays. Although the 2-position conjugation has given slightly better antibody binding than conjugation at the 4-position, synthesis of 4-thioethers offers a better synthetic method of conjugation for the estrogens in that attachment is specific to one position and does not require difficult column purification of isomers. The thioether synthetic route is straightforward and allows for a range of different intermediate linkers to be attached to the parent steroid.

This study opens a wide range of possible assay formats for small molecules including new conjugation techniques and new biosensor surface modifications. This assay system could easily be modified to detect the estrogen mimics, which are one potential group of analytes of great interest for their environmental and health impacts. This research demonstrates how biosensors and small-molecule conjugates may be significantly improved by an understanding of the underlying organic chemistry involved in antibody epitope recognition and contributes to on-going studies in the development of more sensitive, stable and rapid immunobiosensors.

Chapter 4 – Catecholamine Thioether-Linked Derivatives – Synthesis, Purification and Antibody Binding Studies

4.1 Introduction

The catecholamine neurotransmitters and hormones are another class of aromatic small biomolecules that are of great interest for quantification in biosensors, particularly at the often-low concentrations prevalent in many samples, including vertebrate brain dialysates. The catecholamines can be chemically modified to produce conjugates that are of great interest and have various applications. One can attach linkers to them to produce protein conjugates that can be used to raise antibodies[250, 251] or as immobilisation agents in immunosensing. There is potential also to attach linkers to them to produce drug conjugates that can be targeted to particular tissues expressing receptors for the target compound, or to also produce conjugates with chemiluminescent, enzyme or fluorescent labels for applications in immunosensing or high-throughput screening.

There has been a dearth of studies into the synthetic routes that can be employed to synthesise these conjugates and in systematic studies of their antibody or receptor binding properties. It is of much interest to consider how the position of attachment, whether to the aromatic ring directly or not, and the method of attachment may affect the ability of an antibody or receptor to recognise the target conjugate. The only studies of conjugates of the catecholamines have employed either conjugation directly through an existing functional group such as the amine terminal, the amine being crucial for receptor or antibody recognition; or through use of the Mannich reaction,[172, 173, 175, 176] which produces conjugates attaching *ortho* to a phenol moiety.

Conjugation through the primary amine has been effected by the glutaraldehyde method,[252, 253, 250, 254] which links the primary amine of the catecholamine to amines present in the carrier protein. Naturally such a reaction

will modify the primary amine and so remove a major part of the set of functional groups needed to recognise the catecholamine target. This is of particular concern with very small molecule targets like the catecholamines where there are few functional groups to begin with and little uniqueness in the shape of the target. Carbodiimide linkage through the amine has the same problems,[251, 255] as would any conjugation through the hydroxyl moieties. It has been shown that conjugation by glutaraldehyde and carbodiimide results in changes of charge in the hapten and a sterically different hapten structure.[255] Further studies with protein conjugates of the catecholamines linked through the glutaraldehyde method and used to raise antisera, show that these antisera will bind the original protein conjugate well in ELISA but bind very poorly to the free catecholamines, thus further reinforcing the inadequacy of this method.[250] The glutaraldehyde method of conjugation is widely used in immunocytochemistry for a range of catecholamine neurotransmitters.[256]

The problem with the Mannich reaction is that the reaction does not direct to a single position of attachment, and gives mixtures of conjugates with different positions of attachment when the conjugation reaction is performed in the preferred one-step process. In order to achieve attachment direct to the aromatic ring by the Mannich reaction,[256] any primary amine of the catecholamine has to be protected before the conjugation otherwise the reaction will occur through free amines as well as direct to the aromatic ring and may produce dimers. Whilst the Mannich reaction can be used for conjugation to the aromatic ring if adequate protection can be used and position of attachment identified, it is possible to have an alternative that can be easily synthesised and also allows direct attachment to the aromatic ring by production of a thioether derivative. The problems with the Mannich reaction have been outlined in previous work, with conjugates of serotonin linked in this way to generate antibodies, resulting in the antibody binding the conjugated serotonin strongly but the free serotonin very weakly.[251]

Thioether linkages offer significant potential for conjugation to the aromatic ring without the problems inherent in use of the Mannich reaction. Thioether conjugates to glutathione and cysteine have been reported[257, 258, 259] proceeding via production of the *o*-quinone and subsequent addition of a thiol-containing compound, a route possible only through *ortho*-dihydroxylated aromatics and so unavailable for use with 17β-estradiol and estrone. These cysteine and

glutathione conjugates have also been synthesised by enzyme-catalysed routes.[260, 261] Such thioether derivatives are well known metabolites of the catecholamines.[262, 263, 264, 265, 266] 6-Mercaptodopamine has been synthesised by thiocyanation.[267] Thioether bridging would produce stable compounds that could be easily reacted further with other intermediate linkers to produce conjugates. The ultra-polar nature of these compounds would make purification in reasonable quantities a significant challenge, though any purification could be observed clearly by UV-Visible detection by HPLC. If mercaptoalkanoic acids are used as the reacting thiol, then linkers can be attached that will terminate in a carboxylic acid, thus enabling activation with NHS / DCC and subsequent conjugation to amines in a carrier protein or label, which is a reliable and repeatable method.

These novel compounds would be of much interest in antibody and receptor binding studies to systematically assess how changes to target structure in the formation of conjugates affects the antibody or receptor binding abilities of those conjugates. Antibodies and receptors recognise their targets according to shape and functionality and these conjugations should provide the minimum of disruption to the antibody or receptor binding abilities as attachment does not compromise existing functional groups and linkers provide adequate projection of bound label, protein or surface out from the target to allow full binding around virtually the whole hapten. With a wide range of catecholamines available, it would be anticipated that the synthetic techniques could be applied broadly to all catecholamines with *o*-hydroxyl groups.

Reported below is the synthesis of thioether-bridged catecholamine derivatives for dopamine, nor-epinephrine and epinephrine using 3-mercaptopropionic acid (MPA) and 11-mercaptoundecanoic acid (MUA) as the intermediate attaching linkers, which attach directly to the aromatic ring. These compounds are purified using ion-exchange chromatography techniques or normal-phase silica chromatography and their purification is profiled by their characteristic HPLC absorbance patterns. The purified compounds are characterised and their positions of attachment determined with the aid of 2-dimensional NMR spectroscopy. The dopamine mercaptopropionate derivative is then immobilised onto an SPR chip surface specially modified with amine-bearing functional terminals and the bindings to a monoclonal antibody are studied using BIAcore

and compared to immobilisation via existing functional groups and different linker types.

4.2 Experimental

4.2.1 Materials and Instruments

4.2.1.1 General

Dopamine HCl and nor-epinephrine bitartrate were purchased from Sigma (dopamine as the racemate and nor-epinephrine as the R-isomer) and epinephrine was purchased from Aldrich (R-isomer). All other chemicals were from Aldrich. All solvents used were analytical grade except for the HPLC solvents that were HPLC reagent grade ACS. Solvents used were from Scharlau (Barcelona, Spain). The silica gel used in column chromatography and the TLC plates were as for Chapter 3. Melting point determinations, NMR analysis and electrospray mass spectrometry and high resolution mass spectrometry were all done as for Chapter 3. All products synthesised and isolated using the electrochemical methods were purified to one significant HPLC peak.

4.2.1.2 HPLC and Antibody Studies

HPLC was performed on a Shimadzu instrument composed of the following modules: Autoinjector (SIL-10AD VP), pumps (LC-10AD VP), UV/visible detector (SPD-M10 A VP), thermostatted oven (CTO-10AC VP) and a system controller (SCL-10A VP). The UV-visible chromatograms and spectra plots were analysed using Class-VP software 5.032 1999. The column used was a Prodigy, 3 μm ODS 100 x 4.6 mm, 00D-4243-E0, 111274-4 from Phenomenex (Milford, Auckland, New Zealand). All mobile phases used were mixed, pH adjusted, filtered through a Nylon 47 mm diameter, 0.45 μm filter and degassed before use. The HPLC had a degasser also.

BIAcore analysis was done using the same instrument specifications as in Chapter 3 and using a CM5 sensor chip (research grade). The monoclonal antibody used was mouse anti-human dopamine (US Biological, Swampscott,

USA, D9000) raised to dopamine-BSA conjugate conjugated through the primary amine using the glutaraldehyde method, and with an affinity of ~1 x 10^7 L/M.

The ion-exchange column was a Dowex-50W strongly acidic cation exchange resin column (10 g of dry resin slurry packed in deionised water into a glass column to give a bed of dimensions 15 mm x 150 mm). The resin had been thoroughly washed with deionised water, acetone, methanol and deionised water, 2 M HCl and deionised water again, dried down with diethyl ether and vacuum drying and re-hydration in deionised water before use.

4.2.2 Dopamine Thioether Derivatisation by Aromatic Substitution[1]

4.2.2.1 ***5-(2-Aminoethyl)-x-bromobenzene-1,2-diol (1)***

Dopamine (400 mg, 2.12 mmol) was dissolved in dry methanol (30 mL) and *N*-bromosuccinimide (NBS) (375 mg, 2.12 mmol) was added and the solution stirred at room temperature in the dark for 24 h. The solution then had the solvent removed and was reconstituted in distilled water (50 mL) and washed with chloroform (2 x 25 mL, 1 x 50 mL) and the solvent removed from the aqueous phase. The sample was reconstituted in methanol and decoloured thoroughly with activated charcoal. The solvent was then removed to yield **1** as a brown oil. Yield: 71% (347 mg, 1.51 mmol). TLC R_f = 0.62 (40:1 MeOH : acetic acid). IR (KBr disc): 1189 (phenol C-C-O out of phase υ), 3410 (OH υ) cm^{-1}. ^1H NMR (D_2O) δ: 2.94 (2H, t, *J* = 7.2 Hz, Ar-CH_2), 3.17 (2H, t, *J* = 6.9 Hz, $^+NH_3$-CH_2), 6.74 (1H, m, 2-CH), 6.92 (1H, m, 6-CH); ^{13}C NMR δ: 31.0 (Ar-C) 39.4 (C-NH_3^+), 115.7 (2-C), 116.5 (5-C), 116.6 (6-C), 117.0 (1-C), 118.0 (4-C), 124.2 (3-C); ES-MS *m/z* (MeOH, 20 V) 230.7 and 232.7 $[M+H]^+$. HiRes FAB-MS: Calculated: 230.9895, 232.9874, Found: 230.9902, 232.9893 (MH^+).

4.2.2.2 ***3-(5-(2-Aminoethyl)-2,3-dihydroxyphenylthio)propanoic acid (2A)***

1 (338 mg, 1.46 mmol) was dissolved in dry methanol (5 mL) and 3-mercaptopropionic acid (380 μL, 4.37 mmol) was added and the solution stirred

[1] For reaction scheme see p. 166

vigorously. Methanolic KOH (200 mg in 5 mL of dry methanol) was added with vigorous stirring. The solution was then refluxed for 24 h in the dark in oven-dried glassware and with a drying tube. The solvent was removed and the sample constituted in distilled water (25 mL) and washed with ethyl acetate (2 x 12.5 mL, 1 x 25 mL). The aqueous phase then had its pH adjusted to 1 with 2 M HCl solution and then to 10 with 2 M NaOH solution which produced a cream coloured solid flock, which was then separated from the supernatant by a combination of gravity settling and centrifugation to yield **2A**. Yield: 9% (35 mg, 0.135 mmol). IR (KBr disc): 1200 (phenol C-C-O out of phase υ), 1401 (CH_2 deformation), 1561 (COO^-), 3449 (OH υ) cm^{-1}. ^1H NMR (D_2O) δ: 2.53 (2H, t, J = 9.4 Hz, $\mathbf{CH_2}$-COO^-), 2.6-2.75 (2H, m, CH_2-Ar), 2.86 (2H, t, J = 9.4 Hz, S-CH_2), 3.06 (2H, q, J = 9.7 Hz, CH_2-N), 6.39-6.62 (2H, m, aromatic protons). ^{13}C NMR (D_2O) δ: 30.0 (CH_2-S), 34.7 (CH_2-COO^-), 36.9 (CH_2-Ar), 40.7 (CH_2-NH_3^+), 116 (C-2), 119 (C-5), 124 (C-6), 127 (C-1), 172 (COO^-); ES-MS *m/z* (-20 V, H_2O) 253.9 $[M-H]^-$. Mass peak corresponds to the *o*-quinone form, see section 4.3.1.

4.2.3 Catecholamine-Thioether Synthesis by Electrolysis[2]

4.2.3.1 ***3-(5-(2-Amino-ethyl)-2,3-dihydroxyphenylthio)propanoic acid (2B)***

Dopamine (30 mg, 0.158 mmol) was dissolved in 0.1 M HCl (80 mL). The solution had a voltage of 2 V applied across it between two pressed graphite bar electrodes and was vigorously stirred to prevent air bubble formation. The electrolysis was conducted over 2.5-3 h and the initially colourless solution soon turned bright yellow and then bright orange. The formation of the coloured *o*-quinone was monitored by HPLC. Once maximum *o*-quinone formation had occurred, 10%v/v 3-mercaptopropionic acid solution (413 μL, 0.473 mmol in 0.1M HCl) was added rapidly with vigorous stirring. The reaction was monitored and was left overnight as a precaution to ensure maximum product formation. The raw reaction mixture was pH adjusted to 5 with 2 M and 0.1 M NaOH with vigorous stirring to prevent isolated pockets of base destroying the compound.

[2] For reaction scheme see p. 167

The solution was then poured onto a Dowex-50W strongly acidic cation exchange resin column. The solution was eluted straight through the column and the column thoroughly flushed with deionised water until no more 3-mercaptopropionic acid was observed eluting from the column. The 3-mercaptopropionic acid could be seen in the eluant by HPLC, Figure 4.10, with no other compounds eluting straight through. The column was then flushed with HCl (1 M), ethanol (10%v/v) and fractions collected (10-20 mL). Fractions were analysed at regular intervals by HPLC to determine their content. Yield: 34% (14 mg, 0.0545 mmol). Mp: decomposes. IR (KBr disc): 1241 (phenol C-C-O υ), 1400 (CH_2 deformation or COO^- υ), 1638 (COO^- υ), 3434 (OH υ) cm^{-1}. ^1H NMR (D_2O) δ: 2.49 (2H, t, J = 7.9 Hz, CH_2-COO^-), 2.72 (2H, t, J = 9.2 Hz, CH_2-Ar), 2.95 (2H, t, J = 7.0 Hz, CH_2-S), 3.07 (2H, t, J = 9.2 Hz, CH_2-N), 6.68 (1H, s, 2-H), 6.77 (1H, s, 6-H). ^{13}C NMR (D_2O) δ: 28.6 (CH_2-S), 32.0 (CH_2-COO^-), 34.1 (CH_2-Ar), 40.6 (CH_2-NH_3^+), 116.5 (2-C), 120.5 (5-C), 125.3 (6-C), 129.3 (1-C), 144 (4-C), 144.5 (3-C). ES-MS *m/z* (MeCN: H_2O 1:1 5 V) 258.9 $[M+H]^+$.

*4.2.3.2 **11-(5-(2-Aminoethyl)-2,3-dihydroxyphenylthio)undecanoic acid (3)***

Dopamine (30 mg, 0.158 mmol) was dissolved in HCl solution (80 mL, 0.2 M in 1:1 MeCN: H_2O) and electrolysed at 2 V with vigorous stirring for 2.5 h. The *ortho*-quinone formation was followed by HPLC and the current was observed to drop from 20 mA to 9 mA within 30 min. 11-Mercaptoundecanoic acid (104 mg, 0.475 mmol, in 6 mL of 50%v/v MeCN, 0.2 M HCl total) was added rapidly to the vigorously stirring solution. Colour was observed to fade gradually until by 30 min there was no significant colour left. The raw reaction solution after running for 1 h (no further changes detected by HPLC) was pH adjusted to 5 carefully with 2 M NaOH and then 0.1 M NaOH. The solution was run into a Dowex strongly acid cation exchange column as before (10 g) with the column first regenerated by washing with 100 mL of 2 M HCl and then deionised water until washings were stable at pH 3.5. The column was then washed extensively with 50%v/v MeCN to remove all 11-mercaptoundecanoic acid. HPLC analysis revealed that MUA alone eluted through the column and all other compounds were retained.

The column was then eluted with the following elution scheme to chromatographically separate the products and reactant:

1020 mL eluted at 10%v/v EtOH 1M HCl total (2 x 20 mL, 18 x 10 mL, 40x20 mL)

100 mL eluted at 20%v/v EtOH 1M HCl total (5 x 20 mL)

100 mL eluted at 30%v/v EtOH 1M HCl total (5 x 20 mL)

400 mL eluted at 40%v/v EtOH 1M HCl total (20x20 mL)

100 mL eluted at 50%v/v EtOH 1M HCl total (5 x 20 mL)

100 mL eluted at 20%v/v EtOH 2M HCl total (5 x 20 mL)

Fractions were combined and solvent removed (in vacuo) and sample dried (vacuum line) extensively. Yield: 16% (9.2 mg, 0.025 mmol). IR (film): 1413 (COO^- υ), 1638 (COO^- υ), 2855 ($-NH_3^+$ υ, CH_2 symmetric υ), 2929 (CH_2 asymmetric υ), 3437 (OH υ) cm^{-1}. ^1H NMR (D_2O) δ: 1.21 (10H, main chain CH_2 of MUA), 1.36 (2H, MUA), 1.56 (4H, MUA), 2.36 (2H, CH_2-COO^-), 2.87 (2H, CH_2-S), 2.88 (2H, CH_2-Ar), 3.22 (2H, CH_2-N), 6.78 (1H, m, 2-H), 6.88 (1H, m, 6-H). ^{13}C NMR (D_2O) δ: 24.3 (MUA chain), 28.3 (MUA chain), 32.1 (CH_2-COO^-), 33.3 (CH_2-S), 33.9 (CH_2-Ar), 40.6 (CH_2-NH_3^+), 115.5 (2-C), 122.6 (5-C), 123.8 (6-C), 129.3(1-C), 143.0 (4-C), 144.4 (3-C), 179.1 (COOH). ES-MS *m/z* (CH_3CN: H_2O 1:1) 370.6 $[M+H]^+$. Hi-Res FAB-MS: Calculated: 370.2052, Found: 370.2047 MH^+.

4.2.3.3 3-(2-(2-Amino-1-hydroxyethyl)-4,5-dihydroxyphenylthio)propanoic acid (4)

Nor-epinephrine bitartrate (40 mg, 0.125 mmol) was dissolved in HCl solution (80 mL; 0.1 M) and electrolysed at 2 V until maximum conversion to *ortho*-quinone was observed (usually 2 h). 3-Mercaptopropionic acid (328 μL of 1/10 solution in 0.1 M HCl, 0.375 mmol) was added with rapid stirring and the bright orange colour left the solution immediately. The reaction was stirred vigorously overnight. The reaction mixture was adjusted to pH 5 with 2 M NaOH and 0.1 M NaOH before eluting into a regenerated Dowex column (as before) and then being flushed with deionised water until no more MPA was visible eluting from the column. The column was then eluted using the following eluant scheme:

100 mL 0.01 M HCl
100 mL 0.1 M HCl
100 mL 0.1 M HCl 10%v/v EtOH
100 mL 0.2 M HCl
460 mL 0.4 M HCl
100 mL 0.3 M HCl 10%v/v EtOH
100 mL 0.3 M HCl
700 mL 0.4 M HCl

Yield 41% (14 mg, 0.0512 mmol). IR (film): 1193 (CH_2 wag), 1470 (CH_2 deformation), 1633 (COO^- υ), 3450 (OH υ) cm^{-1}. ^1H NMR (D_2O) δ: 2.67 (2H, t, *J* = 7.2 Hz, CH_2-COO^-), 3.15 (2H, m, CH_2-S), 3.27 (2H, m, CH_2-N), 4.55 (1H, s, CH-OH), 6.91 (1H, s, 2-H), 7.07 (1H, s, 5-H). ^{13}C NMR (D_2O) δ: 40.5 (CH_2-COO^-), 41.0 (CH-NH_3^+), 123 (6-C), 129 (1-C), 139 (3-C or 4-C). ES-MS *m/z* (MeCN: H_2O 1:1, 20 V) 274.3 $[M+H]^+$.

4.2.3.4 ***11-(2-(2-Amino-1-hydroxyethyl)-4,5-dihydroxyphenylthio)undecanoic acid (5)***

Nor-epinephrine bitartate (40 mg, 0.125 mmol) was dissolved in HCl solution (80 mL; 0.2 M in 1:1 MeCN: H_2O) and electrolysed at 2 V until maximum conversion to *ortho*-quinone was observed (2 h). 11-Mercaptoundecanoic acid (82 mg, 0.375 mmol in 5 mL of 0.2 M HCl in 1:1 MeCN: H_2O) was added quickly to the rapidly stirring solution. After 1 h the colour had almost completely disappeared though colour loss was a lot slower than the corresponding 3-mercaptopropionate derivative, with distinct strong colour still persisting at 20 min. The solution was left stirring overnight at a reduced speed. The reaction mixture was pH adjusted to 5 with 2 M NaOH and 0.1 M NaOH as before and then eluted into the column and the column flushed with 50%v/v acetonitrile in deionised water until all the MUA had eluted according to the HPLC analysis. The column was then eluted using the following elution scheme:

700 mL 0.4 M HCl
600 mL 0.6 M HCl
200 mL 0.6 M HCl total 10%v/v EtOH
200 mL 0.6 M HCl total 20%v/v EtOH

100 mL 0.8 M HCl total 10%v/v EtOH

100 mL 1 M HCl total 10%v/v EtOH

100 mL 1 M HCl total 20%v/v EtOH

100 mL 1 M HCl total 30%v/v EtOH

300 mL 1 M HCl total 20%v/v EtOH

300mL 1M HCl total 30%v/v EtOH

Yield 28% (14 mg, 0.0353 mmol). IR (film): 1456 (CH_2 deformation), 1616 (COO^- υ), 3394 (OH υ), 3429 (OH υ) cm^{-1}. ^1H NMR (D_2O) δ: 1.15 (12H, m, MUA chain CH_2), 1.44 (4H, m, MUA CH_2), 2.26 (2H, m, CH_2-COO^-), 2.62 (2H, m, CH_2-S), 3.10 (2H, m, CH_2-NH_3^+), 6.92 (1H, m, 2-H), 7.07 (1H, m, 5-H). ^{13}C NMR (D_2O) δ: 24.3 (MUA chain CH_2), 28.7 (CH_2-S), 115.8 (2-C). ES-MS *m/z* (MeCN/H_2O, 20 V): 386.5 $[M+H]^+$. HiRes FAB-MS: Calculated 386.2001, Found 386.2010 (MH^+).

4.2.3.5 ***3-(4,5-dihydroxy-2-(1-hydroxy-2-(methylamino)ethyl)phenylthio)propanoic acid (6)***

Epinephrine (30 mg, 0.164 mmol) was dissolved in aqueous HCl (0.1 M; 80 mL) and electrolysed at 2 V until maximum *ortho*-quinone formation was observed by HPLC. 3-Mercaptopropionic acid (428 μL, 0.491 mmol diluted 1/10 in 0.1 M HCl) was then added quickly to the rapidly stirring solution. The solution changed from bright orange through green to a very deep green, almost black after 30 min. At 30 min reaction the columning process was begun. Rather than using an ion-exchange column, the epinephrine derivatives were purified using conventional phase chromatography on silica gel, Merck 60 Å, grade 9385, 230-400 mesh. For compound 6 the elution was MeCN, 5%v/v H_2O in MeCN, 10%v/v H_2O in MeCN, 20%v/v H_2O in MeCN, 10% 0.01 M HCl in MeCN, 10% 0.1 M HCl in MeCN, 20% 0.1 M HCl in MeCN, 10% 1 M HCl in MeCN, 20% 2 M HCl in MeCN and 2 M HCl. Yield 21% (10 mg, 0.035 mmol) Mp: decomposes. IR (KBr disc): 1123 (CH-OH υ), 1638 (COO^- υ), 3447 (OH υ) cm^{-1}. ^1H NMR (D_2O) δ: 2.75 (3H, s, NH-C**H**$_3$), 2.86 (2H, t, J = 6.7 Hz, CH_2-COO^-), 3.01 (2H, t, J = 7.1 Hz, C**H**$_2$-S), 6.91-7.09 (2H, m, aromatics). ^{13}C NMR (D_2O) δ: 16.7 (CH_3-N), 28.7 (**C**H_2-S), 42 (**C**H_2-COO^-), 57.4 (CH_2-N), 115 (2-C), 117 (5-

C), 126 (6-C), 130 (1-C), 138 (4-C), 140 (3-C), 167 (COOH) (low resolution for peaks at 42 and 115-167 ppm). ES-MS *m/z* (CH_3CN: H_2O 1:1, 30 V) 288.5 $[M+H]^+$. (H_2O, 5 V): 214.5 [M-amine side chain + H]$^+$, 306.3 $[M+H_2O+H]^+$.

4.2.3.6 ***11-(4,5-dihydroxy-2-(1-hydroxy-2-(methylamino)ethyl)phenylthio)undecanoic acid (7)***

Epinephrine (30 mg, 0.164 mmol) was dissolved in HCl solution (80 mL; 0.2 M in 1:1 MeCN: H_2O) and electrolysed at 2 V until maximum *ortho*-quinone formation was observed by HPLC. 11-Mercaptoundecanoic acid (107 mg, 0.491 mmol, in 9 mL 0.2 M HCl in 1:1 MeCN: H_2O) was added to the rapidly stirring solution. The colour changed from bright orange to colourless slowly but did not go black. The reaction was allowed to proceed overnight before columning. This compound was also purified using conventional phase silica and using an elution sequence of MeCN, 5% H_2O in MeCN, 10% H_2O in MeCN, 20% H_2O in MeCN and 10% 0.1 M HCl in MeCN. Yield 36% (24 mg 0.0596 mmol), Mp: decomposes. IR (KBr disc): 1120 (CH-OH υ), 1638 (COO^- υ), 3437 (OH υ) cm^{-1}. ^1H NMR (D_2O) δ: 1.24 (10H, s, MUA chain CH_2), 1.33 (2H, m, MUA chain CH_2), 1.51 (2H, m, MUA chain CH_2 β to COOH), 1.66 (2H, m, MUA chain CH_2 β to S), 2.23 (2H, t, J = 9.8 Hz, CH_2-COOH), 2.71 (3H, m, N-CH_3), 2.84 (2H, m, CH_2-S), 3.13 (1H, m, CH-NH), 3.21 (1H, m, CH-NH), 6.87 (2H, m, aromatic). ^{13}C NMR (D_2O + CD_3OD) δ: 24.0, 27.8, 28.3, 28.5, 28.5 (24-28.5 CH_2 chain), 33.1 (N-CH_3), 54.6 (CH_2-N), 68.4 (CH-OH), 113.9 (C-2), 114.5 (C-5), 116.4 (C-6), 118.7 (C-1), 132.2 (C-4). ES-MS *m/z* (MeCN: H_2O 1:1, 40 V): 454.6 $[M+MeOH+Na]^+$.

4.2.3.7 ***Optimisation of the Electrolysis Method***

Optimisation of the electrolysis method was done to three parameters. The first was electrode type with dopamine-*o*-quinone formation being monitored using stainless steel gauze, platinum wire, silver foil and pressed graphite electrodes. The graphite electrodes were the carbon electrodes from D-size cells that were cut out of the casing and soaked in nitric acid and organic solvents and

regularly sonicated until all loose material had been cleaned away and a clean graphite surface was exposed.

4.2.4 HPLC Analysis of Catecholamine Derivatives

4.2.4.1 ***General***

All the thioether reactions carried out by electrolysis were monitored by HPLC using UV/visible detection. All were analysed using the same reverse-phase Prodigy column and all employed an oven temperature of 40 °C and a total flow rate of 1 mL/min. Analysis injections were 10 μL and were done through an autoinjector. The wavelength range employed in the scans was 190 nm-400 nm. A photodiode array detector was used with deuterium and tungsten lamps. All plumbing was in stainless steel. Three-dimensional plots of absorbance *vs* time *vs* wavelength were obtained and these signature peaks used in identification of the products.

4.2.4.2 ***Elution, Pump and Mobile Phase Sequences***

Compounds ***2B, 4, 6***

Mobile Phases: A: 50%v/v MeCN pH adjusted to 2.15 with trifluoroacetic acid (TFA)
B: 5%v/v MeCN pH adjusted to 2.15 with TFA
Gradient: 100% B for 6.5 min then linear gradient to 50%B until 11 min.

Compounds ***3, 5, 7***

Mobile Phases: A: 50% MeCN, pH 2.15 with TFA
B: 5% MeCN pH 2.15 with TFA

1. 0-6.5 min 100%B
6.5-14.5 min 100%B – 0%B
14.5-20 min 0%B

or

2. 0-4 min 100%B-50%B
4-8 min 50%B-0%B
13.5 min 0% B

4.2.5 Determination of Position of Attachment

The positions of attachment of the thioethers to the aromatic ring were determined by use of Nuclear Overhauser Enhancement Spectroscopy (NOESY) NMR spectroscopy combined with close examination of the chemical shifts of the aromatic carbons compared to the chemical shifts expected for the various positions of attachment by addition of the appropriate chemical shift increments around the aromatic ring. NOESY determination was used to assess whether the two aromatic protons were within 5 Å of each other. This could be assessed by running a thorough NOESY over many scans and seeing if there was a cross-peak between the two protons in the 2-D spectrum. If there was a cross-peak and no cross peak in the COSY then attachment was very likely to be at the 5-position and if no cross-peaks, then it was very likely to be at the 6-position, and if there was no NOESY cross-peak but one in the COSY then it was very likely to be at the 2-position.

4.2.6 Antibody Binding Studies

4.2.6.1 ***2,5-Dioxo-1-pyrrolidinyl-3-(5-(2-amino-1-hydroxyethyl)-2,3-dihydroxyphenylthio)propionate (8)***

2B (5 mg, 0.019 mmol) was dissolved in DMF (1 mL, DMF pH adjusted to 4.2 with HCl) and DCC (96 mg, 0.465 mmol in 125 μL of DMF pH = 4.2) and NHS (54 mg, 0.465 mmol in 125 μL of DMF pH = 4.2) were then added drop-wise to the stirring solution of catecholamine. The reaction was stirred at room temperature in the dark for 3 h. The production of the ester was confirmed by ES-MS and the raw reaction mixture used as is immediately to minimise risk of internal cyclisation. ES-MS: (MeOH, 40 V): 354.4 $[M+H]^+$.

4.2.6.2 Immobilisation of SPR Flow Cells

A new CM5 chip was docked and primed x2 with HBS-EP running buffer and flow cell two activated with 100 μL of EDC/NHS 1:1 (5 μL/min) (150 μL of EDC

coupling solution mixed with 150 μL of NHS solution and take 100 μL to inject). To the flow cell 4,7,10-trioxa-1,13-tridecanediamine was injected (2 x 200 μL, quick inject, 5 μL/min, 1% w/v, pH = 9.7 aqueous) and then immediately followed by more 4,7,10-trioxa-1,13-tridecanediamine (2 x 200 μL, quick inject, 5 μL/min, 1% w/v, pH = 11.3 aqueous). The flow cell was then deactivated with ethanolamine (50 μL, 5 μL/min). Flow cell three was then activated as above and injected with 1,6-hexanediamine exactly as for the 4,7,10-trioxa-1,13-tridecanediamine and was then deactivated as above. Flow cell one was activated and then deactivated as above to serve as the blank flow cell.

The chip was primed with deionised water and flow cell two was washed with 50 mM NaOH (4 x 20 μL, 5 μL/min), 100 mM Na_2CO_3 (100 μL, 5 μL/min) and then 50 mM NaOH (2 x 20 μL, 5 μL/min) before quick injecting the raw **8** reaction solution (1/4 dilution in deionised water centrifuged at 14k x g for 8 min, 1 x 200 μL, 4 x 50 μL injected at 5 μL/min). Flow cell 3 was then treated in the exact same way. The reaction solution of **8** (¼ dilution in deionised water and pH adjusted to 7.0 using 50 mM NaOH, freshly prepared) was then injected over flow cell 2 (8 x 50 μL at 5 μL/min) after centrifugation as before, before and after pH adjustment. Flow cell 3 was then treated exactly as for flow cell 2.

Flow cell 4 was equilibrated to HBS-EP running buffer and activated with EDC/NHS as above. This was immediately followed by ε-aminocaproic acid (1%w/v, pH = 9.7 aqueous, 2 x 200 μL injections at 5 μL/min) and then the same at pH = 11.3. The surface was then deactivated with ethanolamine (as above). The flow cell was then equilibrated in deionised water and activated with EDC/NHS (as above but 200 μL injected). The flow cell was then immediately injected with dopamine (1% w/v, pH = 5.5 aqueous, 1 x 200 μL, 4 x 50 μL, 5 μL/min) and then dopamine (1%w/v pH = 7.0 aqueous, 8 x 50 μL). The chip was then deactivated with ethanolamine (50 μL, 5 μL/min).

4.2.6.3 Antibody Binding Tests

The flow cells were primed with 0.15 M NaCl, 0.01 M phosphate buffer pH = 5.2 (used as running buffer) and monoclonal anti-dopamine injected (100 μg/mL and 50 μg/mL, 60 μL, 20 μL/min). The surface was regenerated with HCl solution

(pH = 3.5 in 20%v/v MeCN). An antibody binding study was then set up. mAb (0, 5, 10, 25, 50, 100, 150 μg/mL in PBS (phosphate buffered saline) pH = 5.2) was injected (60 μL 20 μL/min). The surface was then regenerated as above. Five replicates of each antibody concentration were run. The running buffer was PBS pH = 5.2. Another binding study was set up as for the first, using mAb concentrations of 0, 2.5, 5, 10, 25, 50, 75, 150, 225, 300 μg/mL with five or four replicates of each concentration prepared in PBS pH = 7.0. This was then mixed 1:2 with PBS pH = 5.2 in microwells and injected immediately (60 μL, 5 μL/min). Regeneration was as above. mAb injection was also done using the buffer PBS pH = 6.2 by direct injection (60 μL) for 100 μg/mL mAb and blank injections.

4.3 Results and Discussion

4.3.1 Synthesis of the Dopamine-Thioether Derivative by Aromatic Substitution

When developing the aromatic substitution chemistry for the estrogens at their aromatic A-ring, it was thought that this principle should be applicable to other important biomolecules with an aromatic ring. This would thus allow direct ring attachment without compromising the exisiting functional groups and continuing use of a thioether linkage that has proven to be so stable and to demonstrate such good antibody binding properties as an immunoassay linkage in the past.[10, 15] The obvious choice for such a new class of aromatic biomolecules are the catecholamines.

Like the estrogens, the catecholamines have free aromatic ring positions for conjugation thus enabling the aromatic substitution of a halo derivative, *e.g.* bromo, in the same way as for the estrogens. Once again, like the estrogens studied in Chapter 3, the aromatic ring positions are deactivated with respect to nucleophilic aromatic substitution by the presence of hydroxyl moieties but substitution could be envisaged to proceed via a radical $S_{RN}1$ mechanism. To this end bromodopamine was synthesised through reaction with *N*-bromosuccinimide

(NBS). Chemical synthesis of bromodopamine has not been previously reported, with only one report of 6-bromodopamine having been synthesised biochemically by enzymatic cleavage of bromo-L-DOPA.[268]

Simple treatment of a dopamine solution with a solution of NBS resulted in intense colour changes ranging from blue, green, and red to dark crimson. The product could be isolated by washing the aqueous phase with chloroform to remove the unreacted NBS and the succimide side product and then treating it with activated charcoal to decolourise. The compound had strong electrospray twin peaks at 231 and 233 m/z corresponding to the twin isotopes of bromine, Figure 4.1. The proton NMR spectrum showed clearly monobromo product but the carbon-13 spectrum indicated more than one positional isomer was present.

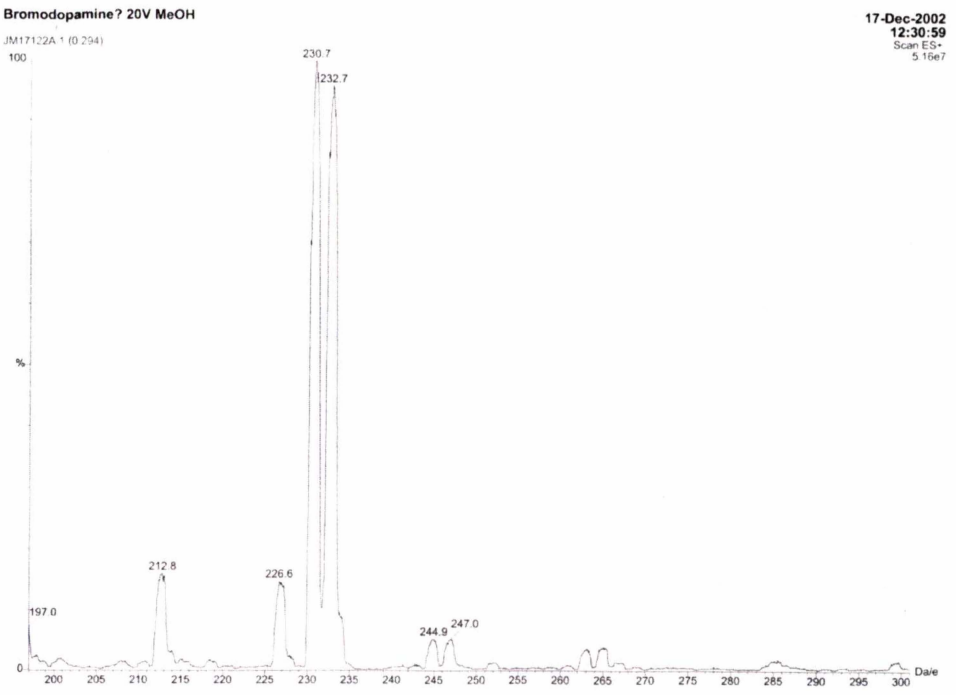

Figure 4.1 Electrospray Mass Spectrum of Bromodopamine

The next step in the synthesis would then be the aromatic substitution of the bromodopamine with a thiol to form a thioether linkage to the aromatic ring. This was done for the estrogens by heating under reflux in methanolic KOH with 3-mercaptopropionic acid. The problem with such a reaction for the catecholamines is that it is well documented that in alkaline conditions the catecholamines undergo superoxide-mediated radical oxidation to produce a number of oxidation

products including the *ortho*-quinone.[170] From these products polymerisation can occur to produce black melanin-type polymers that are insoluble tars. Basic conditions however, are needed in this reaction, as the thiol must be present in the $^{-}$S-R form.

This reaction was attempted from the bromodopamine and through careful purification, the product was able to be isolated this way but in quite low yield, as one would expect (9%). The overall reaction scheme is given in Figure 4.2. The numbering given in the scheme is given to minimise confusion and has been used in discussions of attachment positions of thioethers. The numbering may differ from that used for the systematic names. The purification was effected by constituting the raw reaction in water and then washing with ethyl acetate to remove excess 3-mercaptopropionic acid (MPA) and then pH adjustment to precipitate the product as the less soluble sodium salt. The electrospray mass spectrum gives a peak consistent with the *o*-quinone form and most probably reflects simply the conditions prevalent in the ESMS instrument, as ring ketone signals are not visible in the NMR spectrum. The NMR spectrum of the propionate derivative suggests that attachment has occurred at the 5-position judging from the lack of coupling between the aromatic protons and from the chemical shifts of the carbons. The purification of these catecholamine products is made more difficult by not being able to see them very clearly in TLC analyses. The catecholamines have a UV-visible absorbance that can be seen quite clearly on HPLC but is somewhat weak on TLC, and ninhydrin staining of the plates had only limited success in further enhancing the spots. Furthermore, the amine group tends to produce spots that are smeared and thus hard to discriminate. A further obvious disadvantage is that the compounds are extremely hard to move from the baseline using conventional phase silica plates and the reversed phase plates seem to be of limited use in visualisation of the spots.

4.3.2 Electrolysis to Produce Catecholamine Ortho-*Quinones*

Whilst this substitution approach to production of the thioether derivatives of catecholamines has been shown to work for dopamine, it is clearly not an ideal method. It would be far simpler and would produce better yields if the reaction

were to be done in such a way that no oxidised by-products are produced. The work of groups such as Dryhurst et al. suggest a way of doing this.[167, 168] Thioethers can be formed from the *ortho*-quinone of the catecholamine in a reaction mimicking the body's natural metabolism of catecholamines. To produce the *ortho*-quinones in a controlled way it is necessary to apply a potential difference through an electrolyte. As the catecholamines are quite stable in mineral acid such as HCl, this is a good electrolyte to use.

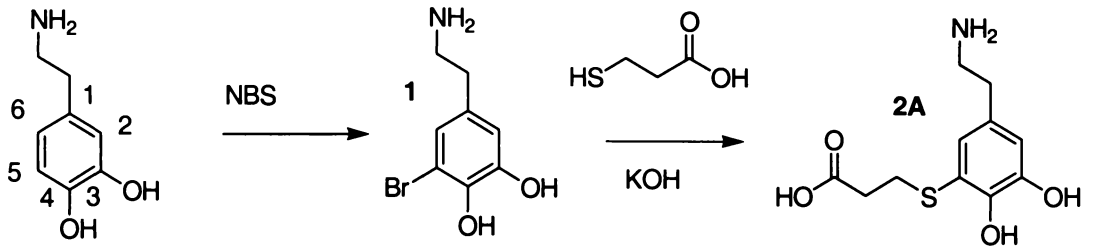

Figure 4.2 Reaction Scheme for Aromatic Substitution to Produce Dopamine-Thioether

Here the methods of previous papers for glutathione and cysteine conjugates of dopamine have been adapted to produce 3-mercaptopropionic acid (MPA) and 11-mercaptoundecanoic acid (MUA) derivatives of three different catecholamines – dopamine, nor-epinephrine and epinephrine. The reaction scheme is given in Figure 4.3. Before proceeding with these reactions it was necessary to optimise the conditions for electrolysis by considering the types of electrode that would work best and the concentration of electrolyte and the potential difference that can be safely applied without electrolytic degradation. Several different types of electrode were tried, these being stainless steel mesh, platinum wire, silver foil and pressed graphite electrodes. The stainless steel meshes were used in different sizes and were able to deliver effective currents that were shown to produce the *ortho*-quinone products, however they leached metal ions into the solutions producing a green colour that masked the formation of the *ortho*-quinone and were not the most effective electrodes. The platinum wire, whilst being inert, presented too small a surface area to the solution and the levels of dopamine-*o*-quinone formation were not adequate. The silver foil tarnished and oxidised and once again did not produce enough current. Pressed graphite electrodes were eventually decided upon as they were inert, leaching nothing into the electrolyte,

had comparatively large surface area and produced good levels of current and the best conversion rates to *o*-quinone.

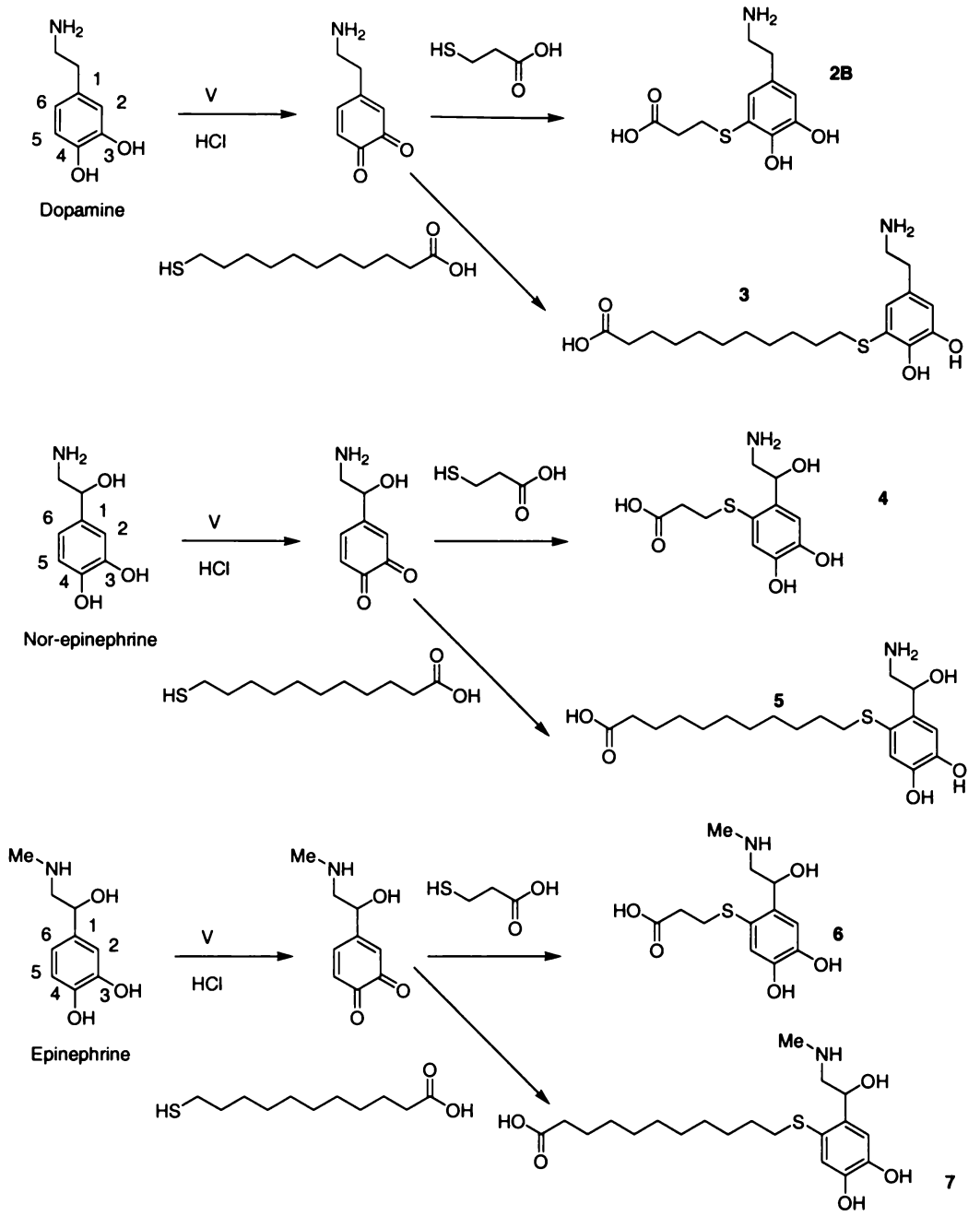

Figure 4.3 Reaction Scheme for the Production of Catecholamine Thioethers via the Corresponding *o*-Quinones

The electrolyte concentration was altered to above 0.1 M HCl but no improvement in *o*-quinone formation was seen. The electrode potential was altered and *o*-quinone formation traced relative to the change. It was found that above 2 V potential difference there was a clear electrolytic degradation of the product and dopamine into a mass of product peaks in the HPLC, and that lesser

voltages led to a reduction in rate of formation of the *o*-quinone and in final product levels. The reaction apparatus is shown in Figure 4.4.

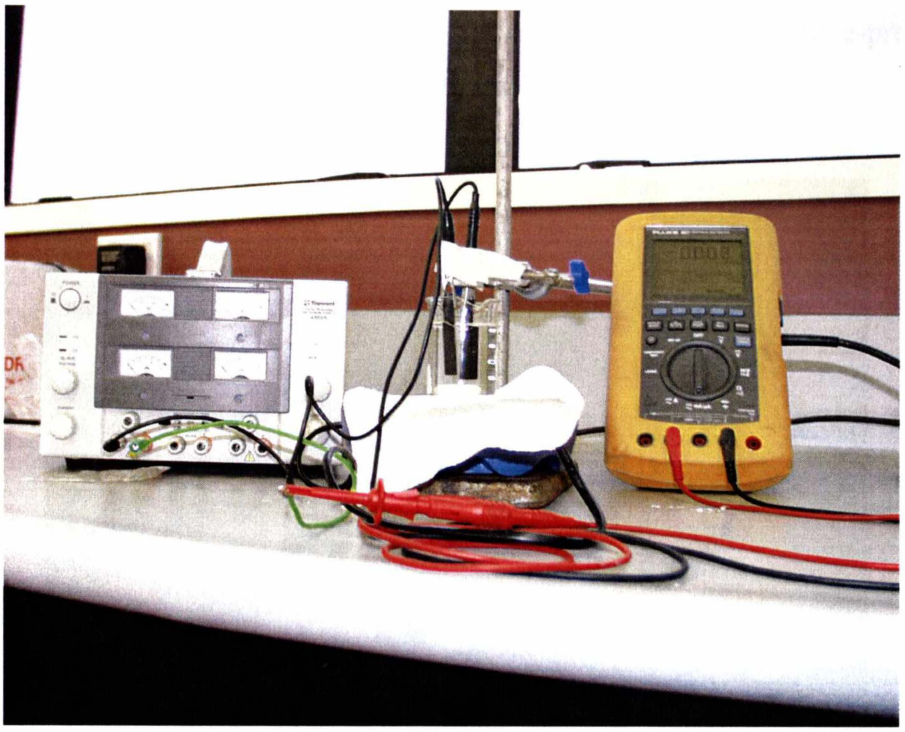

Figure 4.4 Electrolysis Reaction Apparatus

The reactions were done at around 30 mg scale successfully, making them of sufficient scale to not require very many multiple runs but still being low enough to ensure efficient production of the *o*-quinone under electrolysis. In all cases, upon electrolysis there was a clear change in colour from a colourless solution through to a bright orange colour with colour change beginning almost immediately, Figure 4.5. The colour arises from *o*-quinone formation. Another phenomenon observed in all the *o*-quinone reactions is that the current begins high and immediately drops rapidly and eventually evens out at a stable value. This suggests speculatively that at first there is a lot of charged dopamine present but as the reaction proceeds to *o*-quinone these levels drop down until equilibrium is achieved between dopamine and *o*-quinone product.

The formation of the *o*-quinones can be traced clearly by reverse-phase HPLC with the catecholamine and its corresponding *o*-quinone producing characteristic HPLC peaks. To take the example of dopamine, the *o*-quinone peak comes at R_t

= 1.7 min whilst the dopamine comes at an R_t = 1.95 min. The two peaks have signature absorbances that are different across the wavelength scale, Figure 4.6. Dopamine has a characteristic double peaking at 204 nm and 279 nm, the dopamine-*o*-quinone has a single peak at 202 nm, and the dopamine-propionic acid product has peaks at 204 nm and 291 nm.

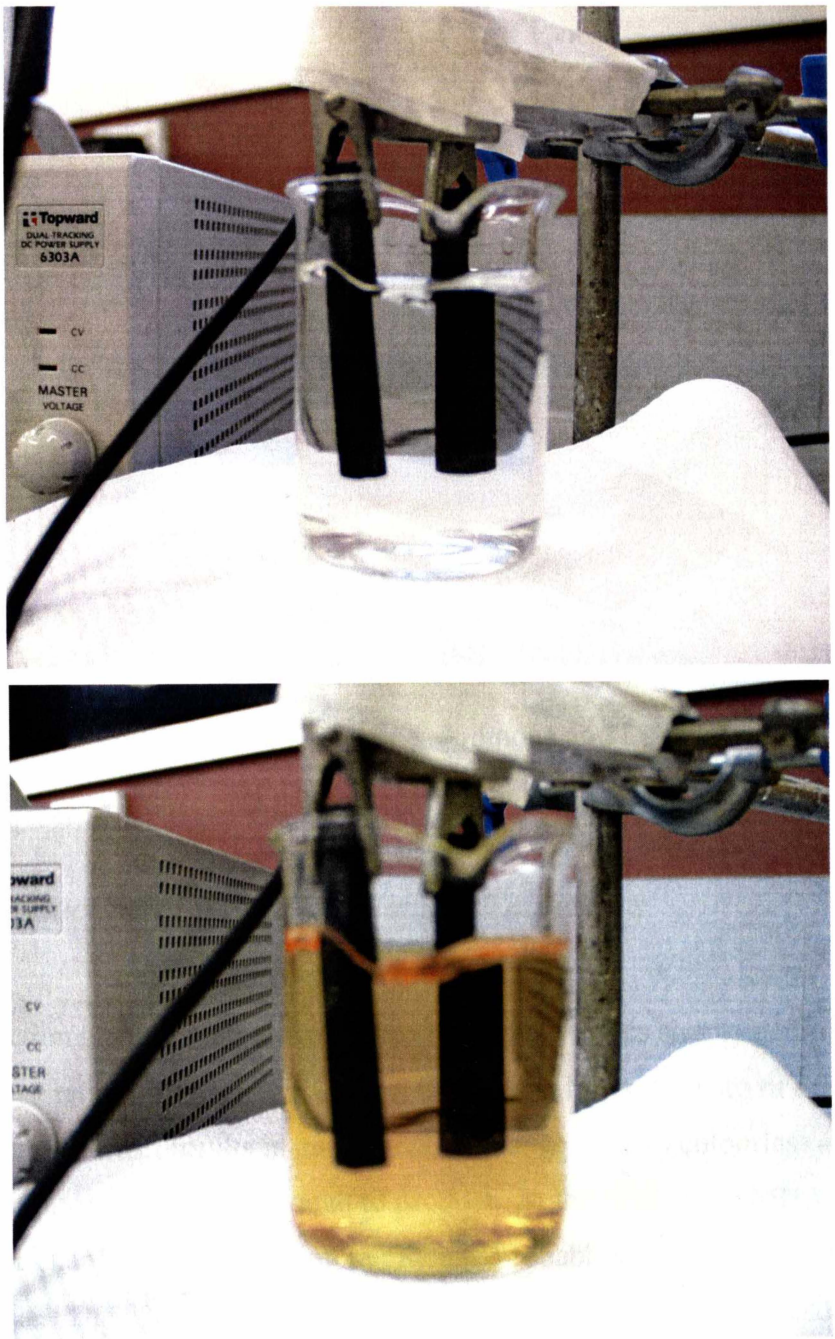

Figure 4.5 Illustration of the Colour Change in Solution Upon Formation of the *o*-Quinone Using Dopamine as an Example

In the case of preparing the *o*-quinones for production of the MUA thioether derivatives, it is necessary to adjust the electrolyte so as to have an acetonitrile component to ensure solubility of the MUA. In order to compensate for the 50%v/v acetonitrile loadings in the electrolyte, it was necessary to increase the electrolyte concentration up to 0.2 M HCl in total.

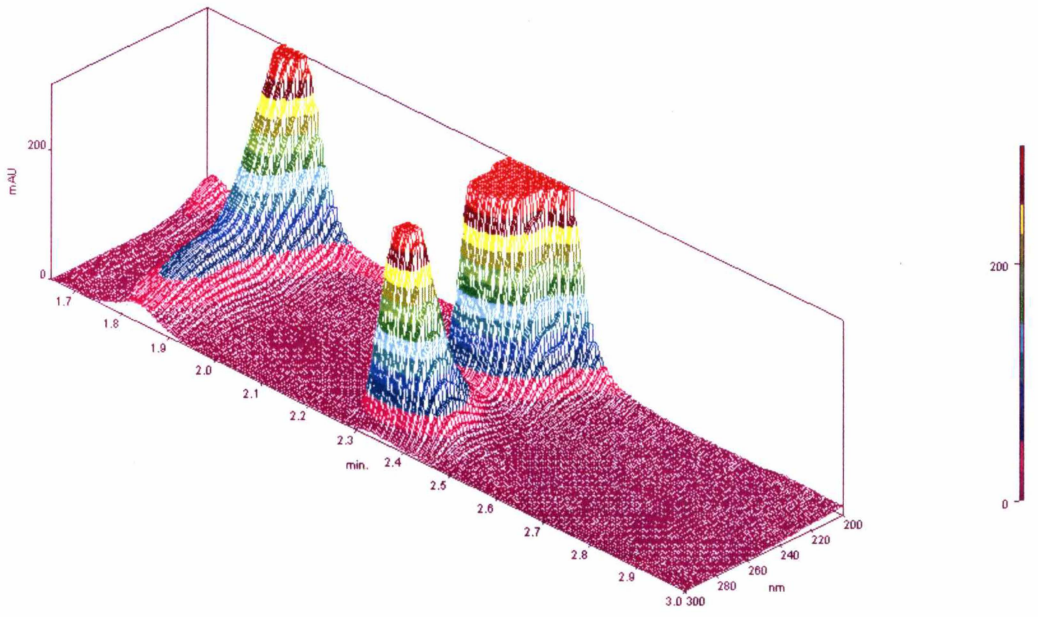

Figure 4.6 3-D Profiles of the Dopamine *o*-quinone and Dopamine Peaks by HPLC

4.3.3 Production of the Catecholamine Thioethers

Production of the thioether from the *o*-quinone involves simply adding the thiol under a fast rate of stirring. This, in the case of the MPA derivatives of dopamine and nor-epinephrine, results in an immediate change back to colourless solution as all the *o*-quinone is reacted through to product. In the case of the MUA reactions, the colour change is somewhat more gradual, probably due to the presence of the acetonitrile. The epinephrine MPA reaction had a slightly different colour change with changes from orange to green to deep green to black within 30 min of addition. The reasons for this difference are unclear.

The addition of the MPA produced several products in each case, corresponding most probably to the different positional isomers. The products,

like the original catecholamines had a main peak in the UV with lesser peaks and shoulders at higher wavelength. A typical example would be the dopamine mercaptopropionate, which is shown in Figure 4.7 with peaks at 204 nm and 291 nm. The original catecholamines themselves have one main UV peak at around 205 nm and then one associated peak usually around 280 nm, rather than a shoulder. Use of water / acetonitrile combinations has enabled the fine adjustment of polarity conditions necessary to achieve chromatographic resolution of these compounds.

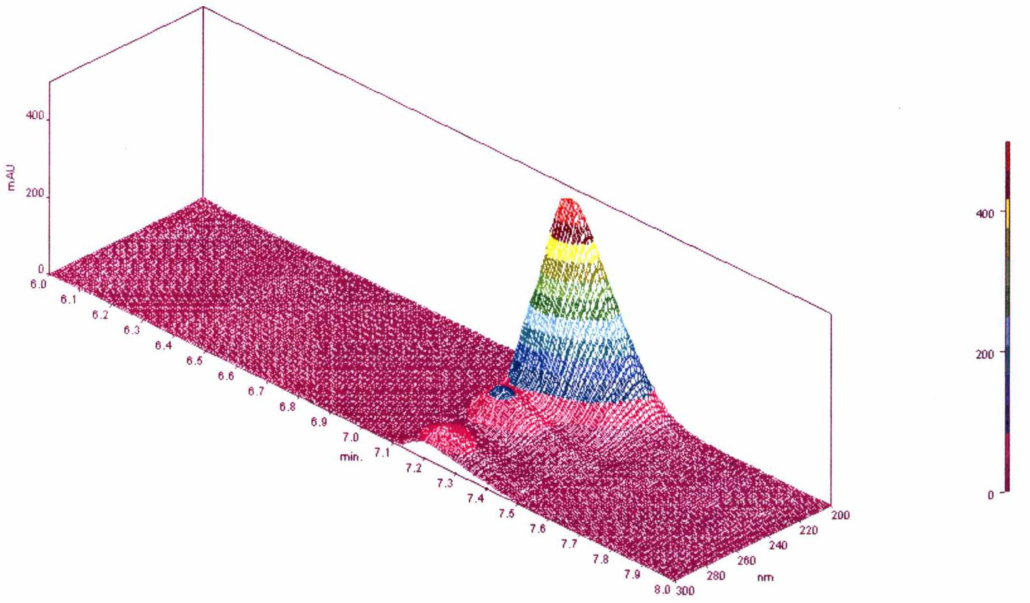

Figure 4.7 3-D HPLC Plot of the Dopamine-Propionate Peak

For each reaction the main product was the one that was the focus of purification efforts. Whilst other positional isomers have clearly been produced in each case, no attempt was made at purifying them out as they were present in lesser quantities and thus were of lesser interest. The MPA peak in each of the MPA reactions was found at R_t = 5.2 min and consisted of just one UV absorbance peak. The MUA was correspondingly seen as two peaks at R_t = 5.7 and 6.5 min. The MUA was observed to persist in the HPLC column for a time, leaching out slowly, which had to be allowed for in assessment of purification.

4.3.4 Ion Exchange Chromatography of the Catecholamine Thioethers

4.3.4.1 General Considerations

The purification of such complex reaction mixtures posed special problems. The foremost of these was that the compounds were so polar that they could not be expected to be separated on conventional phase silica. The use of reversed phase silica should work but this has been complicated by the inability to visualise the compounds on reversed phase silica TLC plates and is not a cost-effective method as reversed phase silica costs approximately NZ$ 400 per 50 g. Previous researchers have relied upon the use of analytical reversed phase HPLC columns for purification and whilst these can be anticipated to work, the columns are very expensive (of the order of NZ$ 4000) and only provide quite small amounts of pure product, with several runs usually needing to be done. The use of ion-exchange resin columns offers an alternative to these techniques. The columns can be used to uptake the desired compound from solution by charge interactions and then release the compounds in a chromatographic fashion upon application of carefully chosen eluants. Small ion-exchange columns have been used in work-up of biological samples containing multiple catecholamines[181] but have previously tended to use small volumes and low concentrations of catecholamines.

Ion-exchange columns were used here to purify the derivatives of dopamine and nor-epinephrine. Weakly acidic cation exchange resins have been used for the catecholamines previously[269, 180] but did not retain the catecholamines strongly enough in this case. A strongly acidic cation exchanger, Dowex 50W, was used. This resin presents carboxylic acid residues on the surface of the beads. Before use, the resin had to be washed to ensure that all loosely held material was washed away and then had to be fully converted to its H^+ form, Figure 4.8. Once this was done, excess acid needed to be washed away so that the compounds being eluted through the column would not be excluded from attaching to the resin due to high competition for binding sites from free H^+ ions in the column. The catecholamines can be purified from the MPA or MUA by attaching the basic amine group to the acid groups of the resin. The MPA and MUA do not possess basic groups capable of binding and so would be expected to flow straight

through. In order for this to work, the catecholamines should be predominantly in the $-NH_2$ form, rather than the $-NH_3^+$ form so the amine group can be protonated by the acid group of the resin. To do this it is necessary to pH adjust the solution to more basic pH. The problem is however, that the catecholamines cannot be adjusted to alkaline pH without some degradation and are not completely stable even at neutral pH. Consequently, the pH was adjusted to 5 very carefully with NaOH solutions and very vigorous stirring to prevent localised alkalinity. The solutions were then eluted into the column as is shown.

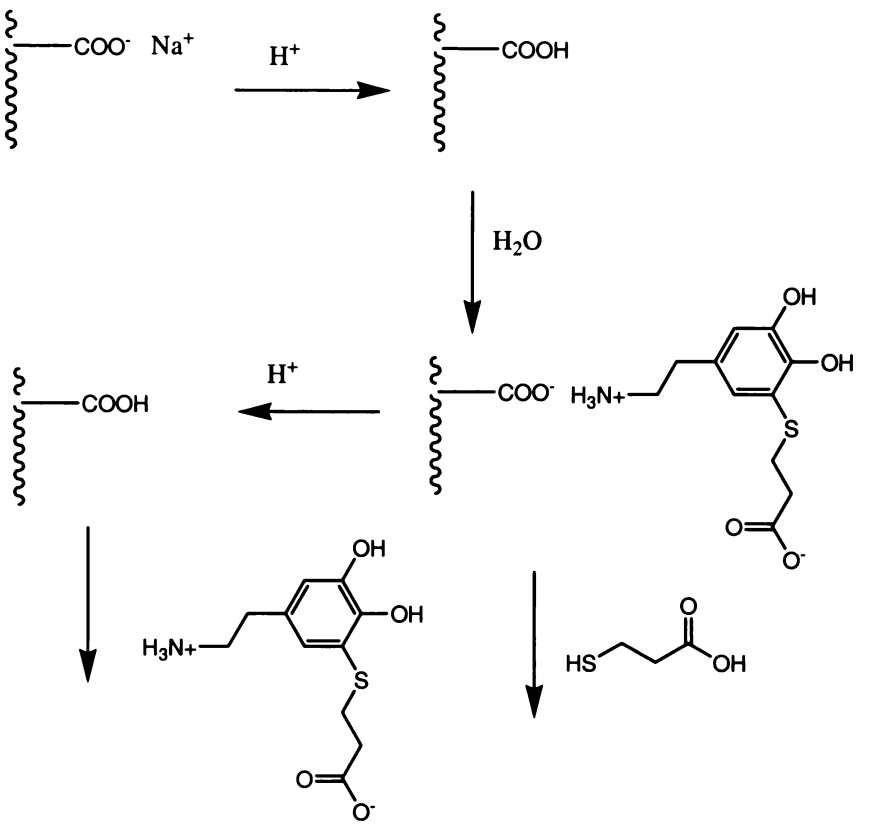

Figure 4.8 Schematic Representation of the Ion-Exchange Separation and Chromatography

The column used in these purifications was gravity fed. Flow was controlled simply by a tap and fractions collected as required. All of the reaction solution was eluted into the one column. Experiments were done using smaller volumes but these resulted in no improvement in chromatographic resolution. In the case of the MPA derivatives, it could be seen that as the sample was eluted into the column and then flushed with deionised water that the MPA flowed straight

through the column whilst all other compounds, *i.e.* the catecholamines, remained adsorbed to the resin. Equivalent results were obtained for the MUA derivatives. By carefully tuning the acid concentration it is possible to elute the adsorbed compounds chromatographically from the column. It has been previously reported that one may use organic solvents with the acid to elute the compounds in a compressed volume[181] and this has been employed here using ethanol combinations.

Between runs the resin must be regenerated. This is done by flushing concentrated HCl solutions through the column to remove any remaining counter ion material and restore all sites to the protonated form. This regeneration must be followed by flushing with deionised water to ensure that all residual acid is gone from the column.

Ion-exchange purification using two resins was attempted. Under this format, the first resin was the same as above and adsorbed the catecholamines. The second was an Amberlite anion-exchange resin, which was supposed to adsorb the carboxylic acid containing products and elute out the un-modified catecholamine. This method failed as the Amberlite resin liberated OH^- ions upon product adsorption and blackened the column with oxidised catecholamines.

4.3.4.2 3-(5-(2-Amino-1-hydroxyethyl)-2,3-dihydroxyphenylthio)propanoic acid (2B)

The dopamine product and unreacted dopamine were eluted from the column using acid solutions with ethanol content. The fractions were analysed at regular intervals by HPLC to determine their content. The dopamine was seen to elute first appearing at 50 mL total eluant. Practically all of the dopamine had gone by 645 mL. The product first appeared at 210 mL as a small peak and this small peak was seen throughout the rest of the dopamine elution and beyond until 765 mL. The product appears to be somewhat more concentrated in the later fractions that are devoid of unreacted dopamine and it was these that were combined. Without the use of ethanol to compress elution volume, separation is still possible with about the same efficiency but this requires more than twice the eluant volume and requires the use of 2 M HCl to get the compounds to elute. It is far better for the purposes of purification to use less acid and less volume as this

allows for easier product recovery. Attempts were made at using 50%v/v ethanol instead of 10%v/v ethanol but whilst this compressed the elution volume much more again, in doing so it completely compromised all separation. The ion-exchange resin elution order reflects the order in which the products elute from the HPLC column, *i.e.* in order of decreasing hydrophilicity with dopamine first and then the dopamine thioether product.

The mass spectrum gave an $[M+H]^+$ ion peak when run in 1:1 H_2O: acetonitrile. The NMR could be run in D_2O. These results demonstrate how ion-exchange chromatography may be used to effectively purify a catecholamine derivative in good yield and to a good level of purity.

4.3.4.3 ***11-(5-(2-Amino-1-hydroxyethyl)-2,3-dihydroxyphenylthio)undecanoic acid (3)***

For this compound, reaction only needed to proceed for 1 h before HPLC showed that maximum product formation had been achieved. In the raw reaction chromatogram one could clearly see the dopamine peak at 1.5 min and the principal product peak at 14.8 min and a secondary product peak at 17.6 min, Figure 4.9. The ion exchange chromatography proceeded successfully by again using 1 M HCl solutions with varying amounts of ethanol to achieve separation. The separation can be followed by plotting peak integral *vs* elution volume and this plot is given in Figure 4.10. One can see how the dopamine has eluted well before the product and how the product and dopamine elutions do not overlap. The pure product exhibits one principal peak and two lesser peaks in the UV-Visible spectrum characteristic of such compounds.

The yield for this reaction was not as good as that for the dopamine-MPA thioether at only 16%. This is perhaps due to the introduction of acetonitrile to the reaction mixture reducing formation of the *o*-quinone. The mass spectrum shows a clear $[M+H]^+$ signal in H_2O / acetonitrile, Figure 4.11. The NMR spectrum shows the characteristic undecanoic acid chain signals including the S-CH_2 signal of the thioether.

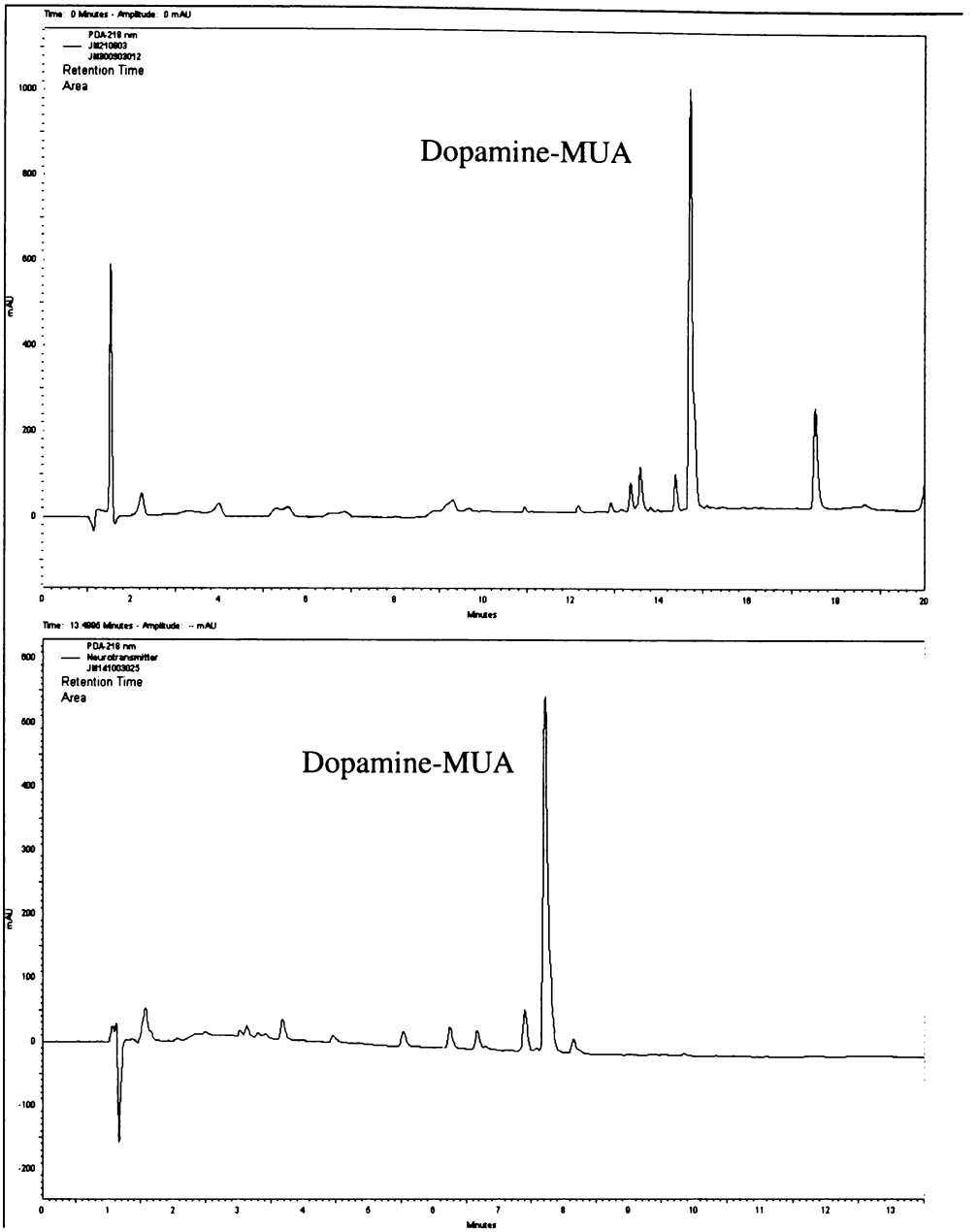

Figure 4.9 Raw reaction using HPLC method 1 (Top) and purified chromatogram using HPLC method 2 (Bottom) – Dopamine-MUA Thioether at 218 nm

4.3.4.4 3-(2-(2-Amino-1-hydroxyethyl)-4,5-dihydroxyphenylthio)propanoic acid (4)

The purification was much the same as for the dopamine-MPA. Once again there was substantial overlap of nor-epinephrine and MPA thioether as the compounds eluted and this can be seen in Figure 4.12. The greater polarity of the catecholamine starting compound and the thioether products meant that more dilute acid was needed to elute the compounds from the column and finer control of acid concentration was needed. Clear purification of the 3.31 min peak could

be seen, the other peaks being too close to nor-epinephrine to resolve. There was some residual 2.33 min peak but this was quite small.

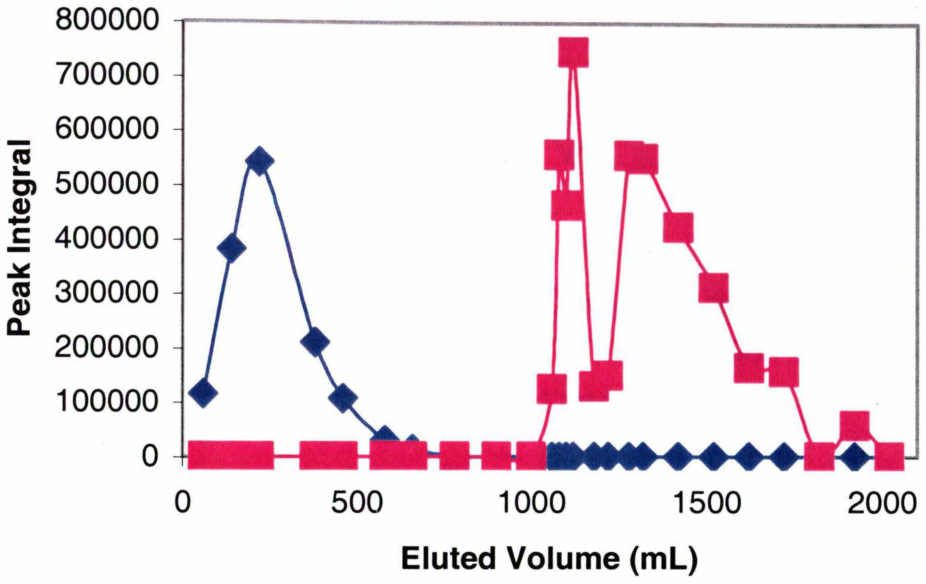

Figure 4.10 Plot of Peak Integral *vs* Elution Volume for Dopamine-mercaptoundecanoate Purification, ♦ (dopamine), ■ (**3**).

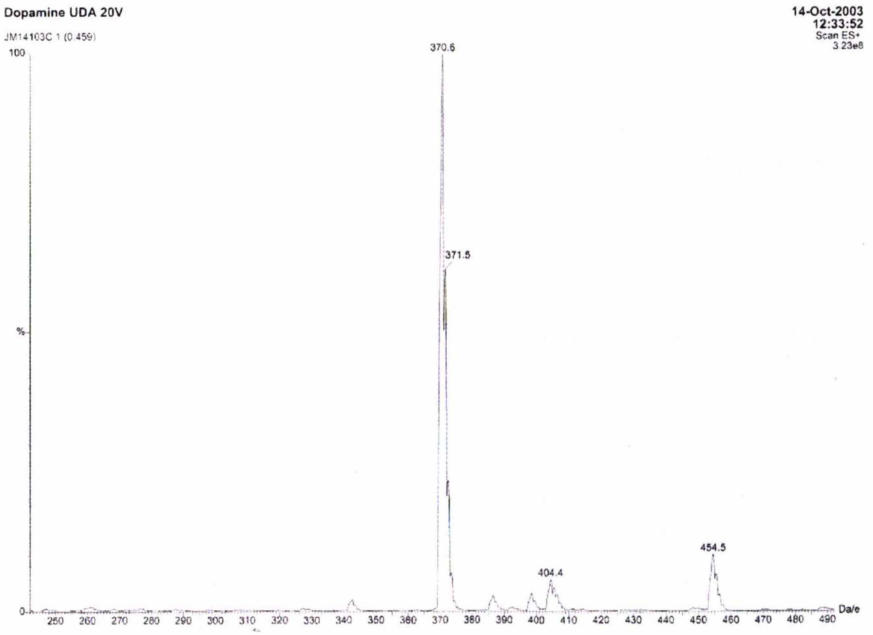

Figure 4.11 Electrospray Mass Spectrum of Dopamine-Mercaptoundecanoate

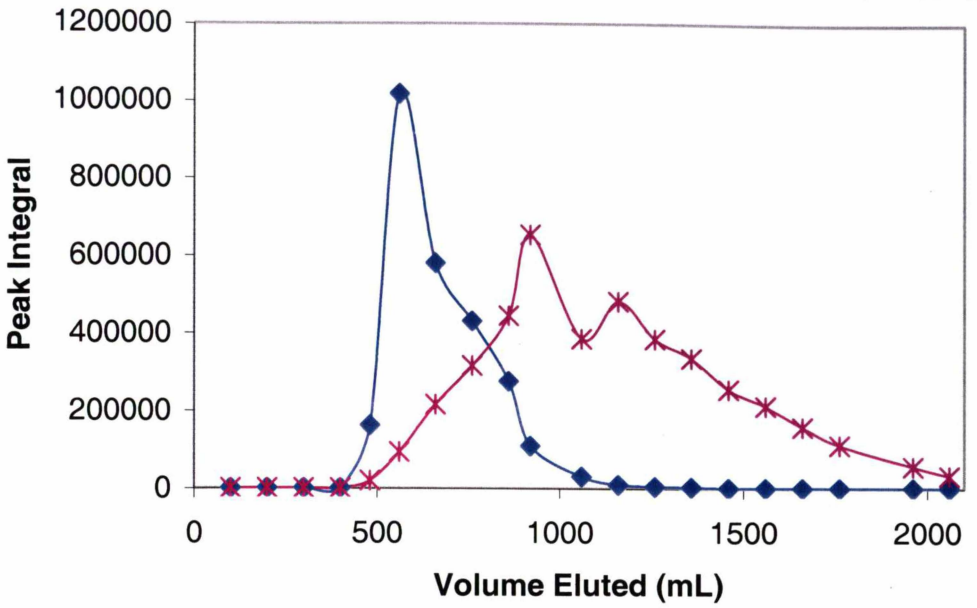

Figure 4.12 Plot of Peak Integral *vs* Eluent Volume for Nor-epinephrine-MPA Column: ♦ Nor-epinephrine, * Nor-epinephrine-propionate.

The yield was quite good at 41% and ^{1}H NMR showed all the required signals including those for the CH-OH moiety. The ultra-polar nature of the nor-epinephrine acid compound means that NMR spectra are correspondingly much weaker as they are less soluble in D_2O. The proton spectra are very clear but some of the aromatic carbon signals are hard to detect.

4.3.4.5 ***11-(2-(2-Amino-1-hydroxyethyl)-4,5-dihydroxyphenylthio)undecanoic acid (5)***

This compound was done in the same manner as for the dopamine derivative but once again finer acid control was needed as the compound was more polar. The pure chromatogram is given in Figure 4.13. One can see that the product is eluting much sooner under these HPLC conditions, as one would expect for these more polar compounds. The 5.79 min peak was isolated and was quite pure.

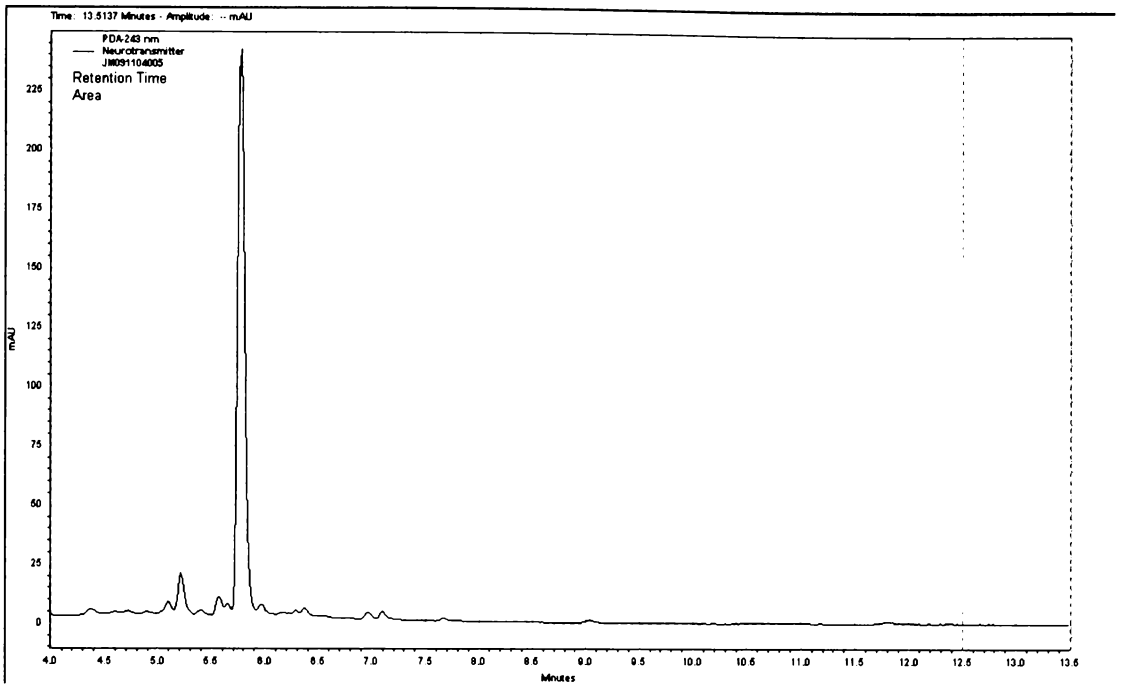

Figure 4.13 Purified Chromatogram for **5** Reaction

4.3.5 Epinephrine Thioether Purification

The epinephrine thioether compounds were originally chromatographed by ion-exchange chromatography like the other catecholamine thioethers. The column still retained the catecholamines even though they now contained only a secondary amine, indicating that the resin was sufficiently strongly acidic to adsorb even weaker basic groups. Purification of epinephrine-MPA was attempted but was only partially successful with there still being significant contamination with epinephrine and other products. Whilst the purified sample was mostly the 4.69 min product there was still a significant amount of both epinephrine and another product. Purification of the epinephrine-MUA thioether was completely unsuccessful despite quite fine gradations in acid concentration. It was clear that another approach was needed to ensure properly purified product. The epinephrine compounds are significantly less polar than the other catecholamines studied as the amino group is a secondary amine not a primary one. It made sense then to try conventional phase chromatography to achieve purification. Methods were developed using eluants composed of acetonitrile and HCl solutions of increasing polarity.

For the epinephrine-MPA reaction the silica column purification gave a single peak upon HPLC examination and so is clearly an efficient way of purifying the sample. Likewise for the epinephrine-MUA reaction there was a clear single peak upon HPLC examination. The retention times for all the purified products are given in Table 4.1.

Table 4.1 Retention Times for the Thioether-Linked Products

Compound	Retention Time (min)
2	7.3
3	14.8
4	3.31
5	5.79
6	6.95
7	7.68

4.3.6 Determination of Positions of Attachment

Thioether groups could attach at any of the 2-, 5- or 6-position of the aromatic ring. The 5- and 6-positions would be favoured over the 2-position on steric grounds. Position can be determined by a combination of 2-D NMR spectroscopy and studying carbon chemical shift increments. COSY NMR can be used to show cross-peaks between protons that are one C-C bond apart and so should only show an aromatic cross-peak for the 2-position of substitution. Nuclear Overhauser Enhancement Spectroscopy (NOESY) gives cross-peaks between protons that are less than ~ 5 Å apart where the intensity of the cross peak signals is inversely proportional to the sixth power of the distance between the protons. In the case of the aromatic protons of the thioether derivatives, one would expect to see the cross-peak between the 6- and 2-protons if the compound is the 5-thioether and no cross-peak if the compound is the 6-thioether (too far away). Combining these methods with an assessment of the carbon chemical shifts, one can determine with good certainty the position of attachment.

For the dopamine-MPA, the ^{1}H NMR spectrum is given in Figure 4.14 and the NOESY spectrum is given in Figure 4.15. This shows a clear cross-peak between the aromatic protons and as COSY shows no cross-peak, this indicates attachment at the 5-position. This is further supported by the incremental carbon chemical

shifts that can be tabulated as in Table 4.2. One can see from the table that the signals for the carbons on the opposite side of the ring to the 5/6 position are very little altered from dopamine to the product as one would expect for attachment at the 5 or 6 position and both peaks in the aromatic region of the proton spectrum are singlets providing evidence that there is no 2-substitution. Considering the C-5 signal, it is seen that the product closely matches the signal of the 5-derivative, with the signal of the 6-derivative matching that of dopamine. Furthermore, the C-5 signal has no peak in the Dept 135 which is completely inconsistent with the 6-derivative and dopamine but wholly consistent with the 5-derivative. When considering C-6 it is seen that the product peak matches that predicted for the 5-derivative closely and has the correct phase. This is good evidence of attachment at the 5-position.

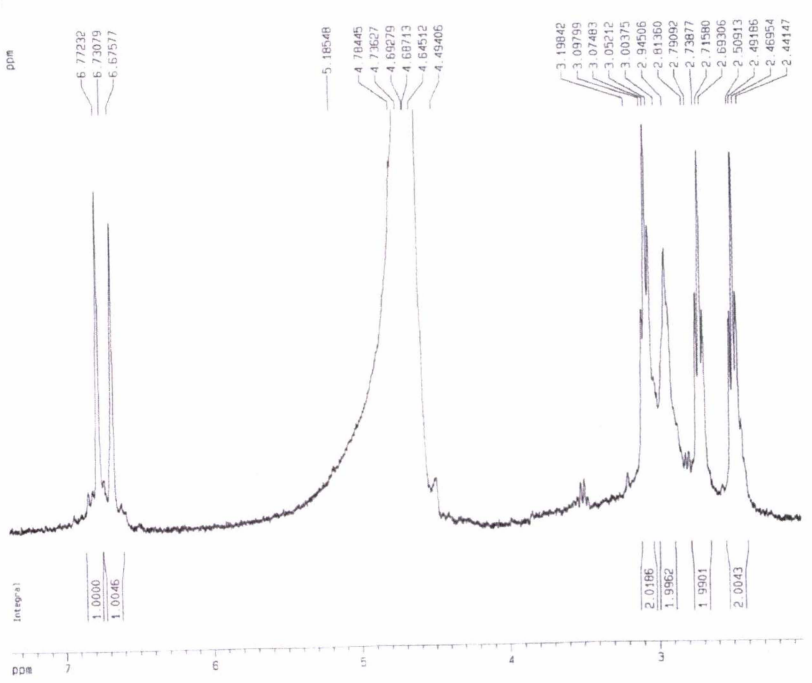

Figure 4.14 ^{1}H NMR Spectrum of Dopamine-MPA Thioether

The dopamine-MUA **3** NOESY spectrum once again showed proton cross-peak but no cross-peak in the COSY, and thus supported 5-position attachment. The analysis of the chemical shifts is shown in Table 4.3. This shows clearly that the 5-position attachment best supports the chemical shift data. For the nor-epinephrine-MPA **4** there was no cross-peak visible in the NOESY or COSY and

the NMR data was consistent with the 6-position also. For the nor-epinephrine-MUA **5** there were no cross-peaks in the NOESY or COSY thus supporting 6-position attachment. In the case of the epinephrine-MPA **6**, the NOESY shows no cross-peak and neither does the COSY and the carbon signals are consistent with 6-position attachment. The epinephrine-MUA **7** has no cross-peak in the NOESY and no cross-peak in the COSY and shows carbon chemical shifts consistent with 6-position attachment. The catecholamine derivatives were found to decompose at high temperatures and so clear melting points could not be obtained. The catecholamine thioethers when in the solid state or protic solvents will be in the zwitterion form (COO- / NH_3^+).

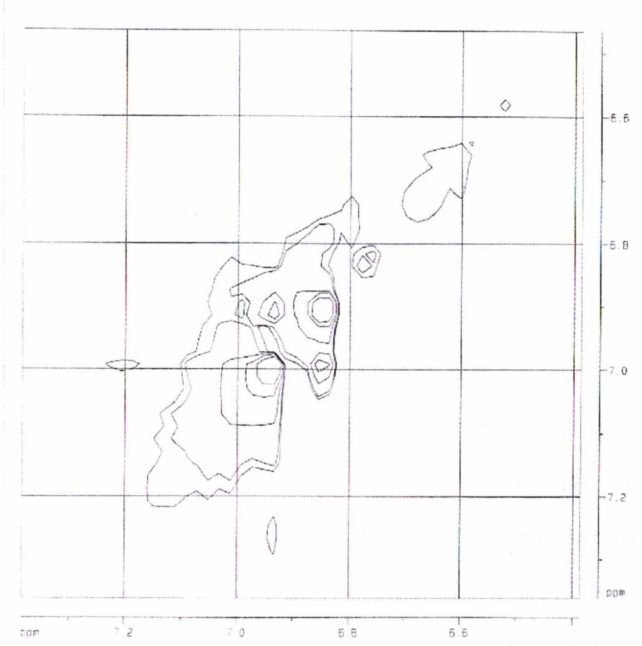

Figure 4.15 NOESY Spectrum of Dopamine-Mercaptopropionate Showing the Aromatic Region

Table 4.2 Chemical Shift Data for Dopamine – MPA Thioether Aromatic Region (ppm) with Dept 135 Phase in Brackets (0 = No Peak)

Assignment	Dopamine	5-Derivative	6-Derivative	Product
C-2	116 (+)	113 (+)	117 (+)	117 (+)
C-5	116 (+)	120 (0)	117 (+)	121 (0)
C-6	119 (+)	123 (+)	126 (0)	125 (+)
C-1	128 (0)	138 (0)	138 (0)	129(0)
C-3	144 (0)	143 (0)	139 (0)	144 (0)
C-4	147 (0)	143 (0)	141 (0)	145 (0)

Table 4.3 Chemical Shift Data – Dopamine-MUA Thioether Aromatic Region (ppm) with Dept 135 Phase in Brackets (0 = No Peak)

Assignment	Dopamine	5-derivative	6-derivative	Product
C-2	116(+)	113(+)	117(+)	116(+)
C-5	116(+)	120(0)	117(+)	123 (0)
C-6	119(+)	123(+)	126(0)	124(+)
C-1	128(0)	138(0)	138(0)	129(0)
C-3	144(0)	143(0)	139(0)	143(0)
C-4	147(0)	143(0)	141(0)	144(0)

4.3.7 Antibody Binding Studies – Monoclonal Anti-Dopamine

4.3.7.1 Formation of the Dopamine-Mercaptopropionate Active Ester (8)

The production of active esters to the thioether-bridged derivatives of the steroids has been done in DMF successfully with simple room temperature stirring overnight. There are two factors that prevent use of this method with the dopamine-mercaptopropionate. The first is that the alkaline conditions of the DMF may result in oxidation of the product, the second is that if the active ester is left for many hours then it will probably internally cyclise with the primary amine. The reaction was thus conducted under acid conditions at pH = 4.2 and the reaction was restricted to 3 h to minimise internal cyclisation. The reaction was analysed by mass spectrometry and showed a strong $[M+H]^+$ peak for the ester and no sign of any peaks corresponding to the internally cyclised product. Any such product will of course just pass straight over the surface without being immobilised; and should have no effect on the immobilisation provided plenty of the active ester is still present as indicated by the electrospray. The reaction mixture had to be used without purification, as rapid conjugation was needed to minimise cyclisation. The structure of **8** is given in Figure 4.16.

4.3.7.2 Immobilisation of Dopamine Derivatives Onto the Flow Cells

To construct flow cells that contain the small molecule antigen immobilised on the surface, it is necessary to introduce intermediate linkers to space the antigen

from the surface and thus minimise steric obstruction to binding. The best way to introduce such linkers is to assemble them in situ on the sensor chip itself. This can be done by first activating the carboxylic acid bearing dextran surface with EDC / NHS to produce the active ester. This was done with large excess in each flow cell to ensure saturation of the surface. The next step was to pass the intermediate linker over the surface. The linker must contain a primary amine group to couple covalently to the surface. The linkers were attached first at pH = 9.7 which was just below the pKa of the linkers and was not so alkaline as to risk degradation of the active esters on the surface. Once a large excess of the linkers had been passed to ensure saturation at this pH, the linkers were then passed at pH = 11.3, which was above the pKa of the amines and thus ensured maximum $-NH_2$ form and so maximum attachment. The use of these two pHs and large excess in both volume and concentration of linker compounds coupled with a slow flow rate should ensure that saturation immobilisation takes place. Three different linkers were used here. The first was the oligoethylene glycol (OEG) linker used in the SPR experiments in Chapters 3 and 5, the second was 1,6-hexanediamine, a somewhat shorter and less water-soluble linker and the third was the heterobifunctional linker ε-aminocaproic acid which is of nearly identical length to the hexanediamine. The first two linkers had two terminal primary amines and the pHs were selected to maximise coupling to one of the amines only. There may be some immobilization at both amine terminals, but the selection of pH and the short length of the linkers should minimise this effect. The caproic acid linker has only one primary amine and is otherwise very similar to the 1,6-hexanediamine.

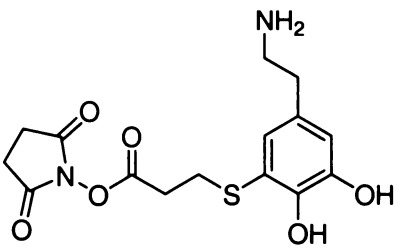

Figure 4.16 Structure of Dopamine-Mercaptopropionate Active Ester **8**.

The next step was to attach the dopamine-mercaptopropionate to the first two linkers in situ on the surface. The active ester reaction mixture had to first be

diluted in deionised water as the integrated microfluidics cartridge (IFC) of the BIAcore instrument could be damaged if straight DMF was used. The addition of the water precipitated unreacted NHS and DCC and DCU on top of that which had already precipitated. This solid was removed by centrifugation before injection. The running buffer used could no longer be HBS-EP (pH = 7.4) as this may have oxidised the dopamine derivative. Instead, deionised water was used as the dopamine could withstand this for short periods without significant oxidation. An acidic buffer could not be used as it would convert much of the amine to the $-NH_3^+$ form and thus diminish reaction. To ensure that the amines were in their $-NH_2$ form, the linker surface was flushed with base before addition of the ester. Once again, a large excess of the ester was used to ensure saturation of the surface. The ester was first passed at pH = 5.2 (the pH resulting from deionised water dilution) and then at pH = 7.0. This treatment was applied to the OEG and hexanediamine linkers.

For the caproate linker, the carboxylic acid unit now needed to be activated with EDC/NHS and this was done in excess to ensure maximum activation of the linker ends. Dopamine was then passed over the surface at pH = 5.5 in excess and was then followed by dopamine again at pH = 7.0 to ensure saturation conjugation through the primary amine of the dopamine. These immobilisations are summarised in Figure 4.17.

4.3.7.3 Antibody Binding Studies

To conduct the antibody binding studies, the running buffer had to be specially modified to ensure that the pH was acidic so as to minimise any risk of oxidation of the immobilised dopamine hapten. The running buffer selected was 0.15 M NaCl 0.01 M phosphate buffer (pH = 5.2). The surface was primed and flushed with this running buffer and stable baseline obtained before injecting monoclonal antibody that had been raised to a BSA conjugate through the primary amine by the glutaraldehyde method. The binding was tested at both 100 μg/mL and 50 μg/mL antibody concentrations. All three flow cells showed very high antibody binding response with well-shaped sensorgrams. These are shown in Figure 4.18.

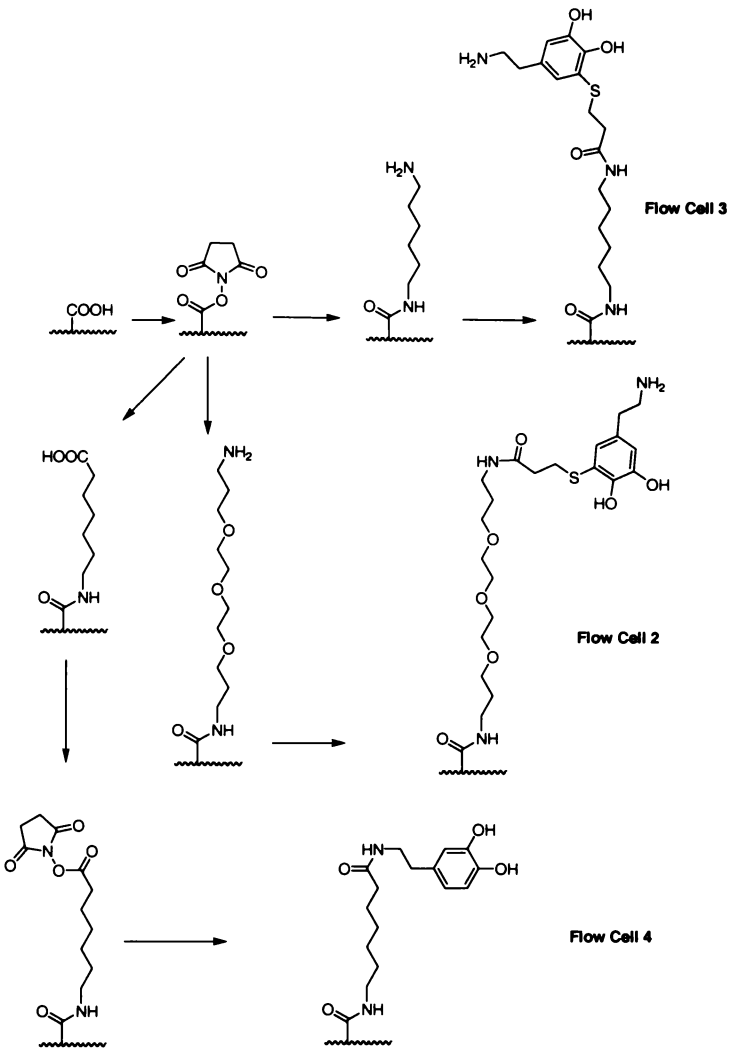

Figure 4.17. Immobilisation of Dopamine to the SPR Chip

One can see from these sensorgrams that the highest antibody binding response was to the caproate-linked dopamine. This makes sense as the antibody has been raised to a conjugate through the amine of the catecholamine and so would be expected to recognise best an antigen immobilised in the same way. The next best binding response in this binding event comes from the OEG-linked surface, which could be explained by the water-soluble OEG linker projecting the dopamine better into the aqueous phase than the less water-soluble hexanediamine. Furthermore, since all the sensorgrams are blank corrected, the significant binding observed with all three linkages suggests that the antibody binding is specific on each surface.

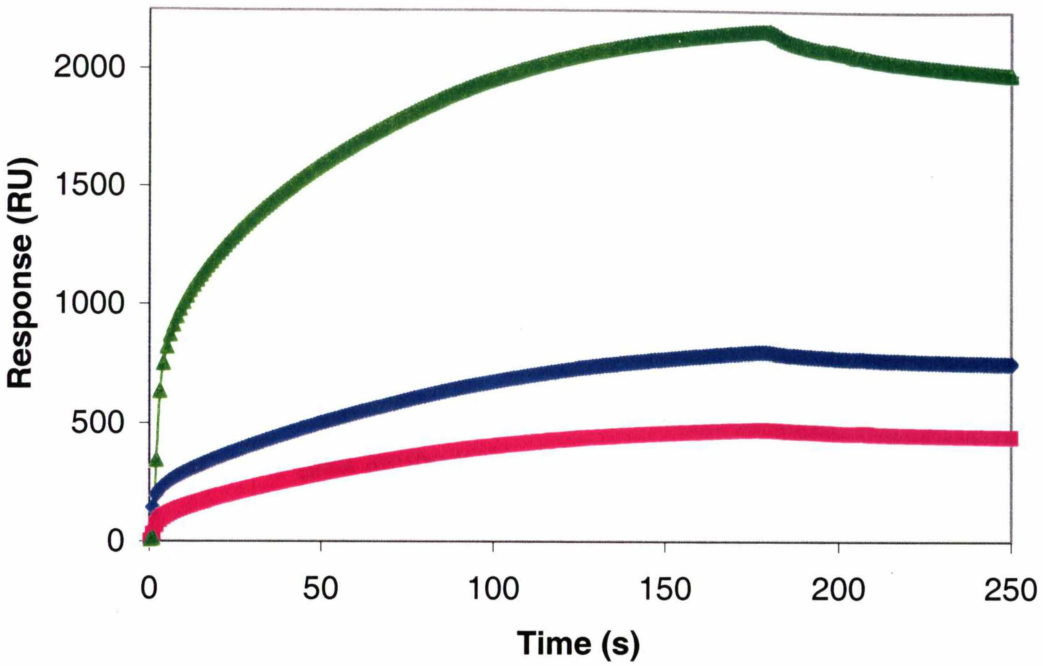

Figure 4.18. Overlay Plot of the Sensorgrams for mAb (100 μg/mL) Binding to the Dopamine Chip. ♦ Flow Cell Two (OEG-Linked), ■ Flow Cell Three (Hexanediamine-Linked), ▲ Flow Cell Four (Caproate-Linked).

Whilst there is strong initial binding, these surfaces suffered from quite rapid degradation, with the binding responses regularly declining in all three flow cells from one cycle to the next. This decline in response was not due to degradation of the antibody, as making solutions of antibody fresh did not have any effect on the decline. It was also not due to poor regeneration, as the responses obtained bore no relationship to any residual baseline rise. The absolute response of the surfaces was seen to decline with time and successive cycles and to decline between docking and undocking of the chip. The surfaces were clearly not stable long-term and this precluded the production of a full antibody binding curve across many concentrations or the construction of an assay using the surfaces. This decline eventually seemed to stop but the CVs of the binding responses were too high to enable any reasonable assay to be done.

The surfaces were stable enough however to determine triplicates of antibody binding at 100 μg/mL and 50 μg/mL antibody concentrations. The CVs were somewhat larger because of the declining responses however the results were still clear and are given in Table 4.4.

Table 4.4. Binding Responses for the Dopamine Flow Cells (RU)

mAb Concentration (μg/mL)	OEG (RU)	Hexanediamine (RU)	Caproate (RU)
50	116 ± 24	135 ± 43	278 ± 22
100	580 ± 100	650 ± 140	1670 ± 210

The errors quoted are standard errors.

Analysis of these values by one-tailed *t*-test showed that the caproate-linked flow cell definitely had higher antibody binding than the other two at both 50 and 100 μg/mL ($P < 0.05$) though the OEG and hexanediamine values cannot be regarded as statistically different from each other. The higher binding observed for the caproate-amine-immobilised conjugate was very likely due to the position of attachment and not to the linker type as the caproate linker is very similar to the hexanediamine linker.

Antibody binding tests were attempted by setting up a "wizard" program to run mAb injections in phosphate buffer pH = 5.2, but the binding responses declined rapidly with time, due either to the deteriorating surface or gradual destruction of the antibody at this pH. The assay was then repeated using injections of the mAb at pH = 7.0 mixed 1:2 with phosphate buffer pH = 5.2 to generate a final solution pH of 6.25. The binding responses here had very high CVs and very low magnitude, largely swamped out by a phase change effect caused by the buffer as it was injected. Injections of mAb in pH = 5.2 buffer were made fresh each time but gave erratic binding. The regeneration buffer used in all cases was HCl solution (pH = 3.5, in 20%v/v MeCN) that regenerated the surface well.

To develop a biosensor assay using this surface, it will be necessary to extensively investigate the conditions under which the surface will be stable. The inherent instability of the catecholamines makes biosensing of them using an antigen-immobilized surface very challenging, and beyond the scope of this investigation. The experiments presented here demonstrate that the surfaces constructed all bind strongly to the monoclonal dopamine antibody and that the immobilization through the primary amine via a caproate linker, gives the strongest antibody binding due to the manner in which the antibody has been raised.

The catecholamine derivatives produced can clearly be used to produce protein conjugates and then be used to raise antibodies. Such antibodies should, regarding the SPR results obtained, show superior binding to the mercaptoalkanoate-modified SPR surfaces. As this conjugation does not compromise existing functional groups on the catecholamine, it could be anticipated that antibodies raised to these conjugates will be better able to recognise the free catecholamine than would the existing antibody raised to conjugates through the primary amine. Clearly such immunogenic protein conjugate studies would be a very interesting area of further research in this field.

4.4 Conclusions

The catecholamines are of great interest as analytical targets for the development of sensitive immunoassay. Conjugation of the catecholamines for immunoassay has previously relied upon the use of conjugation through the primary amine group (glutaraldehyde and carbodiimide methods) or through the unreliable Mannich reaction. Production of thioether-bridged conjugates offers an excellent alternative to these traditional conjugations by allowing attachment directly to the aromatic ring, without compromising existing functional groups, through a simple and rapid reaction, purification to a single positional isomer and no significant undesirable side reactions.

The synthesis of mercaptopropionate and mercaptoundecanoate derivatives of the catecholamines dopamine, norepinephrine and epinephrine by electrochemical production of the corresponding *o*-quinones and then addition of the appropriate linker has been reported. The products have been purified by ion-exchange chromatography for dopamine and norepinephrine using a simple procedure with only one ion-exchange resin. Reactions and purifications have been monitored by HPLC. The positions of attachment have been established with the aid of 2-D NMR spectroscopy in each case.

An SPR sensor chip has been immobilized with the dopamine-mercaptopropionate compound using OEG and hexanediamine linkers assembled in situ on the chip. Dopamine was also immobilized through the primary amine using a caproate linker. The antibody binding to these conjugated surfaces was

assessed and the primary amine-immobilised dopamine gave highest binding by virtue of the antibody being raised to an amine conjugated protein conjugate. All flow cells gave strong antibody binding.

These results demonstrate how a new generation of catecholamine-linker derivatives may be synthesised and applied in conjugations. These derivatives have important potential applications in the raising of antibodies and as coating antigens for antibody binding. In order for antibodies to specifically recognise small molecules that lack a large number of functional groups or specific shapes, it is important that existing functional groups are kept intact when those antibodies are raised. Thioether-linked conjugations provide a simple means of producing specific conjugations direct to the aromatic ring and so open up the possibility of developing a new generation of specific antibodies to the catecholamines and the production of biosensors based around these. This is another illustration of how organic chemistry can help to improve immunosensing.

Chapter 5 – Signal Enhancement of SPR Immunosensing of Small Biomolecules

5.1 Introduction

The lack of sensitivity of SPR-based immunoassays has been a major factor preventing their more widespread implementation as practical biosensing systems. To perform adequately for many applications, the SPR biosensor must demonstrate comparable sensitivity to corresponding ELISA. Sensitivity may be expressed in one of two interrelated ways: first, as the limit of detection of the assay, which is affected by the concentration range of the standard curve and the errors in the concentration determinations; second, as the slope of the active region of the immunoassay curve, and is affected by the signal change per unit concentration change. One of the most critical factors determining the sensitivity of SPR is the level of refractive index change obtained per unit concentration change in the assay. This can be increased by the use of high mass labels of which colloidal gold is the most widespread because of its high mass, its ability to undergo surface plasmon resonance and its ease of production. Nanoparticle labels have been employed in the assay of large size biomolecules such as proteins and oligonucleotides and have achieved immunoassay signal enhancements of around 25-fold[207] and improvements in detection limit of around three-orders of magnitude,[199] but no successful attempt had yet been made to apply these concepts to SPR immunoassay of small biomolecules.

The development of such formats for the small molecule has many great challenges not found for the larger molecules. The principal challenge is how to preserve antibody binding to the small molecule in the face of the steric constraints that a large label produces. Another challenge is how to space the small molecule out from the label to allow antibody binding whilst preserving the gold colloid enhancement effect, bearing in mind that the SPR signal reinforcement will operate only within about 300 nm of the surface. There are further challenges in developing regeneration cocktails strong enough to remove

the bound gold from the surface and still have a surface stable enough to withstand the repeated regeneration cycles needed for a practical system. Further problems can be anticipated to arise by the need to attach the small molecule to the colloidal label via some kind of intermediate compound, thus losing the intimate contact seen in immobilisation of say a protein on the gold label surface, which would be expected to provide more enhancement of the signal. Furthermore, there are potential problems associated with the propensity of gold to bind to surfaces and proteins non-specifically.

In spite of all these potential challenges, the possible benefits of signal enhancement of antibody / antigen binding interactions for small molecules are great, and include the much improved ability to distinguish low target concentrations from the zero response, higher signal/noise ratios, steeper active regions of the assay standard curves and the ability to lower the primary antibody concentration and still have sufficient binding response for an accurate assay.

Progesterone is an ideal model compound for studying small-molecule immunosensing formats as it is the first target to be detected by enzyme immunoassay, and hence its antibody binding interactions have been extensively studied. Monoclonal antibody to progesterone has been fully developed and widely used and is commercially available. Furthermore, progesterone is similar in structure to a range of other biologically important steroids. Progesterone is also of great physiological interest for its role as a female sex steroid hormone, which means that it acts as a biomarker for a range of physiological processes including mammalian estrous cycles. Previous work has established linker attachment chemistries via the 4-position and shown this to provide superior antibody binding in the BIAcore SPR format.[10, 15]

There has been a great dearth of studies on the effect of new immunosensing formats on antigen / antibody binding performance and on how novel labelling technologies and formats might affect immunosensor performance. The principles developed here for progesterone should extend in a generic sense to other small biomolecules, and the formats developed could be easily transferred to other targets.

Reported below is the first successful study of nanoparticle signal enhancement of SPR-based immunoassay for small molecules. Surface immobilisation chemistries, regeneration cocktails and non-specific binding treatments necessary

to achieve a high level of repeatable assay performance are developed along with the use of gold colloids of varying sizes to label antibody binding interactions in SPR, for use in immunoassay, through a range of labelling techniques, including biotin / streptavidin coupling and secondary antibody coupling, and in different label delivery formats, both pre-labelling and sequential binding. All the binding curve and assay standard curve data for all these formats are presented, as are the levels of signal enhancement and the effects on assay detection limits and sensitivities.

5.2 Experimental

5.2.1 Materials and Instruments

5.2.1.1 General

Progesterone for synthetic work was purchased from Applichem (Darmstadt, Germany A06770025) and for preparation of standards was from Sigma (Cell culture tested, P8783, $\geq$ 99%). Di-*tert*-butyl dicarbonate and 4,7,10-trioxa-1,13-tridecanediamine were purchased from Fluka Chemie (Buchs, Germany). DMF was from Aldrich (anhydrous under septum 99.8%, 227056). PEG-400 was from Prolabo (26 602-290), $HAuCl_4.3H_2O$ from Acros (ACS reagent 411070010), trisodium citrate from Aldrich (99% pure, 855782). Biotin *N*-hydroxysuccinimide ester was from Sigma (H1759) as was biotinamidohexanoic acid *N*-hydroxysuccinimide ester (B2643) and OVA (A5503) and BSA (A7030). All other chemicals were from Aldrich. All solvents used were analytical grade except for the HPLC solvents that were HPLC reagent grade ACS. The primary anti-progesterone antibody (monoclonal antibody) was from Sigma (P1922) raised in rat to the 7-position conjugate as for Chapter 2. The secondary antibody was anti-rat IgG (whole molecule) raised in rabbit (Sigma, R5128).

Melting point determinations, NMR spectroscopy and electrospray mass spectrometry were all run as for Chapter 3. Analytical RP-HPLC was done as for Chapter 2 but using a Sphereclone ODS 3 μm column (150 x 4.60 mm) on a Shimadzu instrument using PDA detection.

5.2.1.2 Gold Conjugates

Streptavidin-gold 10 nm conjugate was purchased from Sigma (S-9059, monodisperse 8-12 nm) and was supplied in 0.01 M phosphate buffered saline, pH=7.2, containing 1% BSA, 20% glycerol and 15 mM sodium azide. The concentration of the 10 nm colloid corresponded to an absorbance, $A_{520} \simeq 2.5$, which was verified by additional UV-Visible spectroscopic examination. The streptavidin-gold 20 nm conjugates were purchased from Sigma (S-6514 monodisperse 17-23 nm) supplied in DMSO. The colloid was dialyzed against several changes of PBS/T at 4 °C and was then analysed by UV-Visible spectroscopy and gave an absorbance at λ_{max} at 523 nm of 1.577 $\pm$ 0.001. To ensure that the colloid had preserved streptavidin function during dialysis it was tested in a strip assay with immobilised progesterone – OVA conjugate. The strip was dipped into a microwell with 15 µL of Tween-20 1%v/v in PBS/T, 15 µL of polyvinylpyrrolidone (PVP) 2%v/v in PBS/T, 10 µL of undiluted biotin-mAb in PBS/T and 10 µL of streptavidin gold undiluted. A clear red band was seen, indicative of preservation of streptavidin function.

5.2.1.3 BIAcore Instrumentation and Zetasizer

BIAcore analysis was done using a BIAcore 2000 instrument from the Fraser Group, Department of Molecular Medicine, University of Auckland. The running buffer used was HBS-EP pH = 7.4 (see Appendix 1 for details). All samples were diluted in HBS-EP unless otherwise stated, except for the regeneration buffers, which were prepared using deionised water. All experiments were done at an incubation temperature of 25 °C and a flow rate of 20 µL/min unless otherwise stated. Between injections the flow cells were returned to running buffer as for all SPR experiments in this thesis. Flow rates quoted with the injections refer to the injection period unless otherwise stated. The term "quickinjection" refers to a BIAcore command that injects sample with only a 10 µL pre-injection plug. "Extraclean" refers to another BIAcore function that includes extra cleaning of the needle in the injection. A "wizard" is a computer program for running BIAcore applications. All mixing for assays and binding studies was done in microtitre

plates and the samples were run in random order. The chips used were BIAcore CM5 chips (research grade). The gold colloid particles were sized using a Malvern Zetasizer™ 3000HS with temperature set at 25 °C, a count rate of 260 kCps in a capillary cell with a detector angle of 90° and a wavelength of 633 nm. UV-visible spectra were obtained on a Shimadzu UV-1601 instrument and data processed using UV Probe 1.01 software.

5.2.1.4 Statistical Analysis

All error bars shown on graphs represent one standard deviation of the mean. All assay standard curve data has been fitted to a four-parameter logistic relationship using Sigma Plot 8.02 (SPSS Inc.). All limits of detection have been computed as the concentration corresponding to the blank or curve maximum less two standard deviations of the blank determination. The IC_{50} values have been computed as a parameter of the curve fitting. Standard deviations (SD) in the LOD and IC_{50} have been computed by inputting the standard deviation of a neighbouring standard point into the rearranged four-parameter logistic equation, calculating from the SD in the response. Sensitivities represent the slope of the linear portion of the assay curve. The enhancement ratios are calculated by dividing the slope of the enhanced antibody-binding concentration plot by the slope of the primary antibody concentration plot, or dividing the slope of the active range of the enhanced assay by that of the primary antibody-only assay where the two determinations are greatly different. Errors quoted in the text, including tables, are the standard error of the determination. Outliers have been rejected where they are more than three standard deviations from the mean of the remaining values. All difference comparisons of LOD and IC_{50} mentioned in the text have been examined by two-tailed unpaired *t*-test (or one-tailed where stated) and differences have been found to be statistically significant ($P \leq 0.04$). CVs mentioned in the text are the CVs of the binding responses.

5.2.2 Biotinylation of Antibody

Biotinamidocaproate-*N*-hydroxysuccinimide ester (BcapNHS) (Sigma Aldrich B-2643) was dissolved in dry DMF to make a 5 mg/mL solution. Monoclonal anti-progesterone (100 μL) was added to 0.1 M sodium bicarbonate solution (900 μL) and the BcapNHS solution was added (25 μL in 1 mL of 0.1 M sodium bicarbonate) dropwise to the stirring antibody solution. The solution was stirred for 5 min before leaving without stirring at room temperature for 2 h. The solution was then dialysed against 0.15 M NaCl at 4 °C for four changes including one overnight and then four changes of PBS/T including one overnight. The solution was then passed through a PD-10 column and protein concentration determined by assumption of negligible loss of antibody, as the 2-bincinchonic acid (BCA) method of protein concentration determination was found to be unreliable due to the effects of modifying the antibody with biotin and thus changing the numbers of free lysine residues used in the determination. Antibody was stored frozen until use and once thawed was not refrozen.

5.2.3 Progesterone-Protein Conjugates as Coating Antigens in Biotin-Streptavidin Mediated Gold Labelled SPR

5.2.3.1 Immobilisation

pH scouting was done to determine the best pH for immobilisation of the **C-2** and **C-4** conjugates to the sensor chip. The conjugates are as described in Chapter 2 (11 and 25-atom linkers for **C-2** and **C-4** respectively). The conjugates were prepared at 500 μg/mL and 1.125 mg/mL respectively. For **C-2**, pH of 4, 4.5 and 3.5 10 mM sodium formate were trialed. Flow-rates were 5 μL/min for 2 min.

Immobilisation was done manually aiming for a minimum immobilisation of 2000 RU. **C-2** was immobilised at pH 3.5 and **C-4** at pH 4.0. Flow rates were 5 μL/min and final immobilisations obtained were 2523.9 RU for **C-2** and 2207.7 RU for **C-4**. The chip had a solution of OVA (5 μg/mL in running buffer) passed over the surface to help to stabilise it (10 min at 25 μL/min).

5.2.3.2 Antibody Binding Tests

Monoclonal anti-progesterone (un-modified) was passed over the surface to assess its binding (100 μg/mL in running buffer, 3 min injection, 20 μL/min) and the surface then regenerated with 50 mM glycine pH = 1.5 (2 x 75 μL, 50 μL/min). Biotinylated monoclonal anti-progesterone was then passed over the surface (100 μg/mL in running buffer, 3 min injection at 20 μL/min) and regenerated. Biotinylated monoclonal antibody (100 μg/mL in running buffer, 100 μL) was mixed 1:1 with undiluted 10 nm colloidal gold – streptavidin conjugate and vortex mixed and then incubated at room temperature for 10 min before injection (120 μL, 20 μL/min). The same regeneration conditions were used for all protein conjugate binding work.

To determine the best antibody / gold volume ratio to use for assay development, various ratios were employed and their binding values determined. The biotinylated monoclonal anti-progesterone was set at a concentration of 100 μg/mL. The total mix volume was set at 160 μL to allow for the 120 μL injection plus the 30 μL dead volume. The 10 nm gold colloid – streptavidin was used without prior dilution and the incubation was for 35 min at room temperature with one 5 s vortex mix at the start. The ratios tested were 1:1 (80 μL mAb: 80 μL gold), 1.67:1 (100 μL: 60μL), 3:1 (120 μL: 40 μL), 7:1 (140 μL: 20μL) and 15:1 (150 μL: 10 μL). The same testing was then done but with running buffer instead of gold colloid to determine the degree of gold signal enhancement at each ratio.

5.2.3.3 Progesterone Assay Curves

The progesterone assay curve was determined by mixing 100 μL of progesterone stock solution in running buffer with 100 μL of 7:1 mAb (100 μg/mL): 10 nm gold colloid – streptavidin, incubating at room temperature for 5 min and then injecting at 10 μL/min, 120 μL, with regeneration as above. The antibody gold mixture was incubated at room temperature for 3 h before the assay began to ensure complete biotin-streptavidin binding. Progesterone concentrations of 0, 100 fg/mL, 1 pg/mL, 10 pg/mL, 100 pg/mL, 1 ng/mL, 10 ng/mL, 100 ng/mL and 1 μg/mL were used (in running buffer). Assay curves

were determined for both **C-2** and **C-4** conjugates and each point was done in triplicate.

5.2.3.4 20 nm Gold Colloid

Biotinylated monoclonal antibody (100 µL, 100 µg/mL in running buffer) was mixed with 20 nm gold – streptavidin colloid (undiluted, 100 µL) and vortex mixed and then incubated at room temperature for 10 min before injection (120 µL, 20 µL/min). The incubation time was then extended to 35 min and the experiment repeated.

Monoclonal antibody – biotin was passed over the surface (100 µg/mL, 20 µL/min for 3 min) immediately followed (in co-injection mode) by the 20 nm gold-streptavidin (20 µL/min, 3 min).

To determine the most appropriate antibody / gold ratio to use for development of the assay, different ratios were trialed. The ratios were 2:1 antibody: gold, 1:1 antibody: gold, 1:2 antibody: gold and 5:1 antibody: gold. These were done by co-injecting 80, 60, 40 and 100 µL of biotinylated antibody with 40, 60, 80 and 20 µL of gold colloid respectively (20 µL/min, 6 min) in a sequential format. It was not necessary to run separate antibody blanks as the antibody binding could be clearly seen in the sensorgrams separate from the gold enhancement.

5.2.4 Progesterone-OEG-Biotin and Immobilised Antibody[1]

5.2.4.1 **N-*(13-(t-butoxycarbonylamino)-4,7,10-trioxatridecanyl)-3-(pregn-4-ene-3,20-dione-4-yl)thiopropanamide* (1)**

2,5-Dioxo-1-pyrrolidinyl-3-(pregn-4-ene-3,20-dione-4-yl)thiopropanoate (1.106 g, 2.14 mmol)[10,15] was dissolved in DMF (dry, 5 mL) and *N*-(*t*-butoxycarbonyl)-4,7,10-trioxa-1,13-tridecanediamine (1.371 g, 4.27 mmol) was added drop-wise to the stirring steroid solution. Triethylamine (2 mL) was then added and the solution stirred for 60 h in the dark. The solvent was removed in vacuo and the mixture column-separated on silica gel using 15:1 $CHCl_3$: MeOH

[1] See p. 222 for reaction scheme

eluant to yield **3** as a yellow oil. Yield: 63% (967 mg, 1.341 mmol). TLC R_f = 0.36 (15:1 $CHCl_3$: MeOH). IR (film): 2932 (CH_2 anti-symmetric υ), 1699 (Boc amide C=O υ), 1532 (Boc amide), 1117 (CH_2-O υ) cm^{-1}. ^1H NMR ($CDCl_3$) δ: 0.65 (s, 3H, 18-CH_3), 1.13 (s, 3H, 19-CH_3), 1.41 (s, 9H, Boc CH_3), 2.09 (s, 3H, 21-CH_3), 2.89 (m, 6H, OEG), 3.57 (m, 14H, OEG, CH_2-O). ^{13}C NMR ($CDCl_3$ + CD_3OD) δ: 13.7 (18-CH_3), 18.4 (19-CH_3), 21.5 (11-CH_2), 23.2 (16-CH_2), 24.6 (15-CH_2), 28.8 (Boc CH_3), 29.4 (21-CH_3), 29.6 (C-6), 30.0 (CH_2 OEG chain), 30.9 (CH_2 OEG chain), 31.0 (C-2), 31.7 (C-7), 34.3 (CH_2-S), 34.7 (**C**H_2-CO), 34.9 (C-1), 35.6 (C-8), 37.0 (CH_2N steroid end, C-12), 39.1 (CH_2-NH Boc end), 41.7 (C-10), 44.2 (C-13), 54.5 (C-9), 56.3 (C-14), 63.7 (C-17), 69.8 (OEG CH_2-O), 70.0 (OEG CH_2-O), 70.5 (OEG CH_2-O), 70.9 (OEG CH_2-O), 79 (**C**Me_3) 129.0 (4-C), 156.3 (ester C=O), 171.4 (5-C), 176.2 (C=O), 195.7 (3-C), 209.5 (20-C). ES-MS *m/z* (MeOH) 721.6 $[M+H]^+$, 743.6 $[M+Na]^+$. HiRes FAB-MS: Calculated: 721.4462, Found: 721.4473 (MH^+).

5.2.4.2 (13-Amino-4,7,10-trioxatridecanyl)-3-(pregn-4-ene-3,20-dione-4-yl)thiopropanamide (2)

1 (140 mg, 0.193 mmol) was dissolved in formic acid (8 mL) and stirred in the dark for 3 h. Formic acid was removed in vacuo to leave an oil, which was then column separated on silica gel using 15:1 $CHCl_3$: MeOH. Yield: 73% (94 mg, 0.152 mmol). TLC R_f = 0.29 (5:1 $CHCl_3$: MeOH). IR (film) 2960 (-NH_3^+ υ), 2920 (CH_2 anti-symmetric υ), 1670 (progesterone C=O υ), 1640 (progesterone C=O υ), 1116 (CH_2O υ) cm^{-1}. ^1H NMR ($CDCl_3$) δ: 0.68 (s, 3H, 18-CH_3), 1.26 (s, 3H, 19-CH_3), 2.12 (s, 3H, 21-CH_3), 2.48 (t, 2H, CH_2-CO, *J* = 6.7 Hz), 2.52 (3H, m, OEG), 2.85 (t, 2H, CH_2-S, *J* = 6.8 Hz), 3.26 (2H, t, *J* = 5.0 Hz), 3.35 (2H, t, *J* = 6.1 Hz), 3.48-3.66 (11H, m, OEG CH_2-O), 3.71 (1H, m, 6α-H), 3.73 (2H, t, OEG, *J* = 5.2 Hz). ^{13}C NMR ($CDCl_3$) δ: 13.4 (18-CH_3), 18.1 (19-CH_3), 21.2 (11-C), 23.0 (16-C), 24.3 (15-C), 26.2 (C-6), 29.3 (21-CH_3), 29.7 (CH_2 OEG chain), 31.0 (CH_2 OEG chain), 31.5 (2-C), 32.1 (7-C), 34.4 (CH_2-S), 34.5 (**C**H_2CO, C-1), 35.3 (C-8), 36.6 (CH_2-NH steroid end, C-12), 38.7 (CH_2-NH_2), 40.3 (10-C), 43.9 (13-C), 54.1 (9-C), 55.9 (14-C), 63.5 (17-C), 68.8 (OEG CH_2-O), 69.7 (OEG CH_2-O), 70.5 (OEG CH_2-O), 171.9 (amide C=O), 176.9 (5-C), 196.4 (3-C), 209.2 (20-C).

ES-MS *m/z* (MeOH) 621.8 $[M+H]^+$. Purity: 97% (R_t = 1.20 min, 60: 40 MeOH: H_2O, λ_{max} = 248 nm).

5.2.4.3 1-(3-(Pregn-4-ene-3,20-dione-4-yl)thiopropanoyl)amino) 4, 7, 10-trioxa-13-tridecane-13-amino-biotinylate (3)

2 (160 mg, 0.258 mmol) was dissolved in chloroform (1.5 mL, dried over molecular sieves 4A). Biotin-*N*-hydroxysuccinimide (114 mg, in 1 mL of dry DMF with warming) was added drop-wise to the stirring progesterone – OEG – NH_2 solution. The solution was stirred in the dark for 2 h before addition of triethylamine (0.5 mL) after which it was left stirring for 60 h. A solid initially formed but by the end of the reaction it had gone. The solvent was removed in vacuo and then column-separated using 10 : 1 $CHCl_3$: MeOH then 5 : 1 $CHCl_3$: MeOH eluant. Yield: 44% (96 mg, 0.113 mmol). TLC R_f = 0.70 (5: 1 $CHCl_3$: MeOH). IR (film): 1120 (CH_2O υ), 1672 (amide C=O υ), 2929 (CH_2 anti-symmetric υ) cm^{-1}. ^1H NMR ($CDCl_3$) δ: 0.70 (s, 3H, 18-CH_3), 1.25 (s, 3H, 19-CH_3), 1.72 (m, caproate chain), 1.80 (m, caproate chain), 2.14 (s, 3H, 21-CH_3), 2.95 (m, 5H, OEG), 3.20 (d, 1H, biotin HC**H**-S), 3.37 (m, 2H, OEG), 3.62 (m, 13H, OEG), 4.36 and 4.54 (d of t, 2H, biotin, CH-NH), 5.16 and 5.23 (d, 1H, biotin). ^{13}C NMR ($CDCl_3$) δ: 13.7 (18-CH_3), 18.5 (19-CH_3), 21.5 (C-11), 23.3 (15-CH_2), 24.6 (16-CH_2), 25.3 (CH_2 biotin chain), 25.7 (CH_2 biotin chain), 25.9 (C-6), 28.4 (OEG chain CH_2), 29.3 (OEG chain CH_2), 29.5 (C-2), 31.1 (C-7), 31.8 (S-CH_2), 34.3 (**C**H_2CO), 35.7 (C-8), 36.3 (1-CH_2, **C**H_2CO), 37.1 (C-10), 38.3 (CH_2-NH), 39.0 (CH_2-NH), 40.9 (12-CH_2), 41.7 (CH_2-S biotin), 44.3 (C-13), 54.5 (9-CH/ biotin), 56.3 (14-CH), 60.5 (biotin-ring C-N), 63.8 (17-CH), 70.4 (OEG-CH_2-O), 70.9 (OEG CH_2-O), 129.1 (4-C), 163.7 (biotin C=O), 172 (C=ON biotin end), 173.4 (C=ON steroid end), 176 (5-C), 196 (3 C=O), 209.6 (18 C=O). ES-MS *m/z* (MeOH 80 V): 848.1 $[M+H]^+$, 870.1 $[M+Na]^+$.

5.2.4.4 Format Development for Progesterone-OEG-Biotin

Monoclonal anti-progesterone was immobilised onto flow cell two of a fresh chip with activation as before and using a 35 μL injection of monoclonal antibody

(100 μg/mL) at 5 μL/min flow rate followed by de-activation as before. The immobilisation buffer used was determined by preconcentration using a 2 min injection of 40 μL of monoclonal antibody (100 μg/mL in 10 mM sodium acetate pH = 5.5). Immobilisation of 7475 RU was achieved at the pH 5.5. Flow cell one was used as the blank control flow cell as before.

Rather than use a 100 μg/mL solution which would contain 1%v/v DMF and thus may damage the antibody, **3** was made up to 5 mg/mL in deionised water and diluted one fifth to make a 1 mg/mL solution which was then used to incubate with the gold as above (35 min incubation at room temperature and using a 1:1 volume ratio) and was then injected (120 μL, 10 μL/min). The volume ratio was then changed to 7:1 and all other conditions kept the same. Regeneration was attempted with one pulse of 10 mM glycine (pH 2).

An alternative format was then trialed where the progesterone-biotin (1 mg/mL) was injected (240 μL at 20 μL/min). This was then immediately followed by a quickinjection of the 10 nm gold (60 μL at 10 μL/min). Regeneration was then attempted with two pulses of 75 μL of 10 mM glycine pH = 2 to regenerate the surface. This process was repeated again to test the repeatability of the binding response.

Flow cell 3 was then immobilised with antibody as before giving a final immobilisation value of 3375.5 RU. The following tests were then conducted:

1. 10 nm gold colloid was pre-mixed with 100 μg/mL progesterone-OEG-biotin for 35 min in a 7:1 progesterone-OEG-biotin: gold volume ratio. 60 μL was then injected at 10 μL/min.
2. As for 1 but using 20 nm colloid. The binding response was 10.9 RU indicating that some binding is occurring. Regeneration with 2x 10 mM glycine (pH 2) as before.
3. Sequential injection of progesterone-OEG-biotin (250 μg/mL, 60 μL) gave 0.3 RU bound (10 μL/min) followed immediately by 20 nm gold (30 μL, 10 μL/min). Regeneration as for 2.
4. Premixed 500 μg/mL progesterone-OEG-biotin and 20 nm gold at a 7:1 progesterone-OEG-biotin: gold volume ratio for 35 min and then injected 60 μL at 10 μL/min.

5. Premixed 500 μg/mL progesterone-OEG-biotin and 10 nm gold 7:1 progesterone-OEG-biotin: gold volume ratio, 35 min incubation and then injected 60 μL.

Flow cell four was immobilised with antibody as before to a final immobilisation figure of 6605 RU and the following injections performed:

1. 10 nm gold and 500 μg/mL progesterone-biotin in 7:1 ratio as before – 60 μL injection as before. No binding response was observed. No regeneration attempted.
2. 20 nm gold and 500 μg/mL progesterone-biotin in 7:1 – 60 μL injection. Flow cell 4 (Fc4) = 460.9 RU, flow cell 3 (Fc3) = 70.1 RU, flow cell 2 (Fc2) = 76.1 RU. Regeneration as above.
3. An exact repeat of 2 but with a fresh batch of mixture. The bindings were: Fc4 = 248.9 RU, Fc3 = 30.6 RU, Fc2= 40.1 RU. Regeneration as above.

5.2.5 Progesterone-OEG-NH_2 Mediated Assay – An Ultra-Stable Surface

5.2.5.1 Immobilisation

A solution of **2** was made up in DMF (100 mg/mL). The stock was diluted in PBS/T pH = 9.0 to make a 1 mg/mL solution (1%v/v DMF). A new CM5 chip had flow cell two (Fc2) activated with EDC and NHS (150 μL of each transferred to a vial and then 200 μL mixed and 50 μL injected at 5 μL/min). The **2** solution was then quickinjected (5 μL/min, 100 μL). The surface was then deactivated with ethanolamine (50 μL, 5 μL/min). Flow cell one (Fc1) was activated and deactivated without injection of **2**, as a blank flow cell. The surfaces were then washed with three pulses of 50 mM NaOH (15 μL at 5 μL/min). The washes removed surface material that was not covalently bound. The first pulse removed 211.7 RU, the second 53.1 RU and the third 26.8 RU in Fc2. Flow cell three (Fc3) was also later immobilised as for Fc2 but with about 1.5x the immobilised RU value, and used with Fc2 from section 5.2.6 onwards.

5.2.5.2 Antibody / Gold Ratio Testing

These data were obtained by using the given volume ratio of antibody (100 μg/mL): gold and mixing 1:1 with blank buffer as for the progesterone assay in 5.2.5.3 (using the same wizard). The same applied for the gold only injections mentioned in Section 5.3.4.2. The zero point of the ratio curve was obtained by injecting straight buffer.

5.2.5.3 Aqueous Progesterone Assay Using Biotin / Streptavidin-Mediated 10 nm Gold Labelling

An assay for aqueous progesterone was set up using a wizard which mixed progesterone standard solutions with a pre-incubated (2 h) mixture of 7:1 biotinylated antibody (100 μg/mL): 10 nm gold – streptavidin, in a 1:1 ratio. The components were mixed, incubated for 5 min and then injected (60 μL at 20 μL/min). A 60 s wait was introduced before regeneration with two pulses of 20 μL of 10%v/v MeCN in 50 mM NaOH. The flow rate throughout was 20 μL/min. Five replicates were done of each point. The wizard file is in Appendix 3.

5.2.5.4 Antibody-Only Assay Using The Progesterone – OEG – NH_2 Surface

The program was exactly as for the pre-incubation assay in 5.2.5.3 with biotinylated antibody at a final injection concentration of 43.75 μg/mL (no gold label). Standards of 0, 1 pg/mL, 10 pg/mL, 100 pg/mL, 200 pg/mL, 1 ng/mL, 2 ng/mL, 10 ng/mL, 100 ng/mL and 1 μg/mL were used. Five replicates of each were run.

5.2.5.5 20 nm Pre-incubation Assay

Assay conditions were exactly as for the 10 nm pre-incubation assay in 5.2.5.3 but with 20 nm colloid and 0.84 M ethylene glycol used in the antibody diluent to give a final ethylene glycol concentration of 0.2 M.

5.2.6 Sequential Binding Assay Format

5.2.6.1 Gold Dilution Binding Test

The method for the determination of the relationship between total gold enhanced response and 10 nm gold colloid dilution factor was as follows. Buffer was run at 20 μL/min (same flow rate throughout), and monoclonal anti-progesterone-biotin labelled was quickinjected (50 μg/mL, 60 μL) and binding response determined. The baseline was taken 60 s before antibody injection and the antibody bound point was taken 10 s before quickinjection of gold-streptavidin colloid (30 μL). There was no wait time between quickinjections. The gold quickinjection was finished with an extraclean and a wait of 180 s before quickinjection of three pulses of 20 μL of 20%v/v MeCN 200 mM NaOH total concentration. The final quickinjection had an extraclean and the cycle was then repeated. These conditions of injection are the same as in the corresponding assay (Section 5.2.6.3). This process was repeated for a total of five replicates of each of 0.25, 0.15, 0.10, 0.05, 0.02, 0.01 dilution of gold in HBS-EP (0.2 M ethylene glycol, 10%w/v BSA).

5.2.6.2 Antibody Binding Curve Determination

The antibody binding curve wizard program was set up as follows. Flow rate set at 20 μL/min throughout. The antibody solution (60 μL) was quickinjected followed immediately by the gold (0.15 dilution, 10%w/v BSA total concentration, 0.2 M ethylene glycol total concentration, 30 μL) also quickinjected. There was a wait of 180 s then injection of three 20 μL pulses of 20%v/v MeCN 200 mM NaOH total concentration, one after the other. Antibody concentrations of 0, 5, 10, 15, 25, 35 and 50 μg/mL were used with five replicates per point.

5.2.6.3 Progesterone Sequential Assay

An assay for aqueous progesterone was established that used the following format. 70 μL of biotinylated antibody (30 μg/mL) was transferred to an empty

microtitre plate well. 70 μL of progesterone standard was then transferred to the same well, and the contents mixed (105 μL). The contents were then incubated at 25 °C for 5 min before injecting 60 μL at 20 μL/min flow rate (flow rate the same throughout). Immediately after this injection, 30 μL of gold colloid (0.15 dilution, 10%w/v BSA total concentration, 0.2 M ethylene glycol total concentration) was quickinjected. There was then a wait of 3 min before regeneration by three pulses of 20 μL of 20%v/v MeCN, 200 mM NaOH total concentration. There was then a further wait of 1 min before the next cycle. Ten progesterone concentrations were used: 0, 10 fg/mL, 1 pg/mL, 10 pg/mL, 100 pg/mL, 500 pg/mL, 1 ng/mL, 10 ng/mL, 100 ng/mL and 1 μg/mL. Each point was done with five replicates. The mixings were done in a microtitre plate as for the pre-incubated assay format.

For Section 5.2.6 all injections were quickinjects except for the antibody/progesterone mixes used in the final assay format. The delay between antibody and gold injections when both were quickinjects is 70 s compared to 80 s if the antibody was injected normally and the gold in a quickinject. Quickinject was used to save valuable material but a normal inject was used for all the assay progesterone / antibody injections as this was likely to produce more repeatable antibody bindings and thus lower CV than quickinject.

5.2.6.4 A New Progesterone Sequential Assay

A new assay was set up exactly as before except for these changes:

1. Monoclonal antibody concentration was reduced to 15 μg/mL (diluted 1:1 with progesterone solution to give a final concentration of 7.5 μg/mL)
2. The 60 s wait after regeneration was removed to speed up the assay
3. The progesterone concentrations used were 0, 100 fg/mL, 1, 10, 20, 100, 200 pg/mL, 1, 10, 100 ng/mL.

5.2.7 Antibody Binding Tests and Non-specific Binding Treatments for the Sequential Injection Format

5.2.7.1 Optimisation of the Non-Specific Binding Treatment

In order to determine whether reduction of the gold labelling flow rate would produce additional gold label binding, a test was set up with the same format as for the sequential antibody binding assay but with the gold flow rate set to 10 μL/min rather than 20 μL/min and the antibody was set at 50 μg/mL and blank running buffer used in the place of progesterone solution. The gold was 0.15 dilution in HBS-EP with 5%v/v total PEG-400 and 0.2 M total ethylene glycol.

30 μL of the gold alone was injected over the surface at 10 μL/min flow rate (treatment as above) and the surface was regenerated as before. The gold injection was repeated but at 20 μL/min flow rate. The gold was prepared as above but with 10%v/v PEG-400 and 30 μL injected. Gold with 1%v/v PEG-400 treatment was injected (30 μL) after regeneration as before. Regeneration was followed by injection of the gold with a 0.1%v/v PEG-400 loading. After regeneration, a 0.5%v/v loading was tried.

To test to see if the slope of the antibody curve would be improved by reducing the PEG-400 loading, the biotinylated antibody (50 μg/mL) was used in an assay using the blank with gold at a 0.15 dilution in 1%v/v PEG-400, 0.2 M total EG. This was also then repeated for a 0.5%v/v total PEG-400 loading using regenerations as above.

5.2.7.2 Antibody Binding Test with Reduced Non-Specific Binding

A new antibody-binding test was then set up to determine the binding response *vs* antibody concentration relationship using the new non-specific binding minimisation treatment. The format was exactly the same as for the previous study (5.2.6.2) but with use of a 1%v/v PEG-400, 0.2 M EG treatment for the gold colloid and a 60 s wait at the end of the assay cycle to ensure return to baseline. Five replicates were done at concentrations of 0, 1, 5, 15, 25, 35, 50 μg/mL.

5.2.7.3 Gold Loading – Is it Optimal?

30 µL of 0.25 dilution gold with the same 1%v/v PEG-400 treatment and 0.2 M total EG was injected. An antibody-binding test was run using the same antibody-binding wizard as in 5.2.7.2 with 50 µg/mL antibody and 0.25 dilution of gold.

To assess whether simply increasing the volume of gold label used would improve the binding enhancement, an antibody gold-enhanced assay was attempted using a 60 µL injection of the 0.15 dilution with all other factors the same as 5.2.7.2 with 50 µg/mL mAb-biotin concentration, flow rate 20 µL/min throughout.

To see if increasing the incubation time of progesterone solution with antibody would improve the ability of the assay to discriminate low progesterone concentrations, 100 pg/mL determinations were set up using 0.15 dilution gold (1%v/v PEG-400, 0.2 M EG total) 30 µL, all 20 µL/min, but one with a 600 s wait and one with a 300 s wait, antibody at 15 µg/mL.

5.2.7.4 Gold-Enhanced Assay – Low Antibody

A new progesterone assay was set up using the 0.15 dilution gold with the new treatment, other conditions the same as the previous assay (Section 5.2.6.4) but using a biotinylated antibody concentration of 5 µg/mL (diluted by progesterone solution to 2.5 µg/mL). Five replicates were run of each of 0, 0.1, 1, 5, 10, 50, 100 pg/mL, 1, 10, 100 ng/mL progesterone.

5.2.7.5 Is the Gold Enhancement Mediated Through the Biotin / Streptavidin Couple?

Five replicate injections of the monoclonal un-modified antibody in the antibody-binding wizard of 5.2.7.2 were done *vs* five replicates of the biotinylated antibody, both at 50 µg/mL concentration.

5.2.7.6 Gold Level / Response Relationship with Use of PEG-400

This was repeated exactly as before (Section 5.2.6.1) except using the 1%v/v PEG-400, 0.2 M EG gold treatment and with 15 μg/mL of mAb-biotin (60 μL).

5.2.7.7 Attempts to Remove Non-specific Binding of the Antibody

In an attempt to remove mAb non-specific binding from the surface, the mAb-biotin was made up at 5 μg/mL using HBS-EP but with 1%v/v total PEG-400. This was then incubated with the 100 ng/mL progesterone solution as before (5 min) and then injected (60 μL at 20 μL /min). The process was repeated with 1%w/v BSA total instead of 1%v/v PEG-400. The surface was regenerated as before and then the process repeated with 5%v/v PEG-400. The process was repeated with 1%v/v PEG-400 and 1 μg/mL progesterone. The injection was repeated using 100 ng/mL progesterone and no PEG agent.

To check to see if the non-specific binding may be due to progesterone binding or simply driftings in the baseline, progesterone (1 μg/mL, 30 μL) was injected. All regenerations were done as before.

5.2.7.8 Another Low Monoclonal Antibody Assay

The assay was repeated using 15 μg/mL mAb-biotin 1: 1 with progesterone using a narrower range of concentrations (0, 5, 20, 50, 100, 200, 500 pg/mL, 1, 5, 50 ng/mL) to allow better determination of the standard curve. The gold used was prepared at 0.15 dilution using 1%v/v PEG-400 and 0.2 M EG.

5.2.7.9 20 nm Colloid Sequential Binding – Will the larger colloid substantially improve enhancement?

The antibody binding test wizard from 5.2.7.2 was run as before with 1 x 50 μg/mL biotinylated antibody and 20 nm gold at a 0.5 dilution with 1%v/v PEG-400 total and 0.2 M EG total. Regeneration was attempted (3 pulses of 20 μL of

20%v/v MeCN, 200 mM NaOH). Then 10%v/v MeCN, 50 mM NaOH (70 µL, 50 µL/min) was used. This injection was repeated. An injection of 75 µL (50 µL/min) of 50 mM glycine pH = 3 was made. This was followed by injection of 20%v/v MeCN, 200 mM NaOH total (75 µL, 50 µL/min).

The antibody injection wizard was repeated with a 60 µL injection of 20 nm colloid, all other factors the same as above. The surface was then injected with 20 nm colloid, (1%v/v PEG-400 total, 0.2 M EG total, 30 µL, 0.5 dilution). The first 30 µL gold-antibody injection was repeated after first regenerating the surface with 20%v/v MeCN, 200 mM NaOH (3 x 20 µL) as before using 20 nm gold from a different vial.

To see if steric hindrance could be minimised by lowering the binding concentration of colloid, the dilution was changed to 0.25 (1%v/v PEG-400 total, 0.2 M EG total, 120 µL instead of 60 µL, 20 µL/min). A 15 µL injection of un-diluted 20 nm gold was used as label (20 µL/min), all the rest being the same as the previous test. This was then followed by a check for non-specific binding whereby un-diluted 20 nm colloid was injected (15 µL, 20 µL/min). This process was repeated with 10 nm colloid (0.30 dilution, 1%v/v PEG-400 total, 0.2 M EG total).

5.2.8 Secondary Antibody Labelling

5.2.8.1 The Secondary Antibody Labelling Effect

Secondary antibody enhancement curves were prepared by quickinjecting monoclonal primary antibody (25 µg/mL, 60 µL, 20 µL/min) immediately followed by quickinject of anti-rat IgG secondary antibody (60 µL, 10 µL/min) and then regeneration with one pulse of 20%v/v MeCN, 200 mM NaOH (20 µL, 20 µL/min). Secondary antibody concentrations of 0, 50, 100, 200, 400, 600, 800 µg/mL were used, five replicates each.

5.2.8.2 Secondary Antibody Signal Enhancement of Primary Antibody Binding

Primary antibody binding curves were produced as for section 5.2.8.1 but with secondary antibody concentration held constant at 800 μg/mL and varying the primary antibody concentration using 0, 0.75, 1.5, 3, 6.25, 12.5, 18.75, 25 μg/mL concentrations.

5.2.8.3 Progesterone Assay Using Secondary Antibody Signal Enhancement

The assay was set up using the normal 70 + 70 μL and mix and 5 min incubation method. The primary antibody / progesterone mixture was injected as before (60 μL, 20 μL/min) and then immediately injected anti-rat IgG (60 μL, 10 μL/min, 800 μg/mL) then a 30 s wait and regeneration as for all the above tests (20 μL of 20%v/v MeCN, 200 mM NaOH, 20 μL/min). The progesterone concentrations used were: 0, 0.1, 1, 5, 10, 50, 100 pg/mL, 1, 10, 50 ng/mL. The final primary antibody concentration after 1:1 dilution with progesterone sample was 25 μg/mL. The wizard program is given in Appendix 3.

Another assay was set up as for the preceding assay but with primary antibody at 3 μg/mL final concentration and anti-rat IgG at 400 μg/mL and using progesterone standards prepared by serial dilution at 0, 1, 10, 25, 50, 100 pg/mL, 1, 2.5, 10 ng/mL.

5.2.9 Secondary Antibody-Gold Signal Enhancement

5.2.9.1 Colloid Production and Sizing

Gold colloids were produced by an adaptation of the citrate reduction method of Frens.[266] Specifically, the colloids were prepared as follows:

25 nm: A 0.01%w/v solution of $HAuCl_4$ was prepared (50 mL) and brought to the boil under reflux with no stirring. A 1%w/v tri-sodium citrate solution was added (900 μL) and the colour monitored. Boiling was sustained for 10 min before cooling.

43 nm: Prepared by citrate reduction as for 25 nm at the same scale but with 600 μL of the 1%w/w trisodium citrate and 10 min boiling.

56 nm: A 0.01%w/v solution of $HAuCl_4.3H_2O$ was prepared (50 mL) and brought to the boil with no stirring. A 1%w/v tri-sodium citrate solution was added (500 μL) and the colour monitored. After ~40 s the solution went blue and then a further 1 min to turn red. The boiling was sustained for a total of 10 min before cooling.

70 nm: As for the 41 nm method but using stirring (vigorous, maximum setting) and adding 300 μL of 1%w/v tri-sodium citrate solution. The solution turned black after 49 s and went red at 170 s. The boiling was sustained for 14 min total before cooling. It was found for this colloid that not stirring the solution resulted in too broad a particle distribution.

120 nm: As for the 56 nm method but using reflux conditions and using a 0.01%w/v solution of $HAuCl_4$ (50 mL) and then adding 250 μL of 1%w/v tri-sodium citrate solution and refluxing for 17 min only.

The exact citrate volumes often had to be adjusted slightly based on sizing results. Once cooled to room temperature, the volumes of each were determined and from this the total gold concentration could be calculated. All glassware was washed with aqua regia before use.

Each colloid was examined by the Malvern Zetasizer to determine the average colloid diameter and the diameter distribution by photon correlation spectroscopy. Five runs, each of 10 sub-runs, were completed for each colloid and the Z_{avg} (cumulant mean diameter) parameter used to determine colloid diameter for colloids below 30 nm and the intensity function used to determine colloid diameter for larger colloids. All colloids were either used as is or were centrifugally concentrated as indicated for each experiment. Centrifugal concentration was done with PEG-400 (3%v/v) to prevent aggregation.

5.2.9.2 Optimisation of Gold-Secondary Antibody Conjugate Production

Each of the colloid parameters mentioned in the results section was systematically studied to determine the effects on secondary antibody-gold binding to the surface. Regeneration was as before. Decisions on parameters to

use for colloid-conjugate production were made on the basis of the binding responses obtained and any non-specific bindings obtained. The large number of individual binding tests makes full experimental details space prohibitive.

5.2.9.3 Signal Enhancement with Secondary Antibody-Gold Conjugate by Removing Un-Bound Secondary Antibody

The 25 nm gold-secondary antibody conjugate was prepared as follows. 25 nm gold sol was prepared according to the directions in Section 5.2.9.1 and sized accordingly. The pH of the colloid was adjusted to 8.6, and 10 mL vortex shaken and 1 mL of 900 μg/ mL anti-rat IgG was injected with vortex shaking for 60 s and then shaking at 400 rpm for 10 min. The colloid was then stored at 4 °C for 18.5 h and then BSA (10%w/v, 3.66 mL) was injected while vortex shaking. The sample was vortex shaken for 60 s and then shaken at 400 rpm for 10 min and the sample stored at 4 °C for 3.5 h before centrifuging at 13,000xg for 30 min. The supernatant was removed (Pasteur pipette) and the sample constituted in ½ the volume and sonicated and centrifuged again before supernatant removal and re-constitution to give a 3x concentrated sample relative to the raw reaction mixture.

The binding procedure was done by injection of mAb (60 μL, 20 μL/min), followed immediately by anti-rat IgG-gold 25 nm (60 μL, 10 μL/min, 0.5 dilution, 10%v/v PEG-400), 180 s wait, then regeneration by 1x pulse (20%v/v MeCN, 0.2 M NaOH 20 μL at 20 μL/min). The mAb concentrations used were 0, 0.25, 0.5, 1, 2, and 3 μg/mL, five replicates of each.

5.2.9.4 Signal Enhancement by Secondary Antibody – Gold Conjugate Without Removing Un-bound Secondary Antibody

Gold colloids were produced according to the methods detailed in Section 5.2.9.1 and sized accordingly. Five-fold concentrated gold sols were prepared and conjugated by altering the pH of the sol to 8.5 with dilute NaOH and adding anti-rat IgG secondary antibody (8 mg/mL) in deionised water (pH = 8.5), at 10%v/v to the colloid with vortex agitation. The colloid was then shaken for 5 min at 400 rpm before storage at 4 °C for 18.5 h and then blocking with 20%w/v bovine

serum albumin (BSA) (1%v/v of BSA solution in the colloid making 0.2%w/v final BSA) using the same conditions as for the antibody.

All the colloid sizes produced at both concentrated and non-concentrated levels were run (injected primary antibody 25 μg/mL, 60 μL, 20 μL/min and then immediately gold conjugate undiluted, 60 μL, 10 μL/min) for a minimum of three replicates to determine if there was any difference between colloid sizes and if concentration of the colloid produced a change in binding enhancement. Regeneration was as before.

Primary antibody binding plots were prepared by injecting primary antibody (60 μL, 20 μL/min) and then immediately injecting 25 nm gold-secondary antibody conjugate (0.5 dilution in deionised water 10%v/v PEG-400, 60 μL, 10 μL/min), 180 s wait and then regeneration as above with one pulse. All points were in triplicate and primary antibody concentrations used were 0, 1, 2, 5, 10, 15, 25 μg/mL.

5.2.9.5 Assay Using 25nm Sol-Secondary Antibody Without Centrifugal Purification

The assay was constructed by mixing of primary antibody (3 μg/mL) 1:1 with progesterone solutions in microwells, 5 min incubation at 25 °C and then injection (60 μL, 20 μL/min) immediately followed by secondary antibody – gold 25 nm conjugate (0.5 dilution in deionised water 1%v/v PEG-400, 60 μL, 20 μL/min) and then regeneration with two pulses as above. The progesterone concentrations used were 0, 10, 50, 100 pg/mL, 1, 10 ng/mL. All points were in triplicate.

5.3 Results and Discussion

5.3.1 Biotinylation of Monoclonal Anti-Progesterone

To attach signal-enhancing gold nanoparticle labels to the primary antibody, two different coupling methods were investigated. The first involved the binding of streptavidin-conjugated gold to biotinylated primary antibody. The streptavidin/biotin interaction is very strong and so this linkage should be quite stable, allow good capture binding in flow-through formats, and through the bulk

of the streptavidin and the introduction of a linker between the biotin and the antibody, allow sufficient steric spacing of the antibody from the gold nanoparticle surface.

The biotinylation of the anti-progesterone monoclonal antibody proceeded by an established method that allows for attachment of the biotin via the NHS active ester technique. The biotin was spaced from the antibody by a short 6-carbon caproate chain that ultimately links to the lysine residues of the antibody. Binding tests of this antibody compared to un-modified monoclonal antibody in the BIAcore format revealed that the biotinylated antibody retained $\geq$ 85% of the original antibody binding capacity. The concentration of the biotinylated antibody must be determined by assuming no loss of material upon purification, which is a reasonable approximation as the antibody was handled carefully throughout. Bincinchonic acid (BCA) assay cannot be used as the biotinylation alters the structure of the protein substantially, changing the number of free lysine residues and resulting in unreliable BCA assay determinations. Dialysis would have removed all unbound biotin-caproate and so helped to ensure minimal non-specific signal. The biotinylation procedure is represented schematically in Figure 5.1.

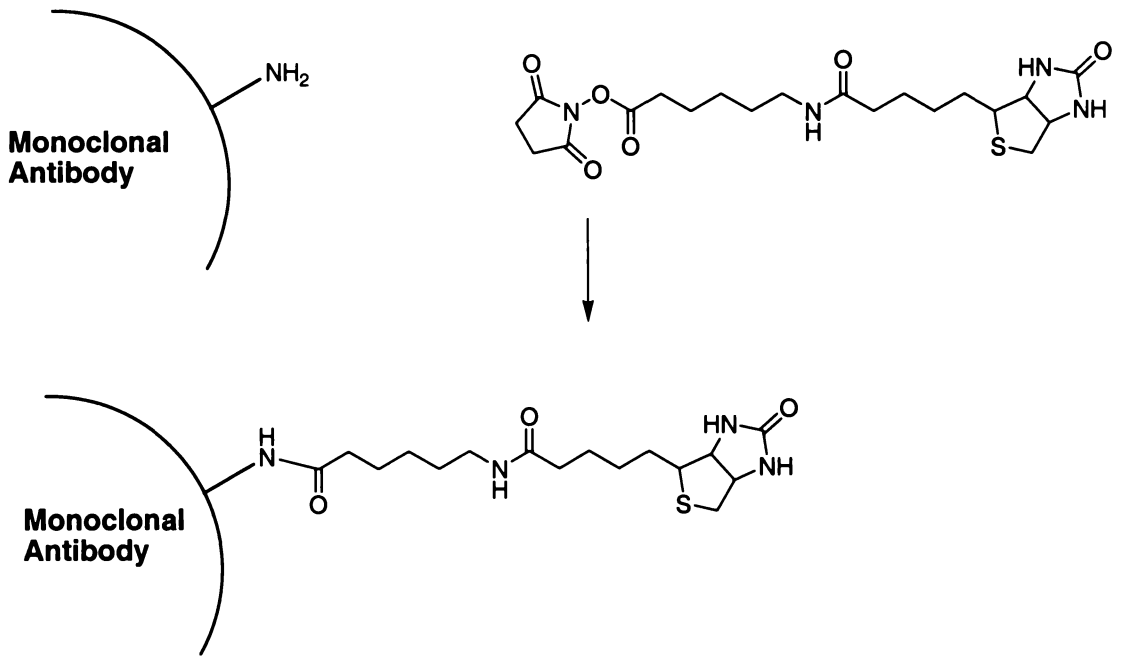

Figure 5.1 Biontinylation of Monoclonal Anti-Progesterone

5.3.2 Progesterone-Protein Conjugates As Coating Antigens in Biotin-Streptavidin-Mediated Gold-Labelled SPR

The first experiments with biotin-streptavidin-mediated gold labelling of primary antibody were done using progesterone-protein conjugate immobilised on SPR sensor chip surfaces.

5.3.2.1 Antibody Binding Tests

An SPR CM5 chip was immobilised with protein conjugates **C-2** and **C-4** to the levels as described in 5.2.3.1. The structures of these conjugates are given in Figure 2.1. Monoclonal anti-progesterone (un-modified) was passed over the surface to assess its binding. This gave positive binding for both conjugates with little non-specific binding. Regeneration was effected with 50 mM glycine pH = 1.5 buffer. Glycine buffers of pHs 2, 1.5 and 1 were tried, but 1.5 gave the best results. Biotinylated monoclonal anti-progesterone was then passed over the surface and gave positive binding for both conjugates. The biotinylated antibody binding sensorgrams are given in Figure 5.2.

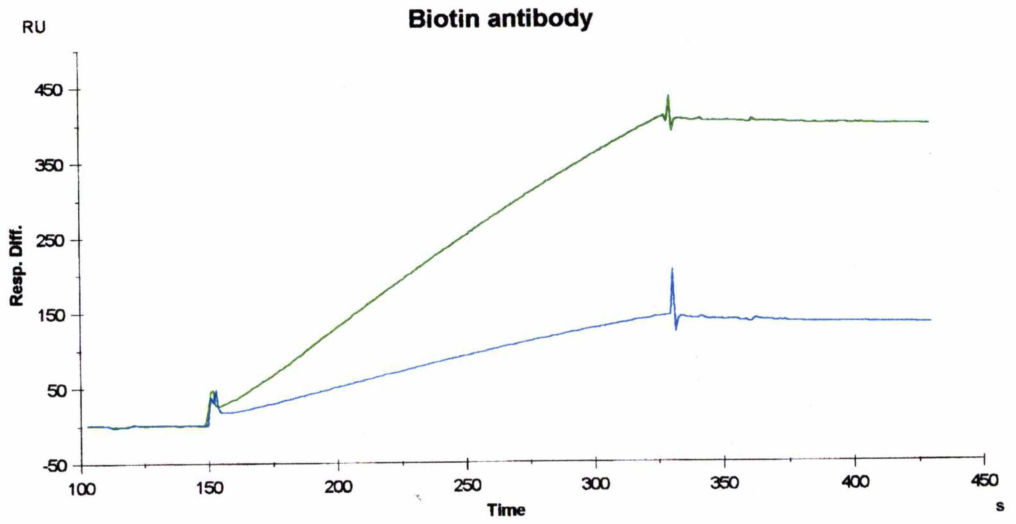

Figure 5.2 Biotinylated Antibody Binding Sensorgrams — **(C-2)**, — **(C-4)**

To determine the best mixing ratio of biotinylated antibody to streptavidin – gold, a series of ratios was examined for its binding enhancement effects. Monoclonal antibody only blanks were run as comparison. The results of the antibody / gold ratio testing are given in Tables 5.1 and 5.2.

Table 5.1. Conjugate **C-2** Ratio data

Volume Ratio mAb/gold	**1**	**1.67**	**3**	**7**	**15**
mAb Only (RU)	497.9		802.3	731.9	
mAb Gold (RU)	796.3	890.5	929	957.1	893.5
Enhancement (RU)	298.4		126.7	225.2	
% Enhancement	60		16	31	

Table 5.2. Conjugate **C-4** Ratio data

Volume Ratio mAb/gold	**1**	**1.67**	**3**	**7**	**15**
mAb Only (RU)	184.4		292.9	266.8	
mAb Gold (RU)	329.6	352.6	371.6	370.2	330.2
Enhancement (RU)	145.2		78.7	103.4	
% Enhancement	79		27	39	

Based on the signals obtained from the ratios above, the ratio giving largest overall signal considering both conjugates (7:1 antibody: gold) was selected for use in development of a progesterone assay curve.

5.3.2.2 Progesterone Assay

Plots of % bound (relative to the blank) *vs* progesterone concentration were prepared, Figure 5.3. The assays for both **C-2** and **C-4** demonstrated preliminary detection limits of < 1 pg/mL progesterone and had a broad active region from 1 μg/mL to < 1 pg/mL, Table 5.3. The IC_{50} values are given below and are taken as 50% bound off the graph.

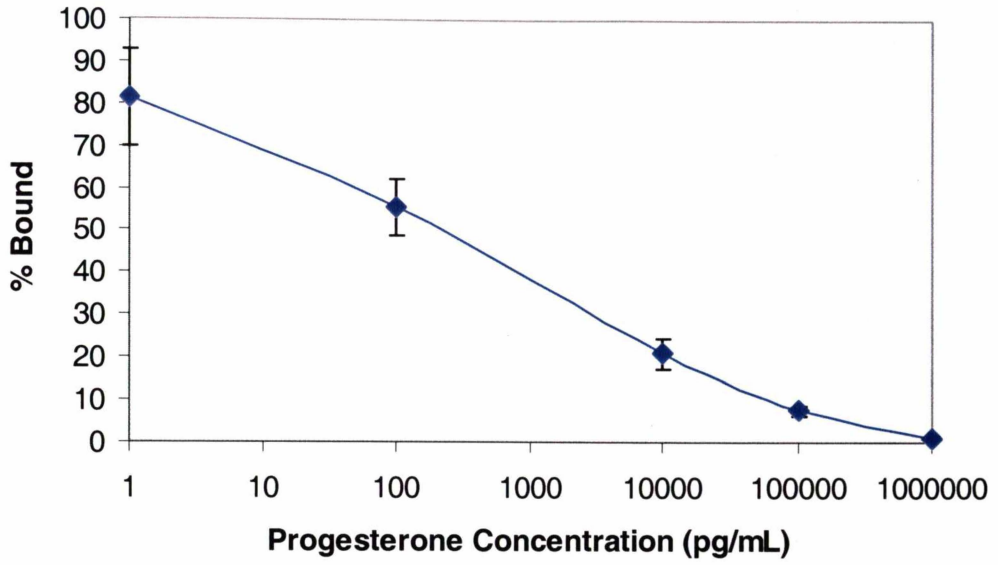

Figure 5.3 Plot of % Bound *vs* Progesterone Concentration (pg/mL) for **C-2**

Table 5.3 Preliminary Assay Data for the **C-2** and **C-4** Conjugates in the Aqueous Progesterone Assay

Conjugate	IC_{50} (pg/mL)	Detection Limit (pg/mL)
C-2	1300	<1
C-4	89	<1

These detection limits seem to be very good, but there was significant drift downwards in the binding values and this was magnifying the errors of each point. It would seem that each regeneration cycle was removing some of the immobilised conjugate from the surface and this resulted in poor assay data. Indeed, eventually the entire antibody binding signal was lost and the baseline seen to decline significantly. This is no doubt due to the regeneration of the bound gold removing protein conjugate from the surface, and so protein conjugate coated surfaces for gold-enhanced progesterone assay seem to not be adequately stable despite promising preliminary assay LOD.

5.3.2.3 20 nm Gold Colloid

Having investigated the use of 10 nm colloids to label primary antibody binding to protein conjugates, it was then advisable to examine a larger colloid

size to see if more enhancement could be obtained. The 20 nm streptavidin-gold conjugate was also commercially available. Incubating the 20 nm streptavidin-gold with primary antibody for 10 min resulted in no binding at all. It was thought that the cause might have been inadequate binding time for the streptavidin-gold to bind the biotin-antibody due to the larger size of the colloid sterically impeding binding. The incubation time was then extended to 35 min and the experiment repeated. This also resulted in no binding. This suggests that speculatively, the streptavidin – gold may be binding the biotinylated antibody but that the larger colloid size may be blocking any binding of the complex to immobilised progesterone. Bearing these observations in mind, it was decided to pass the antibody over the surface first, followed by the streptavidin – gold in a co-injection, *i.e.* a sequential format rather then a pre-incubated format. This resulted in an antibody binding curve similar to those observed above followed by a much stronger binding curve corresponding to the gold conjugate binding to the modified antibody. The curve produced when biotinylated antibody and then 20 nm gold were co-injected is shown in Figure 5.4. It was found that with two pulses of 50 mM glycine pH 12.9 (75 µL, 50 µL/min) complete regeneration could be achieved initially. The results of preliminary antibody/ gold ratio testing are summarised below in Tables 5.4 and Table 5.5.

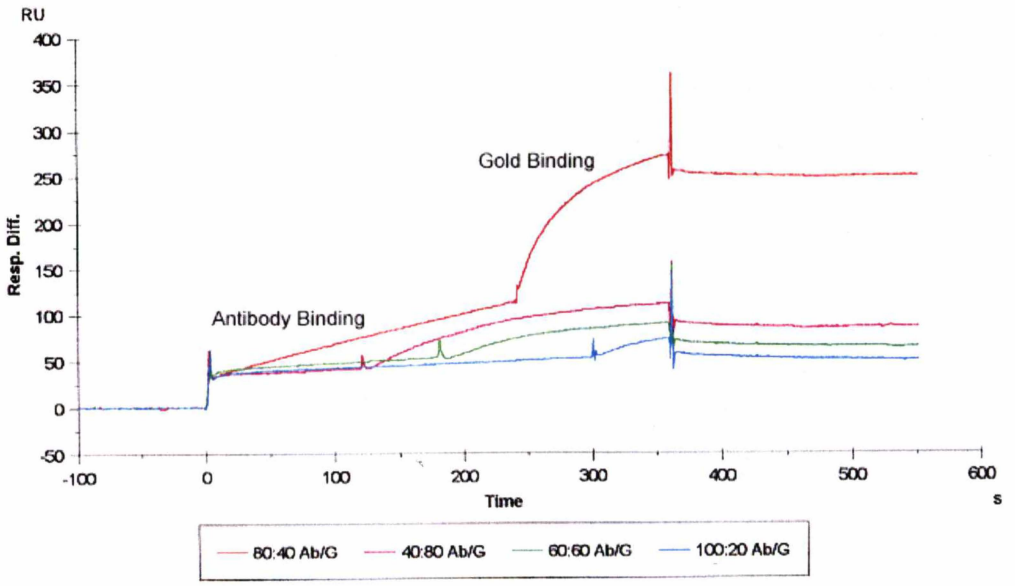

Figure 5.4 Sensorgram Overlay for Various Ratios of mAb to Gold 20 nm for **C-2**.

Table 5.4. C-2 Antibody/Gold Ratio Data

Volume Ratio mAb:gold	0.5	1	2	5
mAb Only (RU)	41.1	52.8	134.7	52.4
mAb Gold (RU)	88.8	67.9	334.8	54.3
Enhancement (RU)	47.7	15.1	200.1	1.9
Enhancement Ratio	2.2	1.3	2.5	1.0

Table 5.5. C-4 Antibody/Gold Ratio Data

Volume Ratio mAb:gold	0.5	1	2	5
mAb Only (RU)	31.8	39.4	38.1	36.6
mAb Gold (RU)	33.6	35	17.3	35.2
Enhancement (RU)	1.8	-4.4	-20.8	-1.4
Enhancement Ratio	1.1	0.88	0.45	0.96

Based on the results above, a ratio of 0.5 monoclonal antibody–biotin to gold 20 nm would give the best enhancement ratio over both conjugates and thus would be most appropriate for use in an assay.

After this data was obtained, regeneration of the surface became very difficult, and though a large range of regeneration cocktails were used to try and regenerate the surface, none was really effective. The 2:1 antibody: gold ratio was repeated under the exact same conditions and an antibody binding of 59.0 RU and a total binding of 75.6 RU were obtained indicating that the flow cell binding capacity had dropped substantially. To use the 20 nm gold colloids in this way, a longer linker may need to be employed between the antibody and the gold colloid to try and ensure that adequate regeneration can be achieved. If this is achieved, then the 20 nm colloid shows promise to give either comparable or better signal enhancements than the 10 nm and possibly even lower detection limit in this conjugate-based format.

Subsequent tests showed that the regeneration of the conjugate immobilised surface produced declines in the binding capacity of the surface even when exposed to weaker regeneration solutions. The 20 nm colloid could not eventually be fully regenerated. This suggests that practical biosensors cannot be constructed around a conjugate- immobilised surface in these formats due to surface instability. The gold seems to be causing the removal of the protein

conjugates from the surface perhaps through strong non-specific interactions. Clearly, another format and / or surface immobilisation technique was required.

5.3.3 Progesterone – OEG – Biotin Format

Another alternative format for gold labelling of the antibody binding in the SPR immunosensor is the labelling of the antigen, progesterone, with the gold through a biotin / streptavidin couple and competing the biotinylated progesterone with free sample progesterone; and then passing over streptavidin-gold to label it. This format would involve immobilising antibody rather than protein conjugate, and is illustrated in Figure 5.5.

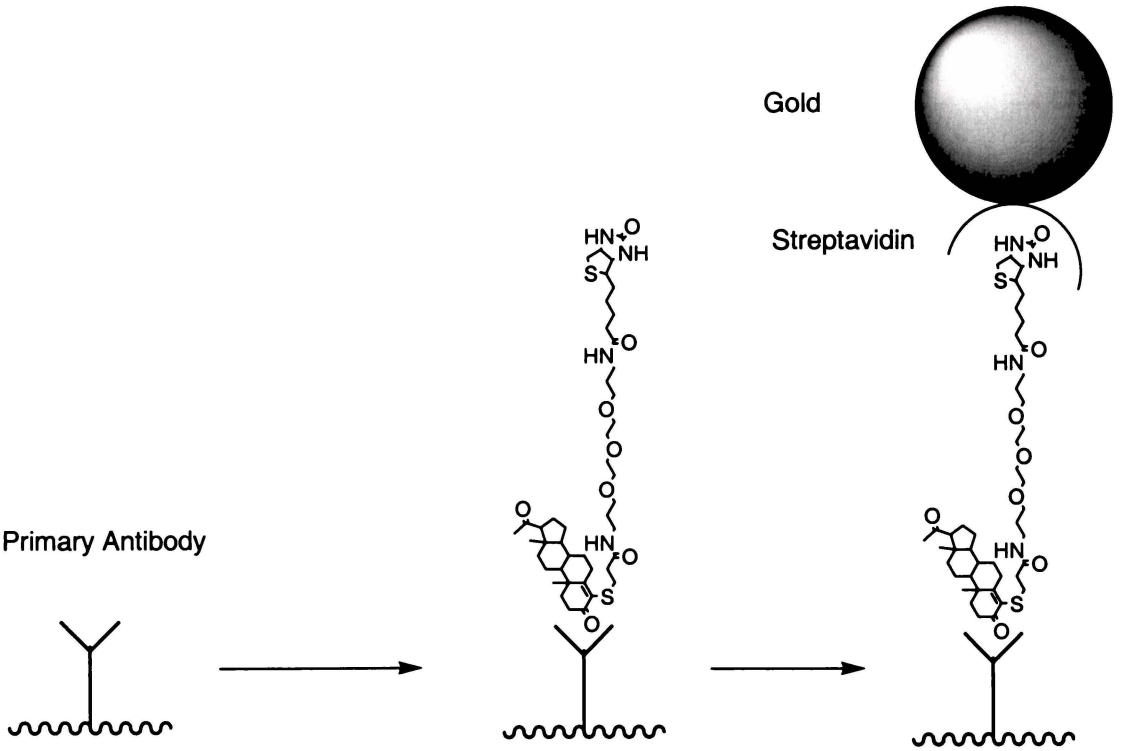

Figure 5.5 Schematic of the Binding of Biotinylated Progesterone to Immobilised Antibody Followed by Streptavidin-Gold

The best method for biotinylating progesterone would be to attach an oligoethylene glycol (OEG) linker at the 4-position and terminate this chain with biotin. This would provide the spatial separation of biotin and progesterone

needed for streptavidin binding at one end and antibody binding at the other, and the water-soluble nature of the OEG chain should help to improve solubility. To do this, the progesterone – OEG derivative must be synthesised first. This can be done by reacting the previously reported progesterone-4-thiopropionate[117, 122] with mono-Boc protected 4,7,10-trioxa-1,13-tridecanediamine. This reaction was effected simply with mild base (triethylamine). The yield was reasonable at 63% and the NMR spectra showed clear S-CH_2 and ethylene glycol signals as well as the characteristic progesterone peaks and the 9H Boc methyl peak at 1.41 ppm in the ^{1}H-NMR. Production of the biotinylated final product can then be achieved by first removing the Boc protecting group simply by stirring in formic acid, and then reacting the free amine with biotin-*N*-hydroxysuccinimide active ester under dry conditions. The NMR spectra showed the peaks characteristic for progesterone, the ethylene glycol units and biotin with no sign of any residual Boc signal. The synthesis scheme is shown in Figure 5.6.

The use of a 1 mg/mL solution of progesterone-OEG-biotin did not produce any binding response to the immobilised antibody when a 35 min pre-incubation at the volume ratio of 1:1 with 10 nm streptavidin-gold was used. Changing the volume ratio to 7:1 progesterone-OEG-biotin: gold led to a response of 68.7 RU. Regeneration was attempted with one pulse of 10 mM glycine pH= 2 and this totally regenerated the surface. An alternative format was then tried where the progesterone-OEG-biotin (1 mg/mL) was injected (240 μL at 20 μL/min) giving a binding of 55.5 RU. This was then immediately followed by a quickinjection of the 10 nm gold (60 μL at 10 μL/min). This produced a binding of 933.6 RU. Regeneration was then attempted with two pulses of 75 μL of 10 mM glycine pH = 2 which seemed to have completely regenerated the surface. This process was repeated again to test the repeatability of the binding response. The second test gave 179.0 RU response for the progesterone-biotin binding but gave 914.8 RU for the gold response (a variation of only 2%). This seemed to offer promise as an alternative assay technique, which could potentially be used for the 20 nm gold colloid. However, flow cell 2 began to exhibit no binding response to progesterone-OEG-Biotin, and testing by passing progesterone protein conjugate over the surface revealed no binding.

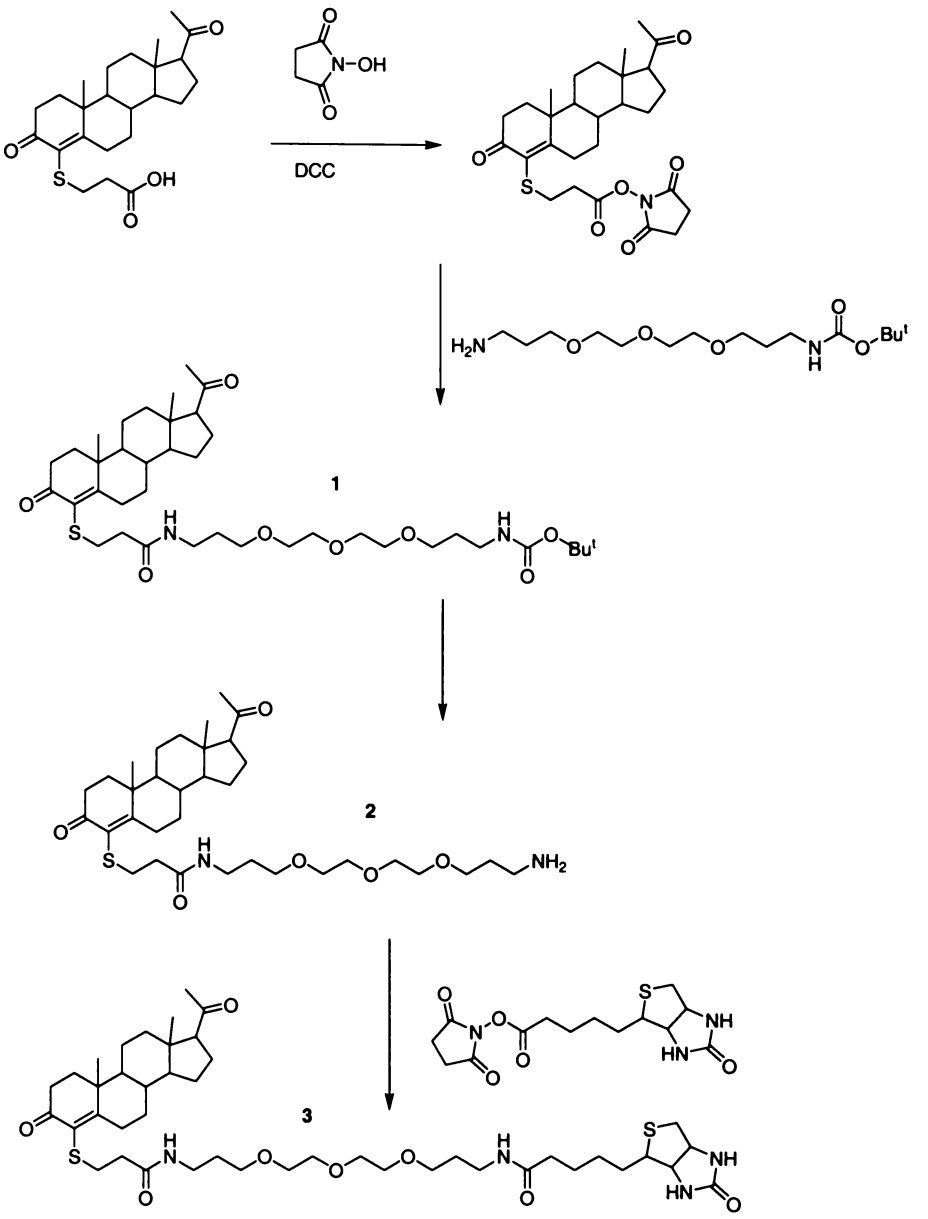

Figure 5.6 Synthesis Scheme for Production of Biotinylated Progesterone

The antibody appeared to be de-natured. This was possibly caused by the DMF content of the progesterone-OEG-biotin solution. It should be noted that it was found to be impossible to dissolve a 10 mg/mL solution of progesterone-biotin in aqueous DMF less concentrated than 10%.

From the series of tests done on surface stability, as detailed in the experimental section (5.2.4.4), there were a number of conclusions that could be made from the binding responses obtained.

- The sequential injection method was shown to be ineffective when using the progesterone-OEG-biotin
- The 10 nm colloid size did not produce significant binding even after overnight incubation
- Overnight incubation with the 20 nm colloid was necessary to obtain responses of reasonable size
- Preliminary binding test data indicated that total response would change in accordance with changing progesterone-OEG-Biotin concentration.

The sequential injection method likely failed as there were too few biotin units projecting from the surface (only one per bound progesterone) for the streptavidin-gold to bind when it was being flowed over the surface. Likewise this low abundance of biotin units was possibly the cause of short time incubations producing low binding, long incubation times being necessary for the streptavidin to bind the biotin. To get higher response one may need a larger colloid size to increase the degree of SPR signal enhancement.

The low responses obtained mean that an assay in this format is probably not advisable. The high progesterone – biotin concentration needed for binding response means that it is unlikely to compete suitably with free progesterone as it would require too high a concentration of free progesterone to inhibit binding of the progesterone-biotin. Furthermore, the regeneration solutions used to remove the gold will damage the antibody irreparably after only a few cycles. The best way to develop a reliable assay seemed to be to develop a very stable immobilised chip surface that will not be stripped by gold colloid or damaged by the regeneration solutions. The covalent attachment of progesterone to the surface, mediated by an OEG linkage, offered the best chance for a stable surface coating.

5.3.4 Progesterone-OEG-NH_2 Mediated Assay – An Ultra-Stable Surface

5.3.4.1 Immobilisation

From the above results, it had become apparent that BIAcore chip surfaces that have proteins immobilised, whether they be protein conjugate or antibody, would not be stable under the regeneration conditions needed to remove the gold labels from the surface. In some cases this had been probably due to the strength of the regeneration solutions destroying the surface, and in others likely due to the gold binding non-specifically to the protein and stripping it from the surface. Having a stable biosensor surface that is capable of withstanding many binding and regeneration cycles is an important part of a viable biosensor. Covalent bond attachment of a target to the surface offers a potential means by which the stability of the surface can be improved. Proteins are immobilised to the surface covalently but their linkages to the surface have not been very stable and they have been easily stripped by gold labels or through exposure to extreme regeneration conditions. As a further advantage, immobilisation of a non-antibody target means that harsher regeneration conditions can be used without needing to worry about loss of immunochemical function.

Small molecules will need to be projected out from the surface so as to provide room for antibody binding, however they cannot be too far from the surface as this will potentially compromise the surface plasmon enhancement of gold labels. The use of short OEG chains gives the ability to project the antigen out into the fluid stream whilst keeping it close enough to the surface for enhancement. A 15-atom chain would be about the right length in such a compromise. OEG has the further advantages of not being immunogenic; making the progesterone-linker compound water soluble and thus aiding projection in the aqueous phase; and being quite inert to potential regeneration cocktails.

Immobilisation can be achieved by passing pure compound **2** (Figure 5.6) over the surface. Once the dextran surface has been activated by formation of NHS esters, one can simply flow **2** over the surface at high concentration and low flow rate for immobilisation, Figure 5.7. The immobilisation curve for attachment of

the progesterone-OEG-NH_2 is given below in Figure 5.8. One can therefore actually see the compound being immobilised despite its small size of 623 g/mol. The immobilisation value was 638.9 RU after de-activation. This suggests that the progesterone-OEG-NH_2 was immobilised to quite high surface concentrations given the small size of the immobilising agent.

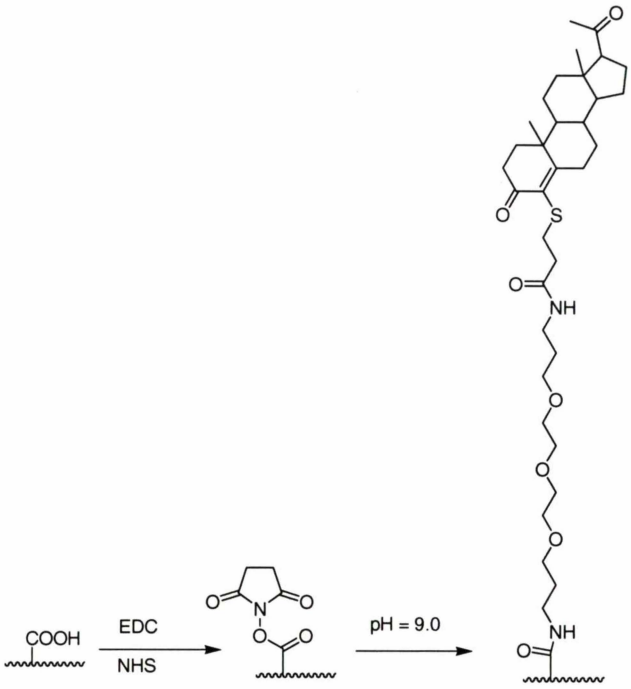

Figure 5.7 Covalent Immobilisation of Progesterone via a 15-atom OEG Linker

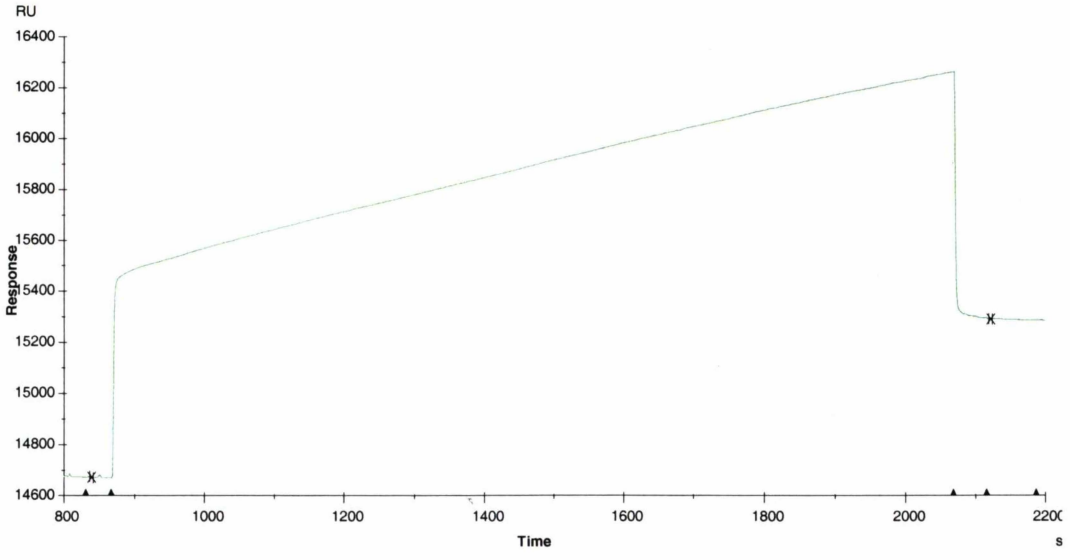

Figure 5.8 Immobilisation Sensorgram of Flow cell 2 with Progesterone-OEG Derivative (**2**)

5.3.4.2 Antibody / Gold Ratio Testing

To understand how binding response varies with varying ratios of antibody-biotin / streptavidin-gold, a plot of response *vs* antibody / gold volume ratio was produced, Figure 5.9. This plot shows how the amount of binding response obtained increases with increasing antibody / gold ratio up to about 5:1 where it levels off. It seems from this that the quantity of antibody present is the limiting factor in the amount of binding obtained. The ratio of 7:1 was chosen as this gives comparable binding to 5:1 but with lower consumption of the gold label thus reducing cost, and also the 7:1 ratio gave slightly better CVs than 5:1.

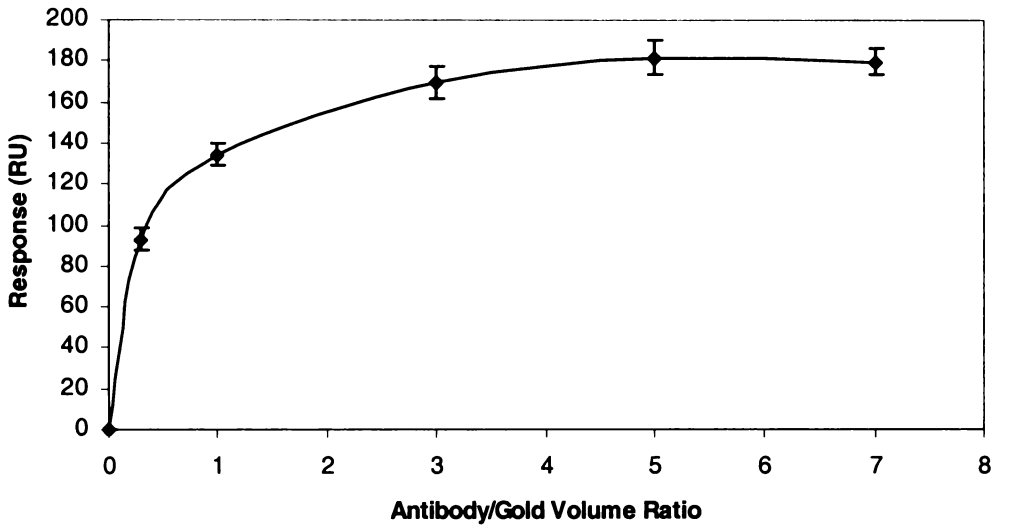

Figure 5.9 Plot of Response (RU) *vs* Antibody / Gold Volume Ratio for the 10 nm Gold Colloid Streptavidin / Biotin Pre-incubation Method

An important point to note is that injection of gold over the surface without the presence of antibody resulted in large (~380 RU) non-specific binding, which was not observed in the presence of antibody even down to an antibody / gold ratio of 0.30. The magnitude of this non-specific gold binding was unaffected by dilution of the gold in buffer. Using both undiluted gold and 7:1 buffer: gold the same final response was obtained. This suggests that the antibody was preventing non-specific binding that would otherwise be very significant. As will be seen later in this chapter, the binding of antibody to gold was specific to the biotin / streptavidin interaction.

It should be noted that this data was obtained by using the given volume ratio of antibody (100 μg/mL): gold and mixing 1:1 with blank buffer as for the progesterone assay in 5.3.4.3 (using the same wizard). The same applied for the gold only injections above. The zero point of the ratio curve was obtained by injecting straight buffer.

5.3.4.3 Aqueous Progesterone Assay Using Biotin / Streptavidin Mediated 10 nm Gold Labelling

An assay was then developed for progesterone using the 10 nm gold-streptavidin conjugate pre-incubated with the biotinylated antibody mixed 1:1 with the free progesterone standard solutions in a 5 min incubation, and then injected over the progesterone-OEG surface.

The progesterone assay standard curve was established using the new surface and this is shown in Figure 5.10. The assay curve had good shape and CVs were all acceptable and no outliers were present. All CVs except one were below 10% and five of the CVs were on or below 5%. All standard deviations were less than 10 RU. The assay parameters are detailed below in Table 5.6. Our previous SPR assays of progesterone using immobilised protein conjugate[10, 15] have given very high errors for progesterone determinations below 1 ng/mL, due to shallow assay curve slope, limiting detection to concentrations above 1 ng/mL. The IC_{50} for our earlier assay was 4.441 $\pm$ 0.019 ng/mL, which whilst being comparable to many ELISA, was still far larger than the IC_{50} of the gold-labelled assay. This gold-labelled assay also has a broader linear range caused by the lowering of the detection limit (0.1 – 10 ng/mL compared with 2.0-7.3 ng/mL previously[10]). As well as demonstrating better detection capabilities than the previous progesterone aqueous assays, this method gave a far lower LOD than that previously reported for milk progesterone determination by SPR (3.56 ng/mL).[86]

5.3.4.4 Baseline Stability

A plot of the baseline response with each cycle is given in Figure 5.11. The baseline is quite steady, with gradual declines being corrected by later rises, often these rises occur when the chip is undocked and then re-docked and primed and

may be due to salt deposition but does not affect antibody binding at all. Such good surface stability no doubt plays a major role in the low CVs obtained for the assays.

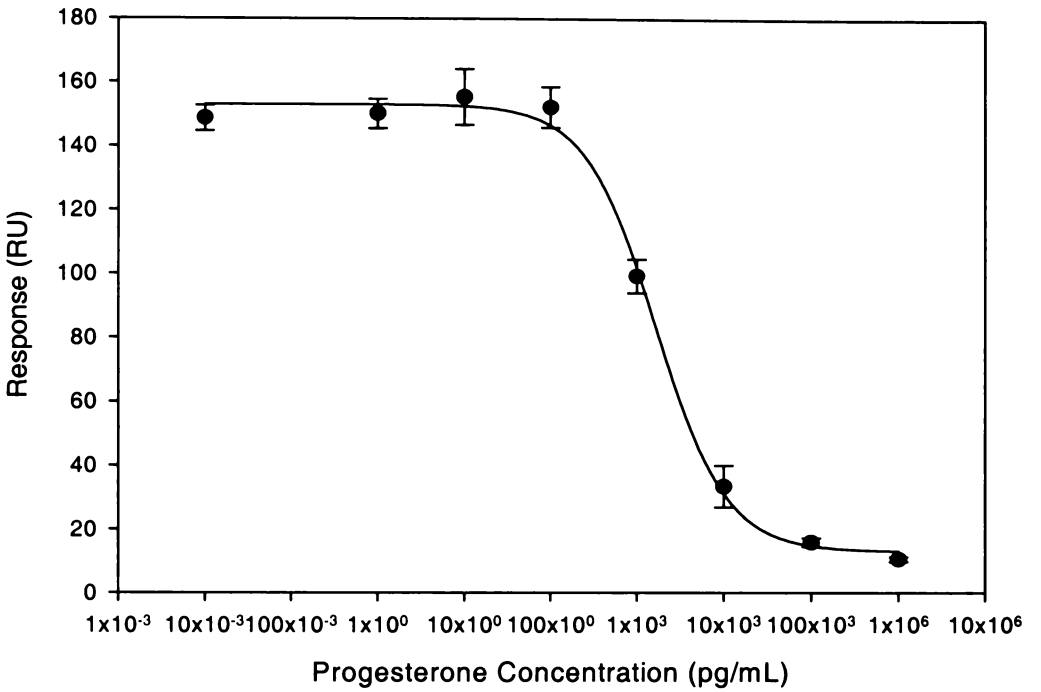

Figure 5.10 Assay Standard Curve Using 10nm-Streptavidin / Biotinylated Antibody Pre-Incubation (43.75 μg/mL final mAb concentration)

Table 5.6 Assay Parameters for the 10 nm Pre-incubation Method

mAb Concentration (μg/mL)	LOD (pg/mL)	IC50 (pg/mL)	Sensitivity (RU.mL/ng)	Enhancement Ratio
43.75	143 ± 35	1670 ± 100	57	1

Such good surface stability did not stop with this assay. The same chip was used successfully throughout all of the gold enhancement work of this thesis and, at the time of writing this thesis, was still functioning well without any appreciable loss in antibody binding capacity. This meant that the chip could withstand more than 1100 binding and regeneration cycles intact without significant loss of binding capacity over a period of about 14 months. This surface treatment is clearly far more stable than that used for most sensor chips where the chip is limited to about 100 cycles. Gillis et al.[86] have reported a sensor surface that could withstand 3600 cycles before losing binding response. Their

surface was prepared by removing the gold chip from the cartridge and manually pipetting EDC and NHS solutions onto the chip and then contacting progesterone-3-CMO with the surface, also manually. The method used in this thesis is to immobilise in situ which is clearly much more convenient than stripping apart the CM5 cartridge. The progesterone-3-CMO method used would not work as well as the 4-OEG attachment as the linker used would not be long enough to provide the necessary spatial separation from the surface and attachment at the 3-position compromises an existing functional group on the antigen.

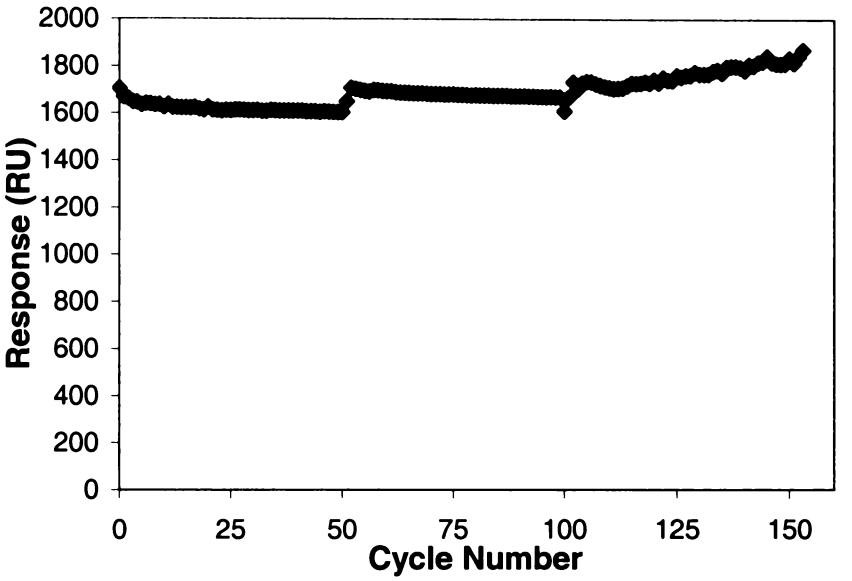

Figure 5.11 Plot of Baseline Absolute Response *vs* Cycle Number for 153 Binding Cycles

5.3.4.5 Antibody Only Assay Using The Progesterone – OEG – NH_2 Surface

To determine the effect that the gold labelling was having on the curve position and limit of detection in the pre-incubation method, it was necessary to determine the assay curve for the biotinylated antibody only, using the new surface at the same concentrations of antibody applied in the pre-incubation format above.

The standard curve for the biotinylated mAb only is plotted below in Figure 5.12. The assay data is summarised in Table 5.7.

The assay constructed on the OEG-linked surface using biotinylated antibody without gold, at the same concentration, gave an LOD of 387 $\pm$ 67 pg/mL, so

clearly the gold nanoparticle labelling was improving the detection limit. However, comparing biotinylated antibody response to the gold-labelled response, it was found that there had been no significant signal enhancement. Speculatively, this could be caused by the steric bulk of the nanoparticle hindering approach of the antigen to the antibody binding site and so reducing binding and counteracting the signal enhancement effects of the nanoparticle. The steric bulk of the nanoparticle would then make approach easier for the free antigen than for the bound antigen and so inhibition of surface binding by the free antigen would be greater and the assay curve shifted to lower LOD.

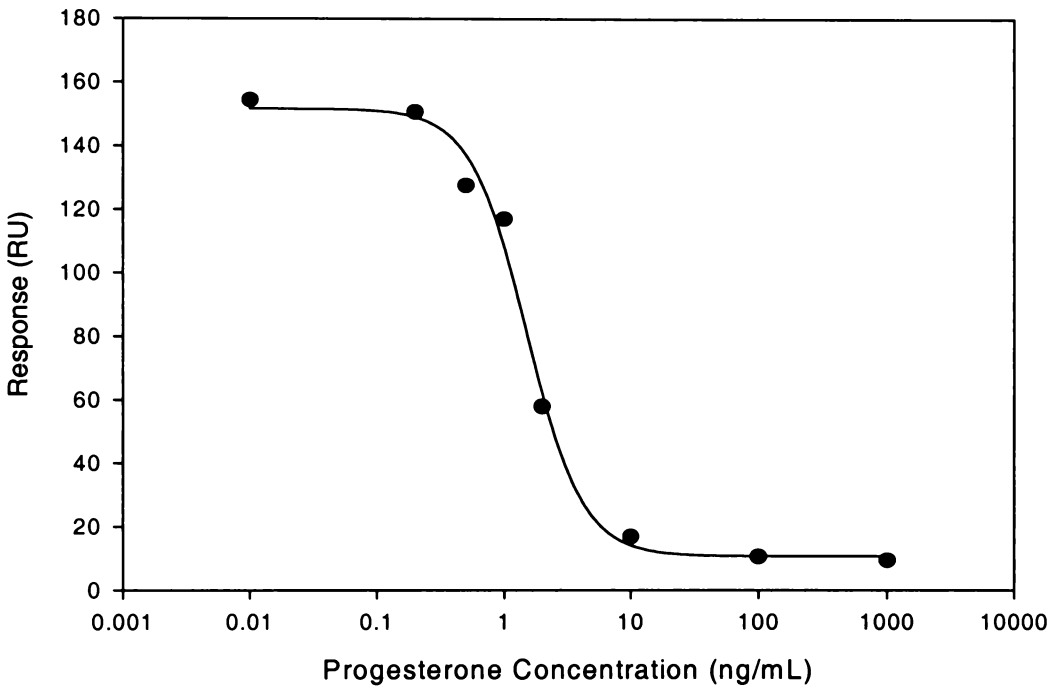

Figure 5.12 Assay Standard Curve for Biotinylated mAb Binding Only

Table 5.7 Biotinylated mAb Only Assay Parameters

mAb Concentration (µg/mL)	LOD (pg/mL)	IC50 (pg/mL)	Sensitivity (RU.mL/ng)	Enhancement Ratio
43.75	387 ± 67	1060 ± 290	9.4	n/a

5.3.4.6 The Pre-Incubation Method With 20 nm Gold Colloid

To compare the signal enhancements possible with a larger colloid size to those obtained with 10 nm colloid, the colloid diameter was increased to 20 nm and the pre-incubation format repeated at the same primary antibody concentration. The

20 nm gold sol was dialysed into PBS/T from the DMSO solution it was stored in, ensuring minimal dilution upon dialysis by allowing no air pocket in the dialysis tube. The UV-Visible spectroscopic analysis showed an $A_{\lambda max} = 1.577$ ($\lambda_{max} = 523$ nm) compared to 2.5 for the 10 nm colloid. The absorbance did not necessarily indicate lower gold loading than for the 10 nm. This was because if the same gold loading was used then doubling of the diameter would drop the particle concentration by 1/8 (assuming spherical particles and homogeneous density) and this could cause an absorbance drop. As the colloid was a commercial preparation, it was decided to use the colloid as is and apply it in the same assay format as for the pre-incubated 10 nm label. The assay standard curve is given below in Figure 5.13.

One can see from the assay results that the 20 nm colloid has, under these conditions, failed to produce any more enhancement of signal than was observed for the 10 nm colloid. The LOD was no different from that of the 10 nm pre-incubation format and the IC_{50} was also fairly similar, Table 5.8. The 20 nm colloid seemed to be performing in the same way as the 10 nm colloid did. Speculatively, it may be sterically restricting binding of the antibody to the surface whilst at the same time enhancing the signal of what has bound in such a way that the two effects largely cancel each other out.

Addition of ethylene glycol was needed to minimise settling of the larger colloid with time, which initially caused drifting binding responses. With ethylene glycol added, the binding responses were fairly constant throughout, even over more than 30 h.

The pre-incubation labelling format had shown no overall enhancement of the binding signal relative to the same concentration of biotinylated antibody alone. However, the detection limits of the assays were substantially better than those previously reported for SPR of progesterone.[10, 86] The steric inhibition arising from having the large gold label attached to the antibody upon binding to progesterone may have reduced the amount of binding signal enhancement that was possible. Speculatively, it may have done this by reducing the amount of antibody that bound to the surface to such an extent that no overall enhancement was observed. The steric impedance of binding to the antibody would be more severe for the surface confined progesterone than for the free progesterone, and this may mean that the inhibition conditions of the assay were weighted in favour

of free progesterone, which would result in an assay capable of detecting lower progesterone levels. In other words, if the antibody could bind free progesterone better than surface bound progesterone then smaller amounts of free progesterone would be needed to inhibit binding, and so the LOD would be lower.

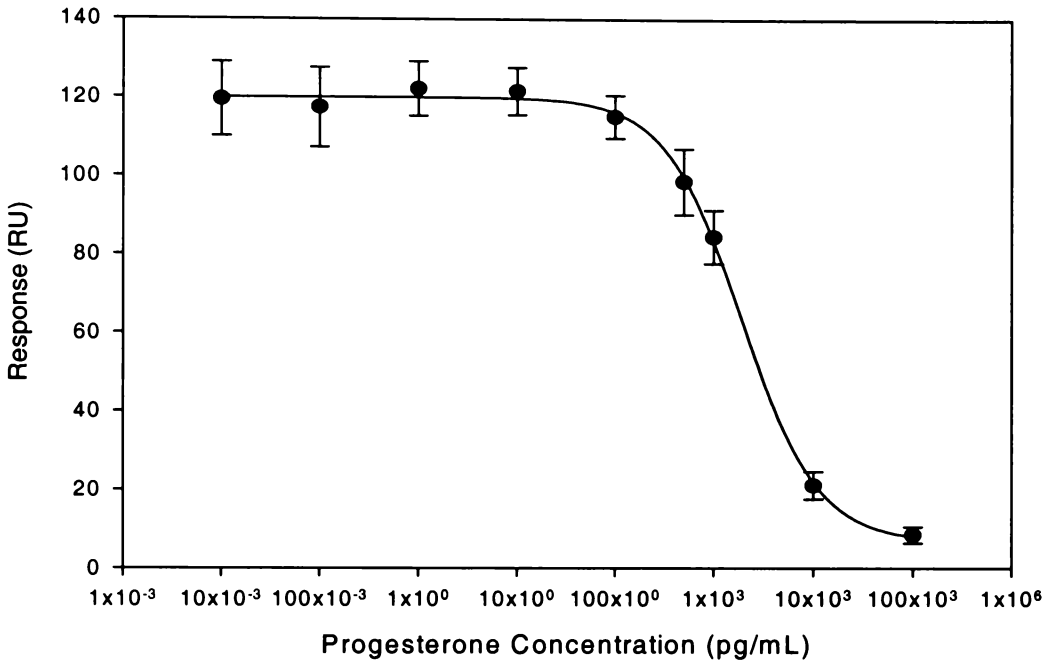

Figure 5.13 Assay Standard Curve for 20 nm Pre-incubation Format

The assay parameters are summarised in Table 5.8.

Table 5.8 Assay Parameters of the 20 nm Pre-incubation Format

mAb Concentration (µg/mL)	LOD (pg/mL)	IC50 (pg/mL)	Sensitivity (RU.mL/ng)	Enhancement Ratio
43.75	198 ± 57	1910 ± 150	28	1

5.3.5 Sequential Binding Assay Format

5.3.5.1 Gold Dilution Binding Test

It is of interest to consider another inhibition assay format whereby the antibody is introduced with the free progesterone and passed over the surface-bound progesterone first, and then a gold-streptavidin label is passed over the surface to label what biotinylated antibody has now bound to the surface. In such a format there would be none of the steric inhibition of binding to the antibody possible in the previous pre-incubation format, but rather the gold would serve to

enhance the antibody binding response already present. This format is shown schematically in Figure 5.14.

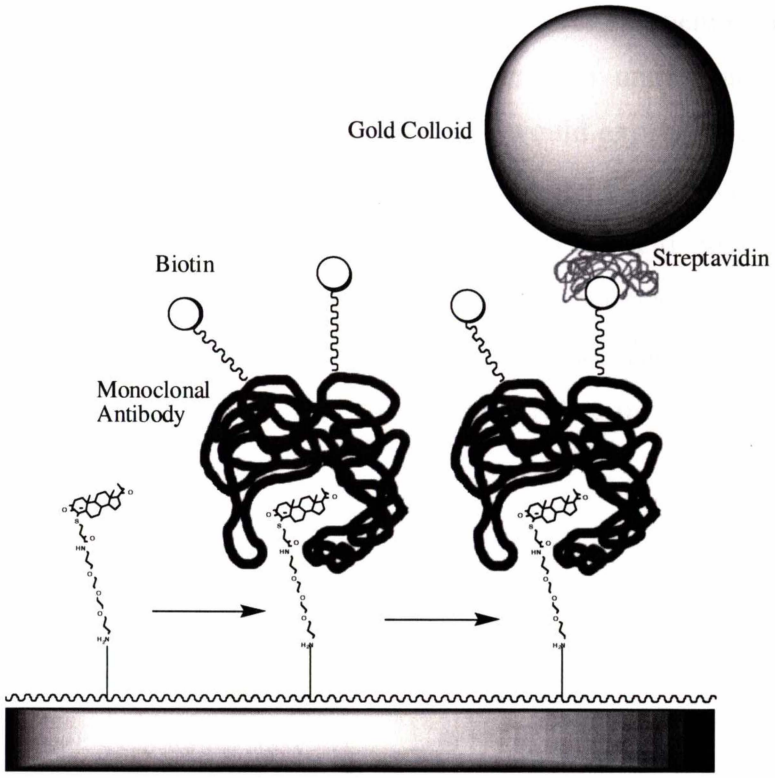

Figure 5.14 Schematic Diagram of the Sequential Binding Format for Gold-Labelling of Biotinylated Primary Antibody

The first step in developing such a format is to determine the best 10 nm gold dilution for use in labelling by formation of a gold dilution binding curve. The results are presented in Figure 5.15 as a plot of total gold enhanced response *vs* gold colloid dilution factor for flow cell two. The plot clearly shows that as the gold dilution ratio is reduced, the binding response is also reduced at an increasing rate down to the antibody–biotin only binding response of about 250 RU. Further testing has shown only slight additional increases in total binding response when increasing the dilution ratio beyond 0.25. Such points have not been included in this curve due to the large wastage of gold this produces for very little further benefit. The CVs of all the points are quite low (< 3%).

The flow cell three curve (about 1.5 times the immobilisation value of flow cell two) completely mirrors that of flow cell two but with higher overall binding responses and slightly higher CVs (< 7%). It is interesting to see how much

enhancement of response is provided at each gold dilution. This can be measured by taking the ratio of the total response over the antibody only response. A plot of the enhancement ratio with different dilutions of the colloid is given in Figure 5.16 for flow cell two. The plot showed an ever-sharpening decline in enhancement as the gold dilution ratio was decreased until finally the ratio reached 1, *i.e.* no enhancement. This was as one would expect given that lower gold dilution ratios produce greater shortages of gold and thus greater restrictions on the degree of gold enhancement. As one approaches and goes above 0.25 dilution, the gold came into excess and no further enhancement was possible for that antibody binding. This mirrored the total response data, as the antibody binding each time was constant. The enhancement ratios in this plot are clearly not corrected for non-specific binding.

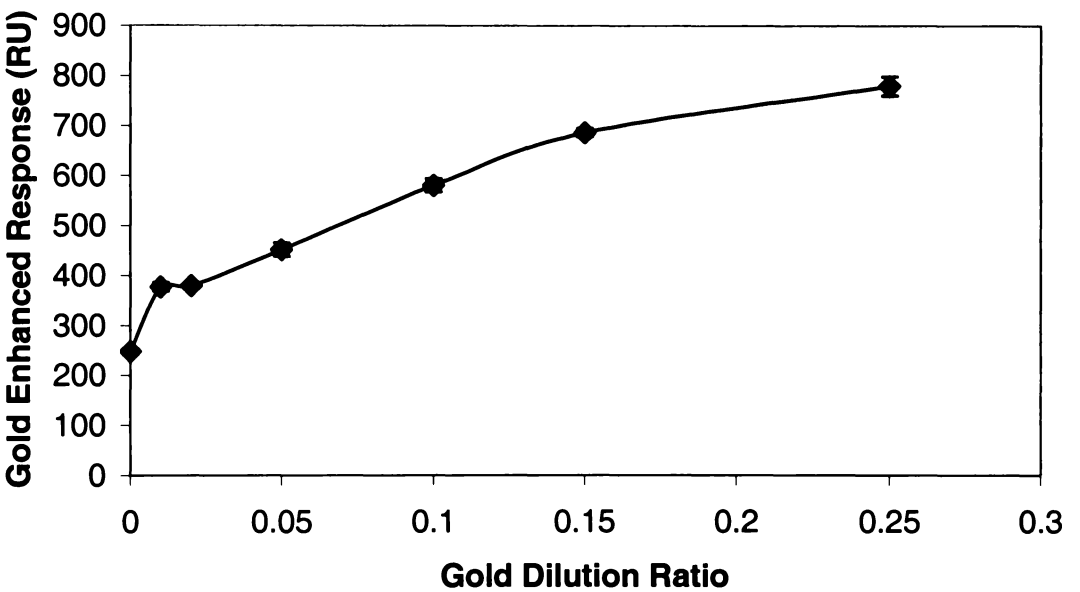

Figure 5.15 Plot of Gold Enhanced Response *vs* Gold Dilution Ratio

Based on this data, it was necessary to select a gold dilution to use for the assay and antibody binding studies. The best dilution to use was 0.15 as this gave high enhancement of signal (2.8 compared to 3.2 for 0.25 dilution) whilst not consuming excessive amounts of gold colloid, which would increase the price of assays, and be more likely to clog the fluidics system.

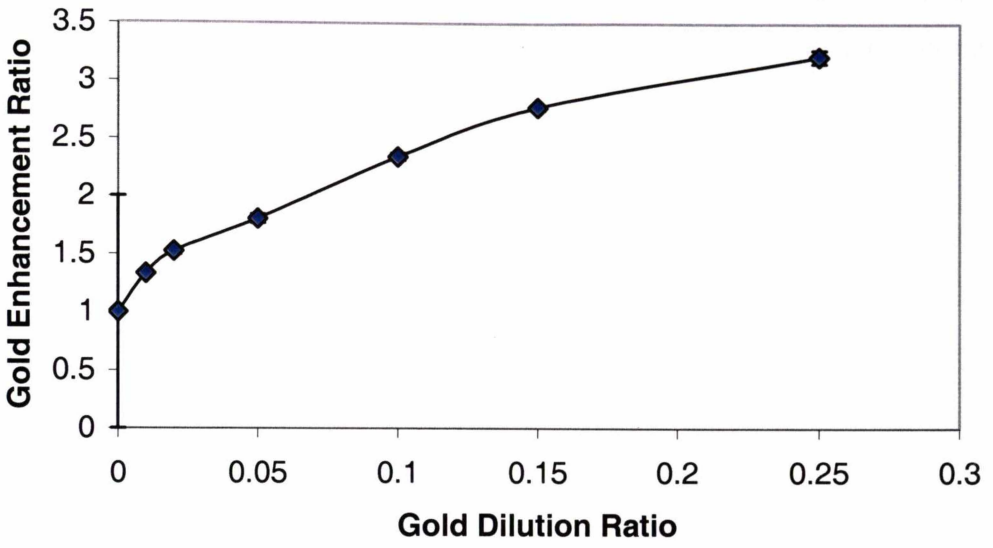

Figure 5.16 Plot of Gold Enhancement Ratio *vs* Gold Dilution Ratio

5.3.5.2 Antibody Binding Curve Determination

A plot of binding response *vs* antibody concentration is given below in Figure 5.17 for flow cell two, showing both total binding response and antibody only binding response. One can see that the responses obtained, both total and antibody only, were directly proportional to the antibody concentration in a linear relationship over the whole range of antibody concentrations considered (R^2 > 0.99). The lines were highly divergent showing that the actual gold enhancement portion of the signal was increasing with increasing antibody concentration. Signals for the pre-incubation method reached a maximum of 150 RU, so one can see from this curve that the antibody concentration can be reduced to at least 15 μg/mL and still retain good levels of binding response. It probably would not be wise to reduce the concentration much further as the gold is demonstrating about 100 RU of non-specific binding making the target gold enhanced signal around 250-300 RU, *i.e.* about 15 μg/mL biotinylated antibody.

From this data, one can compute the signal enhancement ratio by taking the ratio of the slope of the total signal line over the antibody only binding line. This gave a signal enhancement of 2.2. Clearly, gold labelling in a sequential binding format is giving signal enhancement, speculatively due to the gold not sterically reducing binding of the primary antibody. The same enhancement is seen in flow

cell three. All discussion will now be directed to flow cell two unless otherwise stated as flow cell three overall showed worse or equivalent assay performance compared to flow cell two.

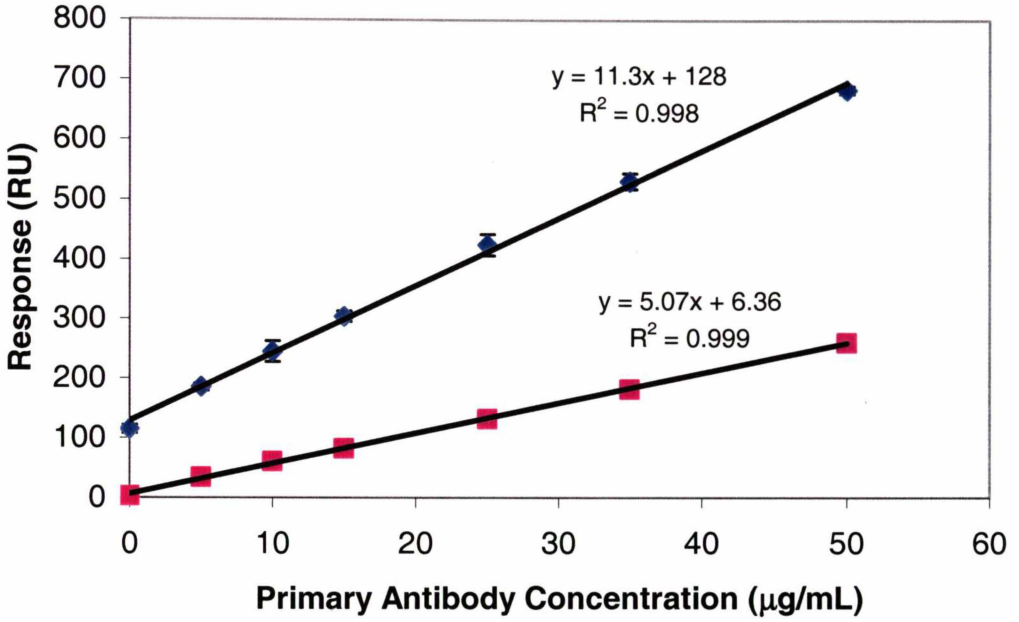

Figure 5.17 Antibody Dilution Plot. ■ Primary Antibody Only, ♦ Gold Enhanced Signal

Based on this data, one can now produce an assay for progesterone. It was hoped that the reduction in the concentration of antibody would mean that substantially smaller amounts of progesterone would produce significant inhibition of binding thus pushing the LOD to lower concentrations.

5.3.5.3 Progesterone Sequential Assay

The assay results were analysed in a number of ways. Firstly the monoclonal antibody only (15 µg/mL injected concentration) responses were plotted to give a calibration curve. This curve is shown below in Figure 5.18.

The curve for the total response was then plotted and is given in Figure 5.19. The CVs were a little better than those of the antibody only curves and the curve gave blank binding of 181 RU. The data for these curves are summarised below in Table 5.9.

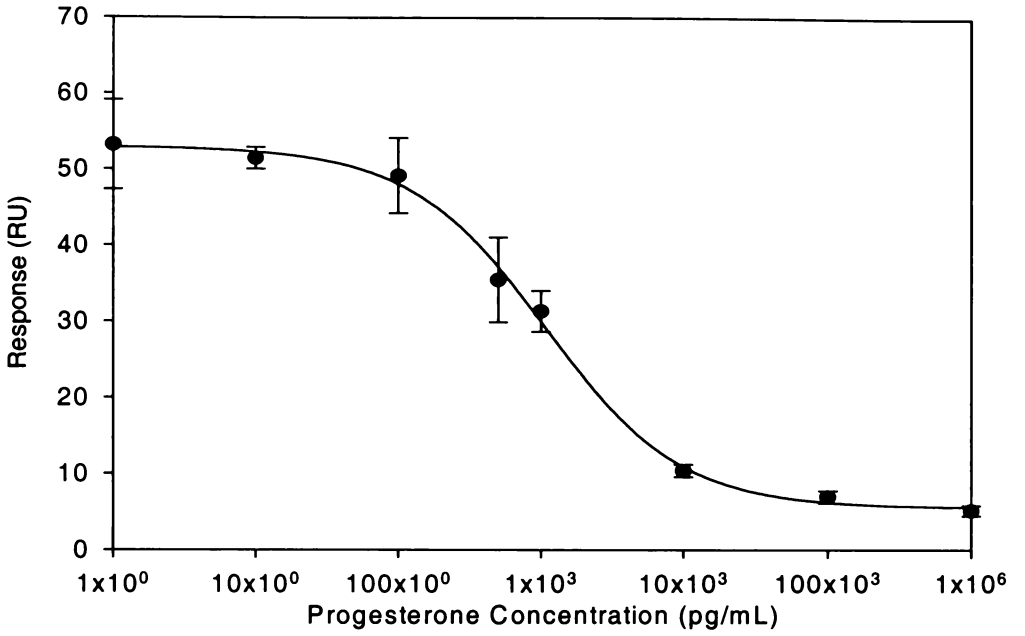

Figure 5.18 Antibody Only Assay Standard Curve, 15 μg/mL Primary mAb (Injected Concentration)

One can see that the antibody-only detection limits are substantially lower than those obtained by antibody alone at a final concentration of 43.75 μg/mL (see Section 5.3.4.5). Dropping the antibody concentration has enabled detection of lower levels of progesterone as expected. This level of non-specific binding was actually less than that anticipated (antibody binding curve data suggested non-specific binding of ~100 RU but it was $\leq$ 40 RU for flow cell 2). This may mean that the presence of progesterone was further diminishing non-specific binding. The CVs were slightly high for a practical assay using the un-labelled antibody, but were significantly better with labelled antibody. The LOD of the assay using antibody only seemed quite low but had high standard error.

Comparing the IC_{50} values, it could be seen that there was no great difference between the unlabelled and labelled binding curve positions, indicating that the gold label was scaling up the binding response without shifting the curve position. This is wholly expected, as the gold is not present during incubation with free progesterone and so will not shift the overall curve position. The slope sensitivity had increased nearly 10-fold on gold labelling.

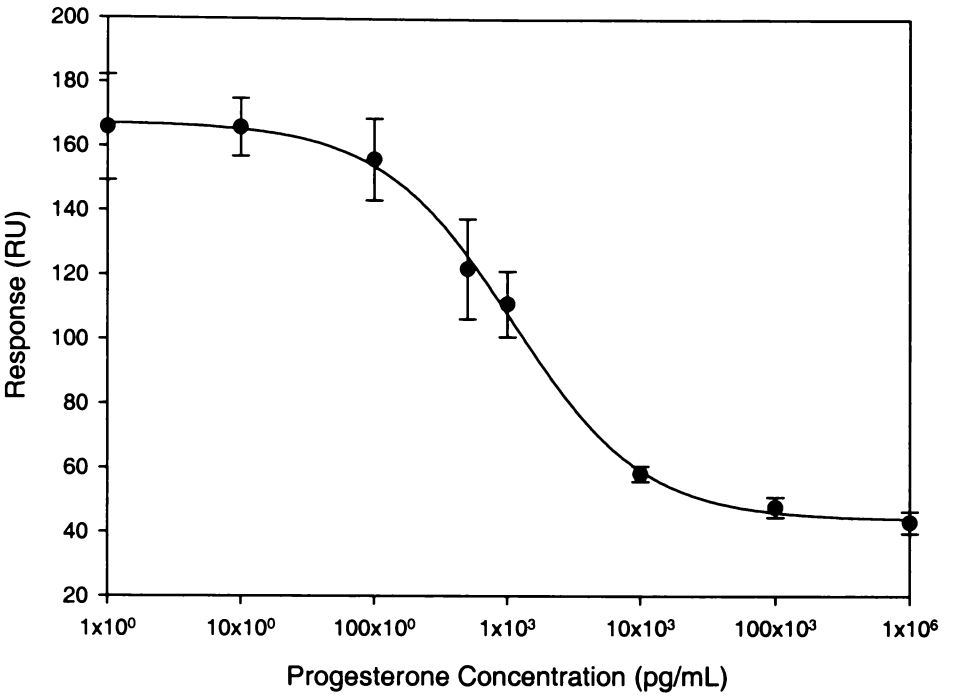

Figure 5.19 Assay Curve with Gold Enhancement, 15 μg/mL Primary mAb

Table 5.9 Data from Calibration Curves of the Progesterone Assay (15 μg/mL Primary mAb)

	mAb Only	Gold Total
LOD (pg/mL)	32 ± 53	150 ± 49
IC_{50} (pg/mL)	1080 ± 120	1000 ± 45
Average CV	7.8%	6.0%
Sensitivity (RU.mL/ng)	3.9	32

The only way that one can further reduce the detection limit of this assay format is to reduce the concentration of the antibody still further. If the final antibody level is halved to 7.5 μg/mL, then one would expect maximum antibody binding of ~27 RU which would be expected to translate to total maximum binding of ~83 RU based on the assay curves. Based on the drop experienced in the detection limit so far, a detection limit then of 25-50 pg/mL would be expected. The question would then remain as to whether the CVs would be low enough. It has been seen that the gold enhancement is capable of improving the CV somewhat.

5.3.5.4 A New Progesterone Sequential Assay

The standard curves for antibody only binding (7.5 μg/mL after dilution with progesterone solutions) and total gold enhanced binding are given in Figure 5.20. The parameters of the assay are summarised below in Table 5.10.

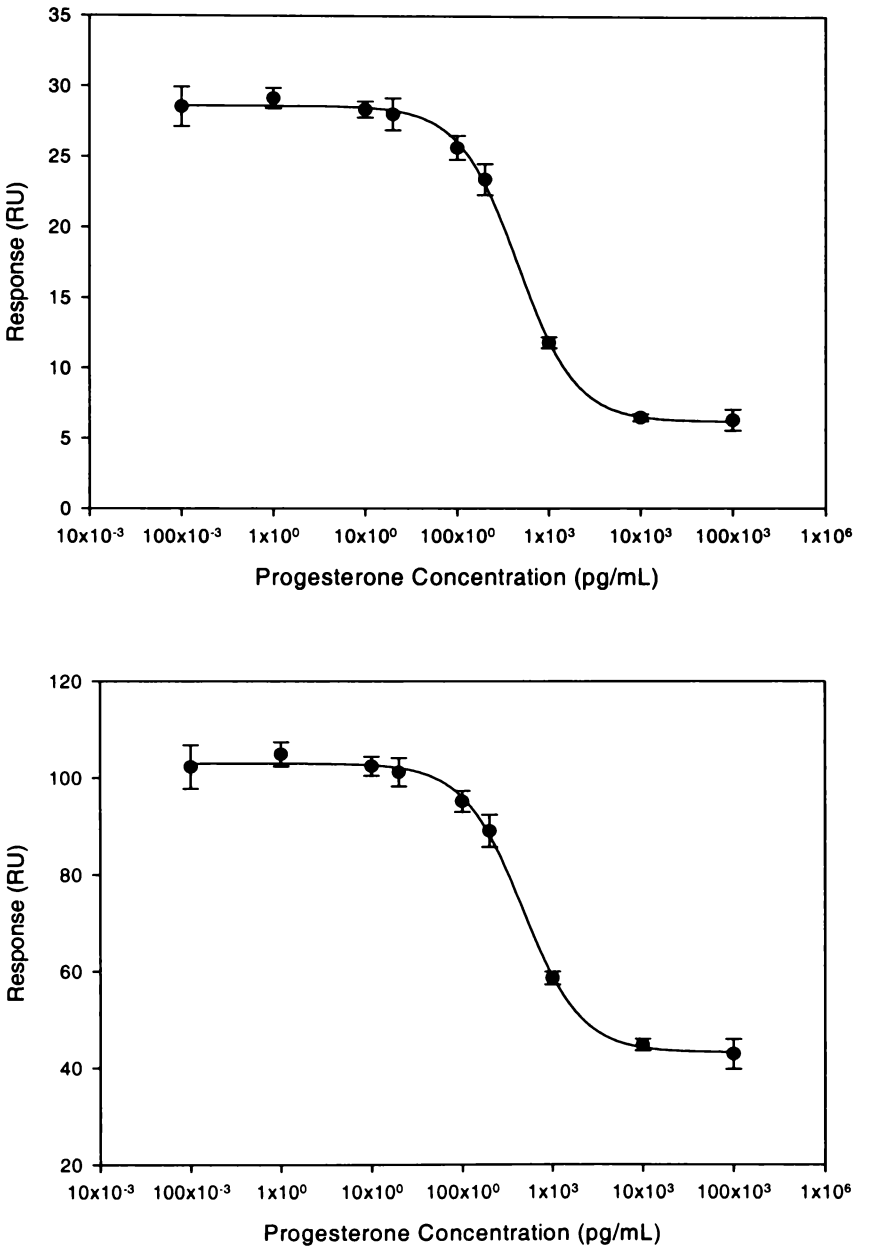

Figure 5.20 Assay Standard Curves with Primary Antibody Only (Top), Gold-Enhanced Signal (Bottom) - 7.5 μg/mL Primary mAb (Injected Concentration)

Table 5.10 Assay Data – New Sequential Assay

	mAb Only	Gold Total
LOD (pg/mL)	28 ± 21	23.1 ± 4.4
IC_{50} (pg/mL)	455 ± 30	460 ± 16
Average CV	4.4	3.3
Dynamic Range	0.01-1 ng/mL	0.01-1 ng/mL
Sensitivity (RU.mL/ng)	14	40

Further reduction of the antibody concentration has significantly reduced the LOD of the enhanced assay to 23.1 ± 4.4 pg/mL. The CV for this assay was quite good and this has probably contributed to the low LOD. The gold has enhanced the signal by a factor of 2 as before. Once again, there is no real shift in the IC_{50} from unlabelled to labelled. It was a little surprising that the antibody bindings have retained good CVs down to such low binding levels (maximum binding response of 30 RU) and indicated the robustness of this surface treatment down to such very low levels of binding. The overall CVs were all acceptable, though the CVs for the gold responses were in practical terms almost double this because of the non-specific binding. It was clear that to further reduce the antibody concentration it would be necessary to largely eliminate the non-specific binding still being exhibited by the gold colloid.

5.3.6 Antibody Binding Tests and Non-specific Binding Treatments for the Sequential Format

5.3.6.1 Optimisation of the Non-Specific Binding Treatment

Slower flow rates for passing of the labelling compounds could possibly have resulted in higher enhancements, so a 10 µL/min flow rate was tried. The enhancement ratios obtained were no better than those for the 20 µL/min flow rate. The biotinylated antibody (50 µg/mL) was injected in the assay format with a blank and with gold at a 0.15 dilution in 1%v/v PEG-400, 0.2 M EG. This was also then repeated for a 0.5%v/v total PEG-400 loading. Preliminary tests indicated that 1%v/v PEG-400 would reduce non-specific binding without reducing the response slope. As the 1%v/v PEG-400 was not decreasing the slope

of the binding curve, it was decided that it be used at this level for use in new binding studies and assays.

5.3.6.2 Antibody Binding Test with Reduced Non-Specific Binding

Using the new treatment to further reduce non-specific binding, the antibody-binding plot was re-done. The plot is given below in Figure 5.21. It was clear that these plots have very good correlation lines and that the non-specific binding is down to 14 RU. The slope of the gold enhanced line as a ratio to the monoclonal antibody line was 2.1. This is an indication that the level of non-specific binding up to at least about 100 RU did not affect the degree of signal enhancement. Clearly this slightly different gold label treatment had significantly reduced non-specific binding and allowed the primary antibody concentration to be dropped further.

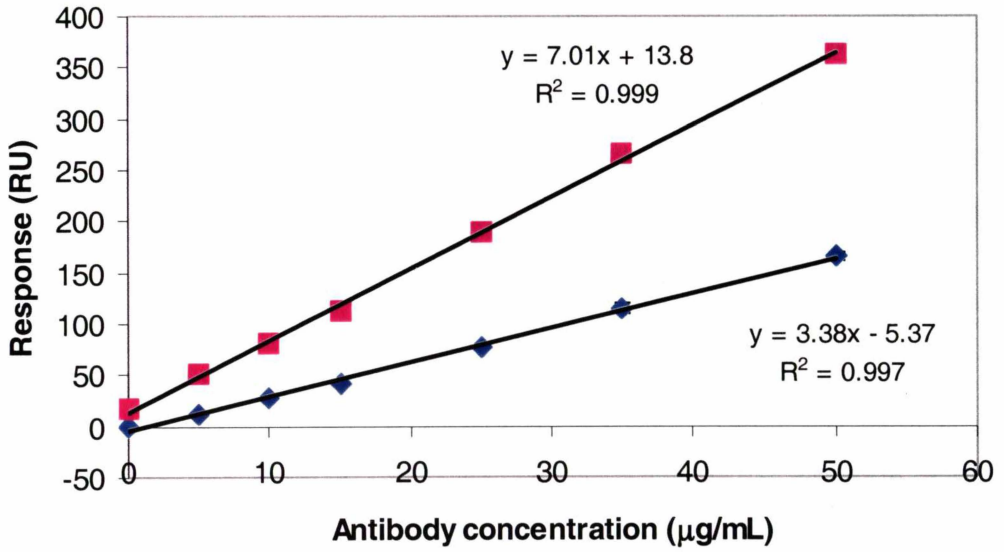

Figure 5.21 Antibody Binding Plot With New Non-Specific Binding Treatment. ♦ Primary Antibody Only, ■ Gold Enhanced Signal

5.3.6.3 Gold Loading – Is it Optimal?

To test whether raising the gold loading in the labelling step had any effect on the enhancement with the new PEG treatment, higher gold loadings of 0.25

dilution were tried. This produced an enhancement of 2.3. One can see that the enhancement was not greatly different from the 0.15 loading (enhancements calculated after correction for non-specific binding).

To assess whether simply increasing the volume of gold label used would improve the binding enhancement, an antibody gold-enhanced binding was done using a 60 μL injection of the 0.15 dilution and 50 μg/mL antibody and flow rate at 20 μL/min. The binding results showed enhancements of 2.3-2.4. Enhancement was not much greater than that achieved previously. Certainly for the 0.15-0.2 extra ratio signal enhancement a lot of gold was wasted (now using twice as much) and the extra benefits were minimal – no better than for the 0.25 dilution. 0.15 dilution and 30 μL injection volume certainly seemed to be the optimal condition for gold labelling.

To see if increasing the incubation time of progesterone solution with antibody would improve the ability of the assay to discriminate low progesterone concentrations, a 100 pg/mL progesterone standard was run using the assay program with 0.15 gold (1%v/v PEG-400, 0.2 M EG total) at 20 μL/min but one with a 10 min incubation and one with a 5 min incubation. The antibody was at 15 μg/mL. This test showed clearly that the increased incubation time was not having any effect whatever on the binding and thus no effect on the discrimination of lower concentrations of progesterone. The 5 min incubation was therefore retained.

5.3.6.4 Gold Enhanced Assay – Low Antibody

Having further minimised the non-specific binding seen on the surface, a new progesterone assay could be constructed using even lower primary antibody concentration. The concentration was thus reduced to 2.5 μg/mL (injected concentration). The assay curves are given below in Figure 5.22. The assay parameters are summarised in Table 5.11.

It can be seen from the LOD that there was no real benefit obtained from reducing the final antibody concentration from 7.5 to 2.5 μg/mL, indeed the LOD was worse than that for the 7.5 μg/mL case. The worsening LOD was caused by the signal dropping too low (sensitivity of only 9.1 RU.mL/ng compared to 40

RU.mL/ng for the 7.5 μg/mL case) causing the CVs to rise and push the LOD to higher concentrations as low concentrations cannot be discriminated from the blank so well. The IC_{50} had continued to drop however, as the lower antibody concentration pushed the curve further to the left. This drop was not as large as might be expected from the reduction in antibody concentration. The linear ranges were the same before and after enhancement, and extended to 50 pg/mL compared with 10 pg/mL for the 7.5 μg/mL antibody concentration.

Clearly, in order to further reduce the LOD at this concentration of antibody, the degree of signal enhancement would need to be increased to much more then 2x, *i.e.* at least around 4x. To achieve this, it may have been necessary to increase the size of the colloid particle employed. The next logical step was to proceed with use of a 20 nm colloid. It is useful to compare the assay plots and linear ranges of the three different antibody concentrations used thus far. These are shown in Figure 5.23.

It was clear that, with decreasing antibody concentration the maximum response declined as expected. Also as expected, the curve flattened substantially at higher progesterone concentration with significant binding response not occurring until lower than 1 ng/mL for the 2.5 μg/mL curve, 10 ng/mL for the 7.5 μg/mL curve and 100 ng/mL for the 15 μg/mL curve. It was of interest to note that the non-enhanced curves did not reach zero response but rather levelled out at between 5-8 RU. This was caused in part by non-specific binding of the antibody to the OEG-progesterone surface.

If lower antibody concentrations were to be used in this format, then this non-specific binding would likely need to be removed, probably by adding an agent to the diluent of the antibody solution. Gold enhancement alone would not solve this problem as the gold enhances the antibody that is present on the surface (see Section 5.3.6.7). The linear regions of the assay curves had improved from 0.1-10 ng/mL for 15 μg/mL to 0.01-0.2 ng/mL for 7.5 μg/mL but for 2.5 μg/mL the linear range was 0.05-1 ng/mL.

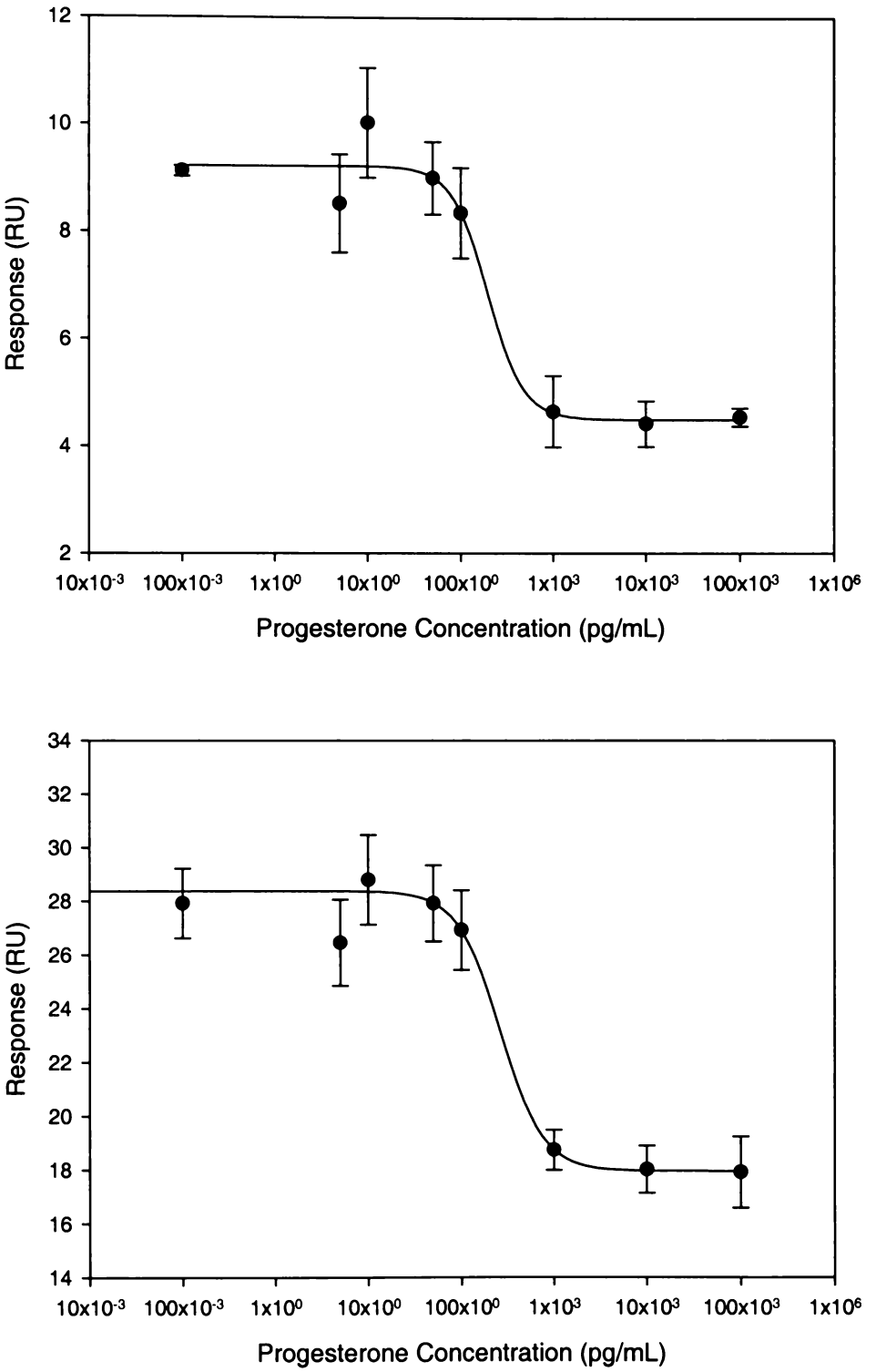

Figure 5.22 Assay Standard Curves With Primary Antibody Only (Top) and With Gold-Enhanced Signal (Bottom) - 2.5 μg/mL Primary mAb (Injected Concentration)

Table 5.11 Assay Parameters for Sequential Binding (2.5 μg/mL Primary Antibody)

	Primary mAb	Gold
LOD (pg/mL)	121 ± 23	104 ± 40
IC_{50} (pg/mL)	195 ± 28	314 ± 21
Average CV (%)	7.7	5.4
Range	0.05-1 ng/mL	0.05-1 ng/mL
Sensitivity (RU.mL/ng)	4.6	9.1

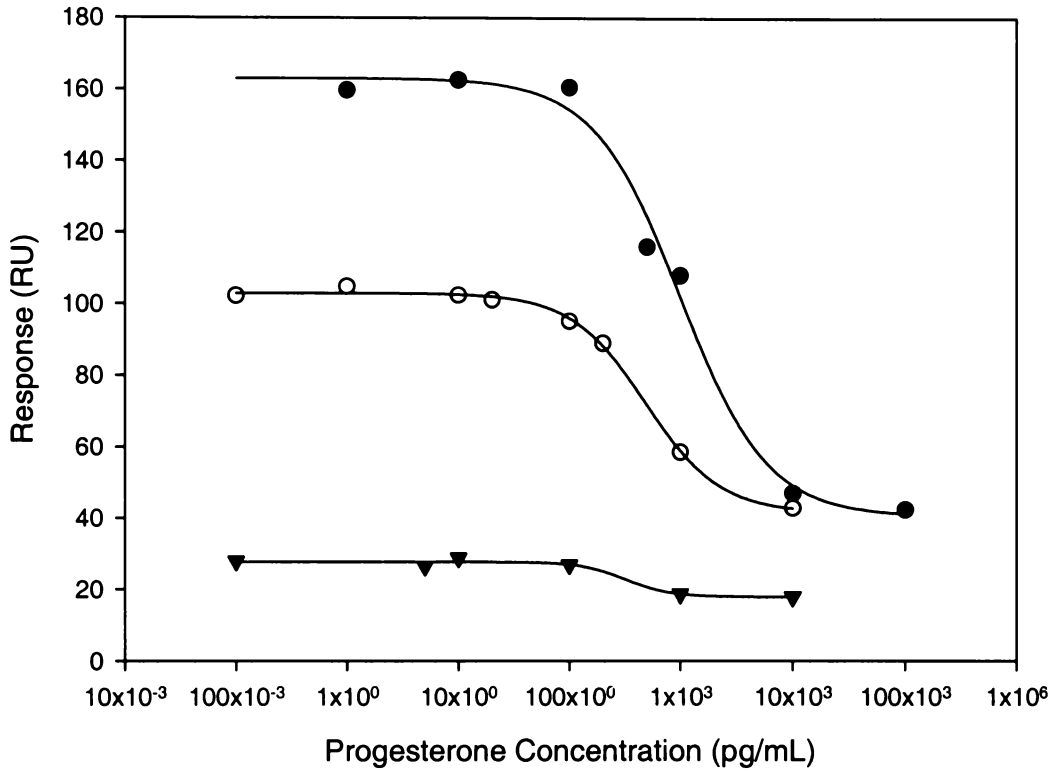

Figure 5.23 Comparison Plot of Gold Enhanced Assay Curves. ▼ 2.5 μg/mL, o 7.5 μg/mL, • 15 μg/mL Primary Antibody

5.3.6.5 Is the Gold Enhancement Mediated Through the Biotin / Streptavidin Couple?

To prove that the gold labelling of the biotinylated antibody was due to coupling via the biotin / streptavidin linkage alone, it was necessary to test any enhancement of the monoclonal antibody unmodified *vs* the enhancements already gained from this data for the biotinylated antibody. The results are summarised in Table 5.12.

Table 5.12 Gold Signal Enhancement Ratios for Un-Modified Antibody and Biotinylated Antibody

	Un-Modified	Biotinylated
Flow Cell 2	1.05	2.2
Flow Cell 3	1.02	2.18

The very small enhancement in the monoclonal un-modified antibody was due to a very small amount of non-specific binding. One can therefore conclude that practically all labelling binding was mediated by the biotin-streptavidin interaction and there was negligible non-specific binding between primary antibody and gold.

5.3.6.6 Gold Level / Response Relationship with Use of PEG-400

Now that the PEG-400 treatment had been successfully employed to reduce non-specific binding, a new gold dilution response curve could be produced. The total response curve is given below in Figure 5.24. When checked against the new antibody concentration curve plot (Figure 5.21), the 0.15 point compared very closely to that predicted by the equations. A more pronounced drop could be seen in the curve at lower gold dilutions here than previously, and once again the 0.15 dilution was revealed as the best dilution as 0.25 was producing little extra enhancement despite using nearly twice as much gold.

5.3.6.7 Attempts to Remove Non-specific Binding of the Antibody

Results have indicated that there was some non-specific binding of the primary antibody to the surface. To construct assays with still lower primary antibody concentrations using the sequential binding format and the biotin/streptavidin couple, this non-specific binding may need to be removed. Attempts were made to remove this by adding in PEG to the antibody solution but this appears to have had no real effect. The progesterone itself at high concentrations seemed to produce some non-specific binding but this does not account for all the non-specific binding observed.

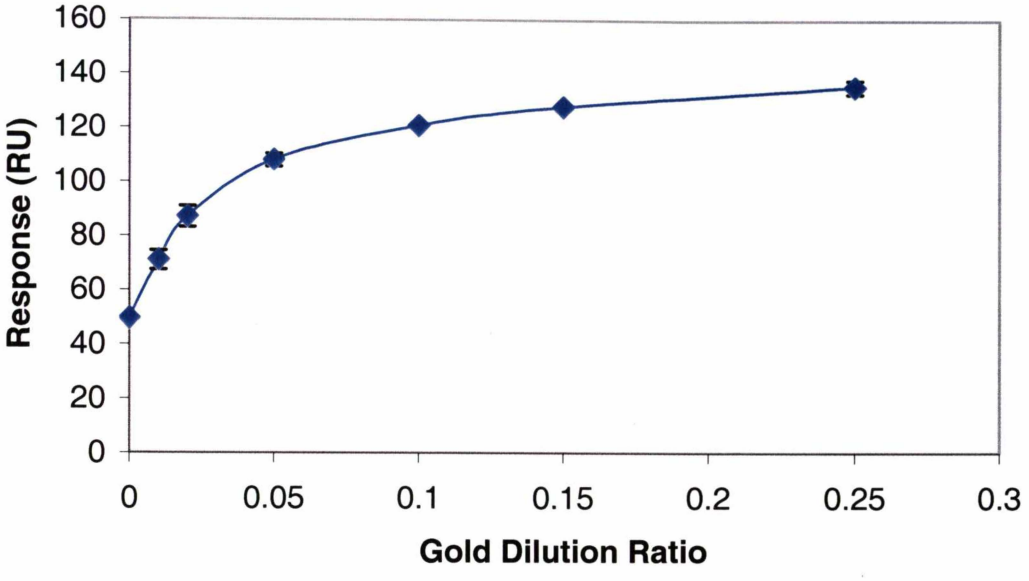

Figure 5.24 Plot of Response (RU) *vs* Gold Dilution Ratio with New Non-Specific Binding Treatment

5.3.6.8 Another Low Monoclonal Antibody Progesterone Assay

The 7.5 μg/mL primary antibody assay method was repeated using the PEG-400 treatment to reduce non-specific binding to see if this would improve the assay results. This method produced good progesterone assay standard curves with almost all CVs equal to or less then 5%. The assay curves are given in Figure 5.25.

Whilst the IC_{50} for this format was somewhat lower than that above, the LOD was not statistically any different from that achieved without the PEG-400 treatment. From the graph, it can be seen that the non-specific binding was no more than 16 RU.

The parameters for this assay are given below in Table 5.13.

5.3.6.9 20 nm Colloid Sequential Binding – Will the Larger Colloid Substantially Improve Enhancement?

It was of interest to examine the effects of increasing the colloid size used for labelling to see if this would greatly improve the binding enhancement under the

sequential injection format. To this end injections of 30 and 60 μL of streptavidin-gold 20 nm were made. The binding results showed that increasing the gold volume had no effect on the enhancement obtained and that these enhancements ranged from 1.5-2.3-fold, *i.e.* less than or similar to the 10 nm colloid.

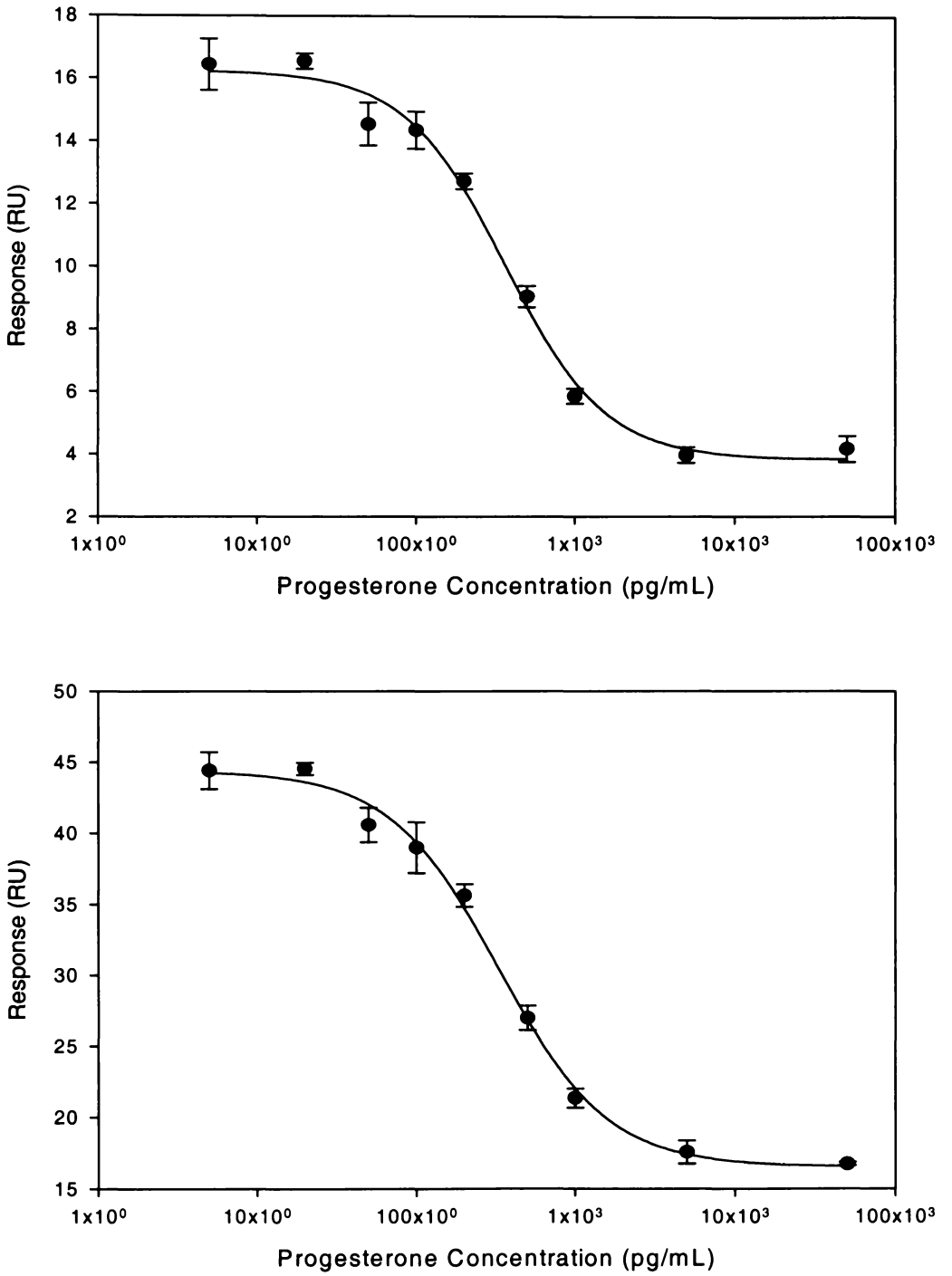

Figure 5.25 Assay Standard Curves. Primary Antibody Only (Top), Gold Signal-Enhanced (Bottom)

Table 5.13 Progesterone Assay Parameters

	Primary mAb	Total
LOD (pg/mL)	55 ± 15	12.8 ± 5.2
IC_{50} (pg/mL)	366 ± 15	328 ± 15
Dynamic Range	20-1000 pg/mL	20-1000 pg/mL
Average CV	4.6%	2.8%
Sensitivity (RU.mL/ng)	9.4	20

The surface was then injected with 0.5 dilution 20 nm colloid (1%v/v PEG-400 total, 0.2 M EG total, 30 μL) and this gave next to no non-specific binding (0.4 RU in flow cell 2 and 1.1 RU in flow cell 3) so the enhancement was antibody-streptavidin gold mediated. Non-specific binding actually appears to be less of a problem than for 10 nm.

So, there has been some improvement in the enhancement ratio but there was still not much more than the 0.15 dilution gives for the 10 nm colloid. The increase in enhancement for a doubling of the injection volume (0.25 dilution) was quite small so further increases in the injection volume are not likely to improve the 20 nm gold enhancement and will only waste gold.

The reason for the lower than expected 20 nm colloid enhancement is possibly that the larger size of the colloid is sterically blocking binding more than for the 10 nm colloid, and so fewer colloid particles are bound, but those that are bound give higher signal enhancement. To see if such steric hindrance could be minimised by lowering the binding concentration of colloid, the dilution was changed to 0.25 (1%v/v PEG-400 total, 0.2 M EG total, 120 μL, 20 μL/min, instead of 60 μL) but this made no difference.

It was thought that putting very concentrated gold in a shorter injection over the surface may improve response enhancement. To this end, a 15 μL injection of un-diluted 20 nm gold was used as label at a flow rate of 20 μL/min. This was then followed by a check for non-specific binding with un-diluted 20 nm colloid (15 μL, 20 μL/min) and gave non-specific binding of around 11 RU. There was a slight increase in the enhancement to 2.42 (correcting for non-specific binding). This was still only a little higher (~0.3) than the 10 nm colloid and the sensorgram

showed binding had just about reached equilibrium so minimal further enhancement could be expected by increasing the injected volume.

It is possible that further increasing the colloid size beyond 20 nm may produce further enhancement, as the larger colloids have been demonstrated in previous studies with large molecules to produce more enhancement. The results with 20 nm are not promising though and there are potential problems with larger sizes as they may result in regeneration or non-specific binding problems or sterically crowd each other around the surface.

5.3.7 Secondary Antibody Labelling

5.3.7.1 The Secondary Antibody Labelling Effect

The biotin/ streptavidin couple has demonstrated enhancement of the binding signal of primary antibody when applied in a sequential format. It is of interest to consider how use of a different binding couple to label the primary antibody binding interaction with the surface may be used to achieve signal enhancement. Another method of labelling is to use secondary antibody directed to the primary antibody. This secondary antibody can increase the bound mass on the surface by binding the primary antibody. In this case, one would use anti-rat IgG, as the primary antibody has been raised in rat. The secondary antibody has mass comparable to the primary antibody, and so one would expect an approximately two-fold enhancement of signal upon secondary antibody binding, assuming a 1:1 binding interaction.

This method of labelling was employed in the progesterone system by injecting secondary antibody solution at high concentration immediately after the primary antibody in the same fashion as for the sequential binding format detailed above. A sensorgram of the binding interactions is given in Figure 5.26.

It can be seen that the secondary antibody binding was very high relative to the primary antibody binding and had achieved maximum binding of the primary antibody as evidenced by the levelling off of the binding response. The secondary antibody had been injected at a flow rate of 10 μL/min to maximise the labelling, as it was found in testing that 20 μL/min resulted in a much lower enhancement.

This was probably because the primary / secondary antibody binding interaction is weaker than the biotin/ streptavidin binding interaction, and so in the flow-through format more exposure time to the surface was needed to effect good binding enhancement. Regeneration of the binding was easily achieved using the same regeneration cocktail as was used for the gold experiments. Regeneration, as shown in Figure 5.26, was complete after just one pulse.

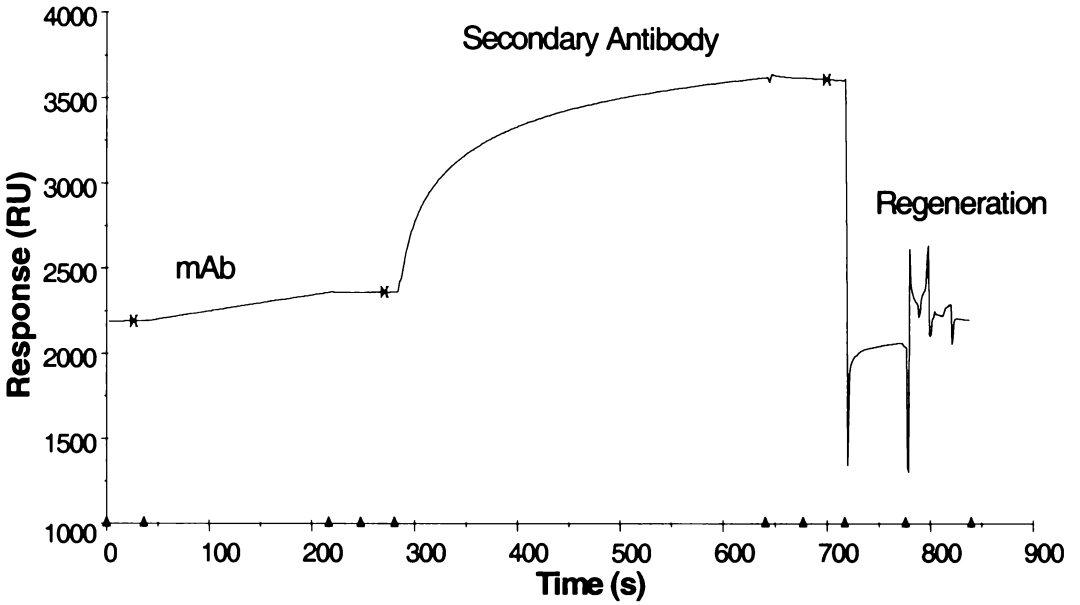

Figure 5.26 Sensorgram of the Binding of Primary mAb (25 μg/mL) Followed by Secondary Antibody (800 μg/mL) and then Regeneration

To determine the effect of secondary antibody concentration on the level of signal obtained, a plot was prepared at varying concentrations of secondary antibody with fixed primary antibody (25 μg/mL). This plot is given in Figure 5.27.

It can be seen that both total binding signal and enhancement ratio increase rapidly with increasing secondary antibody concentration until they level off at high secondary antibody concentrations corresponding to saturation binding of the primary antibody on the surface. Some testing was done at concentrations above 800 μg/mL but showed no significant further increases in signal. One can see clearly from this plot that the enhancement ratios rise up much higher than 2, indicating that there is far more enhancement of signal than would be expected

from a simple 1:1 binding of secondary antibody to the primary antibody. The reason for such a high signal enhancement is not clear and has not to the author's knowledge been reported before, but it may be caused by several secondary antibody molecules binding one primary antibody molecule. Enhancements of 7-8-fold have clearly been obtained with this format.

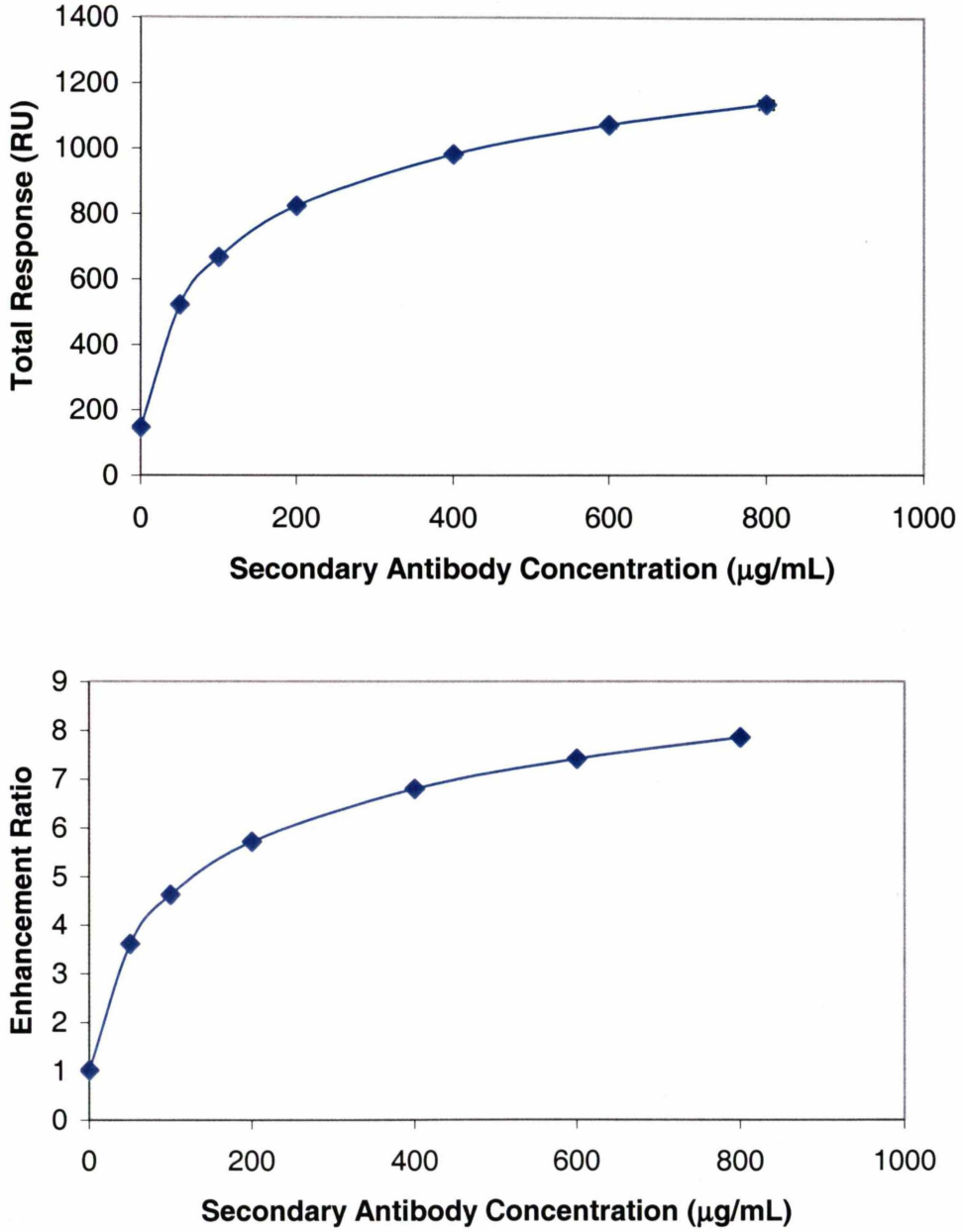

Figure 5.27 Plot of Total Binding Signal *vs* Secondary Antibody Concentration (µg/mL) (Top) and Enhancement Ratio *vs* Secondary Antibody Concentration (Bottom)

5.3.7.2 Secondary Antibody Signal Enhancement of Primary Antibody Binding

To determine the exact enhancement ratio at fixed secondary antibody concentration, and to show the relationship between primary antibody concentration and total response, a plot of response *vs* primary antibody concentration was prepared, Figure 5.28.

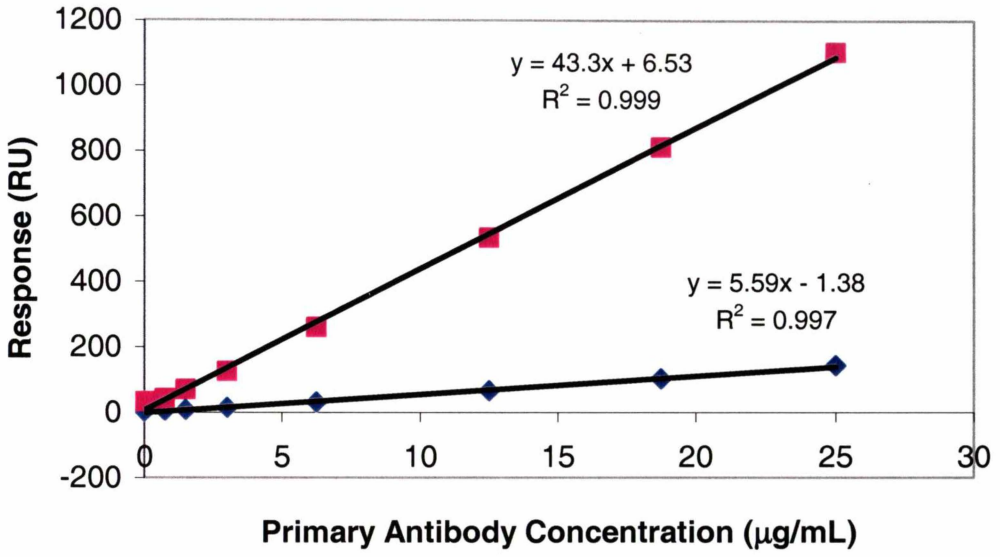

Figure 5.28 Antibody Binding Plot of Response (RU) *vs* Primary Antibody Concentration (µg/mL). ♦ Primary Antibody Response, ■ Total Response

From this plot, it can be seen that the primary antibody only and secondary antibody enhanced binding responses were linear with increasing primary antibody concentration up to 25 µg/mL ($R^2 > 0.99$). The slope of the secondary antibody enhanced plot was 7.7 times that of the primary antibody plot, indicating 7.7-fold signal enhancement and further confirming the results in Figure 5.27. The non-specific binding of the secondary antibody enhanced signal was only 6.5 RU, very small relative to the total signal. On the basis of these data, one could now proceed to constructing assays for progesterone using secondary antibody signal enhancement.

5.3.7.3 Progesterone Assay Using Secondary Antibody Signal Enhancement

Progesterone assays were performed at two concentrations of primary antibody (3 and 25 µg/mL final injected concentration). The assay curves for these two assays are given in Figure 5.29.

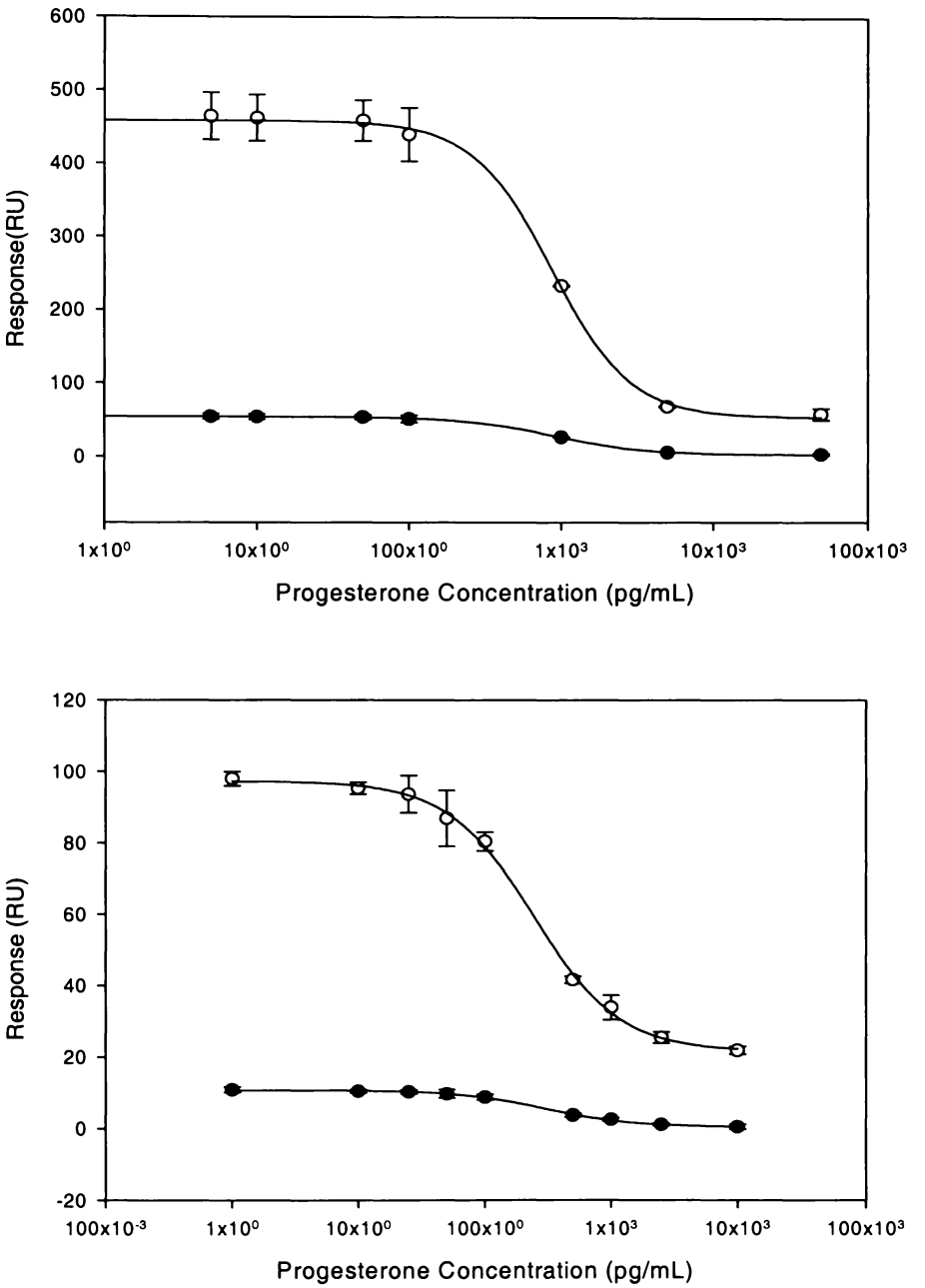

Figure 5.29 Progesterone Assay Standard Curves for 25 µg/mL Primary Antibody (Top) and 3 µg/mL Primary Antibody (Bottom). ♦ Primary Antibody, o Secondary Antibody-Enhanced

The 25 μg/mL assay had a high slope sensitivity caused by high binding responses over a relatively narrow dynamic range. The LOD of the assay (246 ± 41 pg/mL) was indistinguishable from the corresponding un-labelled assay (197 ± 18 pg/mL) as the CVs for the unlabelled assay were adequate to get good LOD and the labelling was only increasing the slope sensitivity. The 3 μg/mL assay was another situation altogether. In this case, the LOD (20.1 ± 4.0 pg/mL) was significantly lower than the corresponding un-labelled assay (46 ± 10 pg/mL) (one-tailed t-test *P* value of 0.04). This arises as the higher signal brings about better CV and thus lower LOD.

The LOD drops from the 25 to the 3 μg/mL assay in rough proportion to the drop in primary antibody concentration, but the IC_{50} does not drop as much. The slope sensitivity of the 3 μg/mL assay was roughly 2.5 times that of the 10 nm sequential binding biotin/streptavidin assay at 2.5 μg/mL. Theoretically, if gold labels are applied to the secondary antibody then one should observe further signal enhancement from the SPR-active nanoparticle. The secondary antibody concentration was dropped to 400 μg/mL for the assay using 3 μg/mL primary antibody.

5.3.7.4 Non-Specific Binding and Regeneration

The secondary antibody has bound the surfaces with very little non-specific binding. No additives were needed to minimise non-specific binding. The secondary antibody format developed here was a quick and simple assay format that generated substantial signal enhancement without needing the use of gold nanoparticles. The format was generically applicable to other small molecule systems such as that detailed in Chapter 3 for estradiol. Regeneration could be very effectively achieved with the same regeneration cocktail as used previously with the gold, and the surface continued to demonstrate excellent stability and consistent antibody binding responses. The CVs for these bindings were all quite low, averaging about 5%.

The assay parameters are given in Table 5.14.

Table 5.14 Assay Parameters for Secondary Antibody Signal Enhancement

mAb Concentration (μg/mL)	LOD (pg/mL)	IC50 (pg/mL)	Sensitivity (RU.mL/ng)	Enhancement Ratio
3	20.1 ± 4.0	242.8 ± 5.1	99	8
25	246 ± 41	865 ± 63	226	8

5.3.8 Secondary Antibody-Gold Signal Enhancement

5.3.8.1 Colloid Production and Sizing

To produce even higher signal enhancement than that obtained with the secondary antibody alone, gold labels were attached to the secondary antibody to examine the level of signal enhancement that could be obtained. The first step in doing this was to produce gold sols of well-defined size.

The citrate reduction method of Frens[230] is an excellent method of producing gold sols in the size range of 20-70 nm. By simply adjusting the volume of citrate solution added to a fixed amount of gold, the colloid size can be altered using a reflux method. To ensure against aggregation, and that a consistent colloid size can be obtained, it was necessary to wash all glassware used with aqua regia to remove all traces of metals on the surface of the glassware. Glassware used in these experiments was washed between every colloid batch produced. All colloids were made to the same gold concentration (0.01%w/v of the $HAuCl_4$, compensating for water of hydration).

The colloids, once cooled, were adjusted for any water losses due to evaporation and were then analysed by the Malvern Zetasizer™. The Zetasizer results could, for all colloids, be done without prior centrifugation or filtering and there were very few large particles formed in the colloids. The sizings matched the Frens method determinations quite closely but tended to suggest that the colloids were on the whole larger than the desired size thus requiring slight changes to the citrate loadings used to ensure the correct size colloids were produced.

As a validating comparison, commercially produced 20 nm gold conjugates that had been sized by TEM were analysed in the Zetasizer. This showed that for

colloid sized by TEM as 19 ± 2.1 nm, the Zetasizer gave 23.0 ± 1.0 nm $n = 30$, *i.e.* the sizings were statistically indistinguishable (values are mean ± SD). This demonstrates the robustness of using the Zetasizer to size the gold sols.

Attempts to produce colloids larger than 70 nm were fraught with problems, as they very easily aggregated under the reaction conditions and also were very hard to produce repeatably, as very small variations in the citrate quantity could produce very large variations in colloid size at low citrate loadings.

The changing sizes could be easily distinguished by the naked eye and a photograph indicating some of the different colloid sizes is given in Figure 5.30.

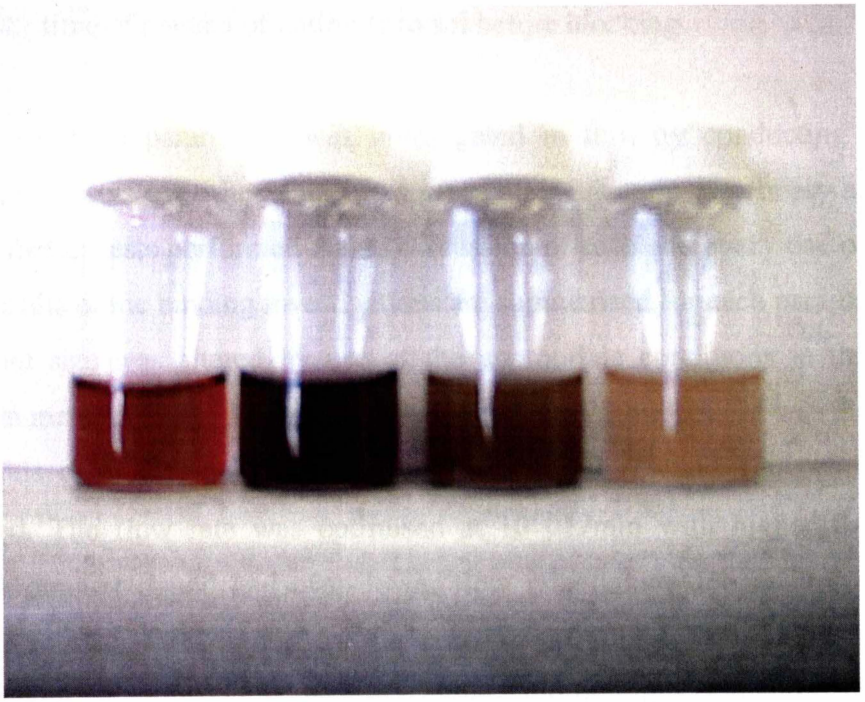

Figure 5.30 Gold Colloid Sizes, Left to Right: Approximately 25, 50, 70, 120 nm

5.3.8.2 Optimisation of Gold-Secondary Antibody Conjugate Production

To produce gold nanoparticle-secondary antibody conjugates which would perform optimally as signal enhancement agents, and to develop the conditions for their use, a large number of parameters had to be optimised. These parameters are listed below.

i. colloid nanoparticle diameter

ii. binding flow rate

iii. gold dilution factor
iv. additives needed to minimise non-specific binding
v. regeneration conditions
vi. concentration of the original colloid
vii. antibody coating concentration
viii. pH used for conjugation
ix. level of BSA blocking agent
x. use of centrifugation
xi. use of sonication
xii. use of azide preservative
xiii. time of contact of antibody to sol before blocking

Each of these parameters was investigated in turn by conducting binding studies of the sols over the SPR chip surface after injection of primary antibody. The number of tests performed makes discussion of each and every one overlong, so the results of the binding investigations are summarised for each parameter.

Colloid size was altered by use of the appropriate conditions in the citrate reduction method. Overall, it was concluded that the 25 nm colloid was the best to use in this case. Sizes of approximately 25, 40, 50, 70 and 120 nm were all examined. The flow rate was optimised at 10 μL/min with higher flow rates reducing amount bound and even lower flow rates taking too much time. The lower flow rate was needed as the secondary antibody / primary antibody interaction is not as strong as the streptavidin / biotin interaction and the gold sol may have been slightly sterically hindering approach of the labelling antibody. It was found that either not diluting the gold at all, or using a 0.5 dilution was best for maximum binding response (see Sections 5.2.9.3-5.2.9.5). The agent used to minimise non-specific binding was 10% v/v PEG-400 for experiments with centrifugal purification and 1%v/v PEG-400 without purification, added straight to the gold-antibody with loadings optimised by binding tests. Other agents tried but not used included 1-octanthiol, PEG-600 diacid, and PEG-4000. Regeneration was achieved with the same regeneration cocktail as used previously (200 mM NaOH, 20%v/v MeCN). Sols were used both as produced and 5x concentrated from their original citrate reduction concentration (concentrated by centrifugation

with PEG-400, 3%v/v) and the 5x concentrated method was found to give slightly higher binding though it did not raise the binding by 5-fold; see Section 5.3.8.4.

The optimal antibody coating concentration for the sols was found to be 900 μg/mL for the purified sol and 8 mg/mL was used for the non-purified sol (concentrations before adding to gold). These concentrations were sufficient to prevent aggregation by NaCl addition. The pH used for the sol on conjugation was pH 8.6 for the purified sol and pH 8.5 for the non-purified. The pH of the antibody solution was 7.2 for the purified sol and 8.5 for the non-purified. In order to optimise the binding of the protein to the sol, the pH should be above the pI of the protein. The typical pI range for IgG is 5.8-7.3. The bovine serum albumin which was used to block the un-bound sites on the sol and so reduce non-specific binding, was applied at 2.5%w/v final concentration for the purified sample and 0.2%w/v final concentration for the un-purified sample.

Centrifugation up to 13k x g was found to have no effect on the integrity of the antibody being conjugated. Sonication also seemed to have minimal effect, as did addition of azide. The amount of time in which the antibody was exposed to the sol before blocking, was found to have a strong effect on the binding intensity of the gold-antibody conjugate. Long, *i.e.* 18 h, binding times at 4 °C were needed to ensure that the antibody was optimally bound to the colloid surface. Only then could BSA blocking agent be applied and the colloid centrifuged if necessary. Attempts to use shorter times before blocking resulted in much lower signal enhancement, due most probably to lower antibody adsorption on the sol.

5.3.8.3 Signal Enhancement with Purification of Un-Bound Secondary Antibody

At first, the secondary antibody-gold conjugate was formed with a step to centrifugally remove any un-bound anti-rat IgG. This enabled the binding enhancement possible with anti-rat IgG-gold alone to be determined. The colloid's signal enhancement was then plotted, Figure 5.31.

This plot shows that the level of enhancement obtained with secondary antibody-gold with removal of unbound antibody is 3.5-fold. This is far less than that obtained by the secondary antibody at 800 μg/mL. The reason for this lower enhancement was that the gold colloid cannot adsorb the entire secondary

antibody that was mixed with it, and so a significant proportion of the antibody was washed away during the centrifugal purification. The only way to further improve the signal enhancement is to either increase the size of the sol at the same particle concentration, or increase the particle concentration of the sol. Both these methods can lead to aggregation of the colloid, which will affect the binding responses obtained and may clog the integrated microfluidics cartridge (IFC) of the BIAcore. It seems that the surface area of the gold sol is a limiting factor in the level of adsorption of the antibody and thus in the level of signal enhancement that can be obtained.

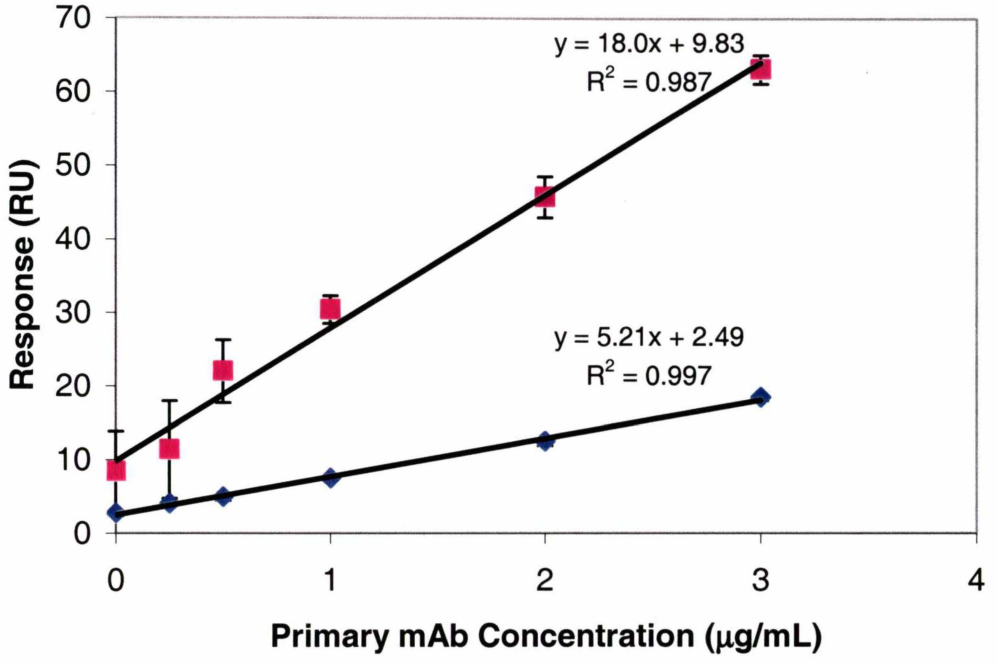

Figure 5.31 Antibody Binding Plot. ♦ Primary Monoclonal Antibody Only, ■ Total Response With Secondary Antibody-Gold Enhancement

The non-specific binding of this colloid, whilst being only 10 RU, was significant relative to the amount of signal response obtained, though this may not necessarily affect an assay. There is no point in doing an assay using these conditions as the level of enhancement is not superior to that of secondary antibody alone and so it cannot be expected that the LOD will be any better as the primary antibody concentration cannot be lowered any further with this enhancement.

5.3.8.4 Signal Enhancement Without Purification of Secondary Antibody – Colloid Sizes

To determine the actual level of enhancement a gold colloid will give to the secondary antibody, it was necessary to compare the gold-secondary antibody labelling to secondary antibody alone at the same final concentration. To do this, one cannot purify out unbound secondary antibody, but rather must leave all the antibody in place.

In such a format, one should first consider the best colloid size to use in the labelling. Previous reports have suggested that larger colloid sizes can allow better SPR signal enhancement increasing from 30-59 nm on a 47 nm gold film.[210] To determine if colloid size was important, a plot was prepared to compare colloid size to signal obtained for five different colloid sizes. They were compared at both the concentrations produced by the citrate method and 5-fold concentrated (by centrifugation with 3%v/v PEG-400 to prevent aggregation). Naturally, as the gold loading was the same for all colloids produced, the particle concentration will be lower for larger colloids, however not so large as to not be compensated for significantly by a five-fold concentration of the colloid. The plot is given in Figure 5.32.

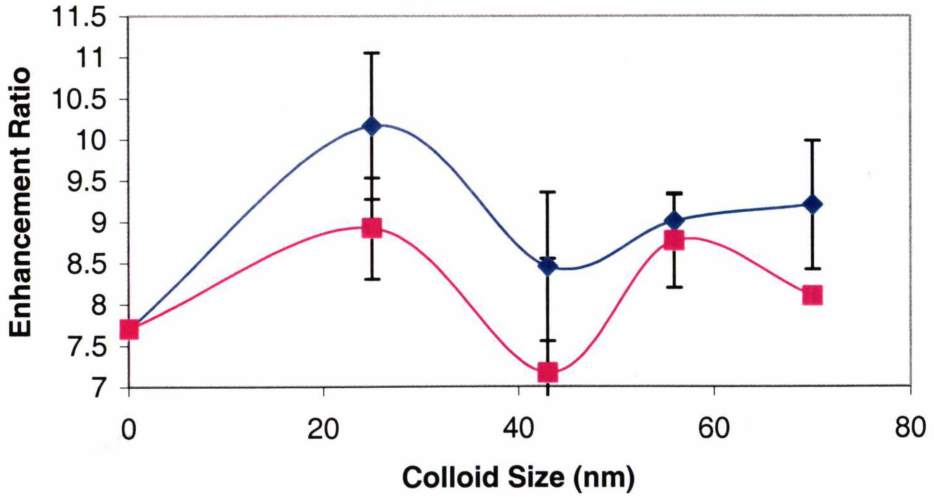

Figure 5.32 Plot of Signal Enhancement *vs* Colloid Size (nm). ■ Non-Concentrated ♦ 5-fold Concentrated

One can see from this plot that the five-fold concentration has made very little difference to the enhancement obtained and furthermore, there is no statistically significant difference between the sizes. This effect may be produced by the sol being a larger distance out from the surface than was previously reported for protein work. As the larger sols are much more prone to aggregation, it was decided to keep using the 25 nm sol, which was comparatively stable.

5.3.8.5 Assay Using 25 nm Sol-Secondary Antibody Without Centrifugal Purification

Having decided on the colloid size to use, it was then necessary to determine the level of enhancement that could be obtained with the conjugate. The antibody binding plot is given in Figure 5.33.

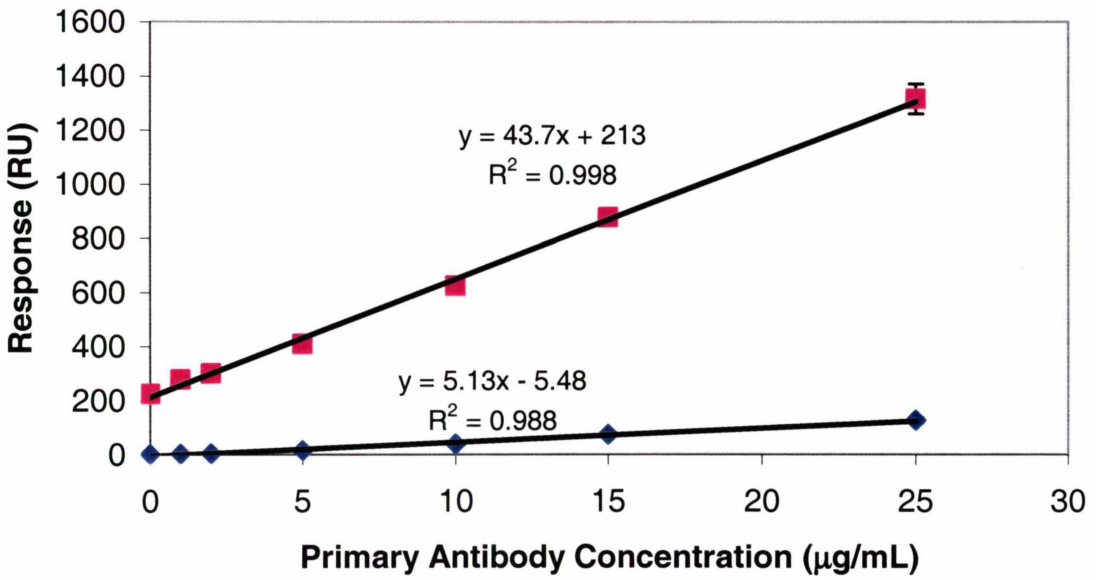

Figure 5.33 Antibody Binding Plot for 25 nm Gold-Secondary Antibody Enhancement

The signal enhancement observed here is 8.5-fold, much better than that obtained for the purified gold-secondary antibody conjugate, but seemingly not much better than the secondary antibody alone. The gold sol gives some significant non-specific binding (about 200 RU) and this may affect low-level antibody assays. To get a true picture of the enhancement ratio it was wise to perform the assay and assess the actual enhancement of the active region of the

curve, which up until now has been the same as that computed from the antibody binding plot.

A progesterone assay was then constructed using the 25 nm gold-secondary antibody conjugate at the same secondary antibody loading as the original secondary antibody-only assays. The primary antibody concentration used was 1.5 μg/mL (final injected concentration). The assay standard curve for flow cell 3 is given in Figure 5.34. The assay parameters from flow cell 3 are summarised in Table 5.15.

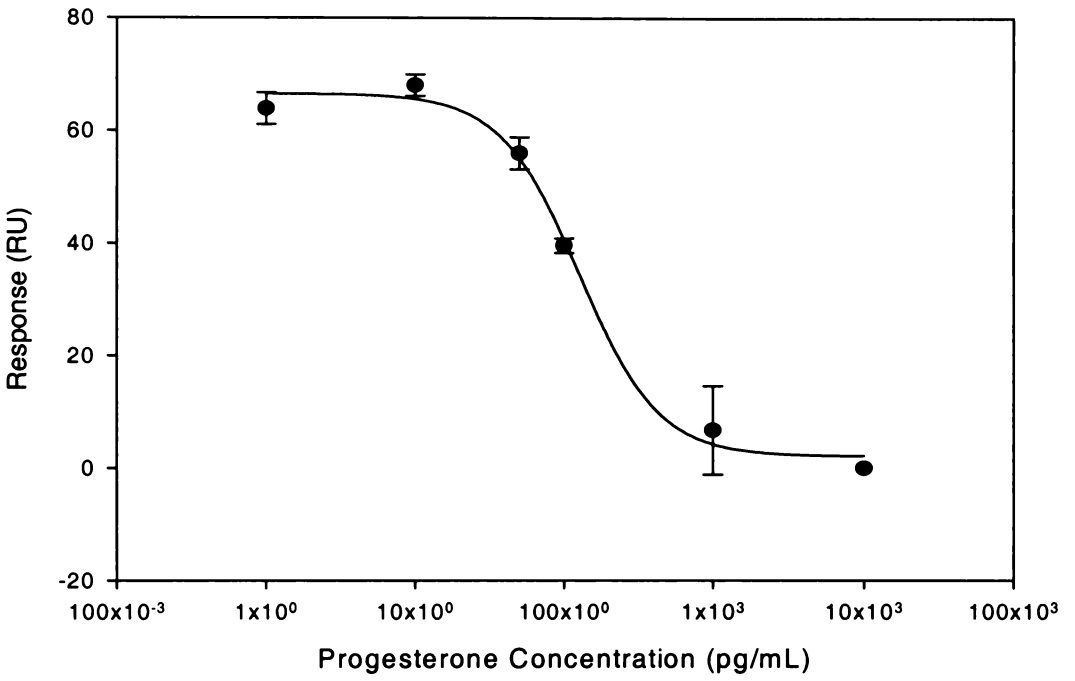

Figure 5.34 Assay Standard Curve for 25 nm Gold-Secondary Antibody-Enhanced Assay

The enhancement ratio of this assay is 13-fold, much higher than the antibody binding plot suggested, and the highest signal enhancement ratio yet attained in these studies. The LOD was 8.6 ± 3.2 pg/mL, which was the lowest LOD yet attained, and shows very clearly that higher signal enhancement can lead to better LOD through reduction in primary antibody concentration. This LOD was about what one would expect given that the assay uses half the primary antibody concentration of the 3 μg/mL secondary antibody enhanced assay, and that gave an LOD of 20.1 ± 4.0 RU. The IC_{50} had also decreased with the decreasing primary antibody concentration. This lower curve position, coupled with the

sustained binding signal has led to the highest assay slope sensitivity of this study (308 RU.mL/ng). Clearly this assay format has given the best performance overall and shows that addition of the gold label to the secondary antibody can enhance the signal obtained to about 1.6-times that of the secondary antibody alone. Flow cell 3 gave slightly better assay performance than flow cell 2 for this assay only.

This assay does have some non-specific binding to the surface (~150 RU), but this does not appear to have affected the assay performance in any way and can just be subtracted out as has been done in Figure 5.34. It may be of interest in future to try and reduce this non-specific binding component.

Table 5.15 Assay Parameters for 25 nm Gold – Secondary Antibody-Enhanced Assay

mAb Concentration (µg/mL)	LOD (pg/mL)	IC50 (pg/mL)	Sensitivity (RU.mL/ng)	Enhancement Ratio
1.5	8.6 ± 3.2	151.7 ± 2.1	308	13

5.3.9 Overall Results Summary

To enable easier comparison of the assay data obtained, a table of the assay parameters for all the main assay formats is given in Table 5.16. The primary antibody concentrations given are the final concentrations after 1:1 mixing with progesterone solutions.

5.3.10 Regeneration Solutions

The successful regeneration of the biosensor surface was critical to maintaining repeatable antibody binding responses. The regeneration cocktail used in this study is a combination of strong base (200 mM NaOH) and the chaotrophic reagent acetonitrile. Acidic pH and weaker base have proven to be ineffective in regenerating the surface, and acetonitrile was also needed to achieve complete regeneration. This cocktail did not damage the surface to any appreciable extent and yet was very effective in removing bound gold label.

Table 5.16 Summary of the Assay Parameters for Each of the Progesterone Assay Formats

Assay Format	Primary Antibody Concentration (µg/mL)	LOD (pg/mL)	IC_{50} (pg/mL)	Sensitivity (RU.mL/ng)	Enhancement Ratio
Primary Antibody Only	43.75	387± 67	1060 ± 290	9.4	n/a
Pre-incubation 10nm	43.75	143 ± 35	1670 ± 100	57	1
Pre-incubation 20nm	43.75	198 ± 57	1910 ± 150	28	1
Sequential 10nm	15	150 ± 49	1000 ± 145	32	2
Sequential 10nm	7.5	23.1 ± 4.4	460 ± 16	40	2
Sequential 10nm	2.5	104 ± 40	314 ± 21	9.1	2
Secondary Antibody	3	20.1 ± 4.0	242.8 ± 5.1	99	8
Secondary Antibody	25	246 ± 41	865 ± 63	226	8
Secondary Antibody- Gold 25nm	1.5	8.6 ± 3.2	151.7 ± 2.1	308	13

[a] All errors quoted are standard errors

5.3.11 Statistics Discussion

A thorough statistical analysis of immunoassay data is important in drawing valid conclusions about the assay data and to make valid comparisons between different assay formats. It is necessary therefore to discuss the statistical methods employed in this study. The limit of detection (LOD) was computed as the concentration corresponding to the response value that is two standard deviations below the blank response value. This definition is one that is widely used for immunoassay[22, 128, 129] and ensures that the figure quoted is the minimum value the assay can distinguish from the blank. As the value is dependent upon the standard deviation of the blank, assays with better blank CV can give better LOD as can assays with steeper slopes in the assay curve close to the blank value. Limit of detection therefore is a combination of precision of the assay's concentration determination at low levels and the position of the assay curve. The errors in the LOD needed to be computed to give accurate comparisons of LOD. These were computed by translating the error in the response of a point nearest the LOD on the assay curve into error in the concentration by use of the 4-parameter logistic fitting equation. All the curve data have been fitted to 4-parameter logistic relationships and calculations made using their formula. The inhibitory

concentration at 50% bound (IC_{50}) is determined as a parameter of the curve fitting and so was not affected by non-specific binding. The errors in this parameter were computed in the same fashion as for the LOD. Sensitivity is a measure of the slope of the assay curve's linear region and shows how much signal response can be obtained per unit concentration change. It is affected by both the signal strength and the assay curve position. This means that if the active concentration region of the curve is lower then the sensitivity will be higher, and if the response is higher then the sensitivity will be higher. In comparison, the enhancement ratio is simply the ratio of enhanced signal over non-enhanced signal calculated by taking the ratio of the slopes of the antibody binding response plots or the assay response ranges. The active or dynamic region of the curve is the concentration band between 10-90% bound that in these studies has been referenced to the nearest standard at either end.

All comparisons of assay curves are validated by use of t-test. In most cases this was two-tailed, but in some cases as mentioned they are one-tailed (*i.e.* show that one average is higher than the other). In this chapter all the *P*-values ≤ 0.04, *i.e.* they meet the requirements for a statistically significant difference. All the errors quoted in the tables were standard errors.

5.4 Conclusions

SPR biosensors for small molecules have long suffered from poorer detection capability compared with more traditional ELISA techniques. Such biosensors exhibit limits of detection often many orders of magnitude higher than ELISA and have low signal strength due to their reliance on the primary antibody to produce signal through its mass. Whilst there have been extensive investigations of signal enhancement of large molecules through use of nanoparticle and other high mass labels, there has been a complete absence of successful studies directed to small molecule immunoassay. The importance of immunosensing of small molecules cannot be overlooked and so it is of clear interest to develop more sensitive SPR biosensor assays through the use of signal-enhancing labels.

In this study, a robust SPR chip surface has been constructed by covalently immobilising progesterone through an OEG linker to the chip surface in situ. This easily produced surface has proven to be stable for in excess of 1100 binding and

regeneration cycles without appreciable loss of antibody binding capacity. The biotin / streptavidin linkage has been used to attach gold nanoparticle labels to primary antibody. This was done firstly in a pre-incubation format where the LOD was significantly improved over non-labelled antibody but there was no overall signal enhancement. Both 10 nm and 20 nm colloids were used and showed no difference in enhancement. When applied in a sequential binding format, the gold labelling gave 2-fold signal enhancement and enabled substantial reduction in the concentrations of primary antibody used. This enabled the LOD to be reduced to as low as 23.1 $\pm$ 4.4 pg/mL.

Secondary antibody can also be used to label bound primary antibody and was used as a binding label giving an 8-fold signal enhancement. This enabled reduction of primary antibody sufficient to achieve LOD of 20.1 $\pm$ 4.0 pg/mL and slope sensitivities much higher than those for streptavidin-bound gold. Use of secondary antibody-gold conjugates with purification of the conjugates to remove unbound secondary antibody, resulted in enhancements of about 3-fold due to the limited ability of the colloid to adsorb antibody. When the secondary antibody-gold conjugate is used without purification at the same loadings as for the secondary antibody alone, the enhancement is improved to 13-fold and the LOD drops still further to 8.6 $\pm$ 3.2 pg/mL.

Conditions of regeneration, and additives to reduce non-specific binding have been developed and discussed. Full antibody binding studies have been conducted for each format and the effects of labelling concentrations have been examined.

This study represents the first successful report of gold nanoparticle signal enhancement of small molecule immunoassay using SPR and shows how technologies that until now have been limited to large molecules can be applied to small molecules. Such enhancements have been successfully achieved through use of a "double-linker" system whereby the antigen is projected from the sensor surface by one linker and the labelling particle has been spaced from the antibody by use of another linker or spacer. The major problems of surface stability, reliable regeneration, steric obstruction from labelling particles and reduction of non-specific binding have all been successfully addressed.

The formats developed here for progesterone are very generic in nature and can be applied to a whole range of different small molecule antigens through appropriate conjugation chemistries, and examples of this are clearly shown in

Chapters 3 and 4. High mass label signal enhancement of small molecule binding interactions has enormous future potential for the development of sensitive SPR immunosensors for small molecules. The limits of detection achieved in this study are comparable to or better than most ELISA for progesterone[11,15,74] and now enable SPR technology to compete on a more equal footing with ELISA in detection capability.

Chapter 6 – The Chemistry of Immunosensing

6.1 Chemistry and the Immunoassay

The development of biosensors that utilise immunochemical binding interactions has been greatly hindered by a number of fundamental problems. These include unstable sensor surfaces, poor signal on antibody binding, the ease with which antibodies can be destroyed, and difficulties with adapting to new biological media. ELISA continues to be the mainstay of the immunochemical diagnostics market as they demonstrate limits of detection and sensitivities superior to most biosensors. This is despite the major limitations of ELISA, *i.e.* that they are laboratory-based, labour intensive and can give unreliable signal responses.

If the immunosensor is to truly compete with ELISA then new technologies need to be developed to address the outstanding problems. The chemist is in a unique position to apply knowledge of organic and physical chemistry to solving some of these problems. It has been the principal objective of this thesis to logically develop new immunosensory systems that demonstrate clear advantages over existing technology through the application of organic chemistry and nanotechnology. All the parts of this thesis contribute to this, and taken together they demonstrate, in a wide range of applications, how new chemical architectures can improve immunosensing.

6.2 Protein Conjugate-Based Immunoassay of Whole Milk Progesterone

The development of protein conjugate-based ELISA has many advantages over enzyme-antigen conjugate-based systems. Progesterone-protein conjugates have been applied as coating antigens in ELISA of whole milk progesterone. Studies have been conducted that show a clear pattern of increasing antibody binding with increasing linker length of the conjugate in the whole milk medium up to 18-

atoms in linker length, in contrast with results previously reported in the aqueous medium. The detection limit of the immunoassay is considerably improved when the linker length is increased up to 18-atoms in length. An ELISA format was developed that requires no pre-dilution of milk samples and is rapid and does not require enzyme-antigen conjugates. The assay was validated against existing RIA, and variability and recovery values assessed. The immunoassay was applied to the detection of progesterone in bovine whole milk samples to form a profile of the estrous cycle of the cow.

This study demonstrates how re-designing the assay format can lead to improvement in the ELISA through elimination of the enzyme-antigen conjugate, production of a potentially more stable assay surface, generation of an assay with a broad detection range for full profiling of bovine estrous cycles and no pre-treatment of the milk samples. The assay system gives significant additional benefit to the farmer by making routine whole milk ELISA testing for progesterone much easier.

6.3 Thioether Derivatives of the Estrogens – Synthesis and Antibody Binding Studies

Attachment of linkers directly to the ring structure of a steroid enables immunogenic conjugates to be produced that do not modify existing functional groups and so closely resemble the free antigen. This enables production of immunogenic conjugates that can raise antibodies that are highly specific to the small molecule target. It also enables immobilisation of binding antigens on biosensor surfaces that demonstrate high binding strength to specific antibodies. Thioether derivatives at the 4-position of estradiol and estrone were synthesised through substitution of their corresponding bromo-derivatives. These compounds were then used to link to OEG linkers through NHS activation.

An SPR chip was immobilised with the estradiol derivative and compared to reference compounds conjugated through the 2-position by Mannich reaction and the 3-position by hemisuccinate conjugation through the 3-OH, also attached to the surface via OEG linkers. Antibody binding studies showed that conjugation at the 2-position by Mannich reaction gave 19% more binding than the thioether but

the hemisuccinate gave very little binding at all. This supports the theory that conjugation through functional groups will greatly reduce specific antibody binding in the flow-through format, and interestingly shows that binding to the 2-conjugate using an antibody produced to a 6-position conjugate still gives strong antibody binding. Sensitive estradiol assays could then be constructed from this surface.

This study shows how a rational consideration of the position of attachment can optimise the antibody binding strength in flow-through assays and gives important information on antibody binding properties to different conjugates. A sensitive SPR immunoassay of estradiol has been developed and through the use of secondary antibody labelling technology has an LOD of 25 pg/mL.

6.4 Catecholamine Thioether Linked Derivatives – Synthesis, Purification and Antibody Binding Studies

Attachment of linkers to the aromatic ring by formation of thioether bridges has been demonstrated for the catecholamines dopamine, nor-epinephrine and epinephrine. The use of electrolysis methods proved to be an efficient means of producing the thioether conjugates without degradation of the catecholamine. This was done through formation of the *o*-quinone followed by addition of the thiol. This was demonstrated for both three and 11-carbon thiol chains. Convenient purification was developed by ion-exchange chromatography, and reactions and separations monitored by HPLC. These compounds were then analysed by 2-dimensional NMR spectroscopy to help determine the position of attachment in each case. The dopamine-propionate derivative was used as coating antigen in the in situ immobilisation of the neurotransmitter using OEG and hexanediamine linkers and in comparing to conjugation through the amine. As the antibody was raised to glutaraldehyde-conjugated dopamine it exhibited highest binding to the amine-conjugated surface.

This study has demonstrated the synthesis of a new group of catecholamine-thioether derivatives tailored for use in bioconjugates that do not compromise existing functional groups on the catecholamine and may be used to raise specific antibodies, to construct enzyme or protein conjugates or immobilize onto the biosensor surface as coating antigens for better immunoassays in future.

6.5 Signal Enhancement of SPR Immunosensing of Small Biomolecules

The use of gold colloids to enhance the binding signal in SPR-based immunosensing of small biomolecules was examined in detail. Protein conjugates were initially used as coating antigens, but whilst they produced promising preliminary assay results, they were found to be unstable when exposed to gold colloids and the regeneration solutions needed. Similarly, progesterone-OEG-biotin used as a competitive agent with free progesterone for limited bound antibody and with signal enhancement via streptavidin-gold, was found to be unreliable because of denaturing of the immobilised antibody.

A novel covalent immobilisation system was developed for progesterone using attachment of an OEG linker at the 4-position and in situ immobilisation of the amine terminus of the chain on the dextran surface by NHS mediated coupling. This produced a surface capable of withstanding more than 1100 binding and regeneration cycles without loss of binding capacity. The surface was employed in two labelling formats. In the first, biotinylated monoclonal antibody was pre-incubated with streptavidin-gold and the labelled antibody used in an assay of progesterone. This produced no signal enhancement but enabled reduction of the detection limit to as low as 143 pg/mL. In the second format, free progesterone competed with bound progesterone for binding to biotinylated antibody and the bound biotinylated antibody was labelled by passing over streptavidin-gold. This resulted in a two-fold signal enhancement and enabled the detection limit to be reduced to 23.1 pg/mL through reduction of primary antibody concentration.

Enhancement of the binding interaction of eight-fold was achieved with use of secondary antibody as the label in a sequential binding format. The use of secondary antibody-labelled gold sols resulted in a four-fold enhancement of signal when the excess secondary antibody was removed and a 13-fold signal enhancement when the secondary antibody total concentration was set the same as for the assay with secondary antibody alone. In none of the formats, except the protein conjugate or progesterone-biotin conjugate work, was increasing colloid size from 10 nm for streptavidin-biotin labelling or 25 nm for secondary antibody labelling seen to improve the degree of enhancement.

Treatments for regeneration of the surface and the minimisation of non-specific binding were examined in full, as was confirmation of the nature of the labelling interactions, and optimisation of antibody coating in secondary antibody-mediated gold coupling.

This study represents the first successful nanoparticle signal enhancement of small molecule SPR-based immunoassay and demonstrates how careful chemical design of the assay system through use of a double-linker format can allow the use of nanoparticle enhancement for small molecules causing large-scale signal enhancement and improvements in assay performance including a reduction in limit of detection of about two orders of magnitude.

6.6 Future Work

There is a large number of different possibilities for future research building on the work of this thesis. In the area of milk progesterone immunoassay, the development of SPR-based biosensors around 4-position attachment to the steroid offers great promise in the development of sensitive and stable biosensing systems, particularly through the OEG intermediate linkage system. The protein-conjugate method of ELISA immobilisation has been much underused and there is great potential for expanding ELISA technologies based on this system to a range of other targets and media.

In the field of estrogen A-ring-linked conjugates, there is the possibility of forming drug conjugates to the estrogens using this attachment and linker technology and to direct them to estrogen receptors *in vivo* for the purposes of treating diseases where these receptors proliferate, *e.g.* breast cancer. The OEG linker offers much promise here because of its low immunogenicity and its inertness and water solubility.

In the field of catecholamine thioethers there is also the possibility of developing drug conjugates analogously to the estrogens or attaching chemiluminescent agents for the study of brain tissues *in vitro*.

The field of gold-labelled SPR interactions of small biomolecules for immunoassay is completely new as this work represents the first SPR immunosensing system to demonstrate this nanoparticle signal enhancement for

small biomolecules, a significant challenge in terms of binding, surface stability and labelling techniques. The possibilities for future research stemming from this are large. The generic in situ chemical immobilization techniques developed open up the possibility of adapting this technology for other small molecule targets. The adaptation of these systems to a non-BIAcore format will be a major future step in developing this technology for practical on-site biosensors.

The diagnostics market for small biomolecules is huge and encompasses a wide range of technologies. This thesis has concentrated on addressing some fundamental questions about the design of small molecule immunoassays and has shown how currently used formats and methods may be substantially improved by the rational application of chemical knowledge to the study and development of immunosensing systems. It is anticipated that the ability of the chemist to further augment and improve immunodiagnostics is immense, with this thesis providing just a small example of what can be gained by rational engineering and fundamental studies of the chemical factors affecting immunochemical interactions in the immunobiosensor.

References

1. Gopel, W.; Schierbaum, K.-D. Chapter 1. Definitions and Typical Examples: In: Gopel, W.; Hesse, J.; Zemel, J. N. Sensors A Comprehensive Survey – Chemical and Biochemical Sensors Part I. VCH Verlagsgesellschaft mbH and VCH Publishers Inc., Weinheim, Germany, **1991**, ISBN 3-527-26768-9, 1-6.
2. Bilitewski, U. ed.; Chapter 2. Technical Principles and Chapter 3. Biochemical Principles: In: Bilitewski, U.; Turner, A. P. F. ed. Biosensors for Environmental Monitoring. Amsterdam, Harwood Academic Publishers The Netherlands, **2000**, ISBN 90-5702-449-7.
3. Ferguson, J.; Boles, C.; Adams, C.; Walt, D. R. A Fiber-optic DNA Biosensor Microarray for the Analysis of Gene Expression. *Nature Biotechnology*. **1996**, *14*, 1681.
4. Pandey, P.; Weetall, H. Detection of Aromatic Compounds Based on DNA Intercalation Using an Evanescent Wave Biosensor. *Anal. Chem.*, **1995**, *67*, 787-792.
5. Chen, R. J.; Bangsaruntip, S.; Drouvalakis, K. A.; Wong Shi Kam, N.; Shim, M; Li, Y.; Kim, W.; Utz, P. J.; Dai, H. Noncovalent Functionalisation of carbon Nanotubes for Highly Specific Electronic Biosensors. *Proc. Natl. Acad. Sci.* **2003**, *92*, 4984-4989.
6. Sellergren, B. ed. Chapter 2. Fundamental Aspects on the Synthesis and Characterization of Imprinted Network Polymers: In: Molecularly Imprinted Polymers Man-Made Mimics of Antibodies and their Applications in Analytical Chemistry. Elsevier Science B.V., Amsterdam, The Netherlands. **2001**, ISBN 0-444-82837-0.
7. Basic Immunochemistry: In: Products for Life Science Research – Sigma Aldrich. Sigma Aldrich, **2003**, 632-634.
8. Kimball, J. W. Introduction to Immunology, Second Edition. Macmillan Publishing Company, New York, USA. **1986**, ISBN 0-02-363830-3.
9. Berson, S. A.; Yallow, R. S. Immunoassay of Endogenous Plasma Insulin in Man. *J. Clin. Invest.* **1960**, *39*, 1157-1175.

10. Mitchell, J. S. Evaluation of Progesterone – Ovalbumin Conjugates with Different Length Linkers in Enzyme-Linked Immunosorbent Assay and Surface Plasmon Resonance-Based Immunoassay – Thesis, Master of Science and Technology, **2001**.

11. Elliott, C. T.; Francis, K. S.; Shortt, H. D.; McCaughey, W. J. Determination of the Concentrations of the Steroids Estradiol, Progesterone and Testosterone in Bovine Sera: Comparison of Commercial Dissociation Enhanced Lanthanide Fluorescence Immunoassay Kits with Conventional Radio and Enzyme Immunoassays. *Analyst*, **1995**, *120*, 1827-1830.

12. Dray, F.; Andrieu, J.; Renaud, F. Enzyme Immunoassay of Progesterone at the Picogram Level Using β-galactosidase as Label. *Biochim. Biophys. Acta*, **1975**, *403*, 131-138.

13. Nakamura, R. M.; Kasahara, Y.; Kasahara, Y.; Ishikawa, E. Chapters 8, 9 and 10: In: Nakamura, R. M.; Kasahara, Y.; Rechnitz, G. A., edit. Immunochemical Assays and Biosensor Technology for the 1990's. American Society for Microbiology, **1992**, ISBN 1-55581-040-3, 149-203.

14. Piran, U.; Riordan, W. J.; Livshin, L. A. New Non-competitive Immunoassays of Small Analytes. *Clin. Chem.*, **1995**, *41*(7), 986-990.

15. Wu, Y.; Mitchell, J. S.; Cook, C. J.; Main, L. Evaluation of Progesterone – Ovalbumin Conjugates with Different Length Linkers in Enzyme-Linked Immunosorbent Assay and Surface Plasmon Resonance-Based Immunoassay. Steroids, **2002**, *67*(7) 565-572.

16. Cook, C. J.; Wu, Y.; Mitchell, J. S. Kinetic Assay. Patent No.: WO02092631, **2002**.

17. Foulds, N. C.; Frew, J. E.; Green, M. J. Immunoelectrodes: In: Cass, A. E. G., editor. Biosensors – A Practical Approach. Oxford, UK: Oxford University Press, **1990**, ISBN 0-19-963047-X, 100.

18. Self, C. H.; Cook, D. B. Advances in Immunoassay Technology. *Curr. Opin. Biotechnol.*, **1996**, *7*(1), 60-65.

19. Sansonno D.; Lauletta G.; Dammacco F. Detection and Quantitation of HCV Core Protein in Single Hepatocytes by Means of Laser Capture

Microdissection and Enzyme-Linked Immunosorbent assay. *J Viral Hepat.* **2004**, *11*(1), 27-32.

20. Self, C. H.; Dessi, J. L.; Winger, L. A. High-Performance Assays of Small Molecules: Enhanced Sensitivity, Rapidity, and Convenience Demonstrated with a Non-Competitive Immunometric Anti-Immune Complex Assay System for *Digoxin. Clin. Chem.* **1994**, *40*(11) 2035-2041.

21. Tanaka M.; Matsuo K.; Enomoto M.; Mizuno K. A Sol Particle Homogeneous Immunoassay for Measuring Serum Cystatin C. *Clin Biochem.* **2004**, *37*(1) 27-35.

22. Van de Wiel, D. F. M.; Koops, W. Development and Validation of an Enzyme Immunoassay For Progesterone in Bovine Milk or Blood Plasma. *Anim. Reprod. Sci,* **1986**, *10*, 201-213.

23. Adamczyk, M.; Chen, Y.; Grote, J.; Mattingly, P. G. *O*-(Fluoresceinylmethyl)hydroxylamine (OFMHA): A Reagent for the Preparation of Fluorescent *O*-(fluoresceinylmethyl)oxime (FMO)-Steroid Conjugates. *Steroids* **1999**, *64*, 283-290.

24. Adamczyk, M.; Grote, J.; Mattingly, P. G.; Pan, Y. *O*-(Acridinium)hydroxylamine (AHA): a Reagent for the Preparation of Chemiluminescent Acridinium Oxime (AO)-Steroid Conjugates. *Steroids* **2000**, *65*, 387-394.

25. Chapter 2: In: Eggins, B. Biosensors – An Introduction. John Wiley and Sons Ltd and B.G. Teubner, Chichester, UK, **1996**, ISBN 0-471-96285-6, 13-30.

26. BIAcore; Surface Plasmon Resonance Biosensors; Internet Document; BIAcore, Uppsala, Sweden; http://www.biosensor.com/bio/plasm.htm.

27. Homola, J.; Yee, S. S.; Gauglitz, G. Surface Plasmon Resonance Sensors: Review. *Sensor. Actuat. B-Chem.* **1999**, *54*, 3-15.

28. Mullett, W.; Lai, E. P. C.; Yeung, J. M. Immunoassay of Fumonisins by a Surface Plasmon Resonance Biosensor. *Anal. Biochem.,* **1998**, *258*, 161-167.

29. Pena, D.; Goodrich, G.; He, L.; Lyon, L. A.; Musick, M.; Holliway, W. D.; The Penn Stat Research Foundation, Natan, M.J. Biosensing Using Surface Plasmon Resonance. Patent No.: WO 01/35081 A1. **2001**.

30. Stenberg, E.; Persson, B.; Roos, H.; Urbaniczky, C. Quantitative Determination of Surface Concentration of Protein with Surface Plasmon Resonance Using Radiolabelled Proteins. *J. Colloid Interface Sci.,* **1991**, *143*, 513-526.

31. Jordan, C. E.; Corn, R. M. Surface Plasmon Resonance Imaging measurements of Electrostatic Biopolymer Adsorption onto Chemically Modified Gold Surfaces. *Anal. Chem.* **1997**, *69*, 1449-56.

32. Kieser, B; Fietzek, C.; Schmidt, R.; Belge, G.; Weimar, U.; Schurig, V.; Gauglitz, G. Use of a Modified Cyclodextran Host for the Enantioselective Detection of a Halogenataed Diether as Chrial Guest via Optical and Electrical Transducers. *Anal. Chem.* **2004**, *74*, 3005-3012.

33. McCormick, A. N.; Leach, M. E.; Savidge, G.; Alhaq, A. Validation of a Quantitative SPR Assay for Recombinant FVIII. *Clin. Lab. Haematol.*, **2004**, *26*(1) 57-64.

34. Zhang, Q.; Pan, R. M.; Ge Y. C.; Xu, P. Expression of the Soluble Extracellular Domain of Human Thrombopoietin Receptor Using a Maltose-Binding Protein-Affinity Fusion System. *Biol. Pharm. Bull.* **2004**, *27*(2) 219-21.

35. Kai, E.; Sawata, S.; Ikebukuro, K.; Iida, T.; Honda, T; Karube, I. Detection of PCR Products in Solution Using Surface Plasmon Resonance. *Anal. Chem.* **1999**, *71*, 796-800.

36. Chen, S.; Yu, Q.; Li, L.; Boozer, C. L.; Hormola, J.; Yee, S. S.; Jiang, S. Detecting the Adsorption of Dye Molecules in Homogeneous Poly(propylene imine) Dendrimer Monolayers by Surface Plasmon Resonance Sensor. *J. Am. Chem. Soc.***2002**, *124*, 3395-3401.

37. Myszka, D. G.; Rich, R. L. Implementing Surface Plasmon Resonance Biosensors in Drug Discovery. *Pharm. Sci. Technol. Today*, **2000**, *3*(9), 310-317.

38. Mullet, W. M.; Lai, E. P. C.; Yeung, J. M. Surface Plasmon Resonance-Based Immunoassays. *Methods,* **2000**, *22* 77-91.

39. Turner, A. P. Biosensors – Sense and Sensitivity. *Science 290* 1315-1317.

40. BIAcore, Determination of Low Molecular Weight Analytes in Serum Using Real-Time BIA, Application Note 202, BIAcore, Uppsala, Sweden.

41. Johnsson, B.; Lofas, S.; Lindquist, G. Immobilisation of Proteins to a Carboxymethyldextran-Modified Gold Surface for Biospecific Interaction Analysis in Surface Plasmon Resonance Sensors. *Anal. Biochem.* **1991**, *198*, 268-277.

42. Chapter 6: In: BIAapplications Handbook, BIAcore Inc., Uppsala, Sweden, 6-1-6-9.

43. Daly, S. J.; Keating, G. J.; Dillon, P. P.; Manning, B. M.; O'Kennedy, R.; Lee, H. A.; Morgan, M. R. A. Development of Surface Plasmon Resonance-Base Immunoassay for Aflatoxin B_1. *J. Agric. Food Chem.*, **2000**, *48*(11), 5097-5104.

44. Wilson, S.; Howell, S. High-throughput Screening in the Diagnostics Industry. *Biochem. Soc. Trans.* **2002** *30*(4) 794-7.

45. Canziani, G. A.; Klakamp, S.; Myszka, D. G. Kinetic Screening of Antibodies from Crude Hybridoma Samples Using Biacore. *Anal. Biochem.* **2004** *325*(2) 301-7.

46. Coille, I.; Gauglitz, G.; Hoebeke, J. Characterisation of Antibodies and Analytes by Surface Plasmon Resonance for the Optimisation of a Competitive Immunoassay Based on Energy Transfer. *Anal. Bioanl. Chem.* **2002**, *372*, 293-300.

47. Cook, C. J. Real-time Measurement of Corticosteroids in Conscious Animals Using an Antibody-Based Electrode. *Nature Biotechnol.* **1997**, *15*, 466-471.

48. Porter, R.; van der Logt, P.; Howell, S.; Kyrolainen-Reay, M.; Badley, A. An Electro-active System of Immuno-assay (EASI assay) Utilising Self Assembled Monolayer Modified Electrodes. *Biosens. Bioelectron.* **2001**, *16*, 875-885.

49. Ekins, R. P. Ligand Assays: from Electrophoresis to Miniaturized Microarrays. *Clin. Chem.* **1998**, *44*(9), 2015-2030.

50. Ekins, R. P. Immunoassay, DNA Analysis, and Other Ligand Binding Assay Techniques: from Electropherograms to Multiplexed, Ultrasensitive Microarrays on a Chip. *J. Chem. Ed.* **1999** *76*(6) 769-780.

51. Gudgin, E. F.; Pollak, A.; Diamandis, E. P. Ultrasensitive Bioanalytical Assays Using Time-Resolved Fluorescence Detection. *Pharmac. Ther.* **1995**, *66*, 207-235.

52. Butenandt, A.; Westphal, U.; Hohlweg, W. *Z. Physiol.*, **1934**, *227*, 84.

53. Allen, W. M.; Wintersteiner, O. *Science*, **1934**, *80*, 190.

54. Slotta, K. H.; Ruschig, H.; Fels, E. *Ber.*, **1934**, *67*, 1270.

55. Hartmann, M.; Wettstein, A. *Helv.*, **1934**, *17*, 1365.

56. Heap, R. B.; Flint, A. P. F. Chapter 6 Progesterone: In: Austin, C. R., Short, R. V., editors. Reproduction in Mammals, Volume 7 Mechanisms of Hormone Action. Cambridge University Press, Cambridge, U. K. **1979**, ISBN 0 521 29737 0, 185-232.

57. Peters, A. R. Hormonal Control of the Bovine Oestrous Cycle I. The Natural Cycle. *Bri. Vet. J.*, **1985**, *141*, 564-575.

58. Bevers, M. M.; Dieleman, S. J.; van den Hurk, R.; Izadyar, F. Regulation and Modulation of Oocyte Maturation in the Bovine. Theriogenology, **1997**, *47*, 13-22.

59. Driancourt, M.; Thuel, B. Control of Oocyte Growth and Maturation by Follicular Cells and Molecules Present in Follicular Fluid. A Review. *Reprod. Nutr. Dev.*, **1998**, *38*, 345-362.

60. Hsueh, A. J. W.; Billig, H.; Tsafriri, A. Ovarian Follicle Atresia: A Hormonally Controlled Apoptotic Process. *Endocr. Rev.*, **1994**, *15*(6), 707-724.

61. Driancourt, M. A. Follicular Dynamics in Sheep and Cattle. Theriogenology, **1991**, *35*(1), 55-69.

62. Diskin, M. G., Sreenan, J. M. Expression and Detection of Oestrus in Cattle. *Reprod. Nutr. Dev.* **2000**, *40*, 481-491.

63. Ginther, O. J.; Knopf, L.; Kastelic, J. P. Temporal Associations Among Ovarian Events in Cattle During Oestrous Cycles With Two and Three Follicular Waves. *J. Reprod. Fertil.* **1989**, *87*, 223-230.

64. O'Connor, M. Heat Detection and Timing of Insemination for Cattle. Extension Circular 402. **1993** Pennsylvania State University, University park, USA.

65. Roosenschoon, P.; Verstege, A.; N. V. Nederlandsche Aparatenfabriek Nedap, Netherlands. Method to Determine Progesterone in Raw Milk. Patent No.: WO 01/14887 A1, **2001**.

66. Foote, R. H.; Oltenacu, E. A. B.; Kummerfeld, H. L.; Smith, R. D.; Riek, P. M.; Braun, R. K. Milk Progesterone as a Diagnostic Aid. *Bri. Vet. J.*, **1979**, *135*, 550-557.

67. Lamming, G. E.; Bulman, D. C. The Use of Milk Progesterone Radioimmunoassay in the Diagnosis and Treatment of Subfertility in Dairy Cows. *Bri. Vet. J.*, **1976**, *132*, 507-517.

68. Boland, M. P.; Lonergan, P.; O'Callaghan, D. O. Effect of Nutrition on Endocrine Parameters, Ovarian Physiology, and Oocyte and Embryo Development. *Theriogenology*, **2001**, *55*, 1323-1340.

69. Senger, P. L. The Oestrus Detection Problem: New Concepts, Technologies and Possibilities. *J. Dairy Sci.*, **1994**, *77*, 2745-2753.

70. Nebel, R. L.; Dransfield, M. G.; Jobst, S. M.; Bame, J. H. Automated Electronic Systems for the Detection and Timing of AI in Cattle. *Anim. Reprod. Sci.* **2000**, *60-61*, 713-723.

71. Suzuki, Y.; Hayashi, N.; Sekiba, K. Automated Direct Assay System for the Measurement of Sex Steroid Hormones Using High-Performance Liquid Chromatography. *J. Chrom.* **1988**, *426*, 33.

72. Schwarzenberger, F.; Son, C. H.; Pretting, R.; Arbeiter, K. Use of Group-Specific Antibodies to Detect Fecal Metabolites During the Estrus Cycle of Cows. *Theriogenology* **1996**, *46*, 23-32.

73. Bulman, D. C. The Measurement of Progesterone in Milk. *Bri. Vet. J.* **1979**, *135*, 460-1.

74. Prakash, B. S.; Meyer, H. H. D.; van de Wiel, D. F. M. Sensitive Enzyme Immunoassay of Progesterone in Skim Milk Using Second-Antibody Technique. *Anim. Reprod. Sci.* **1988**, *16*, 225-235.

75. Waldmann, A. Monoclonal Antibodies to Progesterone: Characterization and Selection Enzyme Immunoassay in Bovine Milk. *Hybridoma* **1999**, *18*(3), 289-296.

76. Ball, P. J. H. Milk Progesterone Profiles in Relation to Dairy Herd Fertility. *Bri. Vet. J.* **1982**, *138*, 546-551.

77. Pennington, J. A.; Spahr, S. L.; Lodge, J. R. Influences on Progesterone Concentration in Bovine Milk. *J. Dairy Sci.* **1981**, *64*, 259-266.

78. O'Connor, M. L. Milk Progesterone Analysis for Determining Reproductive Status. **1998** Department of Dairy and Animal Science Pennsylvania State University, University Park, USA. DAS 98-5 1-5.

79. Chapter 4: In: Toko, K. Biomimetic Sensor Technology. Cambridge, UK: Cambridge University Press, **2000**, ISBN 0 521 59342 5, 77-90.

80. Claycomb, R. W., Delwiche, M. J. Biosensor for On-Line Measurement of Bovine Progesterone During Milking. *Biosens. Bioelectron.*, **1998** *13*(11), 1173-1180.

81. Claycomb, R. W.; Delwichie, M. J.; Munro, C. J.; BonDurant, R. H. Enzyme Immunoassay for On-Line Sensing of Milk Progesterone. *Trans. ASAE* **1996**, *39*(2), 729-734.

82. Delwiche, M; Tang, X.; BonDurant, R.; Munro, C. Improved Biosensor for Measurement of Progesterone in Bovine Milk. *Trans. ASAE* **2001**, *44*(6), 1997-2002.

83. Delwiche, M.; Tang, X.; BonDuranr, R.; Munro, C. Estrus detection with a Progesterone Biosensor. *Trans. ASAE* **2001**, *44* (6) 2003-2008.

84. Pemberton, R. M.; Hart, J. P.; Mottram. An Electrochemical Immunosesnor for Milk Progesterone Using a Continuous Flow System. *Biosens. Bioelectron.* **2001**, *16*, 715-723.

85. Katoch, R.; Korde, S. S.; Deodhar, K. D.; Trivedi, G. K. Synthesis of Potential Pregnenolone and Progesterone Spin Probes for Biomembranes and Immunoassays. *Tetrahedron* **1999,** *55*, 1741-1754.

86. Gillis, E. H.; Gosling, J. P.; Sreenan, J. M.; Kane, M. Development and Validation of a Biosensor-based Immunoassay for Progesterone in Bovine Milk. *J. Immunol. Methods* **2002**, *267*, 131-138.

87. Sternesjo, A.; Mellgren, C.; Bjorck, L. Determination of Sulfamethazine Residues in Milk by a Surface Plasmon Resonance-Based Biosensor Assay. *Anal. Biochem.* **1995**, *226*, 175-181.

88. Homola, J.; Dostalek, J.; Chen, S.; Rasooly, A.; Jiang, S.; Yee, S. S. Spectral Surface Plasmon Resonance Biosensor for Detection of Stapylococcal Enterotoxin B in Milk. *Int. J. Food Microbiol.*, **2002**, *75*, 61-69.

89. Waldmann, A. Enzyme Immunoassay (EIA) for Milk Progesterone Using a Monoclonal Antibody. *Anim. Reprod. Sci.* **1993**, *34*, 19-30.

90. Hermanson, Greg T. Chapter 10: In: Bioconjugate Techniques. Academic Press, San Diego, USA. **1996**, ISBN 0-12-342335-X, 460.

91. Paek, S. Enhanced Performance of Immunoassays with Affinity-Purified Analyte-Enzyme Conjugates as Signal Generators. *Bull. Korean Chem. Soc.* **1997**, *18*(5), 515-519.

92. Paek, S.; Bachas, L. G.; Schramm, W. Defined Analyte-Enzyme Conjugates as Signal Generators in Enzyme Immunoassays. *Anal. Biochem.* **1993**, *210*, 145-154.

93. Glass, T. R.; Saiki, H.; Blake, D.; Blake II, R. C.; Lackie, S. J.; Ohmura, N. Use of Excess Solid-Phase Capacity in Immunoassays: Advantages for Semicontinuous, Near-Real-Time Measurements and for Analysis of Matrix Effects. *Anal. Chem.*, **2003**, *98*, 4205-4210.

94. Pennington, J. A.; Spahr, S. L.; Lodge, J. R. Factors Effecting Progesterone in Milk for Pregnancy Diagnosis in Dairy Cattle. *Brit. Vet. J.* **1976**, *132*(5) 487-495.

95. Thibier, M.; Fourbet, J. F.; Parez, M. Relationship Between Milk Progesterone Concentration and Milk Yield, Fat and Total Nitrogen Content. *Brit. Vet. J.* **1976** *132*(5) 477-486.

96. Ndlovu, P.; Kurtz, D. A.; Rosenberger, J. L. Chapter 20 Calibration of Enzyme-Linked Immunosorbent Assay Data Via a Four Parameter Logistic Regression Model. In: Kurtz, D. A. edit.; Skerritt, J. H. edit.; Stanker edit., L. New Frontiers in Agrochemical Immunoassay. **1995**, Aoac Int. Ltd. ASIN 0935584587 283-303.

97. Rodbard, D.; Frazier, G. R. [1] Statistical Analysis of Radioligand Assay Data. *Methods Enzymol.* **1975**, *37* Pt B, 3-22

98. Raghava, G. P. S.; Joshi, A. K.; Angrewala, J. N. Calculation of Antibody and Antigen Concentrations from ELISA Data Using a Graphical Method. *J. Immunol. Methods* **1992**, *153*, 263-264.

99. Dudley, R. A.; Edwards, P.; Ekins, R. P.; Finnery, D. J.; McKenzie, I. G. M.; Raab, G. M.; Rodbard, D.; Rodger, R. P. C. *Clin. Chem.* **1985**, *31*(8) 1264-1271.

100. Cox, N. Statisticians Notes on ELISA Standard Curve Error Analysis. **2003.**

101. Butenandt, A. *Naturwiss.* **1929**, *17*, 879.

102. MacCorquodale, D. W. J. Biol. Chem. **1936** *115*, 435.

103. Stanczyk, F. Z.; Cho, M. M.; Endres, D. B.; Morrison, J. L.; Patel, S.; Paulson, R. J. Limitations of Direct Estradiol and Testosterone Immunoassay Kits. *Steroids* **2003**, *68*, 1173-1178.

104. Cros, P.; Kururst, R.; Battail, N.; Piga, N.; Bio Merieux, France. Process and Device for Assaying a Hapten. US Patent No.: 5849480. **1998**.

105. Mabilat, C.; Cros, P.; Mandrand, B.; Charles, M. H.; Erout, M. N.; Pichot, C; Bio Merieux, France. Device for the Capture of Target Molecules and Capturing Process Using the Device. US Patent No.: 5723344. **1998**.

106. Sylvia, V. L.; Walton, J.; Lopez, D.; Dean, D. D.; Boyan, B. D.; Schwartz, Z. 17β-estradiol-BSA Conjugates and 17β-Estradiol Regulate Growth Plate Chondrocytes by Common Membrane Associated Mechanisms Involving PKC Dependent and Independent Signal Transduction. *J. Cell Biochem.* **2001**, *81*, 413-429.

107. Meltola, N.; Jauria, P.; Saviranta, P.; Mikola, H. Synthesis of Novel Europium-Labelled Estradiol Derivatives for Time-Resolved Fluoroimmunoassays. *Bioconjugate Chem.* **1999**, *10*, 325-331.

108. England, B.G.; Parsons, G.H.; Possley, R.M.; McConnell, D.S.; Midgley, A.R. Ultrasensitive Semiautomated Chemiluminescent Immunoassay for Estradiol. *Clin. Chem.* **2002**, *48*(9), 1584-6.

109. Kasiotis, K.; Magiatis, P.; Pratsinis, H.; Skaltsounis, A.; Abadju, V.; Charalambous, A.; Moutsatsou, P.; Haroutounian, S. Synthesis and Biological Evaluation of Novel Daunorubicin-estrogen Conjugates. *Steroids* **2001**, *66* 785-791.

110. Devraj, R.; Barrett, J. F.; Fernandez, J. A.; Katzenellenbogen, J. A.; Cushman, M. Design, Synthesis, and Biological Evaluation of Ellipticine-Estradiol Conjugates. *J. Med. Chem.* **1996**, *39*, 3367-3374.

111. Pinto, R.M.; Lerner, U.; Glauberman, M.; Pontelli. H. Influence of Estradiol-17-beta Upon the Oxytocic Action of Oxytocin in the Pregnant Human Uterus. *Am J Obstet Gynecol.* **1966**, *96*(6), 857-62.

112. Wang, C.; Zhao, M.; Cui, W.; Yang, J.; Peng, S. Studies on the Synthesis of Estrogen-GHRPS Linkers. *Syn. Commun.* **2003**, *33*(10), 1633-1641.

113. Baulieu, E. Chapter I Hormones: A Complex Communication Network and Milgrom, E. Chapter IX Steroid Hormones. In: Baulieu, E.; Kelly, P. A. edit. Hormones - From Molecules to Disease. Chapman and Hall Inc. New York, USA **1990**, 394.

114. Allen, R. M.; Redshaw, M. R. The Use of Homologous and Heterologous ^{125}I-radioligands in the Radioimmunoassay of Progesterone. *Steroids* **1978**, *32*(4), 467-86.

115. Janoski, A. H.; Shulman, F. C.; Wright, G. E. Selective 3-(*O*-carboxymethyl)-oxime Formation in Steroidal 3,20-diones for Hapten Immunospecificity. *Steroids* **1974**, *23*(1), 49-64.

116. Stalla, G.; Giesemann, G.; Mueller, O. A.; Wood, W. G.; Scriba, P. C. Non-extractive and Specific Radioimmunoassay for Cortisol: Results Using a Pure Cortisol C3 Derivative for Antigen and Tracer Production. Fresenius' Z. Anal. Chem. **1980**, *301*(2), 129.

117. Lindner, H. R.; Perel, E.; Friedlander, A.; Zeitlin, A. Specificity of Antibodies to Ovarian Hormones in Relation to the Site of Attachment of the Steroid Hapten to the Peptide Carrier. *Steroids* **1972**, *19*, 357-375.

118. Weinstein, A.; Lindner, H. R.; Friedlander, A.; Bauminger, S. Antigenic Complexes of Steroid Hormones Formed by Coupling to Protein Through Position 7: Preparation from Δ^4-3-oxosteroids and Characterisation of Antibodies to Testosterone and Androstenedione. *Steroids* **1972**, *20*, 789-812.

119. Yoshida, H.; Nakai, S.; Nimbari, F.; Yoshimoto, K.; Nishimura, T. Synthesis of 11α-Hydroxyprogesterone Haptens. *Steroids* **1989**, *53*(6), 727-738.

120. Hatzidakis, G.; Stefanakis, A.; Krambovitis, E. Comparison of Different Antibody-Conjugate Derivatives for the Development of a

Sensitive and Specific Progesterone Assay. *J. Reprod. Fertil.* **1993**, *97*, 557-561.

121. Wie, S. I.; Hammock, B. D. Comparison of Coating and Immunising Antigen Structures on the Sensitivity and Specificity of Immunoassays for Benzoyphenylurea Insecticides. *J. Agric. Food Chem.* **1984**, *32*, 1294-1301.

122. Hosoda, H.; Sakai, H.; Yoshida, S.; Miyairi, S.; Nambara, T. Sensitivity and Specificity in Enzyme Immunoassay of Testosterone. *Chem. Pharm. Bull. (Tokyo)* **1980**, *28*(10), 3035-40.

123. Sauer, M. J.; Foulkes, J. A.; O'Neill, P. M. Use of Microtitre Plate EIA For Direct Determination of Progesterone in Whole Milk: Application of Heterologous Systems for Improved Sensitivity. *Bri. Vet. J.* **1982**, *138*, 522-532.

124. Sauer, M. J.; Foulkes, J. A.; O'Neill, P. M. The Influence of Heterology, Enzyme Label and Assay Conditions on the Sensitivity of Microtitre Plate Enzymeimmunoassays for Progesterone in Milk. *J. Steroid Biochem.* **1989**, *33*(3), 433-438.

125. De Boever, J. G.; Kohen, F.; Bosmans, E. Antibody Binding Efficiency of Differently Labelled Steroid Hormones. *Analyt. Chim. Acta* **1993**, *275*, 81-87.

126. Roda, A.; Girotti, S.; Piacentini, A. L.; Preti, S.; Lodi, S. Development of a Sensitive, Direct Luminescent Enzyme Immunoassay for Plasma Estradiol-17 Beta. *Anal. Biochem.* **1986**, *156*, 267-73.

127. Marcus, G. J.; Durnford, R. Estradiol Assay by Microtitre Plate Enzyme Immunoassay. *J. Steroid Biochem.* **1988**, *29*, 207.

128. De Boever, J.; Kohen, F.; Bouve, J., Leyseele, D; Vandekerckhove, D. Direct Chemiluminescence Immunoassay of Estradiol in Saliva. *Clin. Chem.* **1990**, *36*, 2036-41.

129. Silvan, G.; Illera, J. C.; Illera, M. Determination of Follicular Fluid Estradiol Levels by Enzyme-Linked Immunosorbent Assay. *Steroids* **1993**, *58*, 324-329.

130. Webb, R.; Baxter, G.; McBride, D.; Nordblom, G. D.; Shaw, M. P. K. The Measurement of Testosterone and Oestradiol-17β using Iodinated

Tracers and Incorporating an Affinity Chromatography Extraction Procedure. *J. Steroid Biochem.* **1985**, *23*(6A), 1043-1051.

131. Rao, P. N.; Taraporewala, I. B. A Sensitive Enzyme-Linked Immunosorbent Assay (ELISA) for Testosterone: Use of a Novel Heterologous Hapten Conjugated to Penicillinase. *Steroids* **1992**, *57*, 154-161.

132. Franek, M.; Hruska, K. Characterization of Antibodies Against Oestrone-Azo-Protein Conjugates using ^{3}H and ^{125}I Radioligands. *J. Steroid Biochem.* **1983**, *19*(30), 1363-1370.

133. Nambara, T.; Numazawa, M.; Tanaka, T.; Ohkubo, T. Preparation of Specific Antisera to Estradiol 17-glucuronide. *J. Steroid. Biochem.* **1978**, *9*, 785-790.

134. Hosoda, H.; Kobayashi, N.; Nambara, T. Effect of Bridge Heterologous Combination on Sensitivity in Enzyme Immunoassay for 11-Deoxycortisol. *Chem. Pharm. Bull. (Tokyo)* **1983**, *31*(3), 953-958.

135. Hosoda, H.; Kawamura, N.; Nambara, T. Effect of Bridge Heterologous Combination in Enzyme Immunoassay for Cortisol. *Chem. Pharm. Bull.* **1981**, *29*(7), 1969-1974.

136. Bieniarz, C.; Husain, M.; Barnes, G.; King, C. A.; Welch, C. J. Extended Length Heterobifunctional Coupling Agents for Protein Conjugations. *Bioconjug. Chem.* **1996**, *7*, 88-95.

137. Podesta, A.; Nieri, P.; Luisi, M.; Montagnoli, G. Relevance of oestrone Presentation to the Specificity of the Ellicted Antisera, as Revealed by Affinity Separation. *J. Steroid Biochem. Molec. Biol.* **1993**, *46*(6) 847-850.

138. Zheng, H.; Weng, L.; Wang, G.; Deng, L. Studies on Polymer-Supported Drugs: Synthesis of Poly(ethylene glycol)-estrogen compounds. *Yaoxue Xuebao* **1987**, *22*(8), 637-640.

139. Lou, R.; Weng, L.; Zheng, H *Zhongguo Yaowu Huaxue Zazhi.* **1997**, *7*(1), 33-36.

140. Chen, Y.; Weng, L.; Zheng, H. Synthesis of Polyestrones. *Hecheng Huaxue* **2000**, *8*(2), 175-177.

141. Brooks, D. E.; van Alstine, James M.; Sharp, K. A.; Stocks, S. J. PEG-Derivatised Ligands with Hydrophobic and Immunological Specificity:

Applications in Cell Separation. In: Harris, J. M. edit. Poly(ethylene Glycol) Chemistry – Biotechnical and Biomedical Applications. **1992** Plenum Press New York, USA, ISBN 0-306-44078-4.

142. Harris, J. M.; Zalipsky, S. Poly(ethylene glycol) – Chemistry and Biological Applications. **1997** American Chemical Society Washington DC, USA ,ISBN 0-8412-3537-6.

143. Schaub, R.; Weiss, M. J. The Synthesis of Certain 7α-Alkylthio and 7α-Acylthio Steroid Hormone Derivatives. *J. Org. Chem.* **1961**, *26*, 3915-3925.

144. Hosoda, H.; Miyairi, S.; Nambara, T. Synthesis of Corticosteroid Haptens Possessing the Bridge at the C-4 Position. *Chem. Pharm. Bull. (Tokyo)* **1980**, *28*(4), 1294-1299.

145. Jellinck, P. H.; Lewis, J.; Boston, F. Further Evidence for the formation of an Estrogen-peptide Conjugate by Rat Liver *in Vitro*. *Steroids* **1967**, *10*, 329-46.

146. Jellinck, P. H.; Elce, J. S. Synthesis of Estrogen Glutathione and Cysteine Derivatives. *Steroids* **1969**, *13*, 711-718.

147. Ghaffari, M. A.; Abul-Hajj, Y. J. Reaction of Thiol Nucleophiles with 1,2-Epoxy- and 4,5-Epoxy-estrene-3-one-17β-ols. *J. Steroid Biochem.* **1990**, *37*(2), 237-244.

148. Slaunwhite, W. R.; Neely, L. Bromination of Phenolic Steroids I. Substitution of Estrone and 17β-Estradiol in Ring A. *J. Org. Chem.* **1962**, *27*(5), 1749-1752.

149. Utne, T.; Jobson, R. B.; Landgraf, F. W. The Synthesis of 2- and 4-Bromoestradiol. *J. Org. Chem.* **1968**, *33*, 1654-6.

150. Schwenk, E.; Castle, C. G.; Joachim, E. *J. Org. Chem.* **1963** *28* 136.

151. Page, P. C. B.; Hussain, F.; Bonham, N. M.; Morgan, P.; Maggs, J. L.; Park, B. K. Regioselective Synthesis of A-ring Halogenated Derivatives of 17α-Ethynyloestradiol. *Tetrahedron* **1991**, *47*(16/17), 2871-2878.

152. Numazawa, M.; Kimura, K.; Ogata, M.; Nagaoka, M. Reductive Dehalogenation of 2,4-Dihalogeno Estrogens Having a 3-Hydroxy Substituent by Formic Acid, Potassium Iodide, or Ascorbic Acid. *J. Org. Chem.* **1985**, *50*, 5421-5423.

153. Pert, D. J.; Ridley, D. D. An Alternative Route to 2-Bromo and 2-Iodoestradiols from Estradiol. *Aust. J. Chem.* **1987**, *40*, 303-309.

154. Numazawa, M.; Ogura, Y.; Kimura, K.; Nagaoka, M. *J. Chem. Res.* **1985**, 3701-3715.

155. Ali, H. van Lier, J. E. Reaction of benzeneselenenyl Halides with Estrogens *J. Chem. Soc. Perkin Trans. 1* **1991**, 269-271.

156. Lovely, C. J.; Bhat, A. S.; Coughenour, H. D.; Gilbert, N. E.; Bruggemeier, R. W. Synthesis and Biological Evaluation of 4-(Hydroxyalkyl)estradiols and Related Compounds. *J Med. Chem.* **1997**, *40*, 3756-3764.

157. Cook, C. E.; Tallent, C. R.; Christensen, H. D. Antigens from Synthetic and Natural Estrogens: Formation by Conjugation with Protein Through a Thiopropionic Acid Link. *Life Sci.* **1974**, *14*, 1075-1087.

158. Numazawa, M.; Madarame, M.; Ogata, M.; Kimura, K. Stereochemistry of Nucleophilic Substitution Reaction of 16-Bromo-17-oxo Steroids with Thiols. *J. Org. Chem.* **1984**, *49*, 3231-3233.

159. Miller, C. P.; Jirkovsky, I.; Tran, B. D.; Harris, H. A.; Moran, R. A.; Komm, B. S. Synthesis and Estrogenic Activities of Novel 7-thiosubstituted Estratrine Derivatives. *Bioorg. Med. Chem. Lett.* **2000**, *10*, 147-151.

160. Hanson, R. N.; Herman, L. W.; Fiaschi, R.; Napolitano, E. Stereochemical Probes for the Estrogen Receptor: Synthesis and Receptor Binding of (17α, 20E/Z)-21-phenyl-19-norpregna-1,3,5(10),20-tetraene-3,17β-diols. *Steroids* **1996**, *61*, 718-722.

161. Coille I.; Gauglitz G.; Hoebeke J. Characterisation of Antibodies and Analytes by Surface Plasmon Resonance for the Optimisation of a Competitive Immunoassay Based on Energy Transfer. *Anal. Bioanal. Chem.* **2002**, *372*(2), 293-300.

162. Adamczyk, M.; Chen, Y. Y.; Gebler, J.C.; Johnson, D.D.; Mattingly, P.G.; Moore, J. A.; Reddy, R. E.; Wu, J.; Yu, Z. Evaluation of Chemiluminescent Estradiol Conjugates by Using a Surface Plasmon Resonance Detector. *Steroids* **2000**, *65*(6), 295-303.

163. Usami, M.; Mitsunaga, K.; Ohno, Y. Estrogen Receptor Binding Assay of Chemicals with a Surface Plasmon Resonance Biosensor. *J. Steroid Biochem.* **2002**, *81*, 47-55.

164. Butala, H. D.; Sadana, A. A Fractal Analysis of Analyte-estrogen Receptor Binding and Dissociation Kinetics Using Biosensors: Environmental Effects. *J. Colloid Interf. Sci.* **2003**, *263*, 420-431.

165. Reichert, H. Introduction to Neurobiology **1992** Georg Thieme Verlag, Stuttgart, Germany, ISBN 3-13-784701-X.

166. Suszkiw, J. B. Chapter 40 Synaptic Transmission. In: Sperelakis, N. Cell Physiology Source Book. **1998** Academic Press, San Diego, USA, ISBN 0-12-656973-8 610-631.

167. Shen, X.-M.; Dryhurst, G. Synthesis, Redox Properties, *in vivo* Formation and Neurobehavioural Effects of *N*-acetylcysteinyl conjugates of Dopamine, Possible Metabolites of Relevance to Parkinson's Disease. *Chem. Res. Toxicol.* **1996**, *9*, 1117-1126.

168. Shen, X.-M.; Zhang, F.; Dryhurst, G. Oxidation of Dopamine in the Presence of Cysteine: Characterization of New Toxic Products. *Chem. Res. Toxicol.* **1997**, *10*(2), 147-155.

169. Shen, X.-M.; Dryhurst, G. Further Insights into the Influence of L-Cysteine on the Oxidation Chemistry of Dopamine: Reaction Pathways of Potential Relevance to Parkinson's Disease. *Chem. Res. Toxicol.* **1996**, *9*, 751-763.

170. Poirier, J.; Donaldson, J.; Barbeau, A. The Specific Vulnerability of the Substantia Nigra to MPTP is Related to the Presence of Transition Metals. *Biochem. Biophys. Res. Commun.* **1985**, *128*, 25-33.

171. Shen, Y.; Ye, M. Y. Determination of the Stability of Dopamine in Aqueous Solutions by High Performance Liquid Chromatography. *J. Liq. Chromatogr.* **1994**, *17*(7), 1557-1565.

172. Miwa, A.; Yoshioka, M.; Shirahata, A.; Tamura, Z. Preparation of Specific Antibodies to Catecholamines and L-3,4-Dihydroxyphenylalanine. I. Preparation of the Conjugates. *Chem. Pharm. Bull.* **1977**, *25*(8), 1904-1910.

173. Miwa, A.; Yoshioka, M.; Tamura, Z. Preparation of Specific Antibodies to Catecholamines and L-3,4-Dihydroxyphenylalanine. III. Preparation

of Antibody to Epinephrine for Radioimmunoassay. *Chem. Pharm. Bull.* **1978,** *26*(11), 3347-3352.

174. Smith, M. B.; March, J. March's Advanced Organic Chemistry – Reactions Mechanism and Structure 5th Edit. **2001** Wiley-Interscience, New York, ISBN 0-471-58589-0 1189.

175. Miwa, A.; Yoshioka, M.; Tamura, Z. Preparation of Specific Antibodies to Catecholamines and L-3,4-dihydroxyphenylalanine. II. The Site of Attachment on Catechol Moiety in the Conjugates. *Chem. Pharm. Bull.* **1978**, *9,* 2903-2905.

176. Geffard, M.; Kah, O.; Chambolle, P.; Le Moal, M.; Delaage, M. 1st Immunocytochemical Application of an Anti-Dopamine Antibody in the Study of the Central Nervous System. *Cr. Acad. Sci. III-Vie.* **1982**, *295*(13), 797-802.

177. Hirose, K. Akizawa, T.; Asada, K.; Tanaka, Y.; Negoro, Y.; Yoshioka, M. Synthesis of Antigens Conjugated with 3-methoxy-4-hydroxyphenylglycol by Mannich Reaction for Enzyme Immunoassay. *Anal. Chim. Acta* **1998**, *365* 137-145.

178. Merck Index, 12th Edition. Merck Research Laboratories, Whitehouse Station, USA. **1996,** 7956-7957.

179. Dalmaz, Y.; Peyrin, L. Specific Ion-exchange Chromatography and Fluorimetric Assay of Urinary 3-*O*-methyldopamine. *J. Chromatogr.* **1976**, *116*(2), 379-941.

180. Heidbreder, C. A.; Lacroix, L.; Atkins, A. R.; Organ, A. J.; Murray, S.; West, A.; Shah, A. J. Development and Application of a Sensitive High Performance Ion-exchange Chromatography Method for the Simultaneous Measurement of Dopamine, 5-hydroxytryptamine and Norepinephrine in Microdialysates from the Rat Brain. *J. Neurosci. Meth.* **2001**, *112*, 135-144.

181. Atack, C. V.; Magnusson, T. Individual Elution of noradrenaline (Together with Adrenaline), Dopamine, 5-hydroxytryptamine and Histamine from a Single, Strong Cation Exchange Column, by Means of Mineral Acid-Organic Solvent Mixtures. *J. Pharm. Pharmac.* **1970**, *22*, 625-627.

182. Wiegand, R. G.; Scherfling, E. Determination of 5-hydroxytryptophan and Serotonin. *J. Neurochem.* **1962**, *9*, 113-114.

183. Zhang, X.; Hodgetts, K.; Rachwal, S.; Zhao, H.; Wasley, J. W. F.; Craven, K.; Brodbeck, R.; Kieltyka, A.; Hoffman, D.; Bacolod, M. D.; Girard, B.; Tran, J.; Thurkauf, A. *trans*-1-[(2-Phenylcyclopropyl)methyl]-4-arylpiperazines: Mixed Dopamine D_2/D_4 Receptor Antagonists as Potential Antipsychotic Agents. *J. Med. Chem.* **2000**, *43*, 3923-3932.

184. Schreiber, M.; Fogelfeld, L.; Souroujon, M. C.; Kohen, F.; Fuchs, S. Antibodies to Spiroperiodol as Probes for Studying Dopamine Receptors. *Life Sci.* **1983**, *33*(15), 1519-1526.

185. Schiller, P. W.; Nguyen, T. M.-D.; Weltrowska, G.; Wilkes, B. C.; Marsden, B. J.; Lemieux, C.; Chung, N. N. Differential Stereochemical Requirements of μ vs. δ Opioid Receptors for Ligand Binding and Signal Transduction: Development of a Class of Potent and Highly δ-selective Peptide Antagonists. *Proc. Natl. Acad. Sci. USA* **1992**, *89*, 11871-11875.

186. Nikolelis, D. P.; Petropoulou, S. E.; Pergel, E.; Toth, K. Biosensors for the Rapid Detection of Dopamine Using Bilayer Lipid Membranes (BLMs) with Incorporated Calix[4]resorcinarene Receptor. *Electroanal.* **2002**, *14*(11) 783-789.

187. Zhu, Y.; Ran, Y.; Xu, S. Fiber-optic Evanescent Wave Biosensor of Catecholamine Neurotransmitter. *P. Soc. Phot-Opt. Inst.*, **2001**, *4414*, 137-140.

188. Loweth, C. J.; Caldwell, W. B.; Peng, X.; Alivisatos, A. P.; Schultz, P. G. DNA-Based Assembly of Gold Nanoparticles. *Angew. Chem. Int. Ed.* **1999**, *38*(12), 1808-1812.

189. Chan, W. C. W.; Nie, S. Quantum Dot Bioconjugates for Ultrasensitive Non-isotopic Detection. *Science* **1998**, *281*, 2016-2018.

190. Mucic, R. C.; Storhoff, J. J.; Mirkin, C. A.; Letsinger, R. L. DNA-Directed Synthesis of Binary Nanoparticle Network Materials. *J. Am. Chem. Soc.* **1998**, *120*, 12674-12675.

191. Service, R. F. DNA ventures into the World of Designer Materials. Science **1997**, *277* 1036-1037.

192. Battersby, B. J.; Bryant, D.; Meutermans, W.; Matthews, D.; Smythe, M. L.; Trau, M. Toward Larger Chemical Libraries: Encoding with Fluorescent Colloids in Combinatorial Chemistry. *J. Am. Chem. Soc.* **2000**, *122*, 2138-2139.

193. Bruchez, M.; Moronne, M.; Gin, P.; Weiss, S.; Alivisatos, A. P. Semiconductor Nanocrystals as Fluorescent Biological Labels. *Science* **1998**, *281*, 2013-2016.

194. Warhol, M. J. Use of Colloidal Gold in Diagnostic Surgical Pathology. *Am. J. Anat.* **1989**, *185*, 301-309.

195. Lin, S.; Quaroni, L.; White, W. S.; Cotton, T.; Chumanov, G. Localisation of Carotenoids in Plasma Low-Density Lipoprotein Studied by Surface Enhanced-Ramen Spectroscopy. *Biopolymers* **2000**, *57*(4), 249-256.

196. Karlsson, R.; Roos, H.; Bruno, J.; Stolz, L. Practical Aspects Concerning Direct Detection of Low Molecular Weight Analytes using BIAcore 2000. BIA Journal – Special Issue, BIAcore, Uppsala, Sweden, **1997**, 18-21.

197. Karlsson, R.; Stahlberg, R. Surface Plasmon Resonance Detection and Multispot Sensing for Direct Monitoring of Interactions Involving Low-Molecular-Weight Analytes and for Determination of Low Affinities. *Anal. Biochem.* **1995**, *228*, 274-280.

198. Wink, T.; van Zuilne, S. J., Bult, A.; van Bennekom, W. P. Liposome-Mediated Enhancement of the Sensitivity in Immunoassays of Proteins and Peptides in Surface Plasmon Resonance Spectrometry. *Anal. Chem.* **1998**, *70*, 827-832.

199. Kubitschko, S.; Spinke, J.; Bruckner, T.; Pohl, S.; Oranth, N. Sensitivity Enhancement of Optical Immunosensors with Nanoparticles. *Anal. Biochem.* **1997**, *253*, 112-122.

200. Severs, A. H.; Schasfoort, R. B. M. Enhanced Surface Plasmon Resonance Inhibition Test (ESPRIT) Using Latex Particles. *Biosens. Bioelectron.* **1993**, *8*(7-8), 365-370.

201. Lofas, S.; Johnsson, B. *J. Chem. Soc. Chem. Commun.* **1990**, 1526-1528.

202. Jordan, C. E.; Frutos, A. G.; Thiel, A. J.; Corn, R. M. Surface Plasmon Resonance Imaging Measurements of DNA Hybridization Adsorption and Streptavidin/DNA Multilayer Formation at Chemically Modified Gold Surfaces. *Anal. Chem.* **1997**, *69*, 4939-4947.

203. Alterman, M.; Sjobom, H.; Safsten, P.; Markgren, P.; Danielson, U. H.; Hamalainen, M.; Lofas, S.; Hulten, J.; Clason, B.; Samuelsson, B.; Hallberg, A. P1/P1' Modified HIV Protease Inhibitors as Tools in Two New Sensitive Surface Plasmon Resonance Biosensor Screening Assays. *Eur. J. Pharm. Sci.* **2001**, *13*, 203-212.

204. Buckle, P. E.; Davies, R. J.; Kinning, T.; Yeung, D.; Edwards, P. R.; Pollard-Knight, D.; Lowe, C. R. The Resonant Mirror: A Novel Optical Sensor for Direct Sensing of Biomolecular Interactions Part II: Applications. *Biosens. Bioelectron.* **1993**, *8*(7-8), 355-363.

205. Nellen, P. M; Lukosz, W. Model Experiments with Integrated Optical Input Grating Couplers as Direct Immunosensors. *Biosens. Bioelectron.* **1991**, *6*(6), 517-525.

206. Su, K.-H.; Wei, Q.-H.; Zhang, X.; Mock, J. J.; Smith, D. R.; Schultz, S. Interparticle Coupling Effects on Plasmon Resonances of Nanogold Particles. *Nano Letters.* **2003**, *3*(8), 1087-1090.

207. Lyon, L. A.; Musick, M. D.; Natan, M. J. Colloidal Au-Enhanced Surface Plasmon Resonance Immunosensing. *Anal. Chem.* **1998**, *70*, 5177-5183.

208. Lyon, L. A.; Musick, M. D.; Smith, P. C.; Reiss, B. D.; Pena, D. J.; Natan, M. J. Surface Plasmon Resonance of Colloidal Au-modified Gold Films. *Sensor. Actuat. B-Chem.* **1999**, *54*, 118-124.

209. Decher, G.; Natan, M.; Peschel, S.; Smith, E. A. Polyion Multilayer Spacers in Au-Colloid-Enhanced Surface Plasmon Resonance. Book of Abstracts: 219th ACS National Meeting, San Francisco, USA March 26-30 **2000.**

210. Lyon, L. A.; Pena, D. J.; Natan, M. J. Surface Plasmon Resonance of Au Colloid-Modified Au Films: Particle Size Dependence. *J. Phys. Chem. B* **1999**, *103*, 5826-5831.

211. Link, S.; El-Sayad, M. A. Size and Temperature Dependence of the Plasmon Absorption of Colloidal Gold Nanoparticles *J. Phys. Chem. B* **1999** *103*, 4212-4217.

212. Haes, A. J.; Zou, S.; Schatz, G. C.; van Duyne, R. P. A Nanoscale Optical Biosensor: The Long Range Distance Dependence of the Localized Surface Plasmon Resonance of Noble Metal Nanoparticles. *J. Phys. Chem. B* **2004**, *108*, 109-116.

213. Chah, S.; Hutter, E.; Roy, D.; Fendler, J. H.; Yi, J. The Effect of Substrate Metal on 2-aminoethanethiol and Nanoparticle Enhanced Surface Plasmon Resonance Imaging. *Chem. Phys.* **2001**, *272*, 127-136.

214. He, L.; Musick, M. D.; Nicewarner, S. R.; Salinas, F. G.; Benkovic, S. J.; Natan, M. J.; Keating, C. D. Colloidal Au-Enhanced Surface Plasmon Resonance for Ultrasensitive Detection of DNA Hybridization. *J. Am. Chem. Soc.* **2000**, *122*, 9071-9077.

215. Hutter, E.; Pileni, M. Detection of DNA Hybridization by Gold Nanoparticle Enhanced Transmission Surface Plasmon Resonance Spectroscopy. *J. Phys, Chem. B* **2003**, *107*(27), 6497-6499.

216. Natan, M. J.; Goodrich, G., He, L.; The Penn State Research Foundation, USA. Instruments, Methods and Reagents for Surface Plasmon Resonance. Patent No.: WO 01/09388 A1. **2001**.

217. Gu, J. H.; Lu, H.; Chen, Y.; Liu, L. Y.; Wang, P.; Ma, J. M.; Lu, Z. H. Enhancement of the Sensitivity of Surface Plasmon Resonance Biosensor with Colloidal Gold Labelling Technique. *Supramol. Sci.* **1998**, *5*, 695-698.

218. Englebienne, P.; van Hoonacker, Anne; Verhas, M. High-throughput Screening Using the Surface Plasmon Resonance Effect of Colloidal Gold Nanoparticles. *Analyst* **2001**, *126*, 1645-1651.

219. Leung, P.-T., Pollard-Knight, D.; Malan, G. P.; Finlan, M. F. Modelling of Particle-Enhanced Sensitivity of the Surface-Plasmon-Resonance Biosensor. *Sensor. Actuat. B-Chem.* **1994**, *22*(3), 175-180.

220. Johne, B.; Hansen, K.; Mork, E.; Holtlund, J. Colloidal Gold Conjugated Monoclonal Antibodies, Studied in the BIAcore Biosensor and in the Nycocard Immunoassay Format. *J. Immunol. Methods* **1995**, *183*, 167-174.

221. Zayats, M.; Pogorelova, S. P.; Kharitonov, A. B.; Lioubashevski, O.; Katz, E.; Willner, I. Au Nanoparticle-Enhanced Surface Plasmon Resonance Sensing of Biocatalytic Transformations. *Chem. Eur. J.* **2003**, *9*(24), 6108-6114.

222. Jordan, C. E.; Corn, R. M. Surface Plasmon Resonance Imaging Measurements of Electrostatic Biopolymer Adsorption onto Chemically Modified Gold Surfaces. *Anal. Chem.* **1997**, *69*, 1449-1456.

223. Gershon, P. D.; Khilko, S. Stable Chelating Linkage for Reversible Immobilization of Oligohistidine Tagged Proteins in the BIAcore Surface Plasmon Resonance Detector. *J. Immunol. Methods* **1995**, *183*, 65-76.

224. Gopel, W., Heiduschka, P. Interface Analysis in Biosensor Design. *Biosens. Bioelectron.* **1995**, *10*, 853-883.

225. Andersson, K.; Hamalainen, M.; Malmqvist, M. Identification and Optimization of Regeneration Conditions for Affinity-Based Biosensor Assays. A Multivariate Cocktail Approach. *Anal. Chem.* **1999**, *71*, 2475-2481.

226. Peter, J-C.; Briand, J.-P.; Hoebeke, J. How Biotinylation can Interfere with Recognition: A Surface Plasmon Resonance Study of Peptide-Antibody Interactions. *J. Immunol. Methods* **2003**, *274*, 149-158.

227. Li, M.; Wong, K. K. W.; Mann, S. Organisation of Inorganic Nanoparticles Using Biotin-Streptavidin Connectors. *Chem. Mater.* **1999**, *11*, 23-26.

228. Kaiser, T.; Gudat, P.; Stock, W.; Pappert, G.; Grol, M.; Neumeier, D.; Luppa, P. B. Biotinylated Steroid Derivatives as Ligands for Biospecific Interaction Analysis with Monoclonal Antibodies Using Immunosensor Devices. *Anal. Biochem.* **2000**, *282*, 173-185.

229. Oliver, C. Colloidal Gold/Streptavidin Methods *Method. Mol. Bio.* **1994** *34* 309-313.

230. Frens, G. Controlled Nucleation for the Regulation of the Particle Size in Monodisperse Gold Suspensions. *Nature* **1973**, *241*, 20-22.

231. O'Neal, D.; Harrip, P.; Dragicevic, G.; Rae, D.; Best, J. D. A Comparison of LDL Size Determination using Gradient Gel

Electrophoresis and Light-Scattering Methods. *J. Lipid Res.* **1998**, *39*, 2086-2090.

232. Malvern Instruments. Zetasizer – The Zetasizer Range Automated Dispersion Technology Solutions. Malvern Instruments Ref: MRK276-03 http://www.malvern.co.uk/malvern/siteres.nsf/viwdocref/englabhomepage

233. Zhu, T.; Vasilev, K.; Krieter, M.; Mittler, S.; Knoll, W. Surface Modification of Citrate-Reduced Colloidal Gold Nanoparticles with 2-Mercaptosuccinic Acid. *Langmuir* **2003**, *19*, 9518-9525.

234. Goodrich, G. P.; Musick, M. D.; Natan, M. J.; Keating, C. D. Strategies for Optimizing Particle-Amplified SPR. 220th American Chemical Society Meeting **2000**.

235. Otsuka, H.; Akiyama, Y.; Nagasaki, Y.; Kataoka, K. Quantitative and Reversible Lectin-Induced Association of Gold Nanoparticles Modified with α-Lactosyl-ω-mercapto-poly(ethylene glycol). *J. Am. Chem. Soc.* **2001**, *123* 8226-8230.

236. Ishii, T.; Otsuka, H.; Kataoka, K.; Nagasaki, Y. Preparation of Functionally PEGylated Gold Nanoparticles with Narrow Distribution through Autoreduction of Auric Cation by α-Biotinyl-PEG-*block*-[poly(2-(*N,N*-dimethylamino)ethyl methacrylate)]. *Langmuir* **2004**, *20*, 561-564.

237. Otsuka, H.; Nagasaki, Y.; Kataoka, K. PEGylated Nanoparticles for Biological and Pharmaceutical Applications. *Adv. Drug Deliver. Rev.* **2003**, *55*, 403-419.

238. Kurusu, F.; Ohno, H.; Kaneko, M.; Nagasaki, Y.; Kataoka, K. Functionalisation of Gold Electrode Surface with Heterobifunctional Poly(ethylene oxide)s Having both Mercapto and Aldehyde Groups. *Polym. Advan. Technol.* **2003**, *14*, 27-34.

239. Foulkes, J. A., Cookson, A. D., Sauer, M. J. AI in Cattle Based on Daily Microtitre Plate Enzyme Immunoassay of Progesterone in Whole Milk. *Br. Vet. J.* **1982**, *138*, 515-521.

240. Allen, S. E.; Foote, R. H. An Enzyme-Linked Immunoassay of Milk Progesterone as a Diagnositc Aid in Embryo Transfer Programs. *Theriogenology* **1988**, *29*(4), 893-903.

241. Arnstadt, K.-I.; Scmidt-Adamopoulou, B. Direct Enzymeimmunoassay for Determination of Progesterone in Milk from Cows. *Br. Vet. J.* **1982**, *138*, 436-438.

242. Srikandakumar, A. R. H.; Ingraham, M.; Ellsworth, M.; Archbald, L. F.; Liao, A.; Godke, R. A. Comparison of a Solid-Phase, No-extraction Radioimmunoassay for Progesterone with an Extraction Assay for Monitoring Luteal Function in the Mare, Bitch and Cow. *Theriogenology* **1986**, *26*, 779-793.

243. Wilbur, D. S.; Hamlin, D. K.; Buhler, K. R.; Pathare, P. M.; Vessella, R. L.; Stayton, P. S.; To, R. Streptavidin in Antibody Pretargeting. 2. Evaluation of Methods for Decreasing Localisation of Streptavidin to Kidney While Retaining its Tumour-Binding Capacity. *Bioconjugate Chem.* **1998**, *9*, 322-330.

244. Wilbur, D. S.; O'Brian, H. A. A Ring Bromination of Estradiol and 17α-Ethynylestradiol with *N*-Chlorosuccinimide and Bromide Ion. Possible Evidence for Hypobromite Intermediates. *J. Org. Chem.* **1982**, *47*, 359-362.

245. Exley, D.; Woodhams, B. The Specificity of Antisera Raised by Oestradiol-17β-3-hemisuccinyl-Bovine Serum Albumin. *Steroids*, **1976**, *27*(6), 813-20.

246. Won, C.; Chu, C. Dextran-Estrone Conjugate: Synthesis and in Vitro Release Study. *Carbohyd. Polm.*, **1998**, *36*, 327-334.

247. Miyashita, M.; Shimada, T.; Hisashi, M.; Akamatsu, M. Surface Plasmon Resonance-Based Immunoassay for 17Beta-Estradiol and its Application to the Measurement of Estrogen Receptor-Binding Activity. *Anal. Bioanal. Chem.*, **2005**, *381*(3), 667-673.

248. Pearson, J.; Gill, A.; Margison, G. P.; Vadgama, P.; Povey, A. C. A Rapid Receptor-Ligand Assay Determination of Estrogens Using Surface Plasmon Resonance. *Sens. Actuator B-Chem.* **2001**, *76*, 1-7.

249. Sesay, A.; Cullen, D. C. Detection of Hormone Mimics in Water Using a Miniaturised SPR Sensor. *Environ. Monit. Assess.* **2001**, *70*, 83-92.

250. Mons, N.; Geffard, M. Specific Antisera Against the Catecholamines: L-3,4-dihydroxyphenylalanine, Dopamine, Noradrenaline, and Octopamine Tested by an Enzyme-Linked Immunosorbent Assay. *J. Neurochem.* **1987**, *48*, 1826-1833.

251. Flurkey, K.; Bolger, M. B.; Linthicum, D. S. Preparation and Characterization of Antisera and Moncolonal Antibodies to Serotonergic and Dopaminergic Ligands. *J. Neuroimmunol.* **1985**, *8*, 115-127.

252. Geffard, M.; Segeula, P.; Heinrich-Rock; A. Antisera Against Catecholamines: Specificity Studies and Physiochemical Data for Anti-Dopamine and Anti-p-tyramine Antibodies. *Mol. Immunol.* **1984**, *21*, 515-522.

253. Mons, N.; Danel, N.; Geffard, M. Visualisation of L-dihydroxyphenylalanine in Rat brain by Using Specific Antibodies. *Brain Res.* **1988**, *451*, 403-407.

254. Chagnaud, J. L.; Mons, N.; Tuffet, S.; Grandier-Vazeilles, X.; Geffard, M. Monoclonal Antibodies Against Glutaraldehyde-Conjugated Dopamine, **1987**, *49*, 487-494.

255. Kazak, L. E.; Etkin, A. F.; Bol'shakova, T. D.; Ermolin, G. A.; Babayan, S. S. Difficulties in Obtaining Antisera for Immunochemical Assay of Catecholamines and Normetanephrine. *Lab. Delo* **1983**, *5*, 20-22.

256. Geffard, M.; Kah, O.; Onteniente, B.; Seguela, P.; Le Moal, M.; Delaage, M. Antibodies to Dopamine: Radioimmunological Study of Specificity in Relation to Immunocytochemistry. *J. Neurochem.* **1984**, *42*, 1593-1597.

257. Cao, K.; Stack, D. E.; Ramanathan, R.; Gross, M. L.; Rogan, E. G.; Cavalieri, E. L. Synthesis and Structure Elucidation of Estrogen Quinones Conjugated with Cysteine, *N*-acetylcysteine, and Glutathione. *Chem. Res. Toxicol.* **1998**, *11* 909-916.

258. Cao, K.; Devanesan, P. D.; Ramanathan, R.; Gross, M. L.; Rogan, E. G.; Cavalieri, E. L. Covalent Binding of Catechol Estrogens to Glutathione Catalyzed by Horseradish Peroxidase, Lactoperoxidase or Rat Liver Microsomes. *Chem. Res. Toxicol.* **1998**, *11*, 917-924.

259. Nakagomi, M.; Suzuki, E. Quantitation of Catechol Estrogens and Their *N*-acetylcysteine Conjugates in Urine of Rats and Hamsters. Chem. Res. Toxicol. **2000**, *13*, 1208-1213.

260. Miller, R. T.; Lau, S. S., Monks, T. J. Metabolism of 5-(glutathion-*S*-yl)-α-methyldopamine Following Introcerebroventricular Administration to Male Sprague-Dawley Rats. *Chem. Res. Toxicol.* **1995**, *8*, 634-641.

261. Ito, S.; Fujita, K.; Yoshioka, M.; Sienko, D.; Nagatsu, T. Identification of 5-S- and 2-S-cysteinyldopamine and 5-S-glutathionyldopamine Formed from Dopamine by High-Performance Liquid Chromatography with Electrochemical Detection. *J. Chrom.* **1986**, *375*, 134-140.

262. Montine, T. J.; Amarnath, V.; Picklo, M. J.; Sidell, K. R.; Zhang, J.; Graham, D. G. Dopamine Mercaptourate can Augment Dopaminergic Neurodegeneration. *Drug Metab. Rev.* **2000**, *32* (3&4) 363-376.

263. Dagnino-Subiabre, A.; Cassels, B. K.; Baez, S.; Johansson, A.; Mannervik, B.; Segura-Aguilar, J. Glutathione Transferase M2-2 Catalyzes Conjugation of Dopamine and Dopa *o*-Quinones. *Biochem. Biophys. Res. Co.* **2000**, *274* (1), 32-36.

264. Sidell, K. R.; Olson, S. J.; Ou, J. J.; Zhang, Y.; Amarnath, V.; Montine, T. J. Cysteine and Mercapturate Conjugates of Oxidised Dopamine are in Human Striatum but only the Cystein Conjugate Impedes Dopamine Trafficking *in vitro* and *in vivo*. *J. Neurochem.* **2001**, *79*, 510-521.

265. Spencer, J. P. E., Whiteman, M., Jenner, P., Halliwell, B. 5-S-Cysteinyl-Conjugates of Catecholamines Induce Cell Damage, Extensive DNA Base Modification and Increase in Caspase-3 Activity in Neurons. *J. Neurochem.* **2002**, *81*, 122-129.

266. Spencer, J. P. E.; Jenner, P.; Daniel, S. E.; Lees, A. J.; Marsden, D. C.; Halliwell, B. Conjugates of Catecholamines with Cysteine and GSH in Parkinson's Disease: Possible Mechanisms of Formation Involving reactive Oxygen Species. *J. Neurochem.* **1998**, *71*, 2112-2122.

267. Chavdarian, C. G.; Castagnoli, N. Synthesis, Redox Characteristics, and in Vitro Norepinephrine Uptake Inhibiting Properties of 2-(2-Mercapto-4,5-dihydroxyphenyl)ethylamine (6-Mercaptodopamine) *J. Med. Chem.* **1979**, *22*, 1317-1322.

268. Wong, M.; DeJesus, O. T. Synthesis and Enzymatic Decarboxylation of 6-bromo-L-DOPA, a Potential Brain Tracer for L-DOPA. *J. Labelled Compd. Rad.* **1987**, *24* (11), 1373-1380.

269. Seki, T. Chromatographic Separation of Some Biogenic Amines on a Weakly Acidic Ion-Exchange Resin, *J. Chrom.* **1981**, *207*, 286-287.

Appendix 1 – Preparation of Buffers

PBS/T: 10 mM phosphate buffered saline pH 7.4, 0.05%w/v Tween 20, NaCl 138 mM, KCl 2.7 mM. Prepared by dissolving commercial sachet (Sigma P-3563) in 1 L of deionised water. Other pH by adjustment with base or acid as required.

Phosphate buffer, pH 7.2: 36.0 mL of 0.2 M Na_2HPO_4 mixed with 14.0 mL of 0.2 M NaH_2PO_4

pH 7.4: 40.5mL of 0.2 M Na_2HPO_4 mixed with 9.5 mL of 0.2 M NaH_2PO_4

HBS-EP: 0.95 g *N*-[2-Hydroxyethyl]piperazine-*N*'-[2-ethanesulfonic acid] (HEPES), 3.51 g NaCl, 0.44 g EDTA, 200 µL of P-20 surfactant added to 400 mL of deionised water and pH adjusted to 7.4.

0.1 M borate buffer pH 8.5: 0.31 g of boric acid in 25 mL of deionised water, adjusted to pH= 8.5 with 0.1 M NaOH and then made up to 50 mL in deionised water.

0.1 M sodium formate buffer pH 4.3: 0.35 g of sodium formate in 25 mL of deionised water, adjusted to pH 4.3 with formic acid and then made up to 50 mL in deionised water.

0.1 M sodium acetate buffer pH 4.0: 18 mL of 0.2 M sodium acetate is mixed with 82 mL of 0.2 M acetic acid and the pH adjusted to 4.0.

Bicarbonate Buffer pH 9.6: 0.85 g of sodium carbonate and 1.47 g sodium bicarbonate dissolved in 500 mL of deionised water.

0.1 M Sodium Acetate Buffer pH 5.4

1.6406 g of sodium acetate dissolved in 200 mL of deionised water. Add 120 µL of glacial acetic acid. Adjust the pH with acetic acid or sodium acetate as necessary.

TMB Colour Reagent

50 mg of TMB was dissolved in 5 mL of DMSO and protected from light. 250 μL of this stock solution was added to 25 mL of acetate buffer, pH=5.2, along with 250 μL of hydrogen peroxide stock (38 μL of 30% hydrogen peroxide in 2.5 mL of deionised water). The reagent was used immediately. The TMB stock lasts up to three months. The hydrogen peroxide stock must be freshly made each time.

Appendix 2 – BCA Assay

This assay was done using a standard BCA assay kit from Pierce (Rockford, USA) and following the enclosed instructions.

1. BSA standards were prepared at 0, 25, 125, 250, 500, 750, 1000, 1500, 2000 μg/mL in PBS/T.
2. 0.1 mL of standard or sample was added to glass tubes and mixed with 2 mL of working reagent.
3. The tubes were incubated for 30 min at 37 °C and then cooled to room temperature.
4. The absorbance was then measured at 562 nm.
5. Blank corrected plots of absorbance *vs* protein concentration were prepared for the BSA standards and OVA concentrations determined by applying the appropriate correction factor.

   Note: BSA standards should be used because they are of high purity and in combination with the correction factor give accurate results with un-modified antibody.

Appendix 3 – BIAcore Wizards

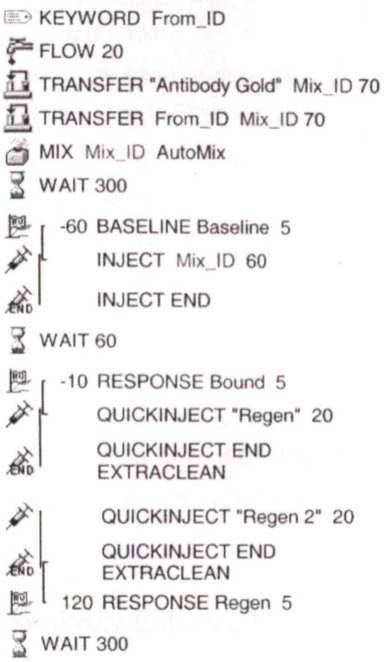

Figure A3.1 Pre-incubation Assay Wizard

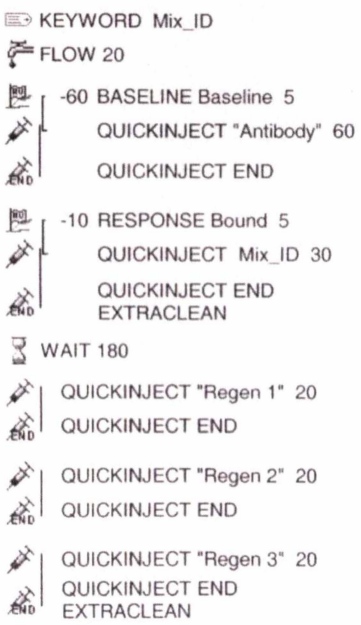

Figure A3.2 Sequential Assay Gold Wizard

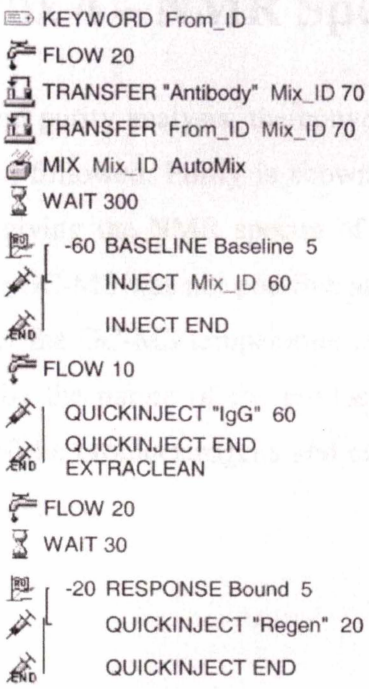

Figure A3.3 Secondary Antibody Enhanced Assay Wizard

Appendix 4 – NMR Spectra

For the purposes of compound purity analysis, the conventions of the Journal of Organic Chemistry have been followed. Purity is shown either by HPLC purity analysis where stated or by giving the NMR spectra of the pure compounds as appended below. Quantitative GC-MS was not possible as most of the compounds were thermally unstable under the GC-MS temperature conditions, and elemental analysis was made difficult by the nature of the products (mostly either oils or waxy solids) or in the case of the bromoestrogens and catecholamines because it does not detect a mixture of isomers.

Chapter 3.

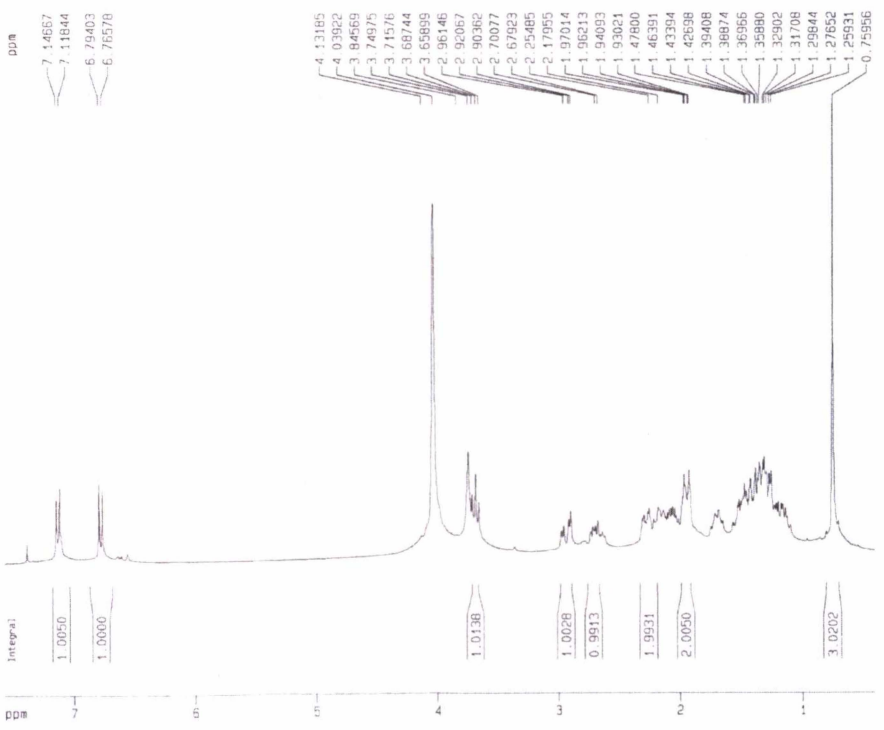

Figure A4.1 ^{1}H NMR of **(1)**

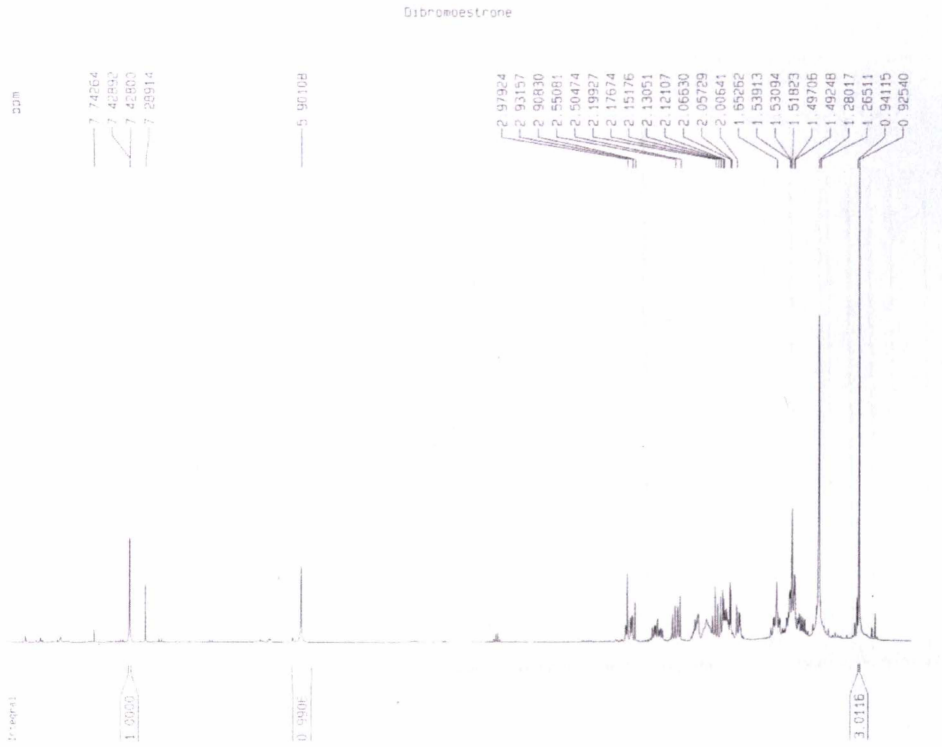

Figure A4.2 ^{1}H NMR of **(2)**

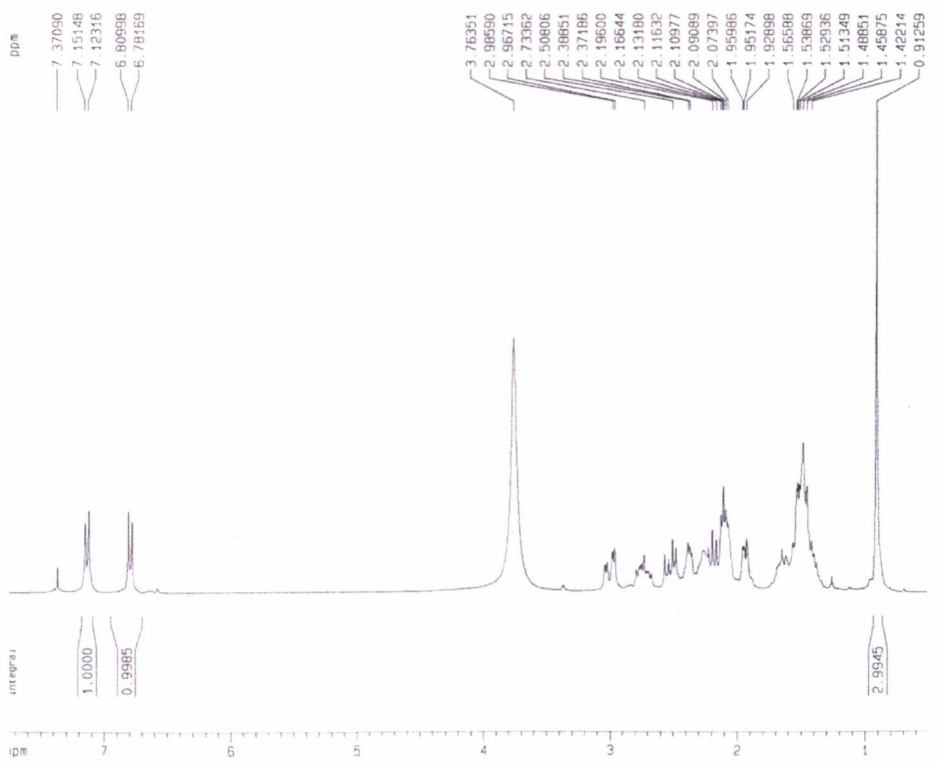

Figure A4.3 ^{1}H NMR of **(3)**

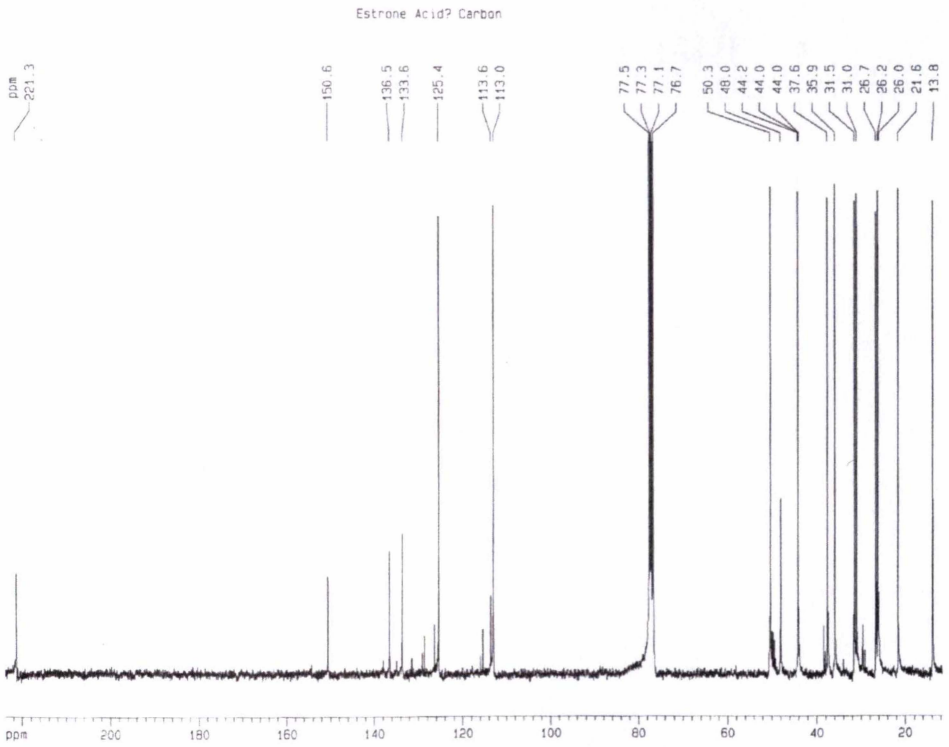

Figure A4.4 ^{13}C NMR of **(5)**

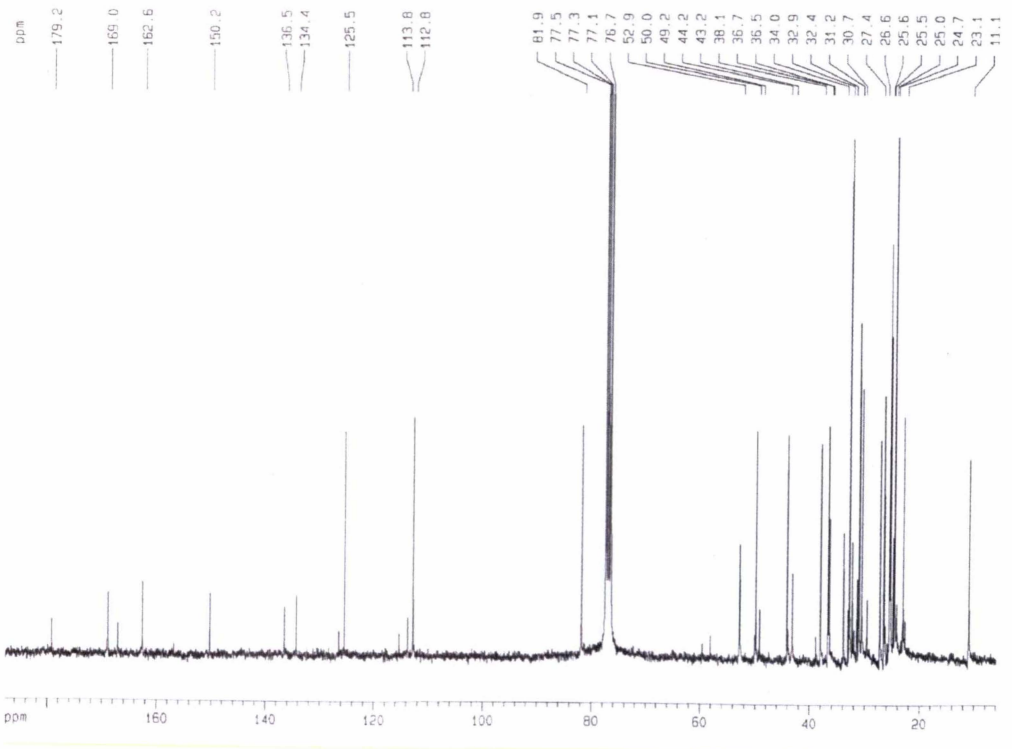

Figure A4.5 ^{13}C NMR of **(6)**

For **(7)** see Chapter 3.

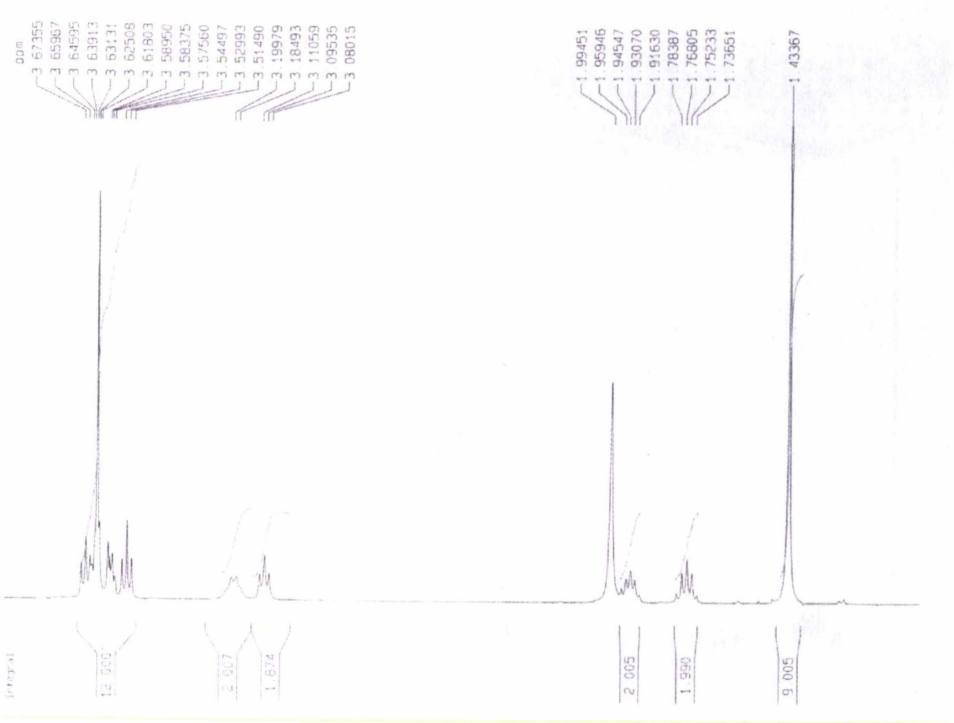

Figure A4.6 ^{1}H NMR of **(8)**

For **(9)** see Chapter 3.

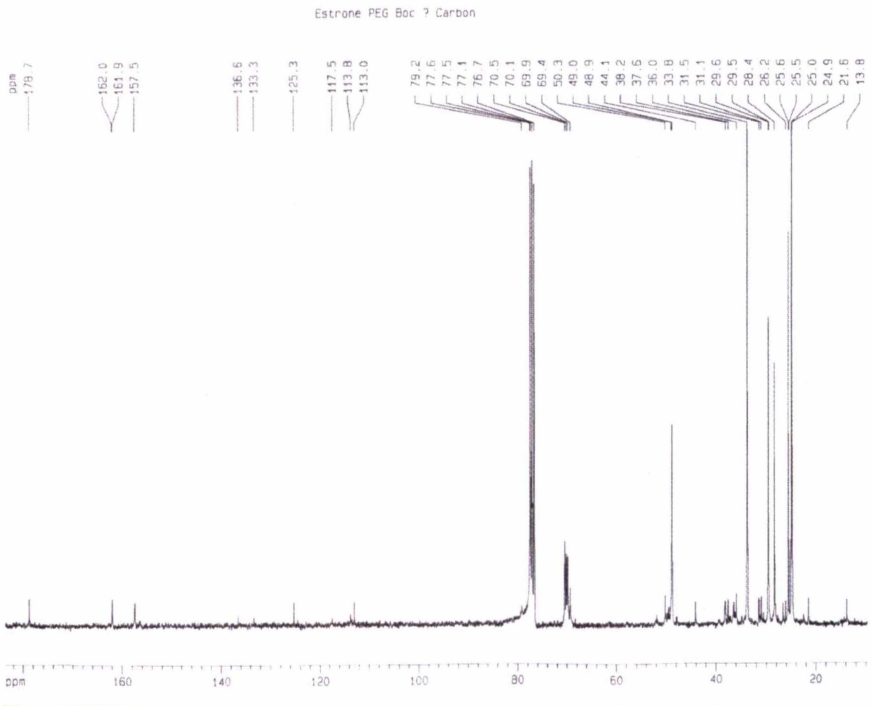

Figure A4.7 ^{13}C NMR of **(12)**

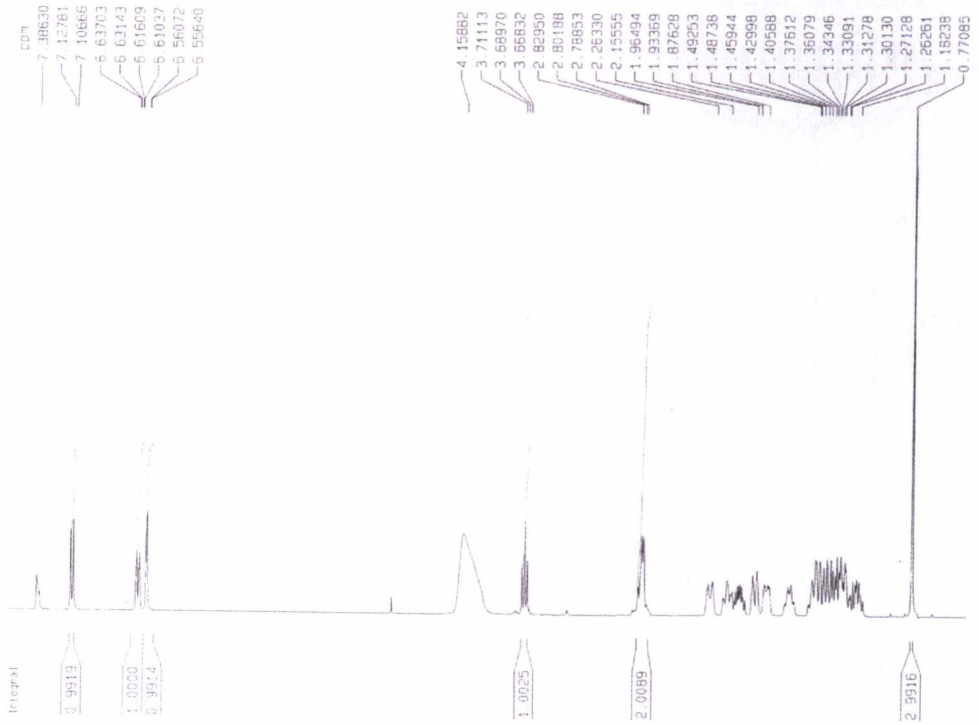

Figure A4.8 ^{1}H NMR Spectrum of **(15)**

For **(16)** see Chapter 3

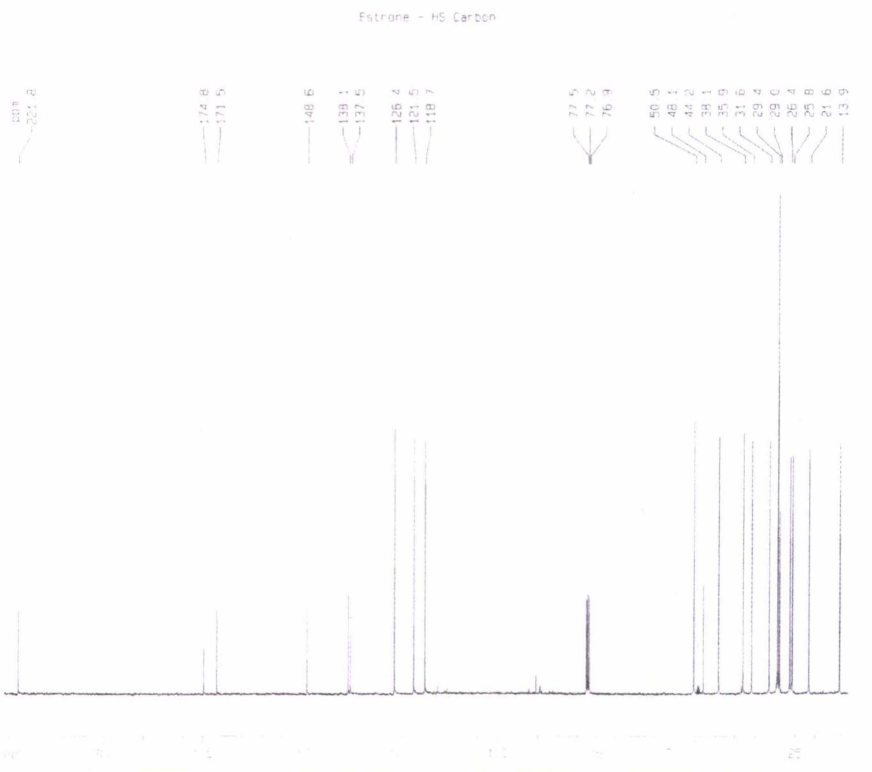

Figure A4.9 ^{13}C NMR Spectrum of **(17)**

UNIVERSITY OF WAIKATO
LIBRARY

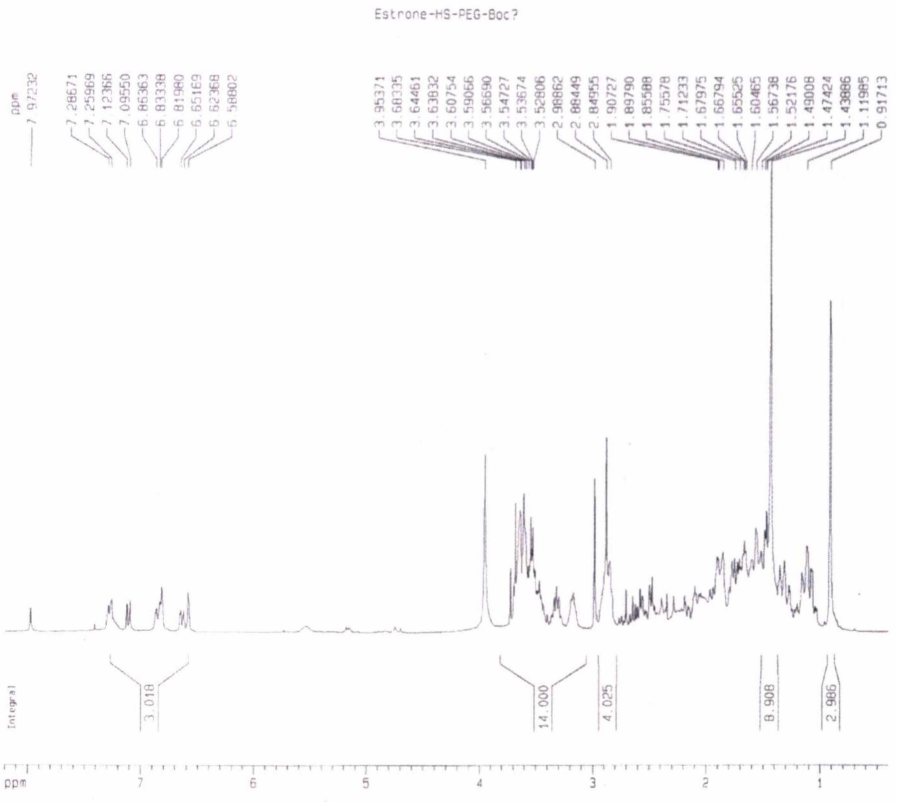

Figure A4.10 ^{1}H NMR Spectrum of **(18)**

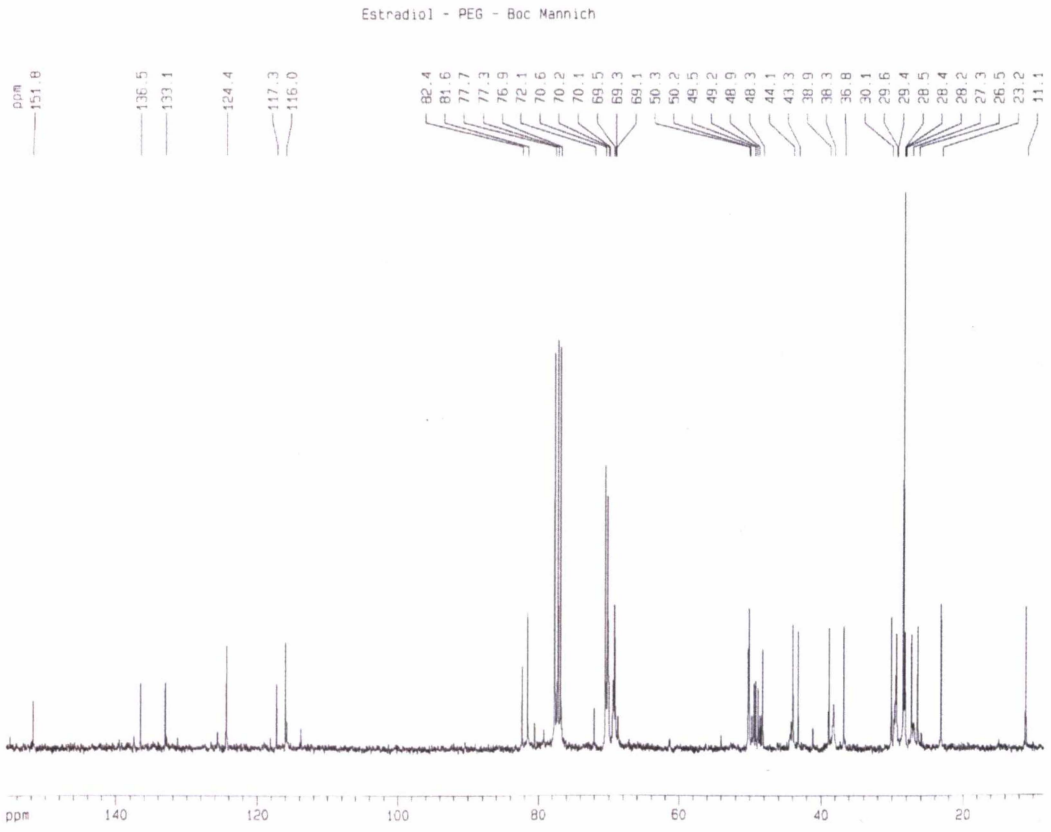

Figure A4.11 ^{13}C NMR Spectrum of **(19)**

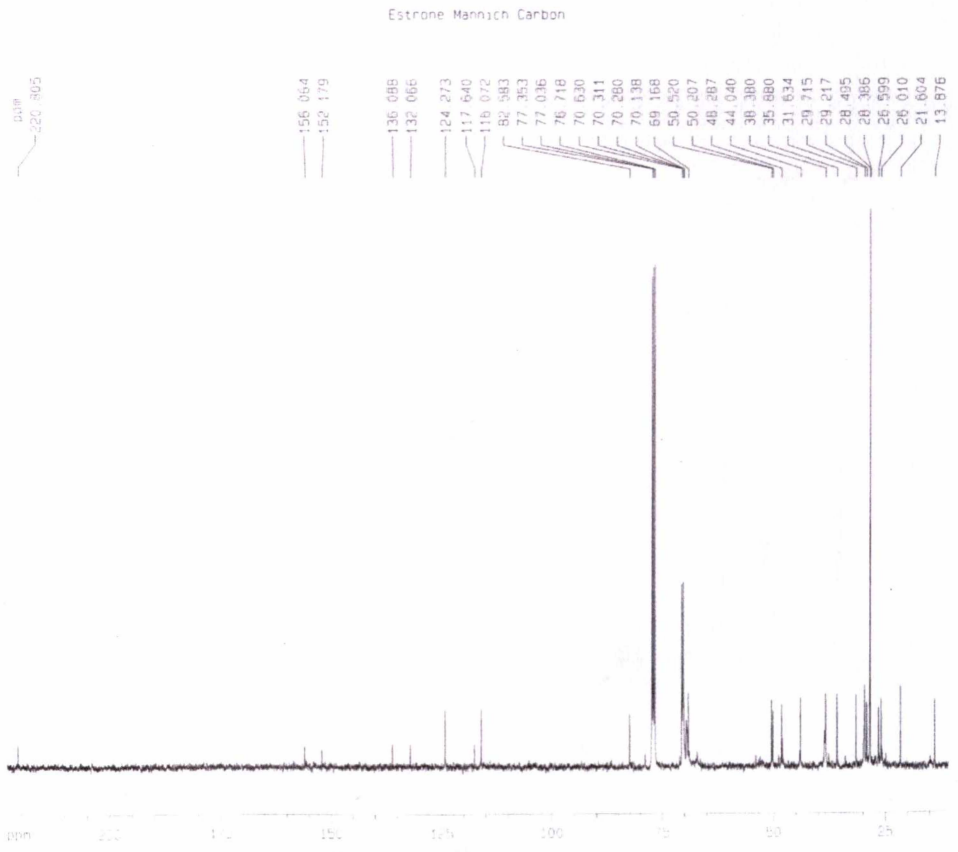

Figure A4.12 ^{13}C NMR Spectrum of **(20)**

Chapter 5.

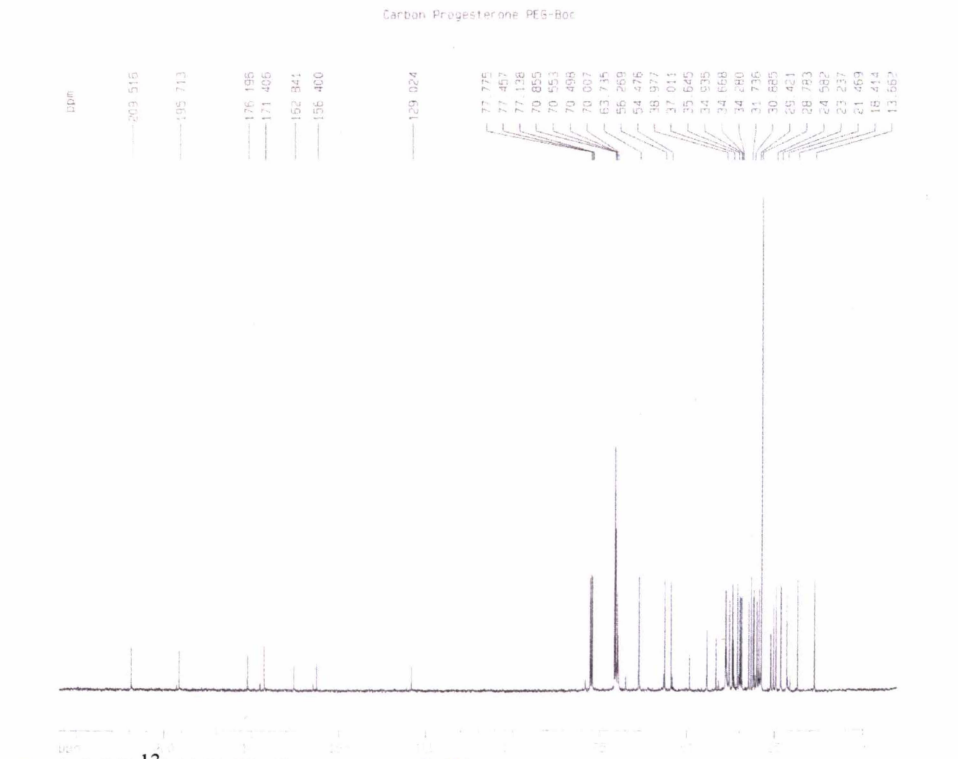

Figure A4.13 ^{13}C NMR Spectrum of **(1)**

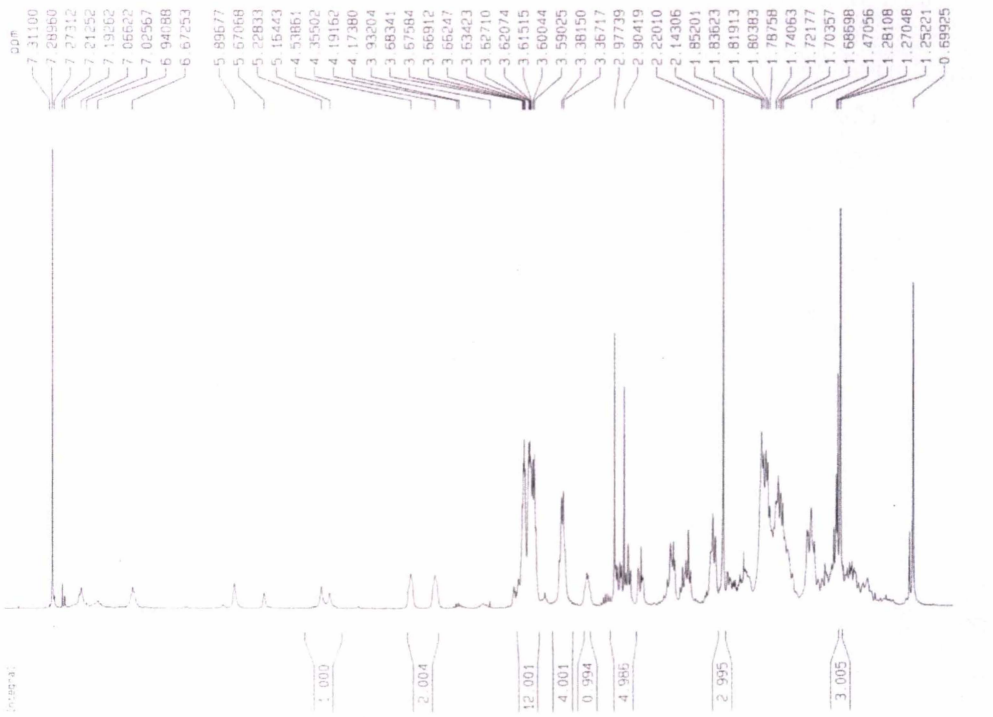

Figure A4.14 ^{1}H NMR Spectrum of **(3)**